SHRP-C-391

Resistance of Concrete to Freezing and Thawing

Donald J. Janssen
University of Washington
Seattle, Washington 98195

Mark B. Snyder
University of Minnesota
Minneapolis, Minnesota 55455

Strategic Highway Research Program
National Research Council
Washington, DC 1994

SHRP-C-391
Contract C-203
ISBN 0-309-05773-6
Product no. 2002, 2004, 2018, 2019, 2020, 2021

Program Manager: *Don M. Harriott*
Project Manager: *Inam Jawed*
Editor: *Katharyn L. Bine*
Production Editors: *Carina S. Hreib, Carrie Kent*

June 1994

key words:
aggregate
D-cracking
durability factor
freezing and thawing
modal analysis
portland cement concrete
quality factor
resonance frequency

Strategic Highway Research Program
National Research Council
2101 Constitution Avenue N.W.
Washington, DC 20418

(202) 334-3774

1.5M/NAP/694

Acknowledgments

The research described herein was supported by the Strategic Highway Research Program (SHRP). SHRP is a unit of the National Research Council that was authorized by section 128 of the Surface Transportation and Uniform Relocation Assistance Act of 1987.

This book represents the efforts of many people and organizations. Appendix D, "Damping Measurements for Nondestructive Evaluation of Concrete Beams," was a collaborative work by Elizabeth A. Vokes, Washington State Department of Transportation; Steven L. Clarke, Archos, Inc.; Donald J. Janssen, University of Washington; and the Washington State Transportation Center (TRAC). The National Science Foundation provided some of the Test Equipment used in this particular study. J. D. Chalupnik and D. W. Storti, Department of Chemical Engineering, and W. D. Scott, Department of Material Science and Engineering assisted in the development of the initial impulse-excitation procedures. Additional support came from the National Science Foundation and in-kind support from Michigan State University and the University of Washington.

Preface

The mechanisms of damage to concrete from repeated cycles of freezing and thawing are not well understood and continue to be intensively studied. Original research was based on the fact that water expands 9 percent when it freezes. Thus, the term "critical saturation" was coined to describe the point at which the concrete pores were 91.7 percent saturated and, therefore, assumed to be susceptible to damage due to freezing and thawing. Further investigation determined that deterioration due to freezing and thawing can affect concrete with lower degrees of saturation.[1]

Four theories have gained wide acceptance in describing the mechanisms of frost action.[2] Although most of these theories were originally used to describe the frost action in cement paste, they are also applicable to concrete.[3] The first was the hydraulic pressure theory Powers proposed in 1945. This was followed by the diffusion and growth of capillary ice theory constructed by Powers and Helmuth in 1953, the dual mechanism theory by Larson and Cady in 1969, and the desorption theory by Litvan in 1972. Other theories have been proposed, but these four form the basis of most research in the area of frost resistance of concrete.

Powers' hydraulic pressure theory proposes that destructive stresses can develop if water is displaced to accommodate the advancing ice front in concrete.[4] If the pores are critically saturated, water will begin to flow to make room for the increased ice volume. Hydraulic pressures generated during the water flow will be dependent upon the length of the flow path, the rate of freezing, the permeability of the concrete, and the viscosity of the water. The concrete will rupture if the hydraulic pressure exceeds its tensile strength.

Further studies by Powers and Helmuth revealed that the hydraulic pressure theory did not account for continued dilation of some specimens and shrinkage of other specimens at a constant temperature.[5] They therefore proposed that the production of ice produces a relatively concentrated alkali solution at the freezing site. Unfrozen water will, in turn, move toward the site because of the differences in solute concentrations in a process similar to osmosis. Hence, the pressure developed was called osmotic pressure.

Larson and Cady produced results that they felt were supported by the hydraulic pressure theory.[6] However, they also noted continued dilation of concrete specimens after the equipment indicated that freezing had ceased. They attributed these dilations to the hydraulic pressures generated by the increase in the specific volume of water during the "ordering," or change of state, from bulk water on the ice and pore surfaces to adsorbed water.

Litvan's desorption theory proposes that vapor pressure differentials, created as the relative humidity decreases in the aggregate pores, force water to migrate out of the aggregate pore.[7] As in Powers' theory, the concrete will rupture if the hydraulic pressures generated during migration exceed the tensile strength of the concrete.

While these theories disagree as to whether water moves toward or away from the point of ice formation, they agree that the amount of water in the pores and the resistance to movement of that water play a role in the frost resistance of concrete. In the case of concrete, it is generally accepted that the pore system is potentially susceptible to damage from freezing and thawing. Efforts to produce frost-resistant concrete have primarily focused on providing a proper system of entrained air voids. In the case of aggregates, some pore systems do not show susceptibility to damage from freezing and thawing while other pore systems do. In addition to the air-entrainment of concrete as mentioned above, efforts have also focused on identifying the aggregates with acceptable pore systems for use in concrete exposed to freezing and thawing.

The work is presented in three parts: Part I, which deals with those factors that relate primarily to the paste portion of the concrete; Part II, which deals with those factors primarily relating to the coarse aggregate portion of the concrete; and Part III, which summarizes and presents preliminary results of the field work for Parts I and II. The first chapter of each part begins with a full description of the scope of the part. The data and other information presented in each part are given in separate appendices.

References

1. Powers, T. C. "Freezing Effects In Concrete," *American Concrete Institute SP 47-1*, 1975, pp. 1-11.

2. Thompson, S. R., M. P. Olsen and B. J. Dempsey. "D-Cracking in Portland Cement Concrete Pavements," 1980, Project IHR-413.

3. Verbeck, G. and R. Landgren. "Influence of Physical Characteristics of Aggregates on Frost Resistance of Concrete," *ASTM Proceedings,* Vol. 60, 1960, pp. 1063-1079.

4. Powers, T. C. "A Working Hypothesis for Further Studies of Frost Resistance of Concrete," *Journal of the American Concrete Institute*, Vol. 16, No. 4, 1945, pp. 245-272.

5. Powers, T. C. and R. A. Helmuth. "Theory of Volume Changes in Hardened Portland-Cement Paste During Freezing," *Highway Research Board Proceedings,* Vol. 32, 1953, pp. 285-297.

6. Larson, T. D. and P. D. Cady. "Identification of Frost-Susceptible Particles in Concrete Aggregates," *NCHRP Report* 66, 1969.

7. Litvan, G. G. "Phase Transitions of Adsorbates, IV, Mechanism of Frost Action in Hardened Cement Paste," *American Ceramic Society Journal,* Vol. 55, No. 1, 1972, pp. 38-42.

Contents

Part I - Frost Resistance of Concrete Made with Durable Aggregate

List of Figures

Part I

Part II

List of Tables

Part I

Part II

Part III

Abstract

This study, aimed at improving the freeze-thaw resistance of concrete, consists of three parts. Part I evaluates parameters affecting the freeze-thaw durability of concrete. A modification of the existing standard of method for determining the durability factor of concrete specimens is proposed, and a new procedure for fundamental transverse frequency (used in durability factor calculations) has been developed. Part II focuses on developing better methods for identifying nondurable aggregates, and has resulted in a rapid new test based on the hydraulic fracture of aggregates. Part III describes field experiments to evaluate the freeze-thaw resistance of a number of specified concrete mixes and the use of sealants to mitigate D-cracking. Preliminary field performance results are presented.

Executive Summary

This document summarizes the results of a four-year program of research into the resistance of concrete to freezing and thawing. The work is presented in three parts. Part I is a discussion of factors primarily relating to the paste portion of the concrete. Part II relates primarily to the coarse aggregate portion of the concrete. Part III summarizes preliminary results for the field work relating to Parts I and II. The appendices contain the data and other information supplemental to the parts. These three parts are summarized below:

Part I: Frost Resistance of Concrete Made with Durable Aggregate

A revised test procedure and a new test procedure for concrete made with durable (frost-resistant) aggregate by rapid freezing and thawing is presented. Durability factor (DF) was measured for a variety of mix parameters, with the emphasis being placed on identifying mix combinations that produced DF values in the 25 to 75 range. Air-void parameters were measured by linear traverse. The water pore systems were evaluated by permeability measurement and by determining the theoretical amount of water that would freeze at -18°C (called freezable moisture in the text).

A modification to AASHTO T 161 was developed to address concerns with current variations of AASHTO T 161 regarding container restraint in Procedure A and specimen drying in Procedure B. The modification consists of wrapping the specimens in terrycloth to keep them moist during freezing without needing containers. The modification is slightly more severe than current procedures, and shows less variability in results.

A new procedure for determining fundamental transverse frequency (used to calculate DF) was developed. The procedure consists of causing a specimen to vibrate by impacting it with an instrumented hammer, then evaluating the frequency response spectrum measured with an accelerometer. The procedure is more than an order of magnitude more precise than the published precision for the current method of determining fundamental transverse frequency, ASTM C 215. No frost resistance models were developed because insufficient freezable moisture data was available to permit adequate modelling.

Part II: Frost Resistance of Concrete Made with Frost-Susceptible Aggregate

The primary focus of this part was to develop a new test procedure for identifying aggregates which are not durable when subjected to freezing and thawing in concrete (D-cracking

susceptible). The procedure, called the Washington Hydraulic Fracture Test, uses compressed gas to force water into the pores of a dry aggregate. When the pressure is released, the aggregate must dissipate internal pressure. Aggregate that cannot dissipate the pressure rapidly fracture. The amount of fracturing is determined, and a value called the hydraulic fracture index (HFI) is calculated. This value is an estimate of the number of pressurization cycles necessary to produce 10 percent of the pieces of aggregate to fracture. The laboratory results were compared to reports of field performances. Aggregates with high (80 to 100 or higher) HFI values tended to be non-D-cracking susceptible, while aggregates with low (less than about 60) HFI values tended to be D-cracking susceptible.

Mitigation for existing D-cracking was also investigated. Findings suggested that the most suitable method of treating existing D-cracked pavements would be to replace the concrete with a full-depth patch. Prior to placing the new concrete, the exposed face of the existing concrete section should be sealed to prevent moisture intrusion. This method would only be appropriate for pavements and other concrete with considerable intact concrete away from joints and cracks. This mitigation method is evaluated in Part III.

Part III: Field Studies

Several questions arose from the work reported in Parts I and II of this report relating to field performance, namely: 1) how the newly-developed modification of AASHTO T 161 relates to field performance; 2) whether non-traditional mixes (such as mixes containing pozzolans or very high cement contents) follow the same accepted criteria for resistance to freezing and thawing as traditional air-entrained mixes; and 3) whether the progression of field D-cracking can be slowed sufficiently to significantly extend the life of pavements containing D-cracking susceptible aggregates. These questions were addressed by the construction of field test sections.

Full-depth concrete patches made with a range of high-performance materials (high cement contents, accelerators, and blended cements used to achieve specified early-opening strengths) were placed. The concrete patches had a range of air contents to produce an expected range of performance. Companion specimens from many of the mixes produced laboratory DF values less than 60, and would be expected to fail. These test patches require further monitoring to evaluate field performance.

Test slabs containing varying amounts of fly ash were placed in Minnesota with a range of air contents to produce an expected range of performance. Companion specimens from most of the mixes produced DF values above 90, even though the air-void systems would be judged to be substandard by conventional wisdom. Further field monitoring will be needed to evaluate field performance of these sections. Many of the patches in Ohio were placed in pavements made with aggregates susceptible to D-cracking. Prior to placing the new concrete, the cut faces of the existing concrete received one of a variety of sealer treatments. Field monitoring will be needed to evaluate differences in field performance of the sealer treatments.

Part I - Frost Resistance of Concrete Made with Durable Aggregate

1.0 Introduction

1.1 Background

Frost resistance of concrete made with durable aggregate is determined by the air-void system's ability to prevent development of destructive pressures due to freezing and associated movement of moisture in the concrete pores. The specific requirements of the air-void system depend on the amount and mobility of the water in the pores. An investigation of the frost resistance of concrete made with durable aggregates should identify the air-void system necessary to protect a variety of concrete water-pore systems.

1.2 Objectives

The goal of this research was to determine the effects of water-cement (w/c) and water-cementitious [w/(c+p)] ratios, various air-entraining admixtures, water-reducing and high-range water reducing admixtures, pozzolanic admixtures, and ground granulated blast furnace slag on the frost resistance of concrete made with durable aggregates. Frost resistance was evaluated by rapid laboratory testing. Field evaluation of selected mixes is discussed in Part III.

In particular, the research examined

1. procedures for rapid freezing and thawing testing with modifications to these procedures if appropriate;
2. procedures for nondestructive evaluation of damage from rapid freezing and thawing. Procedure modifications were made if deemed appropriate;
3. various methods of quantifying the air-void system in hardened concrete;
4. methods of evaluating the water pore system in hardened concrete;
5. combination of the air-void and water pore systems to better predict resistance to freezing and thawing.

2.0 Laboratory Testing Program

2.1 Purpose

The laboratory testing program developed a data set. Because the amount of testing necessary to define durability factor (DF) versus air-void parameter relations for the range of

mix parameters of interest would be prohibitive, an alternate approach was used. Many researchers have shown that this relationship is relatively linear for the midrange of DF values (approximately 25 to 75).[1] Therefore, the initial testing defined the slope of this linear range for base mixes made with 0.40 and 0.45 w/c's. Assuming that these slopes held for other mix combinations with the same w/c values, testing of other mix combinations would concentrate on mixes with marginal DF values in this 25-to-75 range.

This approach required considerable attention to the minimization of testing errors. This involved repeated freezing and thawing testing, along with nondestructive evaluation of specimen deterioration. Chapter 3 descibes the innovative test procedures used.

2.2 Test Matrices

Test matrices were developed that combined the various parameters of:

Parameter	Variable
w/c	0.40, 0.45, 0.52
Cement Type	Type I, Type II, Type III
Air-Entrainment Admixture (AEA)	vinsol resin, two other proprietary AEA's
Water Reducing (WR) and High-Range Water Reducing (HRWR) Admixtures	one WR and two HRWR's
Pozzolan Types	one Class C flyash, one Class F flyash, one silica fume, and one ground granulated blast furnace slag
w/(c+p)	0.40, 0.45 (w/c's of 0.45, 0.46, 0.52 and 0.59, depending upon pozzolan content)
Coarse Aggregate	crushed limestone and glacial gravel
Curing	14, 28 (std.) and 56 days in limewater
Specialty High-Performance Mixes	very early strength and high early strength mixes, Pyrament, Rapid Set cement

The design matrices showing the various combinations of the above parameters are presented in appendix A.

2.3 Air Void System Evaluation

The air-void system in the hardened concrete was evaluated by linear traverse. In addition to the measurements specified in ASTM C 457, individual chord lengths were recorded for all air voids. This permitted the calculation of a spacing factor ($\bar{L}$) with only chords smaller than 1 mm in addition to the standard calculation using all voids, partly eliminating the influence of entrapped air voids in the air-void parameter. Philleo factors ($\bar{P}$)[2, 3] could also be calculated with the individual chord length data. Specific surface (α), and the mean air-void spacing ($\bar{S}$) also were calculated.[4] These parameters were calculated with both the mix design paste contents and paste contents determined by linear traverse.

2.4 Water Pore System Evaluation

The water pore system was evaluated by permeability testing and by drying to equilibrium moisture content at various relative humidities. The permeability testing used an hydraulic gradient of less than ten, and was based upon a procedure developed at the University of Illinois.[5]

Equilibrium moisture contents at various relative humidities were determined by allowing previously saturated (and never dried) specimens to dry to constant mass over saturated salt solutions. Three specimens from each concrete mix, each weighing approximately 1 kg (2.2 lb.), were used for each relative humidity value. The saturated salt solutions and corresponding relative humidities are given in table 1-1. Equilibrium was considered to have been reached when the mass loss was less than 0.03 percent in one week. When equilibrium was reached, the mass of each specimen was determined and the specimen was dried to constant mass at 120°C. The combined equilibrium moisture content for the three specimens at each relative humidity was then determined. An example of the relative humidity drying results is shown in figure 1-1. Some observations of these results are summarized below:

1. The relationship between the moisture content and relative humidity is linear (within the precision of moisture content measurements) for the range of 53 through 97 percent relative humidity. This is the range of greatest interest in the study of freezable water and moisture mobility. The energy level of water that will freeze at temperatures at or above -18°C is equivalent to the energy level of water that will evaporate at approximately 85 percent relative humidity at room temperature, based on calculations by Powers and Brownyard.[6]

2. The saturated, surface-dry (SSD) moisture is always higher than the extrapolation of the humidity data to 100 percent relative humidity. This is possibly due to water left in surface voids after the surface drying process, and probably includes macro-defects in the pore system that are larger than the typical range of the capillary system.

Table 1-1 Relative Humidity at 25°C for Selected Saturated Salt Solutions.

Saturated Salt Solution	Relative Humidity %
K_2SO_4	97
KNO_3	92
NaCl	75
$Mg(N0_3)_2 \cdot 6(H_2O)$	53
$CaCl_2 \cdot 6(H_2O)$	31

3. The moisture content at 31 percent relative humidity is always below the best-fit straight line portion of the data at higher humidities. While this relative humidity range is below the range of interest for freezing in concrete (and the range that would be considered a part of the capillary system), this data may be of interest in the investigation of concrete microstructure.

Two parameters are used to quantify the effects of water in the pore system: permeability and the freezable moisture. Because permeability applies only to a saturated material and concrete is seldom completely saturated, permeability was considered of secondary importance in quantifying the water pore system. Freezable moisture is defined as the amount of moisture in the capillary system of the concrete that would theoretically freeze at or above -18°C. It is determined as the difference between moisture contents taken at 85 and 100 percent relative humidities on the linear portion of the moisture content-humidity relationship shown in figure 1-1. This specifically excludes the moisture characterized as residing in macrodefects in point 2 above. While the selection of -18°C as the reference temperature for determining theoretical freezable moisture is based only upon the minimum temperature reached during rapid freezing and thawing (AASHTO T 161), the linear nature of the moisture content-humidity relationship found for the concretes tested suggests that selection of an alternate freezing temperature would simply apply a scaling factor to all freezable moisture results reported in this work.

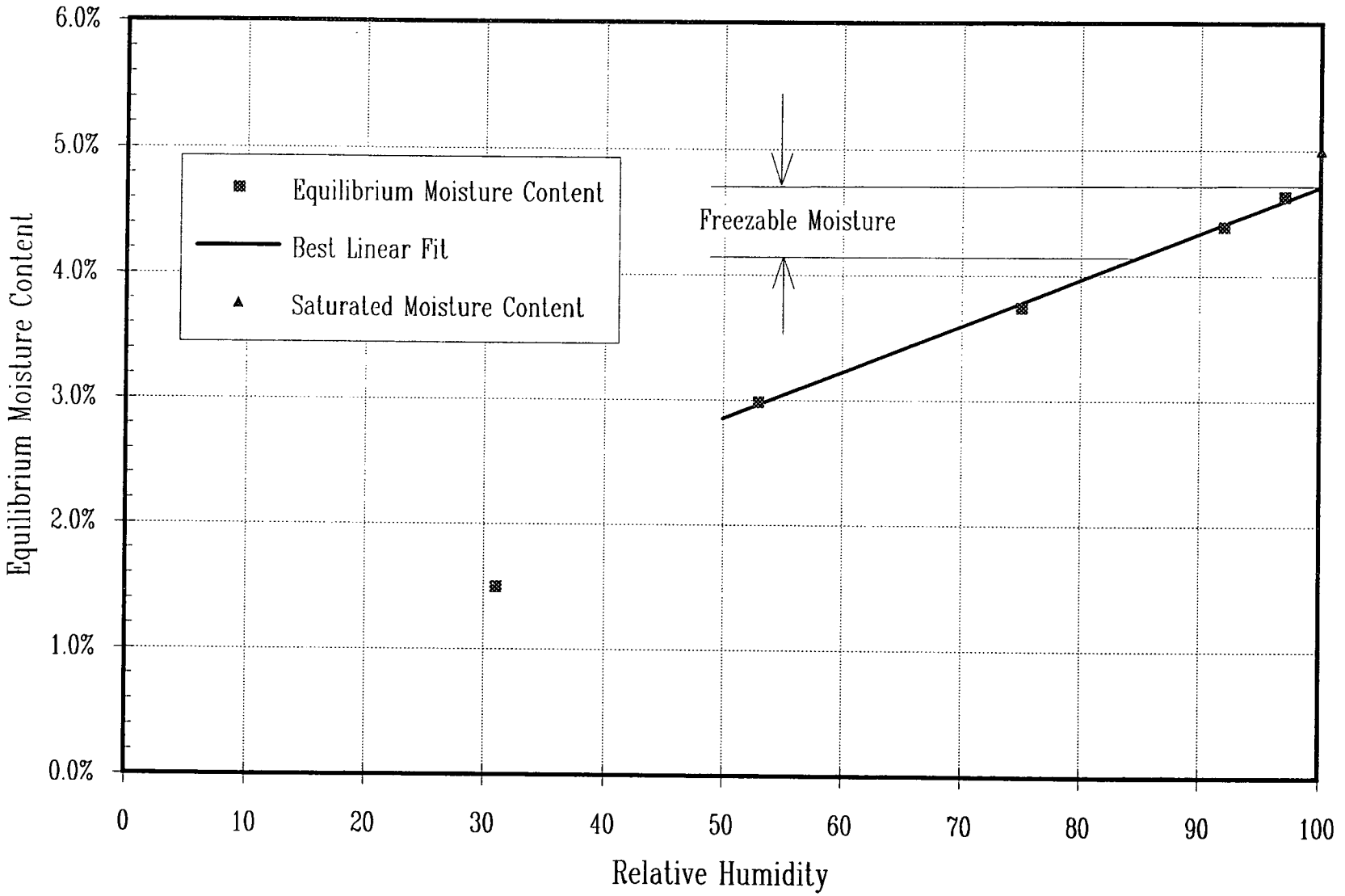

Figure 1-1 Moisture Content versus Equilibrium Relative Humidity.

2.5 Freezing and Thawing Test Procedure

There are a variety of testing procedures available to determine the resistance of concrete to freezing and thawing. The most commonly used procedures in the United States are AASHTO T 161 (ASTM C 666), "Resistance of Concrete to Rapid Freezing and Thawing", and ASTM C 672, "Scaling Resistance of Concrete Surfaces Exposed to Deicing Chemicals". The latter procedure uses a qualitative evaluation of the amount of scaling produced. Results from this procedure would not be suitable for the statistical analysis used to evaluate the influence of the various mix parameters. Efforts to develop a quantitative scaling test were under way in Europe[7] concurrent with the testing summarized in this report. These efforts had not culminated in an acceptable procedure in time for the procedure to be considered in this work.

AASHTO T 161 is the most commonly used laboratory method for the evaluation of the resistance of concrete to freezing and thawing in the United States. Most highway agencies in freezing climates have access to equipment capable of performing this test. Despite (or perhaps because of) the popularity and availability of equipment for AASHTO T 161, considerable controversy exists over the appropriateness of using it to predict field durability and over limitations of the variations of the procedure. The first issue is addressed in Part III of this report.

As for the second issue, AASHTO T 161 describes two primary variations for achieving the specified freezing and thawing: Procedure A, Rapid Freezing and Thawing in Water; and Procedure B, Rapid Freezing in Air and Thawing in Water. Testing by Procedure A generally uses a container of some type that allows the specimen to be surrounded by "not less than 1/32 in. (1 mm) nor more than 1/8 in. (3 mm) of water at all times." Appropriate cautions are given concerning problems associated with rigid containers and the ice pressure that can build up between the container wall and the specimen. In extreme cases, this ice pressure can actually damage the specimens. In any case, the use of a container must result in some amount of pressure on the specimen when the water surrounding the specimen freezes. If the specimen is not perfectly centered in the container, differential pressures will develop due to the differences in thickness of the ice surrounding the specimen during freezing. An additional problem with the containers is maintaining the proper thickness of surrounding water for specimens that exhibit scaling. Containers that start with a water thickness that is close to the maximum could exceed this thickness after some scaling of the specimens. Containers with a water thickness closer to the minimum limit tend to bind against the specimens due to accumulation of scaled material in the lower portions of the container. Removal of these bound specimens from their containers could result in physical damage to the specimens.

The primary objection to Procedure B is that the specimens are allowed to dry during freezing, which slows the accumulation of damage. Most refrigeration equipment cools air by circulating it past refrigerated coils and then over the test specimens. Moisture in the air condenses on the coils. This dried, cooled air removes moisture from the specimens in

addition to removing heat. Many agencies compensate for this delayed accumulation of damage from drying by testing to a minimum of 350 cycles of freezing and thawing rather than 300, which is common for testing by Procedure A.

These problems with the standard variations of AASHTO T 161 were addressed by the development of a new variation which attempts to eliminate the perceived shortcomings described above. This new variation is addressed below.

3.0 Innovative Test Procedures

3.1 Modification of AASHTO T 161 (ASTM C 666)

A modification of AASHTO T 161 (ASTM C 666), Procedure B has been developed that consists of wrapping the specimens with absorbent cloth to keep the specimens wet during freezing. This modification is hereafter called Procedure C, and is in response to the major criticisms described above. Briefly, these criticisms are that in Procedure B, the specimens are allowed to dry during freezing, and that in Procedure A, the physical confinement of specimens by rigid specimen holders could cause damage, along with the problem of maintaining the correct thickness of water surrounding the specimens. A summary of the modifications to the published procedure for AASHTO T 161 is given in appendix B.

Comparison testing of two marginal concrete mixes by Procedure A, Procedure B, the proposed Procedure C, and a variation of Procedure A in which a 3 percent by weight sodium chloride solution was used instead of water to surround the specimens, was conducted. The results are summarized below in table 1-2.

Table 1-2 Summary of Rapid Test Method Comparisons.

	Mix 1	Mix 2
Procedure	Average[a] DF	Average[a] DF
A	62	81
B[b]	64	90
C	37	66
Salt[c]	47	65

[a] Average of five specimens.
[b] Not within ASTM C 666, Procedure B temperature specifications.
[c] Three percent sodium chloride solution instead of water surrounding specimens in containers.

All of the testing took place simultaneously in a single test chamber. The procedures were conducted in the following manner:

1. The containers for Procedure A and the salt solution were plastic rather than metal as used by most investigators. This probably reduced the detrimental effects of unequal ice pressures often associated with the use of metal containers.

2. Procedure B was not within temperature specifications as the lack of any kind of covering permitted the specimen to cool below the specified 0°F±3°F.

3. Cooling rate was more uniform for Procedure C than for Procedure A. Procedure A showed a plateau in the 30-32°F range while the water surrounding the specimen froze, followed by a more rapid drop in temperature. The cloth wrap in Procedure C did not hold sufficient water to produce a pronounced plateau, but probably did inhibit heat transfer from the wrapped specimen during the entire freezing period.

Though original expectations were that the severity of Procedure C would be between that of Procedures A and B, the appearance is that the cloth wraps are slightly more severe than Procedure A when container restraint effects are reduced.

3.2 Modification of ASTM C 215

The relative dynamic modulus, as determined by resonance frequency measurements, is the most frequently used indicator for evaluating damage to concrete beams that are subjected to repeated cycles of freezing and thawing (AASHTO T 161). While sinusoidal excitation (ASTM C 215-85) has been the standard method for measuring resonance frequency, impulse excitation (ASTM C 215-91) has recently been approved as an alternate. With minimal changes in procedure from that specified in ASTM C 215, substantial improvements in precision can be achieved. Also, quality factor Q, the inverse of the damping coefficient, can be determined with no additional testing. A proposed test method, Fundamental Transverse Frequency and Quality Factor of Concrete Prism Specimens, is included as appendix C.

The improvements in precision are shown in table 1-3. The acceptable range for the fundamental transverse frequency of an undamaged concrete beam is reduced by more than an order of magnitude by the new procedure. While a similar comparison cannot be directly made for specimens with substantial deterioration due to freezing and thawing, the relative improvement in precision would be expected to be about the same.

Experience has shown that the variability of DF results from AASHTO T 161 is dependent upon the actual DF value. Both high and low DFs have low variabilities, while intermediate DFs can have rather high variability. Mixes with intermediate DF values were determined to be most significant in the freezing and thawing portion of this study as described in section 2. The influence of this improvement in measurement precision of the fundamental

transverse frequency is shown in table 1-4. This table presents the average standard deviation for groups of five specimens subjected to repeated cycles of freezing and thawing as in AASHTO T 161. The DF values for one set of specimens were determined by measurement of the fundamental transverse frequency determined by the forced vibration method in accordance with ASTM C 215. The DF values for the second set of specimens were determined by measurement of the fundamental transverse frequency using the procedure given in appendix C.

Table 1-3 Comparison of Precision between ASTM C 215 and the Proposed "Fundamental Transverse Frequency and Quality Factor of Concrete Prism Specimens"

Specimen Condition	Acceptable Range of Two Results Fundamental Transverse Frequency (%)[a]	
	ASTM C 215	New Procedure
Undamaged	2.8	0.11
Damaged[b]	—[c]	0.51

[a] *These numbers represent, respectively, the 1S% and D2S% limits as described in ASTM Practice C 670.*
[b] *Specimen was reduced by repeated cycles of freezing and thawing to approximately 60 percent relative dynamic modulus as defined in Test Method T 161.*
[c] *Not specifically given, though ASTM C 215 states both that "(the precision is) for concrete prisms as originally cast. They do not necessarily apply to concrete prisms after they have been subjected to freezing-and-thawing tests," and that "... (the coefficient of variation has) been found to be relatively constant ... for a range of specimen sizes and age or condition of the concrete, within limits."*

Linear changes in damping with early cycles of freezing and thawing were found before significant decreases in resonance frequency could be identified. Comparisons of predicted and actual durability factors show agreement within published testing errors for most of the mixes tested. This work indicates that the durability factor (AASHTO T 161) can be accurately predicted with damping measurements before the actual failure of the concrete beams because of repeated cycles of freezing and thawing. (See appendix D.)

Table 1-4 Comparison of DF Variability for Two Methods of Measuring Fundamental Transverse Frequency.

DF Range	Standard Deviation (ASTM C 215)	Standard Deviation (Appendix C)
20 to 30	4.2	3.0
30 to 50	9.8	4.5
50 to 70	8.0	5.4

4.0 Results

Tables of the results of the laboratory testing program are given in appendix E. This appendix includes mix design information, DF results, linear traverse results, and permeability and freezable moisture results. Portions of the testing were not completed at the time of the preparation of this report, most notably the freezable moisture values. These will be made available as the testing is completed.

5.0 Acceptable Variability and Maximum Expected Errors in Results

Prior to analysis of any results, the variability and maximum expected errors should be determined. These are discussed below for the various results obtained in this study.

5.1 Variability of Durability Factor Results

Section 3 of this report stated that the proposed Procedure C of AASHTO T 161 addressed perceived problems with the existing Procedures A and B. Procedure C also reduces the variability in DF results in all but the highest and lowest DF ranges. Initial testing of cells in Design Matrix A used nine or more specimens per cell to help estimate the number of specimens per cell that would be necessary to provide reasonable confidence in the results. Subsequent testing used a sample size of five specimens. The acceptable variability in the average DF determined for a group of five specimens is shown in figure 1-2. The variability shown is the "difference two-sigma limit (D2S)" as defined in ASTM Practice E 177 and calculated as prescribed in ASTM Practice C 670. These values approximate the range within which 95 percent of all means of five specimens from the same batch would fall. Variabilities are shown for Procedures A and B in addition to the proposed Procedure C. This figure clearly shows that Procedure C substantially reduces the variability, especially in the intermediate DF ranges discussed in section 2.

5.2 Maximum Errors in Linear Traverse Results

When this investigation began, ASTM C 457 (1982 version) did not provide any information on the precision of air-void parameters of hardened concrete determined by the linear traverse method. The guidelines for minimum area of finished surface (71 cm^2) and minimum length of traverse (2.286 m) for a nominal maximum aggregate size of 19 mm were observed. ASTM has since updated C 457 (1990 version) which includes some information on precision of linear traverse measurements. Pleau and Pigeon[8] published procedures for calculating the expected precision of the various hardened air-void parameters given information on traverse length, area, number of voids intercepted, etc.[8] These latter procedures were used for the maximum error values shown. All are for the 95 percent confidence range, described as (D2S) in ASTM Practice C 670.

Air Content of Hardened Concrete - The maximum expected error expressed as a percent of the air content value is shown in figure 1-3. This error is rather high, in part due to the low air contents emphasized in this study, and in part due to the influence that large voids have on the air content determination.

Spacing Factor - Figure 1-4 shows the maximum expected error in the $\bar{L}$ values presented in appendix E. The maximum error is expressed as a percentage of the measured value.

Specific Surface - The maximum expected error in α is shown in figure 1-5. This error is also given as a percent of the measured value.

Philleo Factor - The maximum expected error in $\bar{P}$ was not calculated. Because this value was determined from a curve-fit of the air-void chord length data, the maximum expected error should be substantially less than that shown for $\bar{L}$.

Attiogbe's Mean Void Spacing[4] - The maximum expected error in $\bar{S}$ was not calculated, but the error is probably significantly greater than that shown for $\bar{L}$. This is due to the respective methods of calculating $\bar{L}$ and $\bar{S}$. $\bar{L}$ is proportional to p/A, where p is the volume fraction paste content and A is the volume fraction air content of the concrete, determined as described in ASTM C 457. $\bar{S}$, however, is proportional to p^2/A. The error in p determined by the linear traverse method for the mixes included in this study typically ranged from 15 to 20 percent (as determined by the procedures set forth by Pleau and Pigeon[8]). This additional error would be expected to increase the variability for $\bar{S}$ values.

The possible errors in the various air-void parameters determined by linear traverse analysis are greater than originally anticipated, and may perhaps be too large to permit acceptable modelling of the requirements for frost-resistant concrete. Portions of specimens remaining after rapid freezing and thawing for all of the batches tested have been retained by the research team, and slices of these specimen portions are being prepared for inclusion in the Strategic Highway Research Program (SHRP) Materials Reference Library. This reference library is being maintained under supervision of the Federal Highway Administration (FHWA). Requests for access to these specimens should be directed to:

Federal Highway Administration
HNR-20
6300 Georgetown Pike
McLean, VA 22101

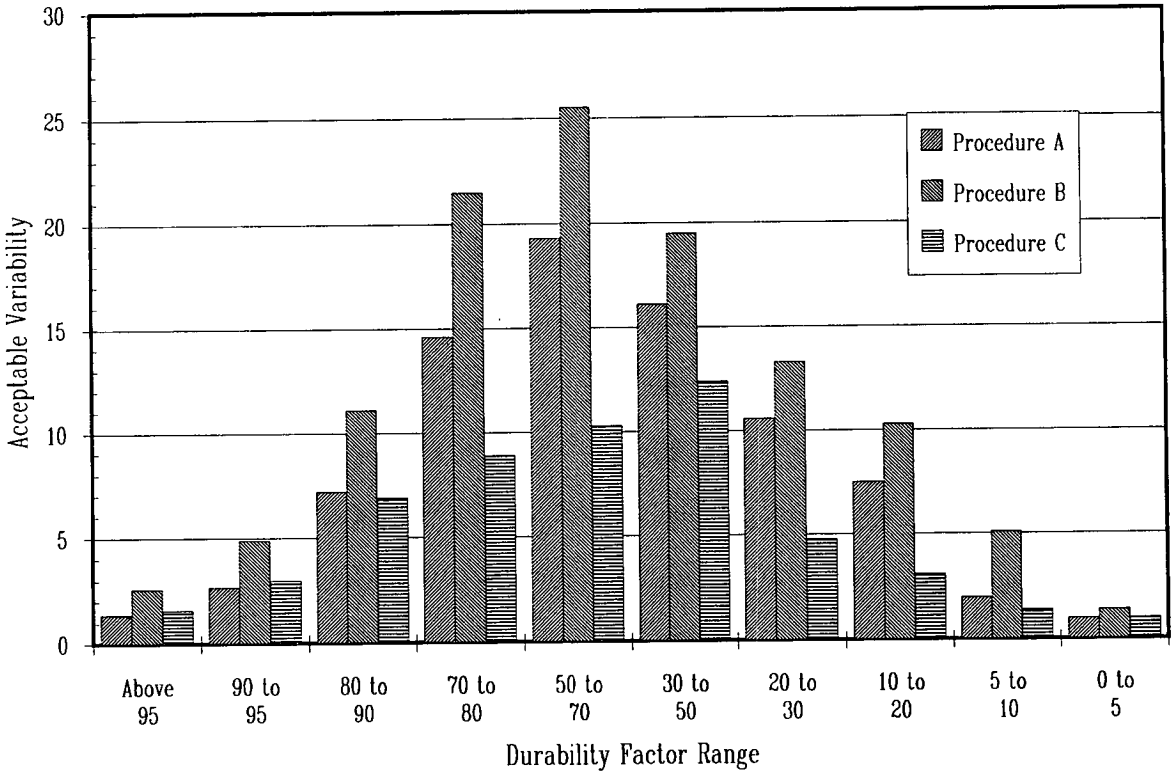

Figure 1-2 Variability of AASHTO T161 Procedures.

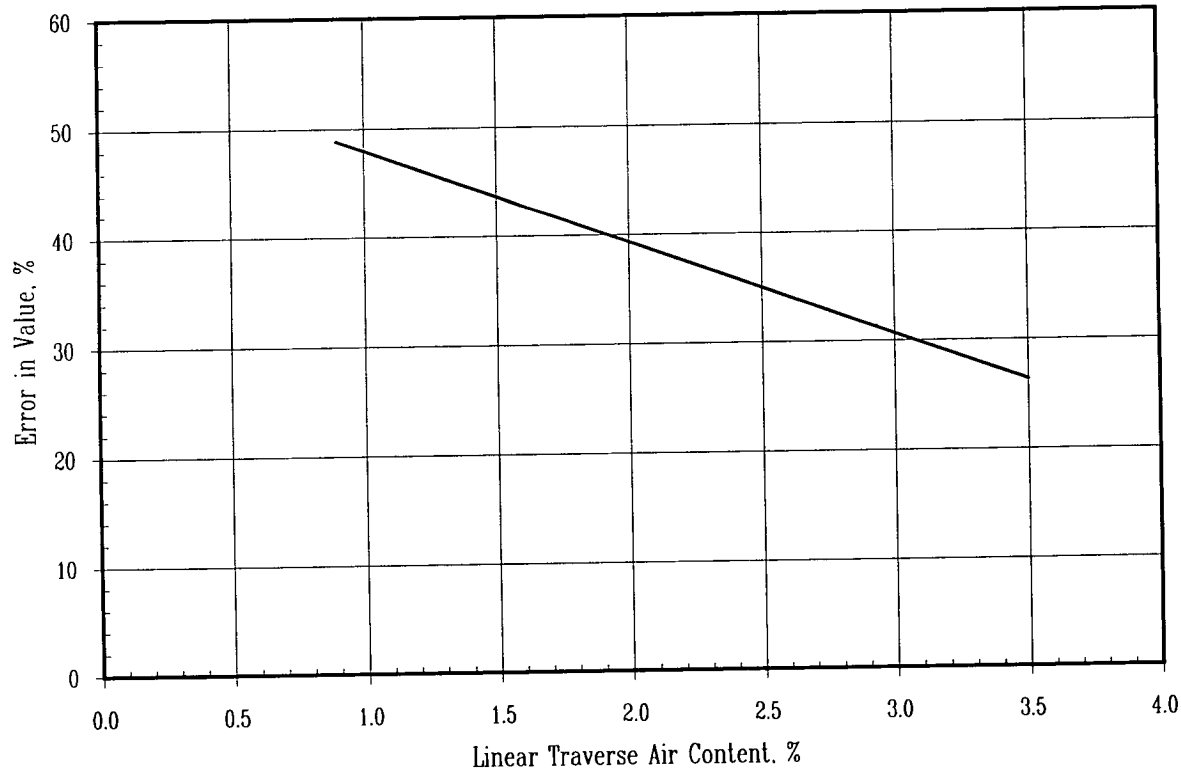

Figure 1-3 Maximum Error of Linear Traverse Air Content (after Pleau and Pigeon, 1992).[8]

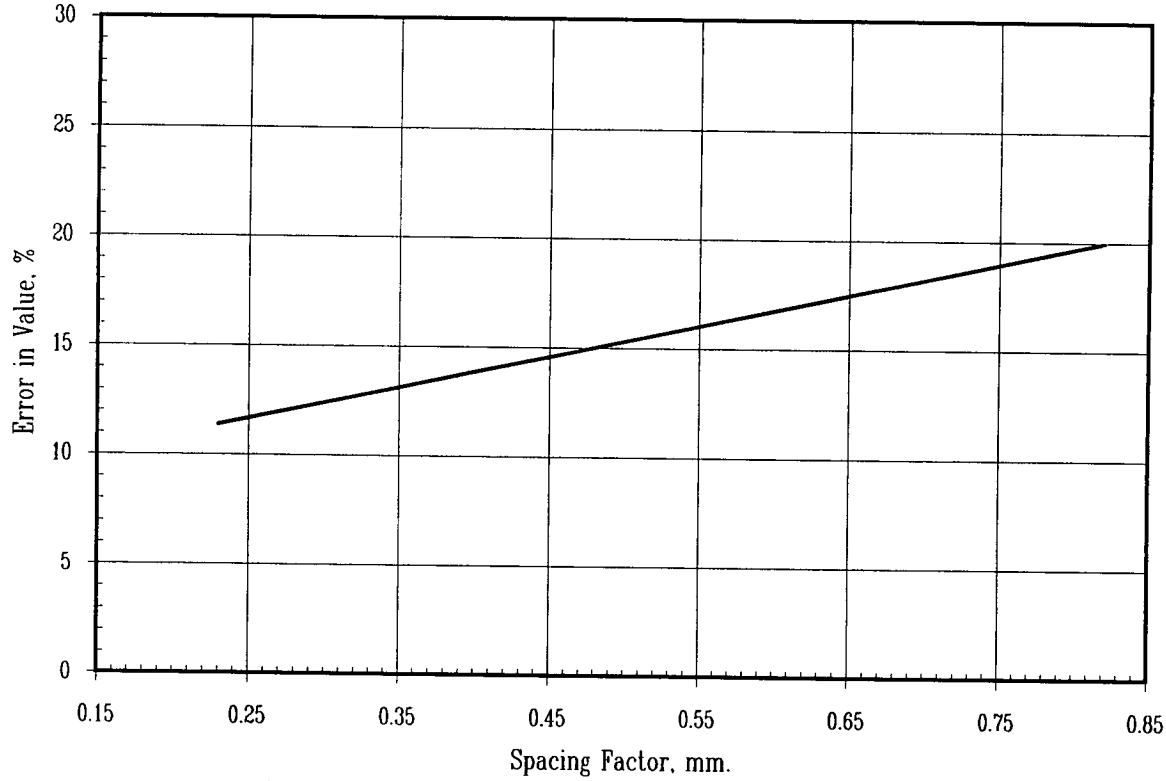

Figure 1-4 Maximum Error of Spacing Factor (after Pleau and Pigeon, 1992).[8]

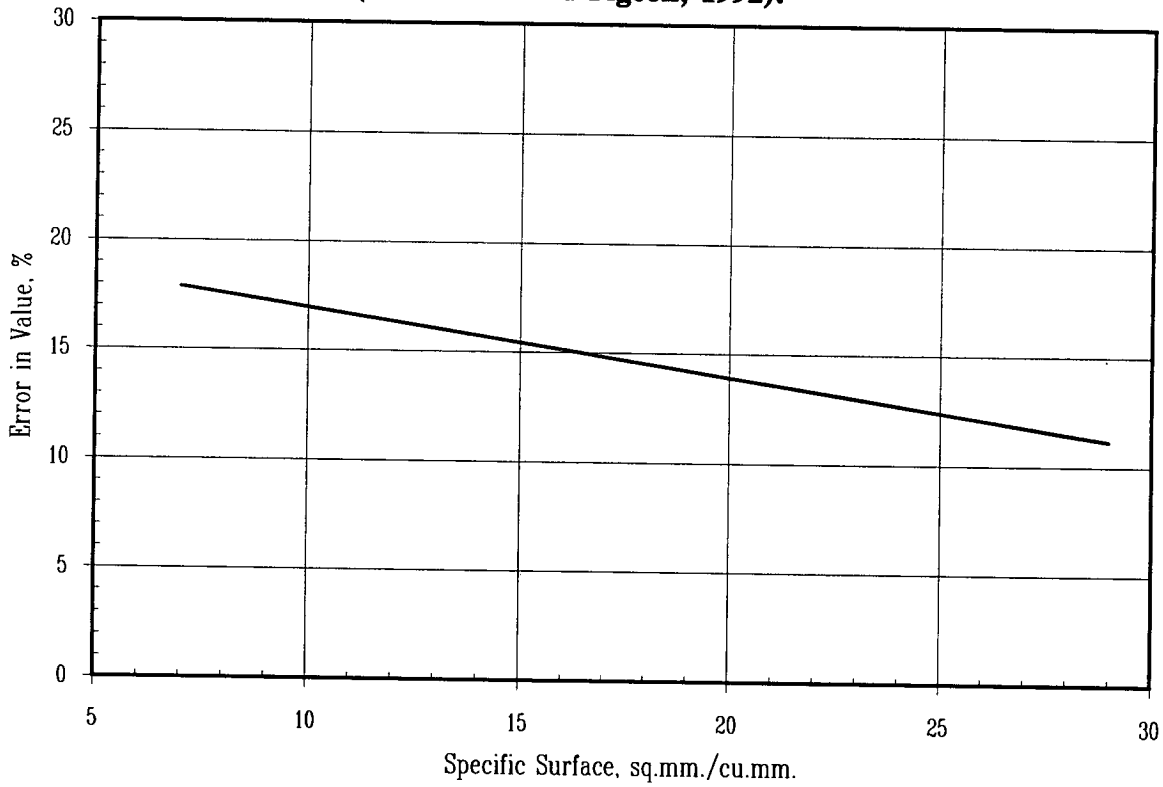

Figure 1-5 Maximum Error of Specific Surface (after Pleau and Pigeon, 1992).[8]

5.3 Reliability of Freezable Moisture Results

The reliability of the freezable moisture results is not known. ASTM C 642, "Specific Gravity, Absorption, and Voids in Hardened Concrete," suggests that "... the sample shall consist of several individual portions of concrete ... each portion shall not be less than ... approximately 800 g." No precision information is given. ASTM C 127, "Specific Gravity and Absorption of Coarse Aggregate," specifies a minimum sample size of 3 kg for an aggregate that has a nominal size of 19 mm. An acceptable range of two percent-absorption results (D2S, ASTM Practice C 670) is given as 0.25 for aggregates with absorptions of less than 2 percent. The sample size for the equilibrium moisture content determinations was approximately 3 kg total for each humidity. The freezable moisture calculation involves taking the difference between two moisture contents, but these moisture contents are from a linear fit of multiple moisture content-humidity measurements. Freezable moisture determinations for multiple sets of samples from the same concrete mix have not been made. Typical standard deviations for freezable moisture measurements from separate mixes but similar mix designs were 0.06 or less. This would suggest a maximum expected difference between freezable moisture determinations of similar mixes to be about 0.17 (D2S, ASTM Practice C 670). This estimate is preliminary, and should probably decrease as additional freezable moisture results are obtained for error analysis.

6.0 Frost-Resistance Model

No frost-resistance modelling has been attempted at this time. As of the preparation of this report, sufficient freezable moisture data has not been collected to adequately characterize the amount of freezable moisture in a given type of concrete mix (i.e., for a given w/c or w/(c+p), or a mix containing a high-range water reducer, etc.). Testing is continuing, and the additional data will be made public as it becomes available.

7.0 Summary and Recommendations for Part I

The effects of the air-void and water-pore systems on the resistance of concrete to repeated cycles of freezing and thawing were examined. To facilitate this work, one new test procedure, and a modification of an existing test procedure were developed. The purpose of developing these procedures was to improve the precision of rapid freezing and thawing testing. These new test procedures were used in the development of a database of air-void, water-pore, and DF information for a variety of concretes made with a range of air-entraining admixtures, normal and high-range water-reducing admixtures, pozzolan types and contents, and other mix and curing parameters. The test procedures and database are summarized on the next page.

7.1 Test Procedures

The new test procedure, "Fundamental Transverse Frequency and Quality Factor of Concrete Prism Specimens," describes the use of an instrumented hammer to produce vibrations in a concrete prism, and the measurement of the fundamental transverse frequency and quality factor for the vibration characteristics of the beam. Modern electronics technology is used for the analysis of the vibration characteristics. The resulting fundamental transverse frequency is much more precise—by an order of magnitude—than measurements made in accordance with the current procedure, ASTM C 215. In addition, the quality factor Q is also measured. This value appears to be an indicator of microcracking, and can be used to predict the accumulation of damage as freezing and thawing progresses.

The modified test procedure, "Procedure C, Rapid Freezing in Air (moist cloth wrapped) and Thawing in Water," was developed as a modification to AASHTO T 161, "Resistance of Concrete to Rapid Freezing and Thawing". The purpose of this modification was to address perceived shortcomings to the current procedures. The modification consists of wrapping concrete specimens with cotton terry cloth in order to keep them moist during freezing in air. Containers (Procedure A) and drying during freezing (Procedure B) are both eliminated. Procedure C appears to be slightly more severe than either of the existing procedures, and is substantially more reproducible in the middle range of DF values. The Procedure C is easily adaptable to existing Procedure B cabinets, with only minor modifications.

7.2 Durability Data Base

The results presented as appendix E represent a considerable database of information pertinent to the resistance of concrete to freezing and thawing. In addition to mix design and DF information, the database includes results of linear traverse and water pore system testing described in this report. The database, by design, emphasizes mixes of marginal durability since these are of greatest interest in identifying the pertinent limits for producing durable concrete. Unfortunately, at the time of this writing, the water pore system testing was not complete. This testing is continuing and revised results summaries will be made public as data becomes available.

7.3 Recommendations

The following specific recommendations are based on the findings of the work described in this report:

1. Agencies with equipment for AASHTO T 161, Procedure B, should consider converting to Procedure C. This procedure has produced results that substantially reduce the variability of rapid freezing and thawing test results.

2. Agencies that soon will purchase AASHTO T 161 equipment with sufficient capacity (typically a capacity of minimum 40 specimens) for a Procedure B chamber should consider specifying a chamber modification (secondary sump below the main chamber level) to allow testing by Procedure C.

3. Agencies that measure, or are considered measuring, fundamental transverse frequency in accordance with ASTM C 215 should consider adopting the "Fundamental Transverse Frequency and Quality Factor of Concrete Prism Specimens" described in appendix C.

4. Information in the database presented in appendix E should be used by agencies that are deciding upon criteria for frost-resistant concrete. This is especially relevant when changes in specifications are being contemplated because of inclusion of pozzolans and/or water reducing and high-range water reducing admixtures. While conclusions cannot be drawn from the database at this time, the information can be of considerable assistance in identifying trends and areas where additional information is needed.

5. When performing linear traverse on concrete suspected of having marginal frost resistance due to inadequacy of the air-void system, minimum specimen area and traverse length should be significantly greater than that suggested by ASTM C 457.

References

1. Pigeon, M., R. Gagne, and C. Foy, "Critical Air Void Spacing Factor for Low Water-Cement Ratio Concrete Made With and Without Silica Fume," *Cement and Concrete Research*, Vol. 17, No. 6, 1987, pp. 896-906.

2. Philleo, R. E., "Method for Analyzing Void Distribution in Air-Entrained Concrete," unpublished report, Portland Cement Association, May 1955.

3. Lord, G. W. and T. F. Willis, "Calculation of Air Bubble Size Distribution from Results of a Rosiwal Traverse of Aerated Concrete," *ASTM Bulletin*, October, 1951, pp. 220-225.

4. Attiogbe, E. K., "Mean Spacing of Air Voids in Hardened Concrete," *ACI Materials Journal*, Vol. 90, No. 2, 1993, pp. 174-181.

5. Ludirdja, D., R. L. Berger, and J. F. Young, "Simple Method for Measuring Water Permeability of Concrete," *ACI Materials Journal*, Vol. 86, No. 5, 1989, pp. 433-439.

6. Powers, T. C. and T. L. Brownyard, "Studies of the Physical Properties of Hardened Cement Paste, Part 8," *Journal of the American Concrete Institute*, Vol. 18, No. 8, 1947, pp. 933-969.

7. Setzer, M. J., Report of Meeting, Technical Committee TC 117, "Freeze-Thaw and Deicing Resistance of Concrete," RILEM, University of Essen, West Germany, May 17-18, 1990.

8. Pleau, R. and M. Pigeon, "Precision Statement for ASTM C 457 Practice for Microscopical Determination of Air-Void Content and Parameters of the Air-Void System in Hardened Concrete," *Cement, Concrete, and Aggregates*, Vol. 14, No. 2, 1992, pp. 118-126.

Appendix A
Design Matrices

Table A-1 Preliminary Tests for Statistical Calibration and Normal Concretes (Matrix A)

Water/Cement Ratio	Air Content		
	Low	Medium	High
0.52	(A09)	(A06)	(A03)
0.45	(A08)	(A05)	(A02)
0/40	(A07)	(A04)	(A01)

Cell numbers are shown in parentheses.
AEA1 used for all concrete mixtures.

Table A-2 Water Reducer and Air-Entraining Admixture Type (Matrix B)

Water Reducer	Air-Entraining Admixture Type					
	AEA1		AEA2		AEA3	
	0.40 w/c	0.45 w/c	0.40 w/c	0.45 w/c	0.40 w/c	0.45 w/c
None	(B01) A07	(B02) A08	(B03)	(B04)	(B05)	(B06)
WR	(B07)	(B08)	(B09)	(B10)	(B11)	(B12)
HRWR1	(B13)	(B14)	(B15)	(B16)	(B17)	(B18)
HRWR2	(B19)	(B20)	(B21)	(B22)	(B23)	(B24)

Cell numbers are shown in parentheses.

Table A-3 Cement and Aggregate Types, including SHRP-C-205 HES Mixes (Method C)

Aggregate	Water/cement ratio	Cement type		
		Type I	Type II	Type III
Crushed limestone	0.40	(C01) A07	(C02)	(C03)
	0.45	(C04) A08	(C05)	(C06)
	0.33 (C-205 HES mix)	(C07)	(C08)	(C09)
Gravel	0.40	(C10)	(C11)	(C12)
	0.45	(C13)	(C14)	(C15)

Cell numbers are shown in parentheses.

Table A-4 Pozzolanic Admixtures (Matrix D)

Pozzolan (by percent weight cement)		High-Range Water Reducer	Air-Entraining Admixture			
			AEA1		AEA2	
			w/(c + p)			
			0.40	0.45	0.40	0.45
15%	None	WR	(D01) B07	(D02) B08	(D03) B09	(D04) B10
		HRWR1	(D05) B13	(D06) B14	(D07) B15	(D08) B16
	Class F fly ash	WR	(D09)	(D10)	(D11)	(D12)
		HRWR1	(D13)	(D14)	(D15)	(D16)
	Class C fly ash	WR	(D17)	(D18)	(D19)	(D20)
		HRWR1	(D21)	(D22)	(D23)	(D24)
	Silica fume	HRWR1	(D25)	(D26)	(D27)	(D28)
40%	Ground blast furnace slag	WR	(D29)	(D30)	(D31)	(D32)
		None	(D33)	(D34)	(D35)	(D36)

Cell numbers are shown in parentheses.

Table A-5 Pozzolan Amount and Curing Period (Matrix E)

Pozzolan Type	Pozzolan Amount (% weight cement)	Cure Time (days)	w/(c + p)	
			0.40	0.45
None (WR only)	None	28	(E01) B07	(E02) B08
		56	(E03)	(E04)
Class F fly ash	15%	28	(E05)	(E06)
		56	(E07)	(E08)
	30%	28	(E09)	(E10)
		56	(E11)	(E12)
Class C fly ash	15%	28	(E13)	(E14)
		56	(E15)	(E16)
	30%	28	(E17)	(E18)
		56	(E19)	(E20)
Silica fume	8%	28	(E21)	(E22)
		56	(E23)	(E24)
	15%	28	(E25)	(E26)
		56	(E27)	(E28)
None (no WR)	None	56	(E29)	(E30)
		14	(E31)	(E32)
		28	(E33) A07	(E34) A08

Cell numbers are shown in parentheses.

Table A-6 List of Admixtures

AEA1	Daravair
AEA2	Microair
AEA3	Darex
WR	Plastocrete 150
HRWR1	Elkem Proprietary (used in silica fume mixture below)
HRWR2	Sikament FF
P1	Class F fly ash, Centralia
P2	Class C fly ash, Laramie River
P3	Silica fume, Elkem Emsac F-100T
P4	Ground granulated blast furnace slag

Appendix B
Proposed Modifications to AASHTO T 161
AASHTO Designation: TP17

Standard Method of Test for Resistance of Concrete to Rapid Freezing and Thawing

AASHTO DESIGNATION: TP17

1. Scope

1.1 This method covers the determination of the resistance of concrete specimens to rapidly repeated cycles of freezing and thawing in the laboratory by two different procedures: Procedure A, Rapid Freezing and Thawing in Water, and Procedure B, Rapid Freezing in Air and Thawing in Water, and Procedure C, Rapid Freezing in Air (moist cloth wrapped) and Thawing in Water. All three are intended for use in determining the effects of variations in the properties of concrete on the resistance of the concrete to the freezing and thawing cycles specified in the particular procedure. The procedures are not intended to provide a quantitative measure of the length of service that may be expected from a specific type of concrete.

1.2 The values stated in SI units are to be regarded as the standard.

1.3 All material in this test method not specifically designated as belonging to Procedure A, Procedure B, or Procedure C applies to any one of the procedures.

1.4 This standard does not purport to address the safety problems associated with its use. It is the responsibility of the user of this standard to establish appropriate safety and health practices and determine the applicability of regulatory limitations prior to use.

2. Reference Documents

2.1 *AASHTO Standards*:

T126	Making and Curing Concrete Test Specimens in the Laboratory
T157	Air-Entraining Admixtures for Concrete
T160	Length Change of Hardened Hydraulic Cement Mortar and Concrete
M194	Chemical Admixtures for Concrete
M210	Apparatus for Use in Measurement of Length Change of Hardened Cement Paste, Mortar, and Concrete

2.2 *ASTM Standards*:

C215	Test for Fundamental Transverse, Longitudinal, and Torsional Frequencies of Concrete Specimens
C341	Length Change of Drilled of Sawed Specimens of Hydraulic Cement Mortar Concrete
C295	Petrographic Examination of Aggregates for Concrete
C670	Preparing Precision and Bias Statements for Test Methods for Construction Materials
C823	Examination and Sampling of Hardened Concrete in Constructions

3. Significance and Use

3.1 As noted in the scope, the two procedures described in this method are intended to determine the effects of variations in both the properties and conditioning of concrete in the resistance to freezing and thawing cycles specified in the particular procedure. Specific applications include specified use in M194, T157, and ranking of coarse aggregates as to their effect on concrete freeze-thaw durability, especially where soundness of the aggregate is questionable.

3.2 It is assumed that the procedures will have no significantly damaging effects on frost-resistant concrete which may be defined as (1) any concrete not critically saturated with water (that is, not sufficiently saturated to be damaged by freezing) and (2) concrete made with frost-resistant aggregates and having an adequate air-void system that has achieved appropriate maturity and thus will prevent critical saturation by water under common conditions.

3.3 If, as a result of performance tests as described in this method, concrete is found to be relatively unaffected, it can be assumed that it was either not critically saturated, or was made with "sound" aggregates, a proper air-void system, and allowed to mature properly.

3.4 No relationship has been established between the resistance to cycles of freezing and thawing of specimens cut from hardened concrete and specimens prepared in the laboratory.

4. Apparatus

4.1 *Freezing and Thawing Apparatus*:

4.1.1 The freezing and thawing apparatus shall consist of a suitable chamber or chambers in which the specimens may be subjected to the specified freezing and thawing cycle, together with the necessary refrigerating and heating equipment and controls to produce continuously and automatically, reproducible cycles within the specified temperature requirements. In the event that the equipment does not operate automatically, provision shall be made for either its continuous manual operation on a 24-h a day basis or for the storage of all specimens in a frozen condition when the equipment is not in operation.

4.1.2 The apparatus shall be so arranged that, except for necessary supports, each specimen is (1) for Procedure A, completely surrounded by not less than 1 mm (1/32 in.) nor more than 3 mm (1/8 in.) of water at all times while it is being subjected to freezing and thawing cycles, or (2) for Procedure B or C, completely surrounded by air during the freezing phase. Specimens for Procedure C should be wrapped with cotton terrycloth to keep the specimens wet during freezing. Rigid containers, which have the potential to damage specimens, are not permitted. Length change specimens in vertical containers shall be supported in a manner to avoid damage to the gage studs.

> Note 1 -- Freezing and Thawing apparatus used for Procedure C, having above-ground sumps, may need modification to allow excess water drainage from the cloth wraps to drain out of the chamber. A miniature sump (approximately 20 to 40-L (5 to 10-gallon) capacity) added to the drain line between the chamber and the drain pump, below the level of the bottom of the chamber, should be sufficient.

> Note 2 -- Experience has indicated that ice or water pressure, during freezing tests, particularly in equipment that uses air rather than a liquid as the heat transfer medium, can cause excessive damage to rigid metal containers, and possibly to the specimens therein. Results of tests during which bulging or other distortion of containers occurs should be interpreted with caution.

Note 3 -- Experience indicates that cloth wraps which cover all sides and ends of specimens produce the same durability factor results as wraps that cover only the sides of the specimens. An advantage of wraps that cover both sides and ends is that material which falls off of specimens during freezing is retained in the cloth wrap, decreasing the frequency that the bottom of the apparatus chamber must be cleaned.

4.1.3 The temperature of the heat-exchanging medium shall be uniform within 3.3°C (6°F) throughout the specimen cabinet when measured at any given time, at any point on the surface of any specimen container for Procedure A or on the surface of any specimen for Procedures B or C, except during the transition between freezing and thawing and vice versa.

4.1.3.1 Support each specimen at the bottom of its container in such a way that the temperature of the heat-exchanging medium will not be transmitted directly through the bottom of the container to the full area of the bottom of the specimen, thereby subjecting it to conditions substantially different from the remainder of the specimen.

Note 4 -- A flat spiral of 3 mm (1/8 in.) wire placed in the bottom of the container has been found adequate for supporting specimens.

4.1.4 For Procedures B or C, it is not contemplated that the specimens will be kept in containers. The supports on which the specimens rest shall be such that they are not in contact with the full area of the supported side or end of the specimen, thereby subjecting this area to conditions substantially different from those imposed on the remainder of the specimen.

Note 5 -- The use of the relatively open gratings, metal rods, or the edges of metal angles has been found adequate for supporting specimens, provided the heat-exchanging medium can circulate in the direction of the long axis of the rods or angles.

4.2 *Temperature-Measuring Equipment*, consisting of thermometers, resistance thermometers, or thermocouples, capable of measuring the temperature at various points within the specimen chamber and at the centers of control specimens to within 1.1°C (2°F)

4.3 *Dynamic Testing Apparatus* conforming to the requirements of ASTM C215.

4.4 *Optional Length Change Test Length, Change Comparator*, conforming to the requirements of M 210. When specimens are longer than the nominal 286 mm (11 1/4 in.) length provided for in M 210 are used for freeze-thaw tests, use an appropriate length reference bar, which otherwise meets the M210 requirements. Dial gage micrometers for use on these longer length change comparators shall meet the gradation interval and accuracy requirements for M210 for either the millimeter or inch calibrations requirements. Prior to the start of measurements on any specimens, fix the comparator at an appropriate length to accommodate all of the specimens to be monitored for length change.

4.5 *Scales* with a capacity approximately 50 percent greater than the weight of the specimens and accurate to at least 4.5 g (0.01 lb) within the range of ± 10 percent of the specimen weight will be satisfactory.

4.6 *Tempering Tank*, with suitable provisions for maintaining the temperature of the test specimen in water, such that when removed from the tank and tested for fundamental transverse frequency and length change, the specimens will be maintained within -1.1°C and +2.2° (-2°F and + 4°F) of the target thaw temperature for specimens in the actual freezing and thawing cycle and equipment being used. The use of the specimen chamber in the freezing and thawing apparatus by stopping the apparatus at the end of the thawing cycle and holding the specimens in it shall be considered as meeting this requirements, provided the specimens are

the thawing cycle and holding the specimens in it shall be considered as meeting this requirements, provided the specimens are tested for fundamental transverse frequency within the above temperature range. It is required that the same target specimen thaw temperature be used throughout the testing of an individual specimen since a change in specimen temperature at the time of length measurement can affect the length of the specimen significantly.

5. Freezing and Thawing Cycle

5.1 Base conformity with the requirements for the freezing and thawing cycle on temperature measurements of control specimens of similar concrete to the specimens under test in which suitable temperature-measuring devices have been imbedded. Change the position of these control specimens frequently in such a way as to indicate the extremes of temperature variation at different locations in the specimen cabinet.

5.2 The nominal freezing and thawing cycle for both procedures of this method shall consist of alternately lowering the temperature of the specimens from 4.4 to -17.8°C (40 to 0°F) and raising it from -17.8 to 4.4°C (0 to 40°F) in not less than 2 nor more than 4 h. for Procedure A, not less than 25 percent of the time shall be used for thawing, and for Procedures B or C, not less than 20 percent of the time shall be used for thawing (Note 6). At the end of the cooling period the temperature at the centers of the specimens shall be -17.8 ± 1.7°C (0 ± 3°F), and at the end of the heating period the temperature shall be 4.4 ± 1.7°C (40 ± 3°F) with no specimen at any time reaching a temperature lower than -19.4°C (-3°F) nor higher than 6.1°C (43°F). The time required for the temperature at the center of any single specimen to be reduced from 2.8 to -16.1°C (37 to 3°F) shall be no less than one-half of the length of the cooling period, and the time required for the temperature at the center of any single specimen to be raised from -16.1 to 2.8°C (3 to 37°F) shall not be less than one-half of the length of the heating period. For specimens to be compared with each other, the time required to change the temperature at the centers of any specimens from 1.7 to -12.2°C (35 to 10°F) shall not differ by more than one-third of the length of the heating period from the time required for any specimen.

> Note 6 -- In most cases, uniform temperature and time conditions can be controlled most conveniently by maintaining a capacity load of specimens in the equipment at all times. In the event that a capacity load of test specimens is not available, dummy specimens can be used to fill empty spaces. This procedure also assists greatly in maintaining uniform fluid level conditions in the specimen and solution tanks. The testing of concrete specimens composed of widely varying materials or with widely varying thermal properties, in the same equipment at the same time, may not permit adherence to the time-temperature requirements for all specimens. It is advisable that such specimens be tested at different times and that appropriate adjustments be made to the equipment.

5.3 The difference between the temperature at the center of a specimen and the temperature at its surface shall at no time exceed 27.8°C (50°F).

5.4 The period of transition between the freezing and thawing phases of the cycle shall not exceed 10 minutes, except when specimens are being tested in accordance with 8.2.

6. Sampling

6.1 Constituent materials for concrete specimens made in the laboratory shall be sampled using applicable standard methods.

6.2 Samples cut from hardened concrete are to be obtained in accordance with ASTM Practice C823.

7. Test Specimens

7.1 The specimens for use in this test shall be prisms made and cured in accordance with the applicable requirements of T126 and M210.

7.2 Specimens used shall not be less than 76 mm (3 in.) nor more than 127 mm (5 in.) in width, depth, or diameter, and not less than 279 mm (11 in.) nor more than 406 mm (16 in.) in length.

7.3 Test specimens may also be cores or prisms cut from hardened concrete. If so, the specimens should not be allowed to dry to a moisture condition below that of the structure from which taken. This may be accomplished by wrapping in plastic or by other suitable means. The specimens so obtained shall be furnished with gage studs in accordance with ASTM C341.

7.4 For this test the specimens shall be sorted in saturated lime water from the time of their removal from the holds until the time freezing and thawing tests are started. All specimens to be compared with each other initially shall be of the same nominal dimensions.

8. Procedure

8.1 Immediately after the specified curing period (Note 7), bring the specimen to a temperature within −3.1°C and +2.2°C (−2°F and +4°F) of the target that temperature that will be used in the freeze-thaw cycle and test for fundamental transverse frequency, determine the mass, determine the average length and cross-section dimensions of the concrete specimen within the tolerance required in ASTM C215, and determine the initial length comparator reading (optional) for the specimen with the length change comparator. Protect the specimens against loss of moisture between the time of removal from curing and the start of the freezing and thawing cycles.

> Note 7 -- Unless some other age is specified, the specimens should be removed from curing and freezing and thawing tests started when the specimens are 14 days old.

8.2 Start freezing and thawing tests by placing the specimens in the thawing water at the beginning of the thawing phase of the cycle. Remove the specimens from the apparatus, in a thawed condition, at intervals not exceeding 36 cycles of exposure to the freezing and thawing cycles, test for fundamental transverse frequency and measure length change (optional) with the specimens within the temperature range specified for the tempering tank in 4.6, determine the mass of each specimen, and return them to the apparatus. To ensure that the specimens are completely thawed and at the specified temperature, place them in the tempering tank or hold them at the end of the thaw cycle in the freezing and thawing apparatus for a sufficient time for this condition to be attained throughout each specimen to be tested. Protect the specimens against loss of moisture while out of the apparatus and turn them end-for-end when returned. For Procedure A, rinse out the container and add clean water. Return the specimens either to random positions in the apparatus or to positions according to some predetermined rotation scheme that will ensure that each specimen that continues under test for any length of time is subjected to conditions in all parts of the freezing apparatus. Continue each specimen in the test until it has been subjected to 300 cycles or until its relative dynamic modulus of elasticity reaches 60 percent of the initial modulus, whichever occurs first, unless other limits are specified (Note 8). For the optional length change test, 0.10 percent expansion may be used as the end of test. Whenever a specimen is removed because of failure, replace it for the remainder of the test by a dummy specimen. Each time a specimen is tested for fundamental frequency (Note 9) and length change, make a note of its visual appearance and make special comment on any defects that develop. (Note 10) When it is anticipated that specimens may deteriorate rapidly they should be tested for fundamental transverse frequency and length change (optional) at intervals not exceeding 10 cycles when initially subjected to freezing and thawing.

Note 8 -- It is not recommended that specimens be continued in the test after their relative dynamic modulus of elasticity has fallen below 50 percent.

Note 9 -- It is recommended that the fundamental longitudinal frequency be determined initially and as a check whenever a question exists concerning the accuracy of determination of fundamental transverse frequency, and that the fundamental torsional frequency be determined initially and periodically as a check on the value of Poisson's ratio.

Note 10 -- In some applications such as airfield pavements and other slabs, popouts may be defects that are a concern. A popout is characterized by the breaking away of a small portion of the concrete surface due to internal pressure thereby leaving a shallow and typically conical spall in the surface of the concrete through the aggregate particle. Popouts may be observed as defects in the test specimens. Where popouts are a concern, the number and general description should be reported as a special comment. The aggregates causing the popout may be identified by petrographic examination as in ASTM C295.

8.3 When the sequence of freezing and thawing cycles must be interrupted, store the specimens in a frozen condition.

Note 11 -- If, due to equipment breakdown or for other reasons, it becomes necessary to interrupt the cycles for a protracted period, store the specimens in a frozen condition in such a way as to prevent loss of moisture. For Procedure A, maintain the specimens in the containers and surround them by ice, if possible. If it is not possible to store the specimens in their containers, wrap and seal them, in as wet a condition as possible, in moisture-proof materials to prevent dehydration and store in a refrigerator or cold room maintained at -17.8 ± 1.7°C (0 ± 3°F). Follow the latter procedure when Procedure B is being used. In general, for specimens to remain in a thawed condition for more than two cycles is undesirable, but a longer period may be permissible if this occurs only once or twice during a complete test.

9. Calculations

9.1 Relative Dynamic Modulus of Elasticity - Calculate the numerical values of relative dynamic modulus of elasticity as follows:

$$P_c = (n_1^2/n^2) \times 100$$

where:

P_c = relative dynamic modulus of elasticity, after c cycles of freezing and thawing, percent,
n = fundamental transverse frequency at 0 cycles of freezing and thawing, and
n_1 = fundamental transverse frequency at c cycles of freezing and thawing.

Note 12 -- This calculation of relative dynamic modulus of elasticity is based on the assumption that the mass and dimensions of the specimen remain constant throughout the test. This assumption is not true in many cases due to disintegration of the specimen. However, if the test is to be used to make comparisons between the relative dynamic moduli of different specimens or of different concrete formulations, P_c as defined is adequate for the purpose.

9.2 Durability Factor - Calculate the durability as follows:

$$DF = PN/M$$

where:

DF = durability factor of the test specimen,
P = relative dynamic modulus or elasticity at N cycles, percent,
N = number of cycles at which P reaches the specified minimum value for discontinuing the test or the specified number of cycles at which the exposure is to be terminated, whichever is less, and,
M = specified number of cycles at which the exposure is to be terminated.

9.3 Length Change in Percent (Optional) - Calculate the length change as follows:

$$L_c = \frac{(l_2 - l_1)}{L_g} \times 100$$

where:

L_c = length change of the test specimen after c cycles of freezing and thawing, percent,
l_1 = length comparator reading at 0 cycles,
l_2 = length comparator reading after c cycles, and
L_g = the effective gage length between the innermost ends of the gage studs as shown in the mold diagram in M210.

10. Report

10.1 Report the following data such as are pertinent to the variable or combination of variables studied in the test:

10.2 *Properties of Concrete Mixture:*

10.2.1 Type and proportions of cement, fine aggregate, and coarse aggregate, including maximum size and grading (or designated grading indices), and ratio of net water content to cement.

10.2.2 Kind and proportion of any addition or admixture used.

10.2.3 Air content of fresh concrete.

10.2.4 Unit weight of fresh concrete.

10.2.5 Consistency of fresh concrete.

10.2.6 Air content of the hardened concrete when available.

10.2.7 Indicate if the test specimens are cut from hardened concrete, and if so, state the size, shape, orientation of the specimens in the structure, and an other pertinent information available.

10.2.8 Curing Period.

10.3 *Mixing, Molding, and Curing Procedures* - Report any departures from the standard procedures for mixing, molding, and curing as prescribed in Section 7.

10.4 Procedure - Report which of the three procedures was used.

10.5 Characteristics of Test Specimens:

10.5.1 Dimensions of specimens at 0 cycles of freezing and thawing.

10.5.2 Mass of specimens at 0 cycles of freezing and thawing, and

10.5.3 Nominal gage length between embedded ends of gage studs, and

10.5.4 Any defects in each specimen present at 0 cycles of freezing and thawing.

10.6 Results:

10.6.1 Values for the durability factor of each specimen and for the average durability factor for each group of similar specimens, and the specified values for minimum relative dynamic modulus and maximum number of cycles (Note 13).

10.6.2 Values for he percent length change of each specimen and for the average percent length change for each group of similar specimens (Note 13).

10.6.3 Values of loss or gain of mass for each specimen and average values for each group of similar specimens, and

10.6.4 Any defects in each specimen which develop during testing, and the number of cycles at which such defects were noted.

> Note 13 -- It is recommended that the results of the test on each specimen, and the average of the results on each group of similar specimens, be plotted as curves showing the value of relative modulus of elasticity or percent length change against time expressed as the number of cycles of freezing and thawing.

11. Precision

11.1 Within-Laboratory Precision (Single Beams) - Criteria for judging the acceptability of durability factor results obtained by the three procedures in the same laboratory on concrete specimens made from the same batch of concrete or from two batches made with the same materials are given in Table 1. Precision data for length change (optional) are not available at this time.

> Note 14 -- The between-batch precision of durability factors has been found to be the same as the within-batch precision. Thus, the limits given in this precision statement apply to specimens from different batches made with the same materials and mix design and having the same air content as well as to specimens from the same batch.

> Note 15 -- The precision of this method for both procedures has been found to depend primarily on the average durability factor and not on the maximum N or minimum P specified for terminating these test nor on the size of the beams within limits. The data on which test precision statements are based cover maximum N's from 100 to 300 cycles, and minimum P's from 50 to 70 percent of E_o. The indexes of precision are thus valid at least over these ranges.

11.1.1 The different specimen sizes represented by the data include the following: 76 by 76 by 406 mm; 76 by 76 by 416 mm; 76 by 102 by 406 mm; 89 by 114 by 406 mm; 76 by 76 by 279 mm; 89 by 102 by 406 mm; and 102 by 76 by 406 mm. (3 by 3 by 16 in.; 3 x 3 by 16¼ in.; 3 by 4 by 16 in.; 3½ by 4½ by 16 in.; 3 by 3 by 11 in.; 3½ by 4 by 16 in.; and 4 by 3 by 16 in.) The first dimension given represents the direction in which the specimens were vibrated in the test for fundamental transverse frequency. The most commonly used size was 76 by 102 by 406 mm (3 by 4 by 16 in.).

11.2 Within-Laboratory Precision (Averages of Two or More Beams) - Specifications sometimes call for comparisons between averages of two or more beams. Tables 2, 3 and 4 give appropriate standard deviations and acceptable ranges for the three procedures for two averages of the number of test beams shown.

11.3 Multilaboratory Precisions - No data are available for evaluation of multilaboratory precision. It is believes that a multilaboratory statement of precision is not appropriate because of the limited possibility that two or more laboratories will be performing freezing and thawing tests on the same concrete.

12. Between Procedure Comparisons

12.1 Comparison of Two Procedures Run Concurrently in the Same Chamber - Limited data comparing results of specimens from the same batch, tested in accordance with Procedures A and C concurrently in the same freezing and thawing apparatus are shown in Table 5. Concurrent comparison of either Procedure A or Procedure C with Procedure B in the same freezing and thawing apparatus is not possible because the temperature conditions given in Section 5 cannot be simultaneously met for Procedure B and either of the other two procedures.

13. Keywords - accelerated testing; concrete-weathering tests; conditioning; freezing and thawing; resistance-frost.

TABLE 1 Within-Laboratory Durability Factor Precision for Single Beams

Range of Average Durability Factor	Procedure A		Procedure B		Procedure C	
	Standard Deviation[A]	Acceptable Range of Two Results[A]	Standard Deviation[A]	Acceptable Range of Two Results[A]	Standard Deviation[A]	Acceptable Range of Two Results[A]
0 to 5	0.8	2.2	1.1	3.0	0.7	2.0
5 to 10	1.5	4.4	4.0	11.4	1.0	2.8
10 to 20	5.9	16.7	8.1	22.9	2.2	6.2
20 to 30	8.4	23.6	10.5	29.8	3.4	9.6
30 to 50	12.7	35.9	15.4	43.5	8.8	24.9
50 to 70	15.3	43.2	20.1	56.9	7.3	20.7
70 to 80	11.6	32.7	17.1	48.3	6.3	12.8
80 to 90	5.7	16.0	8.8	24.9	4.9	13.9
90 to 95	2.1	6.0	3.9	11.0	2.1	5.9
Over 95	1.1	3.1	2.0	5.7	1.1	3.1

NOTE -- The values given in Columns 2, 4 and 6 are the standard deviations that have been found to be appropriate for Procedures A, B and C, respectively, for tests for which the average durability factor as in the corresponding range given in Column 1. The values given in Columns 3, 5 and 7 are the corresponding limits that should not be exceeded by the difference between the results of two single test beams.

[A] These numbers represent the (1S) and (D2S) limits as described in ASTM C 670

TABLE 2 Within-Laboratory Durability Factor Precision for Averages of Two or More Beams--Procedure A

Range of Average Durability Factor	Number of Beams Averaged									
	2		3		4		5		6	
	Standard Deviation[A]	Acceptable Range[A]	Standard Deviation[A]	Acceptable Range[A]	Standard Deviation[A]	Acceptable Range[A]	Standard Deviation[A]	Acceptable Range[A]	Standard Deviation[A]	Acceptable Range[A]
0 to 5	0.6	1.6	0.5	1.3	0.4	1.1	0.4	1.0	0.3	0.9
5 to 10	1.1	3.1	0.9	2.5	0.8	2.2	0.7	2.0	0.6	1.8
10 to 20	4.2	11.8	3.4	9.7	3.0	8.4	2.7	7.5	2.4	6.8
20 to 30	5.9	16.7	4.8	13.7	4.2	11.8	3.7	10.6	3.4	9.7
30 to 50	9.0	25.4	7.4	20.8	6.4	18.0	5.7	16.1	5.2	14.7
50 to 70	10.8	30.6	8.8	25.0	7.6	21.6	6.8	19.3	6.2	17.6
70 to 80	8.2	23.1	6.7	18.9	5.8	16.4	5.2	14.6	4.7	13.4
80 to 90	4.0	11.3	3.3	9.2	2.8	8.0	2.5	7.2	2.3	6.5
90 to 95	1.5	4.2	1.2	3.5	1.1	3.0	0.9	2.7	0.9	2.4
Over 95	0.8	2.2	0.6	1.8	0.5	1.5	0.5	1.4	0.4	1.3

[A] These numbers represent the (1S) and (D2S) limits as described in ASTM C 670

TABLE 3 Within-Laboratory Durability Factor Precision for Averages of Two or More Beams - Procedure B

Range of Average Durability Factor	Number of Beams Averaged									
	2		3		4		5		6	
	Standard Deviation[A]	Acceptable Range[A]	Standard Deviation[A]	Acceptable Range[A]	Standard Deviation[A]	Acceptable Range[A]	Standard Deviation[A]	Acceptable Range[A]	Standard Deviation[A]	Acceptable Range[A]
0 to 5	0.8	2.1	0.6	1.8	0.5	1.5	0.5	1.4	0.4	1.2
5 to 10	2.9	8.1	2.3	6.6	2.0	5.7	1.8	5.1	1.7	4.7
10 to 20	5.7	16.2	4.7	13.2	4.1	11.5	3.6	10.3	3.3	7.4
20 to 30	7.4	21.0	6.1	17.2	5.3	14.9	4.7	13.3	4.3	12.2
30 to 50	10.9	30.8	8.9	25.1	7.7	21.8	6.9	19.5	6.3	17.8
50 to 70	14.2	40.2	11.6	32.9	10.1	28.5	9.0	25.5	8.2	23.2
70 to 80	12.1	34.2	9.9	27.9	8.5	24.2	7.6	11.6	7.0	19.7
80 to 90	6.2	17.6	5.0	14.4	4.4	12.5	3.9	11.1	3.6	10.2
90 to 95	2.8	7.8	2.3	6.4	2.0	5.5	1.7	4.9	1.6	4.5
Over 95	1.4	4.1	1.2	3.3	1.0	2.9	0.9	2.6	0.8	2.3

[A]These numbers represent the (1S) and (D2S) limits as described in ASTM C 670

TABLE 4 - Within-Laboratory Durability Factor Precision for Averages of Two or More Beams - Procedure C

Range of Average Durability Factor	Number of Beams Averaged									
	2		3		4		5		6	
	Standard Deviation[A]	Acceptable Range[A]	Standard Deviation[A]	Acceptable Range[A]	Standard Deviation[A]	Acceptable Range[A]	Standard Deviation[A]	Acceptable Range[A]	Standard Deviation[A]	Acceptable Range[A]
0 to 5	0.5	1.4	0.4	1.1	0.4	1.0	0.4	1.0	0.3	0.8
5 to 10	0.7	2.0	0.6	1.6	0.5	1.4	0.5	1.4	0.4	1.2
10 to 20	1.6	4.4	1.3	3.6	1.1	3.1	1.1	3.1	0.9	2.5
20 to 30	2.4	6.8	2.0	5.6	1.7	4.8	1.7	4.8	1.4	3.9
30 to 50	6.2	17.6	5.1	14.4	4.4	12.4	4.4	12.4	3.6	10.2
50 to 70	5.2	14.6	4.2	11.9	3.7	10.3	3.7	10.3	3.0	8.4
70 to 80	4.5	12.6	3.6	10.3	3.2	8.9	3.2	8.9	2.6	7.3
80 to 90	3.5	9.8	2.8	8.0	2.5	6.9	2.5	6.9	2.0	5.7
90 to 95	1.5	4.2	1.2	3.4	1.1	3.0	1.1	3.0	0.9	2.4
Over 95	0.8	2.2	0.6	1.8	0.6	1.6	0.6	1.6	0.4	1.3

[A]These numbers represent the (1S) and (D2S) limits as described in ASTM C 670

Appendix C
Standard Test Method for Determining the Fundamental Transverse Frequency and Quality Factor of Concrete Prism Specimens

Standard Test Method for Determining the Fundamental Transverse Frequency and Quality Factor of Concrete Prism Specimens

AASHTO Designation TP18[1]

1. Scope

1.1 This test method describes procedures for determining the fundamental transverse frequency and quality factor of concrete prism specimens for the purpose of non-destructively evaluating the condition of the concrete.

1.2 The values stated in SI units are to be regarded as the standard. The values in parentheses are for informational purposes only.

1.3 This procedure may involve hazardous materials, operations, and equipment. This procedure does not purport to address all of the safety problems associated with its use. It is the responsibility of whoever uses this procedure to consult and establish appropriate safety and health practices and determine the applicability of regulatory limitations prior to use.

2. Referenced Documents

2.1 AASHTO Standards

R9 Acceptance Sampling Plans for Highway Construction
T23 Making and Curing Concrete Test Specimens in the Field
T24 Test Method for Obtaining and Testing Drilled Cores and Sawed Beams of Concrete
T126 Making and Curing Concrete Test Specimens in the Laboratory
T161 Test Method for Resistance of Concrete to Rapid Freezing and Thawing

2.2 ASTM Standards

C215 Standard Test Method for Fundamental Transverse, Longitudinal, and Torsional Frequencies of Concrete Specimens
C670 Practice for Preparing Precision and Bias Statements for Test Methods for Construction Materials
D3665 Random Sampling of Construction Materials
E105 Probability Sampling of Materials
E122 Choice of Sample Size to Estimate the Average Quality of a Lot or Process
E141 Acceptance of Evidence Based on the Results of Probability Sampling

3. Terminology

3.1 Description of Terms Specific to this Standard

[1]This standard is based on SHRP Product 2019.

3.1.1 Quality Factor (Q) - the normalized width of the frequency response curve - the inverse of the measure of internal damping

3.1.2 Fundamental Transverse Frequency - the frequency at which a specimen vibrates in the transverse mode with the greatest amplitude for a given amount of input excitation. This frequency is sometimes termed the frequency at which a specimen resonates.

4. Summary of Method

4.1 The fundamental transverse frequency and the quality factor of a concrete prism are determined by analyzing the vibration frequency response spectrum produced when the prism is lightly struck.

4.2 The specimen is supported in such a way as to minimize interference with vibration of the specimen.

4.3 The measured time response of the beam vibrations is converted into a frequency response by a Fast Fourier Transform (FFT). The fundamental transverse frequency and quality factor are then determined by fitting a standard frequency response curve to the measured frequency data.

5. Significance and Use

5.1 This test method is intended primarily for determining the amount of deterioration produced by accelerated durability tests such as T161. The deterioration can be quantified either by evaluating changes in the dynamic modulus of elasticity, or by evaluating changes in the quality factor of the concrete.

5.2 Deterioration from accelerated durability tests results in a decrease in elastic modulus of concrete specimens. This decrease is measured as a decrease in fundamental transverse frequency.

5.3 Prior to the accumulation of sufficient deterioration to produce a measurable decrease in fundamental transverse frequency, a decrease in quality factor occurs. This decrease in quality factor is thought to be an indication of micro-cracking in the concrete specimen. Though the microcracking may not be of sufficient magnitude to produce a change in the fundamental transverse frequency, it does change the amount of internal damping of the vibrations in the specimen.

6. Interferences

6.1 Improper tensioning of the wires supporting the specimen during testing will affect the test results.

6.2 Insecure attachment of the accelerometer to the test specimen surface will affect the test results.

6.3 Improper positioning of the impact point on the test specimen surface will affect the test results.

6.4 Failure to completely damp test specimen vibrations before application of each test impact will affect the test results.

6.5 Supporting the test specimen at locations other than the nodal points of the specimen will affect the test results.

6.6 Using test specimens with shapes and/or dimensions other than those indicated will affect the test results.

7. Apparatus

7.1 Fourier Analyzer - The Fourier analyzer used shall meet the following requirements when coupled with the data analysis and control component:

7.1.1 The Fourier analyzer shall be capable of FFT analysis of vibrational input data to convert time-domain measurements to frequency-domain response.

7.1.2 The Fourier analyzer shall be capable of averaging multiple frequency response measurements from a single specimen prior to determination of fundamental frequency and quality factor.

7.1.3 The Fourier analyzer shall be equipped with a minimum of two input channels.

7.1.4 The Fourier analyzer shall be capable of using the signal from one channel to normalize the signal from a second channel, thus allowing multiple readings to be averaged even though the vibration responses may have been produced by different impact magnitudes.

7.1.5 The Fourier analyzer shall be capable of using a minimal input level in one channel to trigger recording of data in all channels.

7.1.6 The Fourier analyzer shall be equipped with controls for lower and upper limits of the frequency range that may be set independently.

> Note 1 -- The lower limit of the frequency range is set above the frequency of the rigid body motion of the specimen on the support. For the support described under Section 7.1.4 and a normal-weight concrete specimen of dimensions 102 by 76 by 406 mm (4 by 3 by 16 in), a lower limit of 100 Hz. is appropriate. The upper limit of the frequency range should be set $\geq$ 500 Hz above the expected fundamental transverse frequency of the specimens to be measured. This upper limit should not be made too high as the precision of many Fourier analyzers is dependent upon the frequency range being analyzed. An upper limit of 3000 Hz is appropriate for a normal-weight concrete specimen of dimensions 102 by 76 by 406 mm (4 by 3 by 16 in).

7.1.7 The Fourier analyzer shall be capable of recording the time history of the vibrations with an exponential weighting or "window".

> Note 2 -- An exponential weighting of 0.1 provides the best reproducibility for both damaged and un-damaged concrete prisms. (The time response of a vibrating prism is the summation of decaying sinusoids. Included in the measurement is an essentially constant amount of noise. Thus, the signal-to-noise ratio decreases with measurement time. By treating the time-domain measurement to a decreasing exponential weighting, the readings with the best signal-to-noise ratio are weighted greater in the FFT analysis.) This procedure assists in obtaining the reproducibility of the quality factor results given in Section 12.1.1.

7.1.8 The Fourier analyzer shall be capable of storing at least 1024 points for FFT analysis with a maximum frequency capability $\geq$ 8 kHz.

> Note 3 -- A sampling size of 1024 points was found to give the most reproducible fundamental frequency and quality factor results on both damaged and undamaged prisms. While increasing the sampling size from 512 to 1024 points decreased the variability, a higher sampling size (2048 rather than 1024 points) increased variability. This is probably due to the longer measurement time required for the larger number of points and the decreasing signal-to-noise

ratio with increasing sampling times.

7.1.9 The Fourier analyzer shall be capable of restricting the voltage range of any of the inputs that are used for analysis.

7.1.10 The Fourier analyzer shall be equipped with audible and/or visual feedback mechanisms to the operator indicating when an impact of proper magnitude has been delivered.

> Note 4 -- A sensitivity of 0.1 to 1.0 AC volts for the excitation channel and 0 to 5.0 AC volts for the vibration response channel are appropriate for the hammer and accelerometer described in Sections 7.2 and 7.3, below.

7.1.11 The Fourier analyzer shall be capable of producing a visual display of the frequency response spectrum through the data recording and analysis component described in section 7.5.

7.2 Impact Hammer - A modally tuned impact hammer component capable of producing vibrations in the test specimen by impact and meeting the following requirements:

7.2.1 The impact hammer shall be capable of producing a flat frequency response over the entire frequency range being sampled. A modally tuned impact hammer with a mass of 140 g and a frequency response of 0 to 8 kHz produces the appropriate impact.

7.2.2 The impact hammer shall be equipped with a hammer impact tip of sufficient hardness and appropriate shape to neither be damaged by the specimen nor cause damage to the specimen when an impact of proper magnitude is produced. A spherical tip is not mandatory.

7.2.3 The impact hammer shall be equipped with an electronic load cell and appropriate power supply capable of producing an output voltage proportional to the magnitude of the impact with the specimen. The sensitivity of the load cell shall be 12.5 ± 2.5 mV/N or better.

7.3 Accelerometer and Power Supply - The accelerometer shall have a flat base, a mass ≤ 3 g, an operating frequency range of at least 10 to 10000 Hz, and a fundamental frequency at least twice the highest expected fundamental frequency of any of the specimens to be measured. The accelerometer power supply shall provide an output through the accelerometer-power supply combination of at least 50 mV/g.

> Note 5 -- Amplification of the accelerometer output may be necessary to achieve the proper output level.

7.4 Specimen Support - The specimen support shall be fabricated from 2 parallel 0.62 mm diameter piano wires that permit the specimen to vibrate freely, and minimize the amount of vibration energy absorbed from the specimen.

7.4.1 The parallel support wires shall be arranged to support the specimen a distance of 22.4 percent of the specimen length from each end of the specimen. This is approximately the location of the nodal points of the specimen, and vibration magnitude will be minimal at these points.

7.4.2 The parallel support wires shall be positioned at least 25 mm above any horizontal table surface to facilitate placing the specimens on the wires.

7.4.3 The length of the specimen support wires shall be at least 3 times the width of the specimen when the specimen is placed on the support wires.

7.4.4 The parallel support wires shall be tensioned so that they vibrate when plucked at a frequency of at least 400 Hz when there is no specimen on them thus minimizing system damping of the vibrations.

> Note 6 -- Piano wires, 0.62 mm diameter and spanning a distance of 350 mm, have been found to provide a suitable support for normal weight concrete prisms having dimensions of 102 by 762 by 406 mm (4 by 3 by 16 in).

7.5 Data Analysis and Control Equipment - The data analysis and control equipment shall include a personal computer capable of controlling the equipment and recording the data as indicated in Section 7.1.1; performing data analysis to determine fundamental transverse frequency and quality factor; and meeting the minimum compatibility requirements specified by the manufacturer of the Fourier analysis equipment. The computer may or may not be an integral part of the Fourier analysis equipment

7.5.1 The data analysis and control equipment shall include software adequate to perform the required functions. Software to accomplish the curve fit required in Section 11.1.3 is generally available from the supplier of the Fourier analysis equipment or can be written by a person with programming experience and some familiarity with modal analysis techniques.

> Note 7 -- The curve fit is accomplished as a weighted circle fit in the complex Nyquist plane. An appropriate weighting is the square of the distance from the origin in the Nyquist plane. Suggested references for additional information on modal analysis include: Modal Testing and Practice by D.J. Edwins, June, 1985; and assorted papers from the Seminar on Understanding Digital Control and Analysis in Vibration Test Systems, The Shock and Vibration Information Center, 1975.

8. Sampling and Test Specimens

8.1 Determine the number of samples needed based on the concrete under investigation and the purpose for which the test data will be used.

8.2 Samples obtained from concrete pavements and structures.

8.2.1 Stratified patterns for sampling are satisfactory for many concrete elements. On support or substructure elements, a significant factor in the location of sample sites is the geometry of the element. In these cases smaller or larger stratified patterns or non-stratified patterns may be appropriate.

8.2.2 If a stratified pattern is used, locate the sample sites using a stratified random sampling procedure. If geometry dictates a non-stratified pattern, use a random sampling procedure.

> Note 8 -- If geometry of the concrete element under investigation restricts available sample sites to 5 or less, it is generally desirable to sample from all available sites when practical.

> Note 9 -- ASTM D3665 contains a table of random numbers, including instructions for use. Practices R9 and ASTM E105, E122, and E141 contain additional information concerning sampling practices.

8.2.3 Obtain prismatic test specimens cut from hardened concrete in accordance with T24.

8.3 Sampling from Freshly Mixed Concrete in the Field.

8.3.1 Use a stratified random sampling plan for selection of samples from a concrete lot or production process. If the lot or production process is not suitable for stratification (i.e. limited quantity, intermittent batching of small quantities of different concrete mixes, etc.) use a random sampling procedure.

8.3.2 Prepare prismatic test specimens in the field in accordance with T23.

8.4 Sampling from Freshly Mixed Concrete in the Laboratory.

8.4.1 Obtain constituent materials for concrete specimens made in the laboratory using applicable standard methods.

8.4.2 Prepare prismatic test specimens in the laboratory in accordance with T126 or other appropriate procedures.

8.5 Use specimens of rectangular cross section and appropriate dimensions so that fundamental frequencies of either of the two transverse modes, the torsional mode, and the longitudinal mode do not interfere with each other. Square and round cross-sections specifically do not meet these requirements.

> Note 10 -- The data analysis described in Section 11 includes as an assumption that the vibrations are from a single degree of freedom system. This means that other vibration modes are not contributing to the frequency response in the range of frequencies being analyzed. A specimen size of 102 by 76 by 406 mm (4 by 3 by 16 in) meets these requirements.

9. Standardization

9.1 Verify the calibration of the Fourier analyzer at least every 12 months. Use a reference beam with known response for periodic quality control checks when testing is scheduled.

9.2 Verify calibration of the impact hammer and load cell at least every 12 months.

9.3 Verify calibration of the accelerometer at least evey 12 months.

10. Procedure

10.1 Place the specimen (Note 11) on the support wires so that the ends of the specimen extend equal amounts beyond their respective support wires and the specimen is centered on the length of the wire. (Note 12)

> Note 11 -- While the specimen can be tested across either cross-sectional axis, placing the specimen so that cast or cut surfaces are on the top and bottom provide for easier and more reliable testing.

> Note 12 -- Guide marks on the horizontal surface below the wires assist in rapidly placing the concrete specimens in the correct alignment.

10.2 Attach the accelerometer to the specimen with a rubber band. Center the accelerometer on the top face of the specimen, as close to one end as possible. Arrange the base of the accelerometer securely on the specimen, and use a rubber band(s) with sufficient tension to keep the accelerometer firmly in contact with the specimen.

> Note 13 -- While adhesive wax is the generally accepted method of temporarily attaching

accelerometers for modal analysis, this method does not work well with specimens in the cool and damp condition specified in Test Method T161. Drying any portion of the specimen to permit use of adhesive wax is not advised as this could produce variable quality factor measurements. Adhesive wax or another coupling medium can be used in addition to a rubber band in an attempt to improve the contact between the accelerometer and the specimen, but this has not been found to be necessary. If a coupling medium is used, care should be taken to prevent small amounts of scaled material from becoming imbedded in the coupling medium and preventing uniform contact between the accelerometer and specimen.

10.3 Perform any necessary preparations to the Fourier analyzer and take a preliminary reading of the fundamental transverse frequency by impacting the top face of the specimen. Apply the impact vertically, centered on the top face, and on the end opposite to the end on which the accelerometer is attached. Impact as near as practical to the end of the specimen. Record the hammer and accelerometer responses, with said recording activated by the hammer load cell response. The full frequency response curve displayed may include multiple response peaks, representing the various transverse and torsional vibrational modes. If the specimen is of appropriate dimensions, described in Section 8.5, and the accelerometer and impact are properly placed, as described in sections 10.1 and 10.2 above, the greatest amplitude shown corresponds to the fundamental transverse frequency.

10.4 Using the approximate fundamental frequency from this initial impact, reset the frequency measurement range to a total frequency range of 400 Hz, centered on the approximate fundamental transverse frequency.

10.5 Make three successive impacts of the beam as described in Section 10.3, above, taking care to stop any vibrations and/or rigid body swaying between impacts. Observe the displayed frequency response curve after each impact, and repeat any that are not in the expected smooth shape. (Note 14) When the three acceptable frequency responses have been obtained, average the three responses and store this information for later analysis.

Note 14 - Specimen deterioration will cause the frequency response curve to become less smooth; this is normal behavior due to internal cracking in the specimen associated with the deterioration. Major irregularities in the frequency response curve can generally be attributed to failing to completely stop movement of the specimen prior to making the impact. This can result in vibrational interference which looks like a jagged curve. In some cases, irregularities in the curve can also indicate that the accelerometer is not firmly seated on the specimen.

11. Interpretation and Calculation

11.1 Interpretation.

11.1.1 The fundamental transverse frequency, ω_r, is the frequency which produces the highest amplitude in the average of the frequency response spectrums measured in Section 10.5, above.

11.1.2 The quality factor, Q, is the normalized width of the frequency response curve, and is defined as:

$$Q = \frac{\omega_r}{\omega_2 - \omega_1}$$

where:

ω_r = the fundamental transverse frequency,
ω_1 = the frequency below ω_r at which the amplitude of the frequency response curve is $[(2)^{0.5}]/2$ times that at ω_r, and
ω_2 = the frequency above ω_r at which the amplitude of the frequency response curve is $[(2)^{0.5}]/2$ times that at ω_r.

11.1.3 Actual calculation of the fundamental transverse frequency and quality factor values is accomplished by the computer software which fits a standard frequency response curve for a single degree of freedom system to the measured data from Section 10.5, above.

11.2 Calculations

11.2.1 Calculate the dynamic Young's modulus of elasticity, E, in Pa, from the fundamental transverse frequency, mass, and dimensions of the test specimen as follows:

$$\text{Dynamic } E = C_m \varphi \omega_r^2$$

where:

φ = the mass of the specimen, kg,
ω_r = the fundamental transverse frequency, Hz,
C_m = $0.9464(L^3T/bt^3)$, $[(N)(s^2)]/[(kg)(m^2)]$,
L = the length of the specimen, m,
t, b = the cross-section dimensions of the specimen, m, t being in the direction of vibration, and
T = a correction factor which depends on the ratio of radius of gyration, K, (K=0.2887 t) to the length of the specimen, L, and on Poisson's ratio. Values of T for a Poisson's ratio of 1/6 are given in table 1.

TABLE 1 - Values of Correction Factor, T

T	K/L	T	K/L
1.60	0.00	1.00	0.09
1.73	0.01	1.01	0.10
2.03	0.02	1.03	0.12
2.36	0.03	1.07	0.14
2.73	0.04	1.13	0.16
3.14	0.05	1.20	0.18
3.58	0.06	1.28	0.20
4.78	0.07	1.38	0.25
6.07	0.08	1.48	0.30

11.2.1.1 Values of T for a Poisson's ratio of 1/6 are derived from Figure 1 of the paper by G. Pickett, "Equations for Computing Elastic Constants from Flexural and Torsional Resonant Frequencies of Vibration of prisms and Cylinders", Proceedings, ASTM, Volume 45, 1945, P. 846. Poisson's ratio for water-saturated concrete may be higher than 1/6. The correction factor, T', for a different value of Poisson's ratio, μm, and a

given K/L, may be calculated from the following relationship:

$$T' = T[1+(0.26\mu+3.22\mu^2)K/L]/[1+0.1328(K/L)]$$

where:

T is taken from table 1 for the given K/L.

12. Report

12.1 Report the transverse frequency to the nearest Hz.

12.2 Report the quality factor.

13. Precision and Bias

13.1 Precision

13.1.1 The single operator, single laboratory precision for measurements of fundamental transverse frequency and quality factor of a single specimen are shown in table 2. Values are shown for both an undamaged specimen and a specimen whose relative dynamic modulus as defined in T161 has been reduced by repeated cycles of freezing and thawing to approximately 60 percent. These results were determined for specimens having dimensions of 102 by 76 by 406 mm [4 by 3 by 16 in] (the first dimension is the direction of vibration).

TABLE 2 - Single Operator, Single Laboratory, Single Specimen Precision.

Specimen Condition	Fundamental Transverse Frequency		Quality Factor	
	Coefficient of Variation, percent[A]	Acceptable Range of 2 Results, percent of mean[A]	Coefficient of Variation, percent[A]	Acceptable Range of 2 Results, percent of mean[A]
Un-Damaged Specimen	0.04	0.11	3.3	9.4
Damaged Specimen	0.18	0.51	8.8	24.8

[A] These numbers represent, respectively, the 1S% and the D2S% limits as described in the ASTM Practice C 670.

[B] Specimen was reduced by the repeated cycles of freezing and thawing to approximately 60 percent relative dynamic modulus as defined in Test Method T 161

13.1.2 Research required to determine the within-batch and between-batch precision of this method has not been conducted.

13.1.3 Research required to determine the among-laboratories precision of this method has not been conducted.

13.2 Bias - The research required to establish the bias of this method has not been conducted.

14. Keywords - concrete, Young's modulus of elasticity, fundamental transverse frequency, quality factor.

Appendix D
Damping Measurements for Nondestructive Evaluation of Concrete Beams

Synopsis

Change in relative dynamic modulus (RDM), as determined by resonance frequency measurements, is the most frequently used indicator for evaluating damage to concrete beams that are subjected to repeated cycles of freezing and thawing (ASTM C 666). While sinusoidal excitation (ASTM C 215) is the standard method for measuring resonance frequency, impulse excitation has been approved by ASTM as an alternate. Important advantages of the impulse method are that it is rapid, quite reproducible, and also produces information on the damping characteristics of the vibrational modes with no additional testing. The work reported in this paper identifies linear changes in damping with early cycles of freezing and thawing before significant decreases in resonance frequency can be identified. Comparisons of predicted and actual durability factors showed agreement within published testing errors for most of the mixes tested. This work indicates that the durability factor (ASTM C 666) can be accurately predicted with damping measurements before the actual failure of the concrete beams can occur from repeated cycles of freezing and thawing.

Introduction

The frost resistance of concrete is most frequently determined by subjecting concrete beams to repeated cycles of freezing and thawing and periodically measuring the damage in the beams. Because the measurement of damage must be nondestructive, measurement of the concrete's vibration characteristics (modal analysis) has often been employed for damage evaluation. In 1938, Powers[1] presented a method comparing the musical tone of prisms after a hammer impact with a calibrated set of orchestra bells to determine the specimen's dynamic modulus of elasticity (proportional to resonance frequency). In his closure to written discussion of his paper, Powers suggests that monitoring the change in the dynamic modulus of elasticity may indicate deterioration of a sample subjected to repeated cycles of freezing and thawing. The following year, Hornibrook[2] reported the use of electronics to more accurately match frequencies. This report was followed by the discovery of the use of acoustic transducers to excite the specimens and scan for the frequency with maximum amplitude. Notable early research included Thomson in 1940[3], Obert and Duvall in 1941[4], Long and Kurtz in 1943[5], and Stanton in 1944.[6] In the following 20 years, many investigations were performed to determine the results of this dynamic vibration on cement-based materials.[7-10] The method most commonly used today to evaluate damage in concrete beams subjected to repeated cycles of freezing and thawing, (ASTM C 666), still involves the determination of the resonance frequency of the beam (ASTM C 215). Present work

with damping measurements indicates that the durability factor can be accurately predicted before concrete beams fail due to repeated cycles of freezing and thawing. This takes substantially less time than current procedures.

Background

Modal Analysis

Modal analysis has generally been used for nondestructive evaluation of the dynamic characteristics of a structure's modes of vibration. A mode of vibration is defined as the deformation pattern of a structure at a natural frequency. Each mode of vibration is identified by three factors: the resonance frequency; the damping factor; and the mode shape. Resonance frequency is the characteristic frequency at which a maximum response occurs for a given mode of vibration. The damping factor is a measure of the energy dissipated in each cycle of vibration. A mode shape describes the deformed shape of a sample when subjected to a dynamic system.

One method of modal testing uses sinusoidal excitation for the input signal. This method forces a structure to vibrate at a frequency while the response of the structure is monitored with an accelerometer. The excitation frequency is varied until a maximum amplitude is observed, which gives the resonance frequency for a particular mode of vibration. The sinusoidal excitation method is the current standard method for examining damage in concrete prisms (ASTM C 215).[11]

An alternative method of modal testing has recently been suggested as a possible way of determining the resonance frequencies of concrete beams by investigators such as Malhotra and Carino[11] and Gaidis and Rosenberg.[12] The method uses impulse excitation. For instance, a hammer strike can be used to excite vibrations in a beam. A load cell on the hammer measures the impact force (input signal). The response of the beam is recorded with an accelerometer (output signal). A Fast Fourier Transform (FFT) transforms the time domain data (amplitude as a function of time) into the frequency domain (amplitude as a function of frequency). The ratio of the Fourier transform of the output signal to the Fourier transform of the input signal is called the frequency response function. This function is a complete mathematical description of the linear vibration characteristics of the prism over the range of frequencies determined by the hardware and software used.

Resonance Frequency, Relative Dynamic Modulus, and Durability Factor

As mentioned above, a mode of vibration is identified by a resonance frequency and a damping factor. A beam can vibrate at a number of frequencies at the same time. The primary, or resonance frequency, however, is the lowest frequency that has an amplitude substantially greater than both higher and lower frequencies. Figure D-1 shows a portion of

an idealized frequency response curve with the resonance frequency labelled. Isolating a portion of the frequency response curve like this essentially treats the vibration response as a single degree of freedom system (SDOF). While vibrations outside of the limited range around the resonance frequency contribute to the overall response of the beam, they are often ignored in modal analysis.

The dynamic modulus of elasticity for a concrete beam can be calculated from the resonance frequency by the equation given in ASTM C 215:

$$E_D = C \cdot m \cdot \omega_r^2 \qquad (1)$$

where E_D = dynamic modulus of elasticity
C = shape, dimensions, and Poisson's ratio of the beam
m = mass of the beam
ω_r = resonance frequency of the beam

C is defined as follows for a prismatic beam:

$$C = \frac{0.00245 \cdot L^3 T}{bt^3} \qquad (2)$$

where L = length of prism
T = correction factor based on the ratio of the radius of gyration to the length of the specimen, and on Poisson's ratio
A sample with Poisson's ratio of 1/6, 16 in. (406 mm) long, and driven in the 3-in. (76 mm) direction has a T factor of 1.24
b = dimensions of prism
t = driving direction

Both C and ω depend upon whether mode of vibration tested is longitudinal or transverse. Most tests of concrete beams subjected to freezing and thawing use transverse vibration.

As a concrete beam deteriorates from repeated cycles of freezing and thawing, E_D and, therefore, ω_r decrease (ignoring mass and dimensional effects). The relative dynamic modulus is a measure of this deterioration and is defined by ASTM C 666 as follows:

$$P_n = (\omega_{rn} / \omega_{r\circ}^2) \cdot 100 \qquad (3)$$

where P_n = relative dynamic modulus after n cycles of freezing and thawing,
ω_{rn} = resonance frequency after n cycles of freezing and thawing, and
$\omega_{r\circ}$ = resonance frequency at 0 cycles of freezing and thawing.

The effects of mass and dimension changes are ignored in the above equation but should be considered if there is significant change in mass.

A durability factor can be calculated for a concrete beam at the end of freezing and thawing testing as follows (ASTM C 666):

$$DF = P_n \cdot N/M \tag{4}$$

where DF = durability factor
N = number of cycles at which the testing is terminated (because either a minimum P_n is reached or the specified number of cycles is reached)
M = specified number of cycles

A typical value for M is 300 cycles and a typical minimum value for P_n is 60 percent (ASTM C 666). ASTM C 666 also allows the termination of the freezing and thawing testing if the specimen exceeds a 0.10 percent length expansion.

Damping and Quality Factor

Malhotra and Carino[11] have reviewed the damping properties of concrete. Research in materials science by Coppola and Bradt[13] has suggested that viscous damping is more sensitive to thermal damage than elastic modulus. For analysis purposes, a quality factor (Q) is frequently used instead of viscous damping. While viscous damping increases with deterioration, the quality factor decreases and is easier to monitor quantitatively. Q is related to viscous damping by the following equation:

$$Q = \omega_r / (2 \cdot \sigma) \tag{5}$$

where Q = quality factor
ω_r = resonance frequency
σ = damping coefficient

Q is normally calculated as follows:

$$Q = \omega_1 /(\omega_2-\omega_1) \tag{6}$$

where ω_1, ω_2 = frequencies on either side of ω_r at which the vibration amplitude of the beam is 70.7 percent of the amplitude of ω_r

Figure D-1 shows ω_r, ω_1, and ω_2.

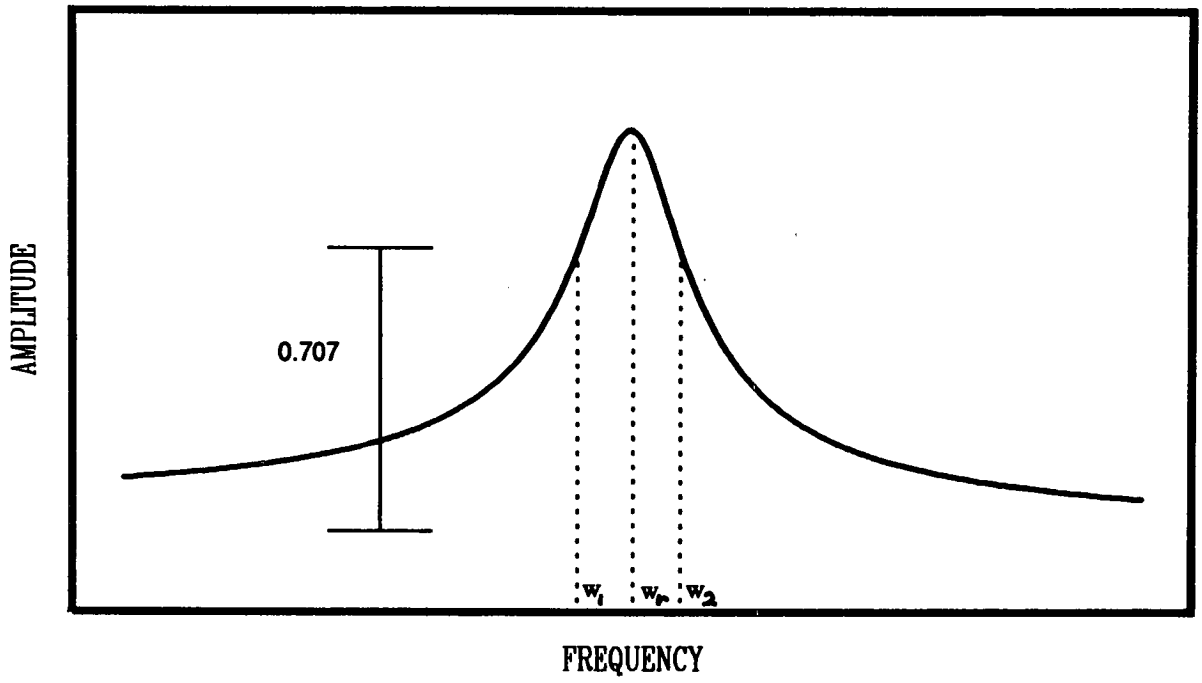

Figure D-1 Idealized Frequency Response Curve

As a concrete prism is subjected to cycles of freezing and thawing, microcracking occurs in the aggregate, in the matrix and at the aggregate-matrix interface. This microcracking creates damping[14] which causes the free vibrations to decrease in amplitude as a function of time. As microcracking occurs, damping increases, and the quality factor decreases. The damping is a result of pumping action as the cracks alternately open and close during the vibration cycle.

To this date, no extensive research has been conducted into how damping might play a role in assessing freeze-thaw damage in concrete prisms. One reason might be the difficulty in obtaining damping information on concrete prisms with the sinusoidal method (as in ASTM C 215). This method requires locating the resonance frequency and the corresponding baseline and maximum amplitudes. The frequencies at which the response is 70.7 percent of the amplitude at the resonance frequency must then be measured. While automated data acquisition processes could obtain the above information quickly, this process has a potential error associated with each measurement.

The impulse excitation method, however, involves no extra laboratory work to get viscous damping information. Once the modal information of the test has been processed by the FFT, the data are in the form of a series of points giving amplitude and frequency. By looking at a limited frequency range, researchers can treat the data as an SDOF system (no interference from other vibrational modes), and the frequency response function can be written in its real and imaginary parts as follows:[15]

Real Portion:

$$H(\omega) = \frac{r_1(\omega_n - \omega) + r_2 \cdot \sigma}{2[(\omega_n - \omega)^2 + \sigma^2]} \tag{7}$$

Imaginary Portion:

$$H(\omega) = \frac{r_2(\omega_n - \omega) - r_1 \cdot \sigma}{2[(\omega_n - \omega)^2 + \sigma^2]} \tag{8}$$

where $H(\omega)$ = frequency response function
ω_n = damped natural frequency
σ = damping coefficient
r_1 = real portion of the complex residue
r_2 = imaginary portion of the complex residue

At resonance, the real and imaginary parts become the following:

Real Portion:

$$H(\omega) = \frac{r_2}{2 \cdot \sigma} \tag{9}$$

Imaginary Portion:

$$H(\omega) = \frac{-r_1}{2 \cdot \sigma} \tag{10}$$

The damping factor (ξ), or percentage of critical damping is calculated as follows:

$$\xi = \frac{\sigma}{\omega_r} = \frac{\sigma}{(\sigma^2 + \omega_n^2)^{0.5}} \tag{11}$$

where ω_r = resonance frequency, and
σ and ω_2 are as defined above in equation 7.

An assumption can be made to simplify the calculation of resonance frequency and damping in the above equations. When the percentage of critical damping in a concrete prism exceeds 5 percent, the relative dynamic modulus is below 60 percent and the ASTM C 666 test will

stop (equation 4). Therefore, substituting ω_n for ω_r introduces a maximum error of 0.13 percent in the calculations for resonance frequency and damping[16] for normal testing of concrete prisms subjected to repeated freezing and thawing in accordance with ASTM C 666.

In practice, the resonance frequency and damping of the data from the FFT can be determined with a least squares "circle fitting" method in the Nyquist plane. The imaginary part of the frequency response function is plotted against the real part, and each mode shows up as a circle. The result is convenient for curve fitting to determine parameter values. "Each resonance arc is approximately tangent with, and lies below, the real axis."[17] Resonance frequency is determined from the point on the circle that is at a maximum distance from the origin in the Nyquist plane. Damping is related to the diameter of the circle. An example of a Nyquist plot is shown in figure D-2.

A weighting function is used to increase the accuracy of the circle fitting. Each point in the Nyquist plot is multiplied by the square of the distance from the origin. Weighting is necessary for two reasons:

1) The data points nearest to the resonance frequency are located in the half of the circle that is farthest away from the origin (figure D-2). This portion of the circle corresponds to the portion of the frequency response curve with higher amplitudes (figure D-1), and which is least affected by background noise in the measurements. There are fewer points in this region of the circle, and curve fitting without weighting would allow the circle fit to be more influenced by the data points closest to the origin (which are more influenced by background noise).

2) Though SDOF is assumed, modes that are outside the range of use can influence the examined mode. Data points near the resonance frequency are affected less by other modes and are therefore weighted more.

Using the circle fitting method for determining Q is more accurate than measurement using the three points determined from a frequency response curve, as in figure D-1 and then applying equation 6[10]. All the data for a given mode are appropriately weighted and used in fitting a circle, while equation 6 uses only three points to determine the resonance frequency and quality factor. As the frequency response curve is rarely as symmetrical as shown in figure 1, potential error exists in determining the baseline amplitude. This asymmetry (figure D-2) is taken into account by the circle fit in the Nyquist plot. The Nyquist plot also has the advantage of having fewer points close to resonance, so that the plot is focused more on the resonance area.[18]

Testing Program

A testing program in which 52 marginally air-entrained concrete beams were subjected to repeated cycles of freezing and thawing in accordance with ASTM C 666 was conducted. The beams were periodically evaluated by an impact method of modal analysis.

Equipment

A modally tuned hammer with a flat frequency response of up to 8 kHz was used to impact the beams. The hammer had a mass of 140 g and a resonance frequency of 31 kHz. A load cell in the hammer with a sensitivity of 12 mV/N was used to measure the magnitude of the hammer impact.

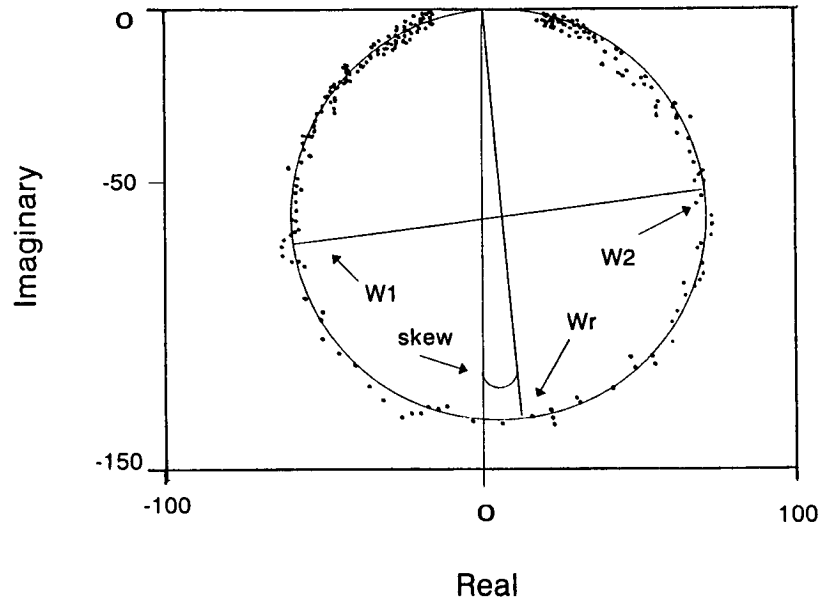

Figure D-2 Typical Nyquist Plot

Vibrations in the beams were measured with an accelerometer with a sensitivity of 10 mV/g (acceleration). It had a mass of 1.9 g and a resonance frequency of 70 kHz. Output from the accelerometer was amplified by a factor of 10 before input into the analyzer.

A Fourier analyzer was used for data acquisition and initial analysis. Sampling rate, bandwidth, and resolution were variable and inter-related. For the testing described in the following section, a bandwidth of 400 Hz was used. This provided a sampling rate of 1,024 Hz and a resolution of slightly less than 0.4 Hz. Inputs were provided for both the load cell from the hammer and the amplified signal from the accelerometer. To improve the accuracy of the frequency spectrum, the procedures included averaging, windowing, resolution, and zoom. These are described below.

Averaging - Results from multiple impacts were combined to improve reproducibility of the test procedure. Increasing the number of impacts used in the average improves the signal to noise ratio of the frequency response function.[15] However, increasing the number of impacts also increases the amount of time necessary to test a beam. An average of three hammer impacts spaced no greater than ten seconds apart was found to produce the best compromise between reducing noise and reducing the time involved to test each beam.[16]

Windowing - The acceleration-response of the response was multiplied by an exponential window to further remove background noise. The time response of a beam is the summation of decaying sinusoids. The exponential window multiplies a weighting factor to the time response so that the initial response of the prism has the greatest influence on the frequency response spectrum, and later decaying sinusoids have an exponentially reduced influence on the frequency response spectrum. This response contains measurement noise that is distributed evenly throughout the time domain. Applying an exponential window to the time domain adds a known amount of damping to the time domain and improves the signal to noise ratio.[16,17] The equipment automatically subtracts the damping introduced by the exponential window.

Resolution - Resolution is a function of the number of sampling points used in the FFT analysis. As described above, a sampling rate of 1,024 Hz was used for this testing. Both higher and lower sampling rates were evaluated, but this rate appeared to give the best results because of the increased noise at the higher sampling rates and inadequate resolution at the lower rates.[16]

Zoom - Zoom was used to isolate the modes and improve the accuracy of the measurements. As mentioned above, a bandwidth of 400 Hz was used for the testing. Because the frequency range between good and damaged beams could approach 1,000 Hz, an approximation of the resonance frequency was necessary to set the 400 Hz bandwidth in the correct range for each beam. This was accomplished by initially setting the bandwidth to 6,000 Hz (sampling from 0 to 6,000 Hz). The specimen was impacted once to establish a frequency spectrum. While this frequency spectrum usually contained multiple modes, the approximate resonance frequency could be determined by observation of the entire bandwidth. The bandwidth was then "zoomed" to a total bandwidth of 400 Hz, with the approximate resonance frequency centered in the range. This procedure is desirable for three reasons. First, the resolution is improved. Second, one mode can be examined because the other modes are outside the frequency range of use. This makes the single degree of freedom (SDOF) assumption essentially valid in the frequency range of use. Third, the frequency for a damaged beam is easier to locate. As the beams deteriorate, the resonance frequency drops. Initially tapping a damaged beam with a larger frequency bandwidth helps locate the desired vibrational mode.[16]

Concrete Beams

Each of the 52 mixes studied in this program contained five concrete beams per batch. The beams had dimensions of 76 mm x 102 mm x 407 mm (3 in. x 4 in. x 16 in.). The mixes were made with a Type I cement and had water/cement (w/c) ratios of either 0.40 or 0.45. All of the mixes contained one of three air-entraining admixtures: neutralized vinsol resin, tall oil, or an organic acid salt. Some of the mixes also contained either a water-reducer based on a salt of hydrocarboxylic acid, or a lignosulfonate- or melamine-based high range water reducer. All but three of the mixes contained a crushed limestone coarse aggregate with a maximum size of 25 mm (1 in.). In one of the mixes without the 25-mm (1-in.)

crushed limestone, all of the aggregate larger than 12.5 mm (1/2 in.) had been sieved out of the fresh concrete mix before specimen consolidation. The other contained a glacial gravel with a maximum size of 22 mm (7/8 in.) in place of the crushed limestone. All mixes were cured for one day in their molds at room temperature and then removed from their molds and placed in a saturated lime water bath at 23°C (73°F) until they reached an age of 28 days.

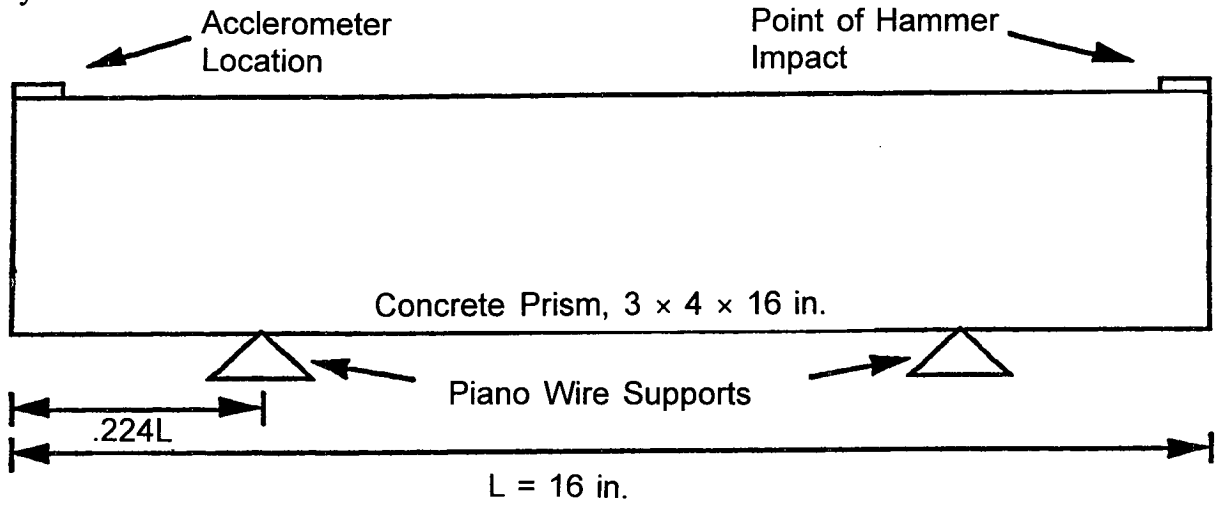

Figure D-3 Schematic of Test Setup

Beam Support

Two options were considered for supporting the concrete prisms: fixing one end (the grounded method) or the unrestrained method (free boundary). The chosen method was the unrestrained method, which requires supporting the prism at the bending modes. This allows the prism to "to vibrate without significant restriction," as specified by ASTM C 215. The unrestrained method also produces more consistent results than the grounded method because of the difficulty in clamping one end of the beam.[18]

The vibrational mode tested for was the first transverse mode, which has two nodes located at 22.4 percent of the length of the prism from each end. A testing support system was constructed with piano wire to support the prisms at each node, as suggested by Obert and Duvall.[4] The tension of the piano wire was adjusted to prevent the support's resonance frequency from interfering with the resonance frequencies of the prisms. Figure D-3 shows the location of the accelerometer and the point of hammer impact for the transverse vibrational mode.

Test Procedure

All concrete beams were subjected to freeze-thaw damage similar to ASTM C 666 Procedure A. The beams underwent six freeze-thaw cycles per day; a freeze-thaw cycle involves cooling the beam so that the center changes from 4°C to -18°C (40°F to 0°F) and then

warming it back to 4°C (40°F) in four hours. At various cycle intervals, the beams were withdrawn from the testing chamber at the end of the thaw cycle and tested for changes in mass, transverse resonance frequency, and quality factor. For the latter two variables, modal analysis was the testing procedure used. The beams were tested until the relative dynamic modulus (P_n, equation 3) reached 50 percent of its initial value, or until the beam had been subjected to at least 300 freeze-thaw cycles.

Analysis

Table D-1 shows typical results for resonance frequency and quality factor measurements taken after various numbers of cycles of freezing and thawing. These values are plotted as average relative dynamic modulus and average relative Q (described in equation 12 below) for the five beams in the mix in figures D-4 and D-5.

$$\text{Rel } Q_n = 100 \cdot (Q_n / Q_0) \tag{12}$$

where $\text{Rel } Q_n$ = relative quality factor after n cycles of freezing and thawing
Q_0 = quality factor at zero cycles of freezing and thawing
Q_n = quality factor after n cycles of freezing and thawing

In all of the beams, regardless of mix characteristics or durability factors, Rel Q was found to drop about 20 percent in the first few cycles. The reason for this drop is unclear, but it occurred in all mixes. This effect is shown in figure D-5. After this drop, Rel Q decreased linearly for a number of cycles of freezing and thawing and eventually levelled out or decreased only slightly thereafter (figure D-5). It is important to note that the linear decrease occurs during early freezing and thawing cycles. The magnitudes of the slopes of the decreasing portions of the Rel Q plots appeared to be greater for mixes that showed greater eventual damage caused by exposure to freezing and thawing.

Determining Q Failure

The data was analyzed by a least squares fit of the early linear portion of the five beam average Rel Q against the number of cycles data. The first four points were used to determine a best-fit linear regression of the Rel Q data. The next data point was added and a new correlation was determined. this procedure of adding the next point continued until the correlation began to decrease (indicating that the end of the linear decreasing portion of the data was reached) or for a maximum of 10 iterations. This best fit line was then extrapolated to get the x-intercept of the Rel Q line. This value will be referred to as the Q failure value (figure D-5). Q failure is a first estimate of the failure cycle of the beam. The best fit line extrapolated to get Q failure can be analyzed for its accuracy. Table D-2 shows the number of actual cycles of freezing and thawing used to get the best correlation, as described above, the correlation coefficient, and the Q failure value for the first beam of each of the mixes tested. For all but two of the mixes tested, the best fit line used had a

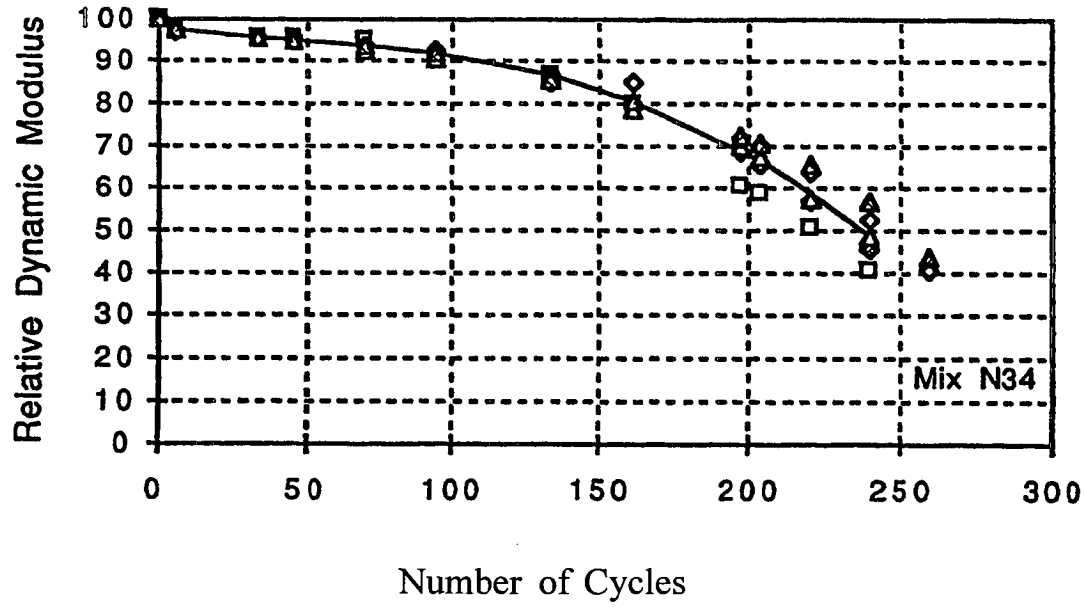

Figure D-4 Changes in Relative Dynamic Modulus

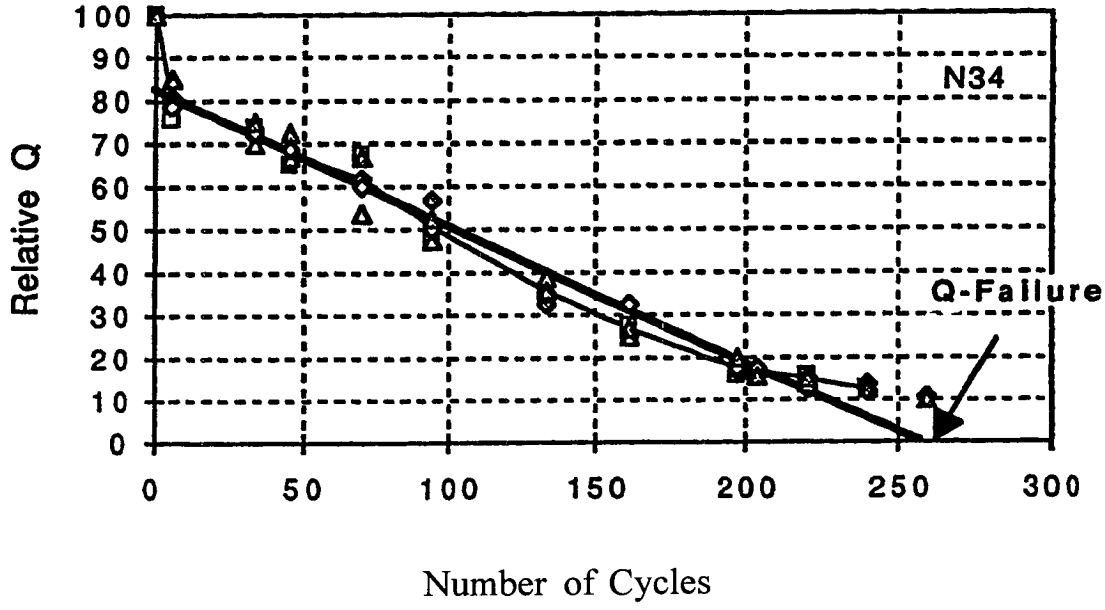

Figure D-5 Changes in Relative Q

correlation coefficient of greater than 0.90. The actual number of cycles performed to achieve a relative dynamic modulus of 60 percent is also shown. This number was determined from interpolation of the relative dynamic modulus values for each beam. For beams that required more than 300 cycles to failure, testing was continued to achieve a relative dynamic modulus of 60 percent. Two of the mixes (N00 and N42) were left in the testing chamber for greater than 300 cycles to obtain results at higher durability factors.

Correlation with Failure

Table D-3 shows the average Q failure and the actual number of cycles necessary to reduce the relative dynamic modulus (RDM) to 60 percent for the five beams of each mix tested. The number of cycles necessary to reduce the RDM to 60 percent are plotted against Q failure values in figure D-6. The linear regression equation for the best fit is as follows:

$$\text{N-fail} = 0.77 \cdot (\text{Q failure}) + 8.9 \qquad (13)$$

where N-fail is the actual number of cycles of freezing and thawing needed to produce a relative dynamic modulus of 60 percent.

The correlation coefficient (r^2) for the above regression was 0.96.

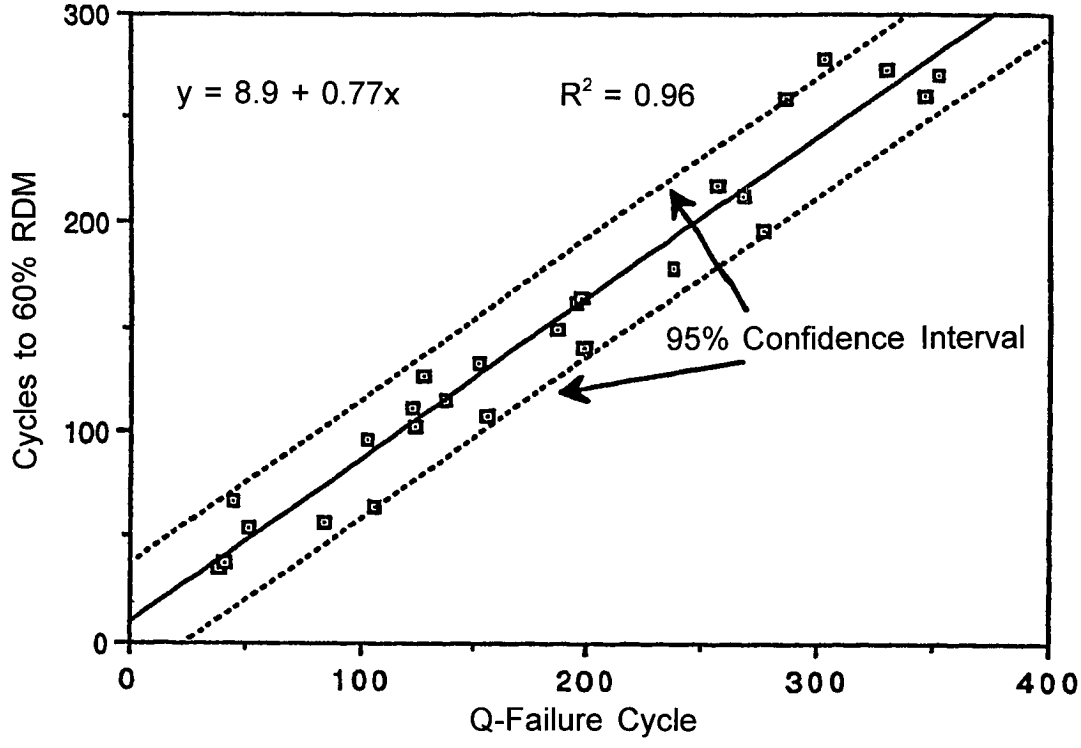

Figure D-6 Q-Failure Cycle versus Cycles to 60 percent RDM

Table D-1 Typical Values for Relative Dynamic Modulus and Quality Factor Measurements.

# of Cycle	Beam 1		Beam 2		Beam 3		Beam 4		Beam 5		Average	
	Res. Freq. (Hz)	Q	Res. Freq. (Hz)	Q	Res. Freq. (Hz)	Q	Res. Freq. (Hz)	Q	Res. Freq. (Hz)	Q	Res. Freq. (Hz)	Q
0	2357	103	2332	107	2343	110	2347	107	2346	104	2345	106
6	2336	78	2304	87	2316	89	2317	85	2317	89	2318	86
34	2314	76	2285	77	2294	77	2303	78	2298	78	2299	77
46	2307	68	2275	71	2284	73	2298	74	2289	76	2291	72
70	2297	70	2261	66	2255	59	2276	65	2275	70	2273	66
94	2249	50	2251	61	2231	52	2245	53	2244	55	2244	54
133	2202	38	2149	35	2190	42	2193	38	2174	37	2182	38
161	2105	29	2090	26	2084	27	2158	35	2105	28	2109	29
197	1839	17	1936	18	1954	19	1986	19	2005	21	1944	19
203	1812	16	1894	17	1931	20	1961	19	1973	16	1914	18
220	1683	16	1758	14	1777	16	1873	16	1906	16	1799	16
240	1517	14	1586	13	1638	15	1716	15	1772	14	1646	14
259	*		*		*	12	1510	12	1558	11	1534	11

* Below 50 percent RDM, the beams were removed from the testing chamber.

Table D-2 Q Failure and Actual Failure Cycle, Single Beam from Each Mix Tested.

Mix # (Beam #1)	Q Failure Cycle	Cycles to Best Correlation	Correlation	Actual Failure Cycle (60 Percent)	Percent of Actual Failure Cycle
M66	191	167	0.98	157	106
M75	150	127	0.98	125	102
M86	146	121	0.97	167	72
M87	90	57	0.99	91	63
M98	195	77	0.99	205	38
N01	425	77	0.96	281	27
N06	198	179	0.97	164	109
N07	235	65	0.99	123	53
N08	82	69	0.97	59	117
N09	81	69	0.96	61	113
N10	39	30	0.91	37	81
N11	37	30	0.92	31	97
N13	71	48	0.99	66	73
N18	43	34	0.96	44	77
N19	78	34	0.99	63	54
N20	194	178	0.94	166	107
N21	117	110	0.97	95	116
N34	247	203	0.97	200	102
N35	331	240	0.98	289	83
N38	107	49	0.99	110	45
N39	199	150	0.99	157	96
N43	204	163	0.78	142	115
N44	311	267	0.90	239	112
N46	234	206	0.98	206	100
N47	541	174	0.86	284	61
N48	140	70	0.99	176	40
N49	149	93	0.99	137	68

Table D-3 Q Failure and Cycles to 60 Percent RDM, Average of Five Beams from Each Mix Tested.

Mix # (Average of 5 Beams)	Q Failure Cycle	Actual Cycles to 60 Percent RDM
M66	276	196
M75	124	103
M86	285	259
M87	199	141
M98	267	213
N01	346	261
N06	196	162
N07	156	108
N08	83	57
N09	106	65
N10	40	38
N11	38	36
N13	44	67
N18	51	54
N20	198	165
N21	103	96
N34	257	218
N35	302	279
N38	123	112
N39	137	115
N43	188	150
N44	330	273
N46	238	178
N47	352	271
N48	128	127
N49	153	133

Predicting Failure

The good correlation found with equation 13 suggested that the Q values obtained from modal analysis could be used to predict cycles to a relative dynamic modulus of 60 percent. However, table D-2 indicates that in some cases the best fit of the Rel Q data occurred at approximately the same number of cycles of freezing and thawing as that required for failure of specimens. The Rel Q data were re-examined to determine the best fit line with data preceding 60 percent RDM. The correlation coefficient (r^2) was above 0.90 for all mixes except N06 (0.81) and N20 (0.70). These new Q failure values are shown in table D-4 along with the cycles to 60 percent RDM from table D-3. For mixes that dropped to 60 percent RDM after more than 100 cycles, the Q failure values were determined with the data collected before 100 cycles of freezing and thawing. For mixes that failed before 100 cycles of freezing and thawing, the Q failure was determined with data collected before 60 percent RDM.

Equation 13 can be used with the Q failure values shown in table D-4 to predict the number of cycles that will cause failure (N-fail) for mixes with actual durability factors of less than 60. Equation 4, the ASTM C 666 method for calculating durability factor of samples that reached 60 percent RDM within 300 cycles, can then be used to calculate a predicted durability factor (DFpred) in combination with the predicted number of cycles to failure from equation 13 (N-fail) for N, 300 for M, and 60 percent for P_n. Table D-5 shows the predicted and actual durability factors for the mixes tested that had Q failure values less than 300 cycles.

Expected Precision

Laboratory durability factor precision are given in ASTM C 666 for the acceptable range between two set of five beams tested by procedure A. This acceptable range varies in relation to the durability factor value, with smaller ranges for very high and very low durability factors. In addition to the predicted and actual durability factors, table D-5 lists the difference between the values and the acceptable range for the actual durability factor, as given in ASTM C 666. The predicted values were within the acceptable range of the actual values for all but three mixes, regardless of the magnitude of the durability factor. The three mixes had low best-fit correlations (N47, r^2=0.47; N44, r^2=0.78; N09, r^2=0.88) when the Q failure value was obtained within 100 cycles, while most of the other mixes had correlation above 0.90.

Summary and Conclusions

To test the durability of concrete, the change in its RDM is measured. An excellent way to get these data is to use impulse excitation to conduct modal analysis. This method is better than the standard sinusoidal method because it is easier, quicker, and also provides data

about changes in damping in the beams. Before the use of impulse excitation, no extended studies had been conducted on the application of damping change to the analysis of damage caused by freezing and thawing.

The change in damping with increasing cycles of freezing and thawing includes a region with a linear decrease in Q for freezing and thawing cycles before the beams reach 60 percent RDM. If sufficient data are collected during this early portion of the freezing and thawing cycles, a least squares fit can be extrapolated to give estimated cycles to 60 percent RDM of the beam. This estimation has been experimentally shown to be closely correlated to the actual cycles to 60 percent RDM of the beam. In addition, the estimated failure cycle can used to predict the durability factor of a beam, and therefore could greatly reduce the amount of testing time needed to assess the extent of freeze-thaw damage in concrete beams.

This relationship between actual and predicted failure cycles is not unique to the chemical admixtures or coarse aggregate in the concrete. Additional testing is required to evaluate mixes containing less durable aggregate, or other non-durable and durable aggregates. Also, mixes with higher air contents and a wider variety of water/cement ratios should be investigated to determine if the damping results found in this study are consistent with other concrete mixes.

Table D-4 Q Failure Determined Prior to 60 Percent RDM and Cycles 60 Percent RDM, Average of Five Beams from Each Mix Tested.

Mix #	Q Failure Cycle (based on correlation before 100 cycles)	Cycles to 60 percent RDM
M66	300	196
M75	122	103
M86	368	259
M87	199	141
M98	267	213
N01	346	261
N06	446	162
N07	156	108
N08	99	57
N09	131	65
N10	40	38
N11	38	36
N13	44	67
N18	51	54
N20	236	165
N21	101	96
N34	265	218
N35	487	279
N38	124	112
N39	136	115
N43	148	150
N44	180	273
N46	256	178
N47	169	271
N48	128	127
N49	152	133

Table D-5 Predicted and Actual Durability Factors.

Mix #	Actual D F	N-Fail	Predicted D F	Difference	Difference Allowed by ASTM
M66	39	240.8	48.2	9.2	16.1
M75	21	103.3	20.7	0.3	10.6
M87	28	162.8	32.6	4.6	10.6
M98	43	215.4	43.1	0.1	16.1
N07	22	129.5	25.9	3.9	10.6
N08	11	85.5	17.1	6.1	7.5
N09	13	110.2	22.0	9.0	7.5
N10	8	39.9	8.0	0	2.0
N11	7	38.3	7.7	0.7	2.0
N13	13	42.9	8.6	4.4	7.5
N18	11	48.4	9.7	1.3	7.5
N20	33	191.4	38.3	5.3	16.1
N21	19	87.0	17.4	1.6	7.5
N34	44	213.8	42.8	1.2	16.1
N38	22	104.8	21.0	1.0	10.6
N39	23	114.1	22.8	0.2	10.6
N43	30	123.4	24.7	5.3	16.1
N44	55	148.1	29.6	25.4	19.3
N46	36	206.8	41.4	5.4	16.1
N47	54	139.6	27.9	26.1	19.3
N48	25	107.9	21.6	3.4	10.6
N49	27	126.4	25.3	1.7	10.6

References

1. Powers, T. C., "Measuring Young's Modulus of Elasticity by Means of Sonic Vibrations," *Proc., ASTM*, Vol. 38, Part II, 460, 1938.

2. Hornibrook, F. B., "Application of Sonic Method to Freezing and Thawing Studies of Concrete," *ASTM Bull.* No. 101, 1939, p. 5.

3. Thomson, W. T., "Measuring Changes in Physical Properties of Concrete by the Dynamic Method," *Proc., ASTM*, Vol. 40, 1940, p. 1113.

4. Obert, L., and W. I. Duvall, "Discussion of Dynamic Methods of Testing Concrete with Suggestions for Standardization," *Proc., ASTM*, Vol. 41, 1941, pp. 1053-1070.

5. Long, B. G., and H. J. Kurtz, "Effect of Curing Method on the Durability of concrete as Measured by Changes in the Dynamic Modulus of Elasticity," *Proc., ASTM,* Vol. 43, 1943, pp. 1051-1065.

6. Stanton, T. E., "Tests Comparing the Modulus of Elasticity of Portland Cement Concrete as Determined by the Dynamic (Sonic) and Compression (Secant at 1000 psi) Methods," *ASTM Bull.* No. 131, 1944, p. 17.

7. Axon, E. O., T. F. Willis, and F. V. Reagel, "Effect of Air-Entrapping Portland Cement on the Resistance to Freezing and Thawing of Concrete Containing Inferior Coarse Aggregate," *Proc., ASTM*, Vol. 43, 1943, pp. 981-1000.

8. Pickett, G., "Equations for Computing Elastic Constants from Flexural and Torsional Resonant Frequencies of Vibration of Prisms and Cylinders," *Proc., ASTM,* Vol. 45, 1945, p. 846.

9. Batchelder, G. M. and D. W. Lewis, "Comparison of Dynamic Methods of Testing Concretes Subjected to Freezing and Thawing," *Proc., ASTM,* Vol. 53, 1953, pp. 1053-1068.

10. Kesler, C. E., and Y. Higuchi, "Determination of Compressive Strength of Concrete by Using its Sonic Properties," *Proc., ASTM,* Vol. 53, 1953, pp. 1044-1051.

11. Malhotra, V. M. and V. Sivasundaram, "Resonance Frequency Methods," *CRC Handbook on Nondestructive Testing of Concrete*, 1991.

12. Gaidis, J. M. and A. M. Rosenberg, "New Test for Determining Fundamental Frequencies of Concrete," *Cement and Concrete Aggregates*, Vol. 8, No. 2, Winter 1986, pp. 117-119.

13. Coppola, J. A., and R. C. Bradt, "Thermal Shock Damage in SiC," *Journal of the American Ceramic Society*, Vol. 56, No. 4, 1973, pp. 214-218.

14. Swamy, R. N. and G. Rigby, "Dynamic Properties of Hardened Paste, Mortar, and Concrete," *Materials and Structures/Research and Testing* (Paris), Vol. 4, No. 19, 1971, p. 13.

15. Richardson, M., "Modal Analysis Using Digital Systems," *Seminar on Understanding Digital Control and Analysis in Vibration Test Systems,* The Shock and Vibration Information Center, 1975.

16. Clarke, S. L., "Improved Method for Non-Destructive Testing of Concrete Prisms," MS Thesis, Department of Mechanical Engineering, University of Washington, 1991.

17. Halvorsen, W. G. and D. L. Brown, "Impulse Technique for Structural Frequency Response Testing," *Sound and Vibration*, Vol. 11, No. 11, 1977, pp. 7-21.

18. Edwins, D. J., *Modal Testing: Theory and Practice*, Research Studies Press (Letchworth, Hertfordshire, England), Wiley (New York), 1984.

Appendix E
Tabulated Results

The following pages contain tabulated test results of all of the laboratory mixtures that were prepared for this project. To the extent possible, these results are grouped according to similar mixture components and properties (e.g., test results for all mixtures made with w/c+p=0.45, 15% Class C fly ash and high-range water reducer are grouped together).

The following abbreviations and notations are used in the tables:

Notation	Description
AEA	air-entraining admixture
WR/HRWR	water reducer or high-range water reducer
w/c	water-to-cement ratio
w/c+p	water to cementitious ratio
BSG (SSD)	bulk specific gravity (saturated, surface-dry condition)
Lbar	Power's spacing factor
Alpha	specific surface
P90	Philleo factor for 90% protected paste volume
P99	Philleo factor for 99% protected paste volume
Wsat	moisture content at saturation
Weq@XX%RH	moisture content at XX% relative humidity
K	coefficient of permeability
DF	durability factor
CA	coarse aggregate
UW	University of Washington
MSU	Michigan State University

Mix Design:	M25	M20	M50	M36	M66	A7	A4	E3A	M67	S1	N19	N41	N09	M73	M52	M37	D1/E1	E3B
Coarse Aggregate (lb)	2088	2086	2082	2082	2116	1899	1849	***	2110	1899	2112	2110	2101	2084	2101	2095	2078	2078
Fine Aggregate (lb)	1268	1267	1264	1264	1161	1266	1246	***	1135	1266	1135	1138	1147	1273	1244	1218	1090	1090
Cement (lb)	530	529	528	528	604	633	623	***	603	633	616	615	613	547	552	550	610	610
Water (lb)	239	238	238	238	242	253	249	***	241	253	246	246	245	219	221	220	244	244
Pozzolan (lb)	0	0	0	0	0	0	0	0	0	0	0	0	0	0	0	0	0	0
Admixtures:																		
AEA	None	None	None	None	AEA1	AEA1	AEA1	AEA1	AEA1	AEA1	AEA1	AEA1	AEA1	AEA1	AEA1	AEA1	AEA1	AEA1
WR/HRWR	None	None	None	None	None	None	None	None	None	None	WR	WR	WR	WR	WR	WR	WR	WR
Pozzolan or Accelerator	None	None	None	None	None	None	None	None	None	None	None	None	None	None	None	None	None	None
Fresh Air (%)	1.1	1.2	1.4	1.4	1.3	2.5	4.5	***	2.1	2.5	1.5	1.5	1.6	1.9	2.0	2.8	2.8	3.0
w/c	0.45	0.45	0.45	0.45	0.40	0.40	0.40	0.40	0.40	0.40	0.40	0.40	0.40	0.40	0.40	0.40	0.40	0.40
w/(c+p)	0.45	0.45	0.45	0.45	0.40	0.40	0.40	0.40	0.40	0.40	0.40	0.40	0.40	0.40	0.40	0.40	0.40	0.40
Physical Properties:																		
Avg. Comp. Strength (MPa)	45.9	40.5	42.2	36.4	45.1	41.9	42.7	46.8	49.0	41.9	43.6	45.9	51.0	43.8	43.2	42.2	43.4	40.6
BSG (SSD)	***	***	***	***	2.489	2.454	2.422	2.432	***	2.446	***	2.468	***	***	***	***	2.452	2.432
Air Void Measurements:																		
Hardened Air, Entrained (%)	***	0.6	0.9	0.4	0.5	1.1	3.2	***	0.7	1.7	***	***	***	***	0.8	0.6	1.7	1.7
Hardened Air, Total (%)	***	2.4	1.4	0.9	1.2	1.8	4.0	***	1.4	2.5	***	***	***	***	2.2	2.5	2.7	4.2
Lbar, Entrained (mm)	***	0.819	0.629	0.439	0.381	0.292	0.183	***	0.594	0.304	***	***	***	***	0.290	0.251	0.257	0.366
Lbar, Total (mm)	***	0.981	0.761	0.525	0.514	0.361	0.203	***	0.777	0.367	***	***	***	***	0.415	0.262	0.322	0.553
Alpha, Entrained (mm-1)	***	15.2	16.1	29.0	33.8	30.2	33.7	***	18.0	25.8	***	***	***	***	35.6	47.1	30.9	22.8
Alpha, Total (mm-1)	***	6.9	10.9	17.5	17.3	19.9	27.4	***	10.4	17.9	***	***	***	***	16.4	25.4	19.9	10.1
P90, Entrained (mm)	***	0.285	0.156	0.096	0.115	0.061	0.040	***	0.157	0.068	***	***	***	***	0.094	0.120	0.066	0.080
P99, Entrained (mm)	***	0.410	0.235	0.138	0.165	0.095	0.073	***	0.233	0.110	***	***	***	***	0.140	0.175	0.106	0.127
Water Pore Measurements:																		
Wsat (%)	***	***	***	***	4.86	5.84	5.92	5.66	***	5.70	***	5.27	***	***	***	***	5.15	5.66
Weq @ 97%RH (%)	***	***	***	***	4.65	5.44	5.52	5.11	***	5.41	***	4.97	***	***	***	***	4.72	5.11
Weq @ 92%RH (%)	***	***	***	***	4.42	5.33	5.41	5.04	***	5.24	***	4.76	***	***	***	***	4.65	5.04
Weq @ 75%RH (%)	***	***	***	***	3.76	4.50	4.70	4.30	***	4.54	***	3.88	***	***	***	***	4.05	4.30
Weq @ 53%RH (%)	***	***	***	***	***	***	***	2.99	***	3.72	***	***	***	***	***	***	2.85	2.99
Weq @ 31%RH (%)	***	***	***	***	***	***	***	***	***	2.57	***	***	***	***	***	***	2.57	***
Freezable Water (%)	***	***	***	***	0.60	0.66	0.58	0.74	***	0.58	***	0.75	***	***	***	***	0.65	0.74
K (m/s x 1E-12)	***	***	3.2	4.6	***	4.3	18.0	3.4	***	***	***	***	12.2	***	***	6.7	2.3	***
Durability Test Results:																		
DF, Avg.	4	***	14	***	39	26	69	51	***	41	15	19	13	95	80	93	8	35
DF, Std. Dev.	0.7	***	1.9	***	5.6	4.2	8.4	8.8	***	4.6	2.0	1.9	1.5	2.2	5.5	1.3	3.4	5.9
Mass Loss (%)	***	***	***	***	***	0.13	0.31	0.14	***	***	***	***	***	***	***	***	0.26	-0.02
Dilation (%)	***	***	***	***	***	0.087	0.082	0.072	***	***	***	***	***	***	***	***	0.127	0.068
Notes:				Cast UW Test MSU				56-day cure	Cast UW Test MSU	Cast MSU Test UW								56-day cure

Mix Design:	M87	M60	M57	N00	N56	M42	N29	N28	E2B	A5A	A2	N26	A5	E4	A8A	A8	S2
Coarse Aggregate (lb)	2101	2093	2099	2096	2101	2101	2110	2095	1894	1879	1888	2101	***	***	1894	***	***
Fine Aggregate (lb)	1243	1320	1284	1142	1153	1263	1168	1160	1352	1252	1258	1141	***	***	1352	***	***
Cement (lb)	550	510	529	599	600	530	558	554	559	554	502	567	***	***	559	***	***
Water (lb)	220	203	212	240	240	212	251	249	251	249	226	255	***	***	251	***	***
Pozzolan (lb)	0	0	0	0	0	0	0	0	0	0	0	0	0	0	0	0	0
Admixtures:																	
AEA	AEA1	AEA1	AEA1	AEA1	AEA1	AEA1	AEA1	AEA1	AEA1	AEA1	AEA1	AEA1	AEA1	AEA1	AEA1	AEA1	AEA1
WR/HRWR	HRWR1	HRWR1	HRWR2	HRWR2	HRWR2	HRWR2	None	None	None	None	None	None	None	None	None	None	None
Pozzolan or Accelerator	None	None	None	None	None	None	None	None	None	None	None	None	None	None	None	None	None
Fresh Air (%)	2.1	2.3	2.1	2.4	2.4	2.5	1.6	2.3	2.2	5.0	7.0	2.0	***	***	2.2	***	***
w/c	0.40	0.40	0.40	0.40	0.40	0.40	0.45	0.45	0.45	0.45	0.45	0.45	0.45	0.45	0.45	0.45	***
w/(c+p)	0.40	0.40	0.40	0.40	0.40	0.40	0.45	0.45	0.45	0.45	0.45	0.45	0.45	0.45	0.45	0.45	***
Physical Properties:																	
Avg. Comp. Strength (MPa)	48.4	42.7	33.7	47.9	44.1	45.3	42.2	43.6	40.9	41.9	35.3	33.7	39.5	45.8	40.9	40.9	***
BSG (SSD)	2.475	2.480	***	2.472	***	***	***	***	***	***	2.390	2.433	2.399	***	***	2.446	2.438
Air Void Measurements:																	
Hardened Air, Entrained (%)	0.3	0.5	***	***	***	***	***	***	1.1	3.0	2.9	***	***	***	1.1	***	1.5
Hardened Air, Total (%)	1.5	1.4	***	***	***	***	***	***	1.8	3.2	3.8	***	***	***	1.8	***	2.4
Lbar, Entrained (mm)	0.654	0.443	***	***	***	***	***	***	0.269	0.288	0.195	***	***	***	0.269	***	0.354
Lbar, Total (mm)	0.588	0.432	***	***	***	***	***	***	0.331	0.294	0.221	***	***	***	0.331	***	0.431
Alpha, Entrained (mm-1)	24.9	27.3	***	***	***	***	***	***	31.3	24.2	30.7	***	***	***	31.3	***	21.8
Alpha, Total (mm-1)	13.8	17.9	***	***	***	***	***	***	20.9	23.3	24.1	***	***	***	20.9	***	14.7
P90, Entrained (mm)	0.236	0.098	***	***	***	***	***	***	0.067	0.044	0.037	***	***	***	0.067	***	0.078
P99, Entrained (mm)	0.328	0.142	***	***	***	***	***	***	0.106	0.075	0.069	***	***	***	0.106	***	0.127
Water Pore Measurements:																	
Wsat (%)	5.15	4.63	***	5.16	***	***	***	***	***	***	6.07	5.66	5.86	***	***	5.67	5.90
Weq @ 97%RH (%)	4.80	4.34	***	4.90	***	***	***	***	***	***	5.30	5.35	5.34	***	***	5.23	5.55
Weq @ 92%RH (%)	4.67	4.23	***	4.67	***	***	***	***	***	***	5.14	5.04	5.20	***	***	5.06	5.30
Weq @ 75%RH (%)	3.87	3.37	***	4.03	***	***	***	***	***	***	4.01	3.69	4.14	***	***	4.17	4.45
Weq @ 53%RH (%)	2.83	2.64	***	***	***	***	***	***	***	***	***	***	***	***	***	3.27	3.55
Weq @ 31%RH (%)	1.83	1.60	***	***	***	***	***	***	***	***	***	***	***	***	***	2.06	2.38
Freezable Water (%)	0.68	0.60	***	0.59	***	***	***	***	***	***	0.91	1.15	0.85	***	***	0.74	0.68
K (m/s x 1E-12)	3.8	8.5	***	***	***	***	***	***	***	***	2.9	***	3.9	16.0	***	***	***
Durability Test Results:																	
DF, Avg.	29	73	58	91	69	94	***	***	28	79	92	***	95	*22	28	55	40
DF, Std. Dev.	7.8	2.3	9.4	2.5	10.0	1.7	***	***	6.8	5.2	3.3	***	2.9	*10	6.8	10.1	3.4
Mass Loss (%)	***	***	***	***	***	***	***	***	-0.10	0.21	0.15	***	0.41	*.285	-0.10	0.65	***
Dilation (%)	***	***	***	***	***	***	***	***	0.089	0.054	0.030	***	0.016	*.1215	0.089	0.081	***
Notes:												14-day cure	51-day cure	56-day cure		42-day cure	Cast MSU Test UW

Mix Design:	M27	M59	M98	M99	N18	N40	N08	M69	M54	M38	D2/E2	E4A	M88	M61	N21	N57
Coarse Aggregate (lb)	2101	2096	2113	2090	2114	2112	2095	2095	2095	2095	2079	2079	2107	2099	2108	2101
Fine Aggregate (lb)	1186	1206	1148	1136	1193	1192	1201	1304	1291	1269	1185	1185	1267	1369	1235	1222
Cement (lb)	533	532	570	564	548	547	543	489	489	489	525	525	501	453	513	511
Water (lb)	240	240	257	254	246	246	244	220	220	220	236	236	226	204	231	230
Pozzolan (lb)	0	0	0	0	0	0	0	0	0	0	0	0	0	0	0	0
Admixtures:																
AEA	AEA1	AEA1	AEA1	AEA1	AEA1	AEA1	AEA1	AEA1	AEA1	AEA1	AEA1	AEA1	AEA1	AEA1	AEA1	AEA1
WR/HRWR	None	None	None	None	WR	WR	WR	WR	WR	WR	WR	WR	HRWR1	HRWR1	HRWR1	HRWR1
Pozzolan or Accelerator	None	None	None	None	None	None	None	None	None	None	None	None	None	None	None	None
Fresh Air (%)	2.5	2.2	1.4	2.5	1.4	1.5	1.9	2.0	2.3	2.8	2.7	2.7	2.0	2.1	2.2	5.2
w/c	0.45	0.45	0.45	0.45	0.45	0.45	0.45	0.45	0.45	0.45	0.45	0.45	0.45	0.45	0.45	0.45
w/(c+p)	0.45	0.45	0.45	0.45	0.45	0.45	0.45	0.45	0.45	0.45	0.45	0.45	0.45	0.45	0.45	0.45
Physical Properties:																
Avg. Comp. Strength (MPa)	29.4	42.8	41.8	43.5	40.2	40.2	45.0	43.0	34.0	33.9	38.8	30.4	43.6	38.1	37.3	32.9
BSG (SSD)	***	***	2.465	2.459	***	***	***	2.472	***	***	2.438	2.446	***	***	2.456	***
Air Void Measurements:																
Hardened Air, Entrained (%)	1.2	0.5	1.0	1.0	***	0.2	***	0.7	0.8	1.0	2.1	2.1	***	0.8	***	***
Hardened Air, Total (%)	2.0	1.3	1.8	1.7	***	1.3	***	1.6	2.0	2.9	3.8	3.8	***	1.5	***	***
Lbar, Entrained (mm)	0.252	0.325	0.429	0.243	***	0.412	***	0.341	0.420	0.263	0.238	0.238	***	0.538	***	***
Lbar, Total (mm)	0.303	0.377	0.550	0.267	***	0.403	***	0.383	0.610	0.305	0.315	0.315	***	0.688	***	***
Alpha, Entrained (mm-1)	32.5	39.1	22.0	38.5	***	42.6	***	28.0	24.4	35.7	30.4	30.4	***	18.0	***	***
Alpha, Total (mm-1)	21.0	22.2	13.2	27.9	***	20.9	***	17.9	11.4	19.1	17.6	17.6	***	10.6	***	***
P90, Entrained (mm)	0.084	0.123	0.140	0.093	***	0.171	***	0.072	0.164	0.089	0.037	0.037	***	0.134	***	***
P99, Entrained (mm)	0.134	0.176	0.213	0.142	***	0.235	***	0.110	0.245	0.136	0.062	0.062	***	0.203	***	***
Water Pore Measurements:																
Wsat (%)	***	***	5.25	5.14	***	***	***	4.99	***	***	5.90	5.68	***	***	5.51	***
Weq @ 97%RH (%)	***	***	4.98	4.85	***	***	***	4.65	***	***	5.55	4.94	***	***	5.15	***
Weq @ 92%RH (%)	***	***	4.81	4.69	***	***	***	4.49	***	***	5.30	4.83	***	***	4.81	***
Weq @ 75%RH (%)	***	***	3.76	3.65	***	***	***	3.50	***	***	4.45	4.00	***	***	3.79	***
Weq @ 53%RH (%)	***	***	***	***	***	***	***	2.50	***	***	3.55	2.70	***	***	***	***
Weq @ 31%RH (%)	***	***	***	***	***	***	***	1.59	***	***	2.38	***	***	***	***	***
Freezable Water (%)	***	***	0.85	0.85	***	***	***	0.75	***	***	0.70	0.78	***	***	0.92	***
K (m/s x 1E-12)	2.4	***	***	***	***	6.1	***	3.4	***	5.2	1.8	5.5	***	25.0	6.2	***
Durability Test Results:																
DF, Avg.	***	57	43	73	11	15	11	72	82	89	16	13	19	23	19	91
DF, Std. Dev.	***	5.0	1.4	4.4	2.2	1.7	0.7	7.8	8.5	1.9	3.9	2.8	5.5	2.1	3.0	4.6
Mass Loss (%)					***	***	***	***	***	***	0.11	0.12	***	***	***	***
Dilation (%)					***	***	***	***	***	***	0.090	0.092	***	***	***	***
Notes:	Original CA	Original CA	Restocked CA	Restocked CA								56-day cure				

Mix Design:	N55	N01	M58	M43	N31	N30	A9	A6	A3	M75	N13	N39	M55
Coarse Aggregate (lb)	2101	2108	2092	2096	2109	2092	2064	2030	1966	2114	2111	2103	2093
Fine Aggregate (lb)	1209	1144	1329	1310	1210	1201	1293	1279	1263	1174	1088	1083	1156
Cement (lb)	533	557	469	470	492	488	462	420	414	604	641	638	598
Water (lb)	240	251	211	212	256	254	238	218	215	241	256	255	239
Pozzolan (lb)	0	0	0	0	0	0	0	0	0	0	0	0	0
Admixtures:													
AEA	AEA1	AEA1	AEA1	AEA1	AEA1	AEA1	AEA1	AEA1	AEA1	AEA2	AEA2	AEA2	AEA2
WR/HRWR	HRWR2	HRWR2	HRWR2	HRWR2	None	None	None	None	None	None	None	None	None
Pozzolan or Accelerator	None	None	None	None	None	None	None	None	None	None	None	None	None
Fresh Air (%)	2.1	2.2	2.4	2.7	1.6	2.4	2.4	5.4	7.5	1.1	1.5	1.9	2.2
w/c	0.45	0.45	0.45	0.45	0.52	0.52	0.51	0.52	0.52	0.40	0.40	0.40	0.40
w/(c+p)	0.45	0.45	0.45	0.45	0.52	0.52	0.51	0.52	0.52	0.40	0.40	0.40	0.40
Physical Properties:													
Avg. Comp. Strength (MPa)	38.5	49.1	36.9	33.3	32.5	32.4	35.4	34.6	25.8	37.9	43.3	45.4	39.1
BSG (SSD)	***	2.472	***	***	***	***	2.454	2.412	2.173	***	***	***	***
Air Void Measurements:													
Hardened Air, Entrained (%)	***	0.4	1.4	***	***	***	1.2	3.5	4.2	0.5	***	***	***
Hardened Air, Total (%)	***	1.8	2.1	***	***	***	1.8	4.4	4.8	1.7	***	***	***
Lbar, Entrained (mm)	***	0.366	0.446	***	***	***	0.427	0.254	0.181	0.536	***	***	***
Lbar, Total (mm)	***	0.423	0.530	***	***	***	0.523	0.279	0.193	0.790	***	***	***
Alpha, Entrained (mm-1)	***	39.0	18.0	***	***	***	24.5	25.0	28.1	23.9	***	***	***
Alpha, Total (mm-1)	***	17.7	12.6	***	***	***	16.6	20.5	24.9	9.6	***	***	***
P90, Entrained (mm)	***	0.134	0.119	***	***	***	0.060	0.054	0.025	0.182	***	***	***
P99, Entrained (mm)	***	0.189	0.191	***	***	***	0.090	0.098	0.057	0.261	***	***	***
Water Pore Measurements:													
Wsat (%)	***	5.09	***	***	***	***	5.72	5.66	5.90	***	***	***	***
Weq @ 97%RH (%)	***	4.85	***	***	***	***	5.23	5.05	5.05	***	***	***	***
Weq @ 92%RH (%)	***	4.57	***	***	***	***	5.05	4.85	4.82	***	***	***	***
Weq @ 75%RH (%)	***	3.89	***	***	***	***	3.77	3.58	3.57	***	***	***	***
Weq @ 53%RH (%)	***	***	***	***	***	***	***	***	***	***	***	***	***
Weq @ 31%RH (%)	***	***	***	***	***	***	***	***	***	***	***	***	***
Freezable Water (%)	***	0.64	***	***	***	***	1.03	1.03	1.03	***	***	***	***
K (m/s x 1E-12)	***	***	5.8	***	***	***	12.0	15.0	1.6	***	***	***	6.8
Durability Test Results:													
DF, Avg.	47	52	52	96	***	***	8	88	86	21	13	23	89
DF, Std. Dev.	4.7	2.8	5.4	1.1	***	***	3.4	4.8	2.9	2.7	1.5	6.1	2.9
Mass Loss (%)	***	***	***	***	***	***	0.26	0.46	0.27	***	***	***	***
Dilation (%)	***	***	***	***	***	***	0.127	0.028	0.042	***	***	***	***
Notes:													

Mix Design:	N15	N34	M72	M51	N11	M71	N35	M39	D3A	D3B	M63	M85	M76	N12	N38	M56
Coarse Aggregate (lb)	2105	2106	2097	2101	2093	2092	2097	2090	2093	2093	2093	2104	2107	2096	2103	2098
Fine Aggregate (lb)	1149	1131	1255	1244	1142	1252	1127	1215	1101	1101	1320	1264	1226	1157	1143	1208
Cement (lb)	614	614	551	552	610	550	611	549	615	615	510	531	535	565	567	533
Water (lb)	245	245	220	221	244	220	244	220	246	246	203	212	241	254	255	240
Pozzolan (lb)	0	0	0	0	0	0	0	0	0	0	0	0	0	0	0	0
Admixtures:																
AEA	AEA2	AEA2	AEA2	AEA2	AEA2	AEA2	AEA2	AEA2	AEA2	AEA2	AEA2	AEA2	AEA2	AEA2	AEA2	AEA2
WR/HRWR	WR	WR	WR	WR	WR	WR	WR	WR	WR	WR	HRWR1	HRWR1	None	None	None	None
Pozzolan or Accelerator	None	None	None	None	None	None	None	None	None	None	None	None	None	None	None	None
Fresh Air (%)	1.4	1.8	1.9	2.0	2.0	2.1	2.2	3.0	2.0	2.0	2.3	2.4	1.4	1.8	1.9	2.1
w/c	0.40	0.40	0.40	0.40	0.40	0.40	0.40	0.40	0.40	0.40	0.40	0.40	0.45	0.45	0.45	0.45
w/(c+p)	0.40	0.40	0.40	0.40	0.40	0.40	0.40	0.40	0.40	0.40	0.40	0.40	0.45	0.45	0.45	0.45
Physical Properties:																
Avg. Comp. Strength (MPa)	48.0	48.1	43.3	49.1	50.5	48.1	47.0	33.3	49.6	49.6	44.7	45.8	33.1	37.2	42.0	35.0
BSG (SSD)	***	2.453	***	***	***	***	***	***	2.459	***	2.471	2.475	***	***	***	2.475
Air Void Measurements:																
Hardened Air, Entrained (%)	***	***	***	***	***	***	***	***	1.7	1.2	0.5	0.2	***	***	***	1.3
Hardened Air, Total (%)	***	***	***	***	***	***	***	***	2.0	2.5	1.8	1.8	***	***	***	1.9
Lbar, Entrained (mm)	***	***	***	***	***	***	***	***	0.133	0.224	0.522	0.382	***	***	***	0.319
Lbar, Total (mm)	***	***	***	***	***	***	***	***	0.147	0.330	0.545	0.536	***	***	***	0.363
Alpha, Entrained (mm-1)	***	***	***	***	***	***	***	***	49.5	43.8	21.7	44.6	***	***	***	26.7
Alpha, Total (mm-1)	***	***	***	***	***	***	***	***	40.9	21.5	12.1	13.4	***	***	***	19.7
P90, Entrained (mm)	***	***	***	***	***	***	***	***	0.038	0.083	0.142	0.173	***	***	***	0.074
P99, Entrained (mm)	***	***	***	***	***	***	***	***	0.066	0.126	0.209	0.239	***	***	***	0.117
Water Pore Measurements:																
Wsat (%)	***	5.31	***	***	***	***	***	***	5.42	***	4.64	5.04	***	***	***	5.19
Weq @ 97%RH (%)	***	5.12	***	***	***	***	***	***	4.81	***	4.35	4.69	***	***	***	4.89
Weq @ 92%RH (%)	***	4.92	***	***	***	***	***	***	4.73	***	4.22	4.54	***	***	***	4.66
Weq @ 75%RH (%)	***	4.03	***	***	***	***	***	***	4.11	***	3.57	3.83	***	***	***	3.80
Weq @ 53%RH (%)	***	***	***	***	***	***	***	***	2.96	***	***	***	***	***	***	***
Weq @ 31%RH (%)	***	***	***	***	***	***	***	***	***	***	***	***	***	***	***	***
Freezable Water (%)	***	0.75	***	***	***	***	***	***	0.64	***	0.54	0.60	***	***	***	0.75
K (m/s x 1E-12)	5.8	***	***	***	***	7.4	***	1.5	***	***	3.7	15.0	***	***	4.5	2.7
Durability Test Results:																
DF, Avg.	10	44	86	90	7	86	56	97	20	20	41	70	13	6	22	70
DF, Std. Dev.	0.7	2.5	5.2	5.2	1.0	4.9	6.8	1.1	4.1	4.1	4.0	11.3	2.0	0.4	3.6	9.2
Mass Loss (%)	***	***	***	***	***	***	***	***	0.10	0.10	***	***	***	***	***	***
Dilation (%)	***	***	***	***	***	***	***	***	0.088	0.088	***	***	***	***	***	***
Notes:									56-day cure	56-day cure						

Mix Design:	N10	N43	M65	M40	N42	D4	M62	N20	M86	N06	M64	M44	M74	N07	N14	M53
Coarse Aggregate (lb)	2101	2101	2100	2100	2084	2072	2096	2102	2110	2103	2107	2101	2109	2103	2090	2092
Fine Aggregate (lb)	1204	1195	1263	1241	1185	1147	1369	1208	1273	1110	1157	1131	1227	1169	1175	1204
Cement (lb)	544	545	507	507	540	541	452	522	482	638	602	600	535	567	564	531
Water (lb)	245	245	228	228	243	243	203	235	217	255	241	240	241	255	254	239
Pozzolan (lb)	0	0	0	0	0	0	0	0	0	0	0	0	0	0	0	0
Admixtures:																
AEA	AEA2	AEA2	AEA2	AEA2	AEA2	AEA2	AEA2	AEA2	AEA2	AEA3	AEA3	AEA3	AEA3	AEA3	AEA3	AEA3
WR/HRWR	WR	WR	WR	WR	WR	WR	HRWR1	HRWR1	HRWR1	None	None	None	None	None	None	None
Pozzolan or Accelerator	None	None	None	None	None	None	None	None	None	None	None	None	None	None	None	None
Fresh Air (%)	1.6	1.8	2.0	2.5	2.6	3.0	2.2	2.5	2.7	1.3	1.7	2.5	1.3	1.3	1.6	2.4
w/c	0.45	0.45	0.45	0.45	0.45	0.45	0.45	0.45	0.45	0.40	0.40	0.40	0.45	0.45	0.45	0.45
w/(c+p)	0.45	0.45	0.45	0.45	0.45	0.45	0.45	0.45	0.45	0.40	0.40	0.40	0.45	0.45	0.45	0.45
Physical Properties:																
Avg. Comp. Strength (MPa)	43.5	37.4	36.9	37.8	38.3	41.9	36.8	39.7	49.7	54.2	47.8	38.4	42.0	45.5	42.7	44.0
BSG (SSD)	***	***	2.481	***	***	2.431	***	2.444	2.465	2.480	2.483	***	2.477	2.469	***	***
Air Void Measurements:																
Hardened Air, Entrained (%)	***	***	1.0	1.2	***	2.1	0.5	0.5	1.2	0.2	0.7	***	0.5	0.4	***	***
Hardened Air, Total (%)	***	***	1.4	2.2	***	3.3	1.6	1.9	1.7	1.1	1.4	***	1.2	1.1	***	***
Lbar, Entrained (mm)	***	***	0.290	0.343	***	0.205	0.466	0.388	0.323	0.727	0.320	***	0.387	0.405	***	***
Lbar, Total (mm)	***	***	0.327	0.440	***	0.256	0.594	0.465	0.367	0.654	0.380	***	0.417	0.488	***	***
Alpha, Entrained (mm-1)	***	***	30.7	24.4	***	37.1	24.3	33.6	26.1	23.6	35.1	***	30.4	36.5	***	***
Alpha, Total (mm-1)	***	***	23.2	14.7	***	24.2	12.2	16.4	19.9	13.9	21.8	***	20.3	19.2	***	***
P90, Entrained (mm)	***	***	0.074	0.094	***	0.054	0.119	0.150	0.084	0.202	0.138	***	0.117	0.120	***	***
P99, Entrained (mm)	***	***	0.115	0.149	***	0.088	0.174	0.214	0.133	0.278	0.203	***	0.171	0.168	***	***
Water Pore Measurements:																
Wsat (%)	***	***	4.92	***	***	5.62	***	5.24	4.70	4.80	4.99	***	5.02	5.13	***	***
Weq @ 97%RH (%)	***	***	4.59	***	***	5.15	***	4.87	4.19	4.55	4.74	***	4.73	4.82	***	***
Weq @ 92%RH (%)	***	***	4.40	***	***	5.04	***	4.64	4.04	4.42	4.64	***	4.58	4.62	***	***
Weq @ 75%RH (%)	***	***	3.61	***	***	4.08	***	3.47	3.19	3.75	3.86	***	3.49	3.62	***	***
Weq @ 53%RH (%)	***	***	***	***	***	2.77	***	***	***	***	2.93	***	***	***	***	***
Weq @ 31%RH (%)	***	***	***	***	***	***	***	***	***	***	1.90	***	***	***	***	***
Freezable Water (%)	***	***	0.68	***	***	0.83	***	0.98	0.70	0.55	0.63	***	0.87	0.84	***	***
K (m/s x 1E-12)	***	21.1	11.0	4.3	3.6	13.0	***	5.3	***	***	5.6	***	***	***	1.9	***
Durability Test Results:																
DF, Avg.	8	30	63	85	86	59	22	35	52	32	63	91	81	22	4	94
DF, Std. Dev.	0.2	2.8	5.4	5.6	3.8	19.3	3.4	5.7	10.9	2.1	11.4	4.0	4.6	2.0	0.3	1.4
Mass Loss (%)	***	***	***	***	***	0.02	***	***	***	***	***	***	***	***	***	***
Dilation (%)	***	***	***	***	***	0.026	***	***	***	***	***	***	***	***	***	***
Notes:																

Mix Design:	D9/E5	D9/E5B	D9/E5A	E7	D17/E13	E15	E9C	E11	E17	E19	D13	D21	D10/E6	E8	D18/E14	E16
Coarse Aggregate (lb)	***	2090	2089	***	2109	2109	2092	2092	2100	2100	2084	2071	2091	2091	2092	2092
Fine Aggregate (lb)	***	1109	1042	***	1078	1078	1093	1093	1082	1082	1120	1206	1152	1152	1177	1177
Cement (lb)	***	517	542	***	547	547	458	458	474	474	516	472	467	467	468	468
Water (lb)	***	238	249	***	251	251	237	237	247	247	237	217	242	242	242	242
Pozzolan (lb)	0	77	81	0	83	83	137	137	142	142	77	71	70	70	70	70
Admixtures:																
AEA	AEA1	AEA1	AEA1	AEA1	AEA1	AEA1	AEA1	AEA1	AEA1	AEA1	AEA1	AEA1	AEA1	AEA1	AEA1	AEA1
WR/HRWR	WR	WR	WR	WR	WR	WR	WR	WR	WR	WR	HRWR1	HRWR1	WR	WR	WR	WR
Pozzolan or Accelerator	15% FAF	15% FAF	15% FAF	15% FAF	15% FAC	15% FAC	30% FAF	30% FAF	30% FAC	30% FAC	15% FAF	15% FAC	15% FAF	15% FAF	15% FAC	15% FAC
Fresh Air (%)		2.2	2.5	***	2.0	2.0	2.8	2.8	2.4	2.4	2.2	3.0	2.8	2.8	2.5	2.5
w/c	0.46	0.46	0.46	0.46	0.46	0.46	0.52	0.52	0.52	0.52	0.46	0.46	0.52	0.52	0.52	0.52
w/(c+p)	0.40	0.40	0.40	0.40	0.40	0.40	0.40	0.40	0.40	0.40	0.40	0.40	0.45	0.45	0.45	0.45
Physical Properties:																
Avg. Comp. Strength (MPa)	42.3	39.9	42.1	44.7	38.2	30.9	36.3	31.0	25.6	32.5	41.5	25.6	38.8	47.9	37.3	30.8
BSG (SSD)	***	2.470	2.441	***	***	***	***	***	2.453	***	2.463	2.464	***	2.432	2.477	2.473
Air Void Measurements:																
Hardened Air, Entrained (%)	***	0.7	1.3	***	1.6	1.6	2.5	2.5	1.6	1.6	1.5	1.0	2.0	2.0	1.2	1.2
Hardened Air, Total (%)	***	1.9	2.6	***	2.2	2.2	2.6	2.6	2.7	2.7	1.8	1.6	2.4	2.4	2.2	2.2
Lbar, Entrained (mm)	***	0.292	0.185	***	0.190	0.190	0.132	0.132	0.236	0.236	0.367	0.400	0.224	0.224	0.284	0.284
Lbar, Total (mm)	***	0.481	0.263	***	0.222	0.222	0.134	0.134	0.302	0.302	0.399	0.512	0.245	0.245	0.383	0.383
Alpha, Entrained (mm-1)	***	43.1	45.6	***	30.1	30.1	38.8	38.8	32.2	32.2	25.7	30.6	32.6	32.6	32.0	32.0
Alpha, Total (mm-1)	***	17.2	23.7	***	21.9	21.9	37.6	37.6	20.2	20.2	21.7	19.4	27.6	27.6	18.3	18.3
P90, Entrained (mm)	***	0.087	0.059	***	0.032	0.032	0.029	0.029	0.049	0.049	0.050	0.074	0.050	0.050	0.043	0.043
P99, Entrained (mm)	***	0.125	0.093	***	0.063	0.063	0.063	0.063	0.080	0.080	0.077	0.107	0.084	0.084	0.066	0.066
Water Pore Measurements:																
Wsat (%)	***	5.36	6.03	***	***	***	***	***	5.37	***	5.20	5.34	***	5.40	5.17	5.31
Weq @ 97%RH (%)	***	4.75	5.42	***	***	***	***	***	***	***	4.74	4.93	***	***	***	***
Weq @ 92%RH (%)	***	4.67	5.27	***	***	***	***	***	4.82	***	4.64	4.81	***	4.79	4.67	4.81
Weq @ 75%RH (%)	***	4.09	4.69	***	***	***	***	***	4.12	***	4.24	4.34	***	4.02	3.83	4.01
Weq @ 53%RH (%)	***	2.89	3.47	***	***	***	***	***	3.25	***	3.16	3.17	***	3.11	2.97	3.10
Weq @ 31%RH (%)	***	***	2.07	***	***	***	***	***	2.14	***	***	***	***	1.88	1.82	1.94
Freezable Water (%)	0.55	0.64	0.66	***	***	***	***	***	0.62	0.45	0.54	0.60	0.59	0.66	0.67	0.67
K (m/s x 1E-12)	1.4	***	***	***	***	***	***	***	6.1	9.3	7.6	9.8	2.2	2.6	2.0	3.0
Durability Test Results:																
DF, Avg.	94	16	13	83	29	24	65	45	62	61	14	12	89	80	15	13
DF, Std. Dev.	2.1	2.1	8.6	1.2	4.6	4.2	8.0	18.0	3.7	4.5	2.2	5.1	5.0	2.4	4.1	5.9
Mass Loss (%)	0.09	-0.00	0.12	0.02	0.23	0.16	0.14	0.16	0.12	0.08	0.30	0.11	0.21	0.13	0.23	0.14
Dilation (%)	0.011	0.086	0.061	0.034	0.089	0.084	0.073	0.106	0.066	0.076	0.099	0.093	0.027	0.043	0.072	0.084
Notes:				56-day cure		56-day cure		56-day cure		56-day cure				56-day cure		56-day cure

Mix Design:	E10	E12	E18	E18A	E20	E20A	D14A	D14B	D22A	D22B	D22C	D11A	D11B	D19	D15	D23
Coarse Aggregate (lb)	2099	2099	2090	2109	2107	2109	2073	2073	2076	2091	2076	2100	2076	2105	2070	2074
Fine Aggregate (lb)	1156	1156	1173	1183	1182	1183	1115	1115	1117	1146	1117	1097	1021	1096	1132	1207
Cement (lb)	409	409	407	411	411	411	478	478	479	475	479	528	555	538	504	472
Water (lb)	238	238	237	239	239	239	247	247	248	246	248	243	255	250	232	215
Pozzolan (lb)	123	123	122	123	123	123	72	72	72	72	72	79	83	81	75	71
Admixtures:																
AEA	AEA1	AEA1	AEA1	AEA1	AEA1	AEA1	AEA1	AEA1	AEA1	AEA1	AEA1	AEA2	AEA2	AEA2	AEA2	AEA2
WR/HRWR	WR	WR	WR	WR	WR	WR	HRWR1	HRWR1	HRWR1	HRWR1	HRWR1	WR	WR	WR	HRWR1	HRWR1
Pozzolan or Accelerator	30% FAF	30% FAF	30% FAC	30% FAC	30% FAC	30% FAC	15% FAF	15% FAF	15% FA	15% FAC	15% FAC	15% FAF	15% FAF	15% FAC	15% FAF	15% FAC
Fresh Air (%)	2.5	2.5	2.9	2.0	2.1	2.0	2.8	2.8	2.9	2.1	2.9	2.4	2.6	2.0	2.8	3.0
w/c	0.58	0.58	0.58	0.58	0.58	0.58	0.52	0.52	0.52	0.52	0.52	0.46	0.46	0.46	0.46	0.46
w/(c+p)	0.45	0.45	0.45	0.45	0.45	0.45	0.45	0.45	0.45	0.45	0.45	0.40	0.40	0.40	0.40	0.40
Physical Properties:																
Avg. Comp. Strength (MPa)	42.6	24.4	25.0	38.7	38.7	***	34.1	30.2	41.7	24.9	41.7	***	39.5	38.5	32.9	31.1
BSG (SSD)	***	***	2.435	2.445	2.466	***	2.437	2.446	2.445	2.441	***	***	2.439	2.450	2.437	2.452
Air Void Measurements:																
Hardened Air, Entrained (%)	0.5	0.5	***	0.6	***	0.6	1.9	0.7	2.7	0.7	2.2	***	1.4	0.9	1.5	1.5
Hardened Air, Total (%)	0.6	0.6	***	1.3	***	1.3	2.3	1.4	3.3	1.5	3.7	***	2.9	1.3	3.0	3.4
Lbar, Entrained (mm)	0.412	0.412	***	0.302	***	0.302	0.198	0.431	0.176	0.668	0.338	***	0.192	0.349	0.213	0.404
Lbar, Total (mm)	0.448	0.448	***	0.433	***	0.433	0.221	0.590	0.194	0.903	0.430	***	0.272	0.421	0.297	0.598
Alpha, Entrained (mm-1)	28.3	28.3	***	43.5	***	43.5	42.2	30.6	43.3	19.7	24.5	***	42.0	29.9	43.2	25.7
Alpha, Total (mm-1)	24.1	24.1	***	22.6	***	22.6	34.5	17.0	36.0	10.7	15.4	***	21.6	21.2	23.4	12.0
P90, Entrained (mm)	0.061	0.061	***	0.066	***	0.066	0.046	0.103	0.043	0.063	0.073	***	0.050	0.108	0.055	0.101
P99, Entrained (mm)	0.089	0.089	***	0.095	***	0.095	0.073	0.147	0.070	0.090	0.116	***	0.080	0.161	0.085	0.151
Water Pore Measurements:																
Wsat (%)	***	***	5.50	5.87	5.09	***	5.75	5.97	5.83	6.30	***	***	5.90	5.37	5.84	5.00
Weq @ 97%RH (%)	***	***	***	5.18	***	***	5.18	5.52	5.21	5.79	***	***	5.48	***	5.39	4.63
Weq @ 92%RH (%)	***	***	4.76	5.06	4.57	***	5.00	5.30	5.07	5.56	***	***	5.35	4.80	5.20	4.39
Weq @ 75%RH (%)	***	***	3.95	4.53	3.80	***	4.39	4.54	4.39	4.41	***	***	4.65	4.15	4.61	3.75
Weq @ 53%RH (%)	***	***	2.99	3.21	3.04	***	3.12	3.64	3.07	3.49	***	***	3.45	3.31	3.75	2.98
Weq @ 31%RH (%)	***	***	1.87	***	2.11	***	***	1.80	***	1.72	***	***	2.09	2.16	2.04	1.50
Freezable Water (%)	***	***	0.70	0.67	0.60	***	0.70	0.64	0.73	0.80	0.98	***	0.70	0.59	0.56	0.56
K (m/s x 1E-12)	***	***	5.5	37.0	5.7	***	10.0	5.5	7.2	***	***	***	***	9.9	5.5	9.9
Durability Test Results:																
DF, Avg.	67	38	***	29	70	***	39	15	35	14	35	70	36	50	43	56
DF, Std. Dev.	14.3	4.5	***	3.1	6.3	***	7.9	3.3	9.7	2.0	9.7	6.5	22.2	12.3	9.8	7.3
Mass Loss (%)	0.21	0.16	***	0.07	0.17	***	-0.02	0.16	0.28	0.12	0.28	0.17	0.13	0.21	0.19	0.08
Dilation (%)	0.066	0.109	***	0.066	0.057	***	0.051	0.054	0.080	0.074	0.080	0.072	0.075	0.077	0.096	0.076
Notes:	f'c= 56-day	56-day cure	Not Tested		56-day cure	56-day cure										

Mix Design:	D12	D20	D16	D24	E21	E23	D25/E25	E27	E22	E24	D26/E26B	E28	D26A/E2	D27	D28
Coarse Aggregate (lb)	2092	2108	2079	2089	2080	2080	2072	2072	2146	2146	2069	2162	2039	2076	2078
Fine Aggregate (lb)	1223	1226	1136	1141	1229	1229	1158	1158	1190	1190	1304	1214	1210	1118	1300
Cement (lb)	438	448	472	474	495	495	488	488	463	463	396	398	419	505	398
Water (lb)	226	232	244	245	214	214	224	224	225	225	205	207	243	233	206
Pozzolan (lb)	66	68	71	71	40	40	73	73	37	37	59	60	63	76	60
Admixtures:															
AEA	AEA2	AEA2	AEA2	AEA2	AEA1	AEA1	AEA1	AEA1	AEA1	AEA1	AEA1	AEA1	AEA1	AEA2	AEA2
WR/HRWR	WR	WR	HRWR1	HRWR1	HRWR1	HRWR1	None	None	HRWR1	HRWR1	WR	HRWR1	HRWR1	None	HRWR1
Pozzolan or Accelerator	15% FAF	15% FAC	15% FAF	15% FAC	8% SF	8% SF	15% SF	15% SF	8% SF	8% SF	15% SF	15% SF	15% SF	15% SF	15% SF
Fresh Air (%)	2.8	2.0	2.5	2.3	2.6	2.6	3.0	3.0	2.7	2.7	3.0	3.5	3.0	2.9	2.8
w/c	0.52	0.52	0.52	0.52	0.43	0.43	0.46	0.46	0.49	0.49	0.52	0.52	0.58	0.46	0.52
w/(c+p)	0.45	0.45	0.45	0.45	0.40	0.40	0.40	0.40	0.45	0.45	0.45	0.45	0.50	0.40	0.45
Physical Properties:															
Avg. Comp. Strength (MPa)	32.1	***	41.6	42.5	46.3	53.5	61.3	53.4	42.7	40.6	37.4	52.9	52.4	59.5	53.1
BSG (SSD)	2.453	2.431	2.451	2.462	2.442	2.435	2.435	***	2.435	2.436	2.407	***	2.433	2.426	2.419
Air Void Measurements:															
Hardened Air, Entrained (%)	1.8	1.4	1.5	1.1	1.4	1.4	2.5	2.5	2.2	2.2	2.1	2.1	2.3	3.0	2.7
Hardened Air, Total (%)	2.6	2.5	3.5	2.8	2.4	2.4	3.4	3.4	3.5	3.5	2.9	2.9	2.9	3.4	3.3
Lbar, Entrained (mm)	0.202	0.254	0.235	0.405	0.237	0.237	0.173	0.173	0.274	0.274	0.369	0.257	0.199	0.200	0.235
Lbar, Total (mm)	0.246	0.336	0.359	0.630	0.306	0.306	0.199	0.199	0.339	0.339	0.423	0.298	0.222	0.215	0.261
Alpha, Entrained (mm-1)	35.6	35.3	41.7	26.9	34.6	34.6	29.0	29.0	24.9	24.9	22.4	28.9	32.7	34.2	27.9
Alpha, Total (mm-1)	24.4	21.1	19.0	11.7	21.0	21.0	21.9	21.9	16.3	16.3	17.1	21.5	26.4	29.7	22.8
P90, Entrained (mm)	0.045	0.079	0.056	0.064	0.031	0.031	0.032	0.032	0.052	0.052	0.139	0.084	0.058	0.056	0.060
P99, Entrained (mm)	0.076	0.122	0.085	0.095	0.049	0.049	0.072	0.072	0.090	0.090	0.221	0.139	0.104	0.097	0.106
Water Pore Measurements:															
Wsat (%)	5.00	5.52	5.49	5.53	5.65	5.91	5.26	***	5.47	5.55	6.04	***	5.08	5.73	5.23
Weq @ 97%RH (%)	***	***	4.94	4.96	5.12	5.44	4.87	***	5.22	5.26	5.57	***	4.77	5.46	4.84
Weq @ 92%RH (%)	4.43	4.88	4.83	4.86	5.03	5.35	4.81	***	5.06	5.10	5.47	***	4.71	5.38	4.78
Weq @ 75%RH (%)	3.83	3.95	4.32	4.29	4.50	4.66	4.65	***	4.65	4.66	4.76	***	4.48	4.78	4.49
Weq @ 53%RH (%)	2.96	3.10	3.13	3.04	3.13	3.60	3.62	***	3.81	3.83	3.21	***	3.50	3.93	3.26
Weq @ 31%RH (%)	1.93	2.06	***	***	***	1.73	***	***	1.88	1.66	***	***	***	2.49	***
Freezable Water (%)	0.58	0.66	0.62	0.66	0.68	0.64	0.42	***	0.47	0.48	0.81	0.35	0.43	0.50	0.53
K (m/s x 1E-12)	18.0	2.5	***	***	***	***	3.2	***	5.1	***	4.4	4.1	2.2	7.3	2.6
Durability Test Results:															
DF, Avg.	78	70	23	37	47	47	88	72	67	67	47	92	93	83	70
DF, Std. Dev.	6.9	2.1	3.3	9.9	25.2	9.7	8.3	18.0	2.8	3.9	24.6	0.7	1.8	4.0	3.6
Mass Loss (%)	0.20	0.22	0.07	0.08	0.08	0.06	-0.07	0.02	0.16	0.03	0.04	0.04	0.00	-0.19	-0.17
Dilation (%)	0.061	0.077	0.063	0.084	0.100	0.126	0.043	0.060	0.105	0.115	0.072	0.025	0.018	0.012	0.029
Notes:						56-day cure		56-day cure		56-day cure		56-day cure			

Mix Design:	D31C	D29	D32	D30C	D30S	N22	N23	N16	N17	N37	N36	N46	N47	N32	N33	N44	N45
Coarse Aggregate (lb)	2099	2094	2085	2093	2105	2113	2105	2109	2103	2115	2113	2108	2105	2116	2111	2107	2092
Fine Aggregate (lb)	1017	1071	1038	1131	1038	1080	1076	1146	1143	1081	1080	1061	1060	1150	1147	1145	1137
Cement (lb)	461	439	419	390	345	641	639	569	567	642	641	652	651	571	569	568	564
Water (lb)	258	246	264	246	259	257	256	256	255	257	257	261	261	257	256	256	254
Pozzolan (lb)	184	176	168	156	230	0	0	0	0	0	0	0	0	0	0	0	0
Admixtures:																	
AEA	AEA1	AEA1	AEA1	AEA1	AEA1	AEA1	AEA1	AEA1	AEA1	AEA1	AEA1	AEA1	AEA1	AEA1	AEA1	AEA1	AEA1
WR/HRWR	None	WR	WR	WR	WR	None	None	None	None	None	None	None	None	None	None	None	None
Pozzolan or Accelerator	40% GBFS	40% GBFS	29% GBF	29% GBF	40% GBFS	None	None	None	None	None	None	None	None	None	None	None	None
Fresh Air (%)	2.2	2.4	2.8	2.4	2.8	1.6	2.0	1.6	1.9	1.5	1.6	1.7	1.8	1.3	1.5	1.7	2.4
w/c	0.56	0.56	0.63	0.63	0.75	0.40	0.40	0.45	0.45	0.40	0.40	0.40	0.40	0.45	0.45	0.45	0.45
w/(c+p)	0.40	0.40	0.45	0.45	0.45	0.40	0.40	0.45	0.45	0.40	0.40	0.40	0.40	0.45	0.45	0.45	0.45
Physical Properties:																	
Avg. Comp. Strength (MPa)	53.3	43.7	43.3	43.1	45.1	50.4	49.1	41.3	36.9	47.2	45.5	48.2	47.1	36.5	37.7	38.4	38.2
BSG (SSD)	2.452	2.433	2.421	2.423	2.441	***	***	***	***	***	***	***	***	***	***	***	***
Air Void Measurements:														***	***	***	***
Hardened Air, Entrained (%)	0.9	1.4	1.8	1.3	1.4	0.5	0.5	0.3	0.4	0.5	0.4	***	***	***	***	***	***
Hardened Air, Total (%)	1.6	2.1	3.7	1.7	3.0	1.7	1.6	1.7	2.0	2.0	1.0	***	***	***	***	***	***
Lbar, Entrained (mm)	0.245	0.205	0.268	0.287	0.300	0.347	0.279	0.473	0.351	0.439	0.574	***	***	***	***	***	***
Lbar, Total (mm)	0.344	0.249	0.385	0.323	0.439	0.497	0.314	0.550	0.444	0.549	0.641	***	***	***	***	***	***
Alpha, Entrained (mm-1)	47.9	37.9	33.7	33.6	33.7	39.0	46.8	31.0	38.2	30.3	25.0	***	***	***	***	***	***
Alpha, Total (mm-1)	26.2	26.1	17.1	26.9	16.7	16.3	26.0	13.8	15.8	13.8	14.6	***	***	***	***	***	***
P90, Entrained (mm)	0.057	0.042	0.065	0.036	0.092	0.134	0.121	0.152	0.144	0.201	0.263	***	***	***	***	***	***
P99, Entrained (mm)	0.083	0.068	0.101	0.055	0.138	0.190	0.173	0.214	0.204	0.286	0.370	***	***	***	***	***	***
Water Pore Measurements:																	
Wsat (%)	5.82	6.10	6.07	6.15	5.38	***	***	***	***	***	***	***	***	***	***	***	***
Weq @ 97%RH (%)	5.34	5.61	5.63	5.61	4.90	***	***	***	***	***	***	***	***	***	***	***	***
Weq @ 92%RH (%)	5.21	5.45	5.49	5.48	4.84	***	***	***	***	***	***	***	***	***	***	***	***
Weq @ 75%RH (%)	4.80	5.10	4.95	4.88	4.57	***	***	***	***	***	***	***	***	***	***	***	***
Weq @ 53%RH (%)	3.88	4.12	3.85	3.75	3.30	***	***	***	***	***	***	***	***	***	***	***	***
Weq @ 31%RH (%)	2.20	2.03	1.92	1.98	***	***	***	***	***	***	***	***	***	***	***	***	***
Freezable Water (%)	0.49	0.50	0.61	0.64	0.54	***	***	***	***	***	***	***	***	***	***	***	***
K (m/s x 1E-12)	9.0	8.9	14.0	6.0	***	***	***	***	***	***	***	***	***	***	***	***	***
Durability Test Results:																	
DF, Avg.	19	15	30	13	31	37	77	24	55	19	13	36	54	7	15	55	88
DF, Std. Dev.	4.8	2.4	2.5	2.4	2.3	6.7	10.2	1.8	4.7	1.8	1.6	4.5	2.5	2.0	3.7	4.3	11.0
Mass Loss (%)	0.25	0.19	0.04	0.26	-6.31	***	***	***	***	***	***	***	***	***	***	***	***
Dilation (%)	0.084	0.070	0.087	0.074	0.027	***	***	***	***	***	***	***	***	***	***	***	***
Notes:					f'c = 57 days	Type II Cement-----		Type II Cement-----		Type III Cement----------				Type III Cement-----		Type III Cement-----	

Mix Design:	N25	N24	M83	M84	N49	N50	M80	M81	M82	N48	N52	N51	N54	N53	D10/E6	D18/E14S	D30S
Coarse Aggregate (lb)	2110	2101	2088	2107	2101	2101	2096	2090	2108	2101	2101	2101	2101	2101	2076	2080	2105
Fine Aggregate (lb)	582	580	1146	1156	1161	1171	1150	1224	1234	1231	1142	1142	1186	1186	1144	1170	1038
Cement (lb)	874	870	596	602	600	600	494	520	524	522	567	567	544	544	464	465	345
Water (lb)	305	304	239	241	240	240	222	234	236	235	255	255	245	245	241	241	259
Pozzolan (lb)	0	0	0	0	0	0	0	0	0	0	0	0	0	0	70	70	230
Admixtures:																	
AEA	AEA1	AEA1	AEA1	AEA1	AEA1	AEA1	AEA1	AEA1	AEA1	AEA1	AEA1	AEA1	AEA1	AEA1	AEA1	AEA1	AEA1
WR/HRWR	HRWR1	HRWR1	None	None	None	None	None	None	None	None	None	None	WR	WR	WR	WR	WR
Pozzolan or Accelerator	DCI	DCI	None	None	None	None	None	None	None	None	None	None	None	None	15% FAF	15% FAC	40% GBFS
Fresh Air (%)	5.6	6.0	2.6	1.7	1.8	1.7	5.2	2.5	1.7	2.0	2.1	3.0	1.9	2.3	2.8	2.4	2.8
w/c	0.35	0.35	0.40	0.40	0.40	0.40	0.45	0.45	0.45	0.45	0.45	0.45	0.45	0.45	0.52	0.52	0.75
w/(c+p)	0.35	0.35	0.40	0.40	0.40	0.40	0.45	0.45	0.45	0.45	0.45	0.45	0.45	0.45	0.45	0.45	0.45
Physical Properties:																	
Avg. Comp. Strength (MPa)	61.1	58.6	44.9	50.6	45.5	46.5	38.4	46.5	46.1	36.6	36.3	39.0	43.1	39.9	27.1	38.8	45.1
BSG (SSD)	2.420	2.353	***	***	***	***	***	***	***	***	***	***	***	***	***	***	***
Air Void Measurements:	***	***	***														
Hardened Air, Entrained (%)	1.1	1.7	***	***	***	***	***	***	***	***	***	***	***	***	1.9	1.2	1.4
Hardened Air, Total (%)	3.3	5.1	***	***	***	***	***	***	***	***	***	***	***	***	3.1	1.3	3.0
Lbar, Entrained (mm)	0.223	0.148	***	***	***	***	***	***	***	***	***	***	***	***	0.261	0.383	0.300
Lbar, Total (mm)	0.264	0.168	***	***	***	***	***	***	***	***	***	***	***	***	0.326	0.402	0.439
Alpha, Entrained (mm-1)	45.3	56.1	***	***	***	***	***	***	***	***	***	***	***	***	33.2	28.4	33.7
Alpha, Total (mm-1)	24.0	30.8	***	***	***	***	***	***	***	***	***	***	***	***	21.7	25.8	16.7
P90, Entrained (mm)	0.098	0.065	***	***	***	***	***	***	***	***	***	***	***	***	0.070	0.105	0.092
P99, Entrained (mm)	0.148	0.103	***	***	***	***	***	***	***	***	***	***	***	***	0.109	0.155	0.138
Water Pore Measurements:																	
Wsat (%)	5.55	6.13	***	***	***	***	***	***	***	***	***	***	***	***	***	***	***
Weq @ 97%RH (%)	4.17	5.64	***	***	***	***	***	***	***	***	***	***	***	***	***	***	***
Weq @ 92%RH (%)	4.10	5.49	***	***	***	***	***	***	***	***	***	***	***	***	***	***	***
Weq @ 75%RH (%)	3.60	5.20	***	***	***	***	***	***	***	***	***	***	***	***	***	***	***
Weq @ 53%RH (%)	***	***	***	***	***	***	***	***	***	***	***	***	***	***	***	***	***
Weq @ 31%RH (%)	***	***	***	***	***	***	***	***	***	***	***	***	***	***	***	***	***
Freezable Water (%)	0.40	0.29	***	***	***	***	***	***	***	***	***	***	***	***	***	***	***
K (m/s x 1E-12)	***	***	***	***	***	***	***	***	16.2	***	***	***	***	***	***	***	***
Durability Test Results:																	
DF, Avg.	28	47	99	99	27	20	100	98	24	25	33	41	31	38	37	21	31
DF, Std. Dev.	3.2	4.9	0.9	0.4	1.2	7.1	0.0	2.4	2.6	9.2	4.5	2.3	3.9	2.7	8.8	4.6	2.3
Mass Loss (%)	***	***	***	***	***	***	***	***	***	***	***	***	***	***	-8.90	-9.27	-6.31
Dilation (%)	***	***	***	***	***	***	***	***	***	***	***	***	***	***	0.068	0.044	0.027
Notes:	Type III Cement		Alt. Coarse Agg.				Alternate Coarse Agg.			F-T in Salt Solution					F-T in Salt Solution		

Part II - Frost Resistance of Concrete Made with Frost-Susceptible Aggregate

1.0 Introduction

Better methods are needed to identify aggregates susceptible to D-cracking, and to mitigate damage in existing pavements caused by such aggregates. Specific goals of this research were to 1) develop a simple and rapid method for identifying aggregates susceptible to D-cracking, and 2) investigate possible methods of mitigating D-cracking in existing pavements.

2.0 Background

2.1 D-Cracking Occurrence

D-cracking is the term used to describe the distress in concrete that results from the disintegration of coarse aggregates after they have become saturated and have been subjected to repeated cycles of freezing and thawing.[1] D-cracking is observed most often in pavements, though it can occur in structural concrete as well. D-cracking occurs most often in portions of the concrete that are exposed to moisture intrusion from multiple directions. For example, at a pavement joint, water can intrude from the top and bottom of the concrete slab, and at the vertical joint face. Intersections of longitudinal and transverse joints provide mutually perpendicular sources of intrusion. Also, bases of concrete walls or columns tend to accumulate snow, and water cannot drain during periodic thaws.

Although D-cracking has been known to exist since the 1930s[2], a simple, rapid and reliable test to identify aggregates susceptible to D-cracking has not been developed.

2.2 Conditions Necessary for D-cracking

The mechanisms of D-cracking have not yet been completely clarified and continue to be intensively studied.[3] D-cracking can occur only when 1) the concrete contains aggregates susceptible to D-cracking in sufficient quantity and size, 2) the concrete is exposed to sufficient moisture, and 3) the concrete is exposed to repeated cycles of freezing and thawing. These conditions work as described below:

1) Sufficient Quantity and Size of D-cracking Aggregate - The concrete must contain D-cracking susceptible aggregate in order to have this distress. Therefore, identifying aggregate susceptible to D-cracking is important. There must be a sufficient number of pieces susceptible to D-cracking to damage the concrete as a whole, rather than cause

localized damage such as a popout. This means that blending a sufficient quantity of non-susceptible aggregate with a D-cracking susceptible aggregate can result in acceptable performance. It should be pointed out that the pieces of the D-cracking susceptible aggregate must be large enough to cause D-cracking. Reducing the maximum aggregate size has been found to decrease the D-cracking potential of the aggregate.[1] This means some other measure of the aggregate (such as pore length) in addition to the pore size distribution is important in determining D-cracking susceptibility.

2) Sufficient Moisture Exposure - The concrete must be exposed to a sufficient amount of moisture in order for D-cracking to occur. Pavement concrete made with D-cracking susceptible aggregates may show substantial deterioration near joints or cracks that allow water intrusion, while cores taken as little as 1 m (3 ft) from the crack or joint show no apparent deterioration.[4, 5] Places where additional water intrudes, such as the intersection of transverse and longitudinal joints, would result in increased deterioration.

3) Sufficient Freezing - The concrete must freeze a sufficient number of times for the D-cracking to be noticeable. Often, five to ten or more years are required for D-cracking to become apparent.[1] Depth of freezing also has an effect on D-cracking, with mild climates producing D-cracking that resembles shallow spalls near joints rather than the traditional deterioration starting at the bottom of concrete slabs.

None of the conditions necessary for D-cracking are related to the air-void system in the concrete. Though deterioration of the paste portion of the concrete due to inadequate entrained air could accelerate D-cracking progression by allowing more moisture to enter the concrete, a properly air-entrained concrete can still develop D-cracking when the above three conditions are met.

3.0 Current Identification Procedures

The complete interrelationship of variables that affect the performance of aggregates in concrete has resulted in a diversity of tests that try to provide a reliable means of separating durable and nondurable aggregates.[6] The current test methods to identify the resistance of aggregate to frost action fall into two primary groups.[7, 8] One group consists of tests that try to simulate the environmental conditions to which the concrete aggregate is exposed. The other group comprises tests that correlate aggregate properties (termed index properties) with known field performances and/or results from environmental tests.

3.1 Environmental Simulation Tests

The environmental simulation tests include the following:

1. Sulfate Soundness (AASHTO T 104)

2. Unconfined Aggregate Freezing and Thawing (AASHTO T 103)
3. Rapid Freezing and Thawing (AASHTO T 161)
4. Powers Slow Cool (ASTM C 671)
5. Single-Cycle Slow-Freeze (Virginia Polytechnic Institute and State University)

3.1.1 Sulfate Soundness (AASHTO T 104)

This test is favored over many other test methods because of the simplicity of the equipment involved and the short amount of time required to run the test.[6] In the sulfate soundness test, aggregate is soaked in a sodium or magnesium sulfate solution and then dried. Repeated cycles result in salt crystal growth in the aggregate pores. The expansive forces generated by the crystal growth supposedly simulate the expansive forces caused by the formation of ice in aggregate pores. However, the major natural cause of disintegration in aggregates, according to some theories, is the hydraulic pressure produced when water attempts to leave the zone of freezing.[6] The growth of the sulfate crystals occurs as the aggregate is dried in an oven; hence, the crystal formation is not generating hydraulic pressures. Additionally, the sulfate test does not account for the effects of confining the aggregate by mortar, which determines the rate and amount of moisture movement into and out of the aggregate.

3.1.2 Unconfined Aggregate Freezing and Thawing (AASHTO T 103)

The unconfined aggregate freezing and thawing test is an outgrowth of the sulfate soundness test.[6] The test has three variations, but, the basic procedure consists of subjecting the aggregate to repeated freezing in water and thawing in air. As with the sulfate test, the unconfined freezing and thawing test does not duplicate confinement of the aggregate by mortar. This test can be less reproducible because of the number of variables involved, such as rate of cooling and final temperature, rate of thawing, the moisture conditions of the samples before each cycle, and the length of time the samples remain frozen and thawed.

3.1.3 Rapid Freezing and Thawing (AASHTO T 161)

The standard test for resistance of concrete to rapid freezing and thawing has two methods, A and B. Method A consists of freezing and thawing specimens in water. Method B consists of freezing specimens in air and thawing them in water.[9] The test can be conducted with concrete cylinder or prism specimens, although prism specimens are most commonly used.[1] A cycle of freezing and thawing is completed by lowering the specimen temperature from 4.4°C (40°F) to -17.8°C (0°F) and raising it back to 4.4°C within a 2- to 5-hour period. Specimen length change and a durability factor, calculated from relative dynamic modulus of elasticity (ASTM C 215), are determined from the test. Measurements are initially taken and repeated after no more than every 36 cycles until completion. The test is completed after 300 cycles or until the modulus is reduced to 60 percent of the initial modulus, whichever occurs first.

Presently, standard specifications provide limited guidance on what constitutes good or bad performance. Except for ranking in relative order of frost resistance, no criteria have been established for the acceptance or rejection of aggregates on the basis of AASHTO T 161[10], although some states have established their own criteria. Furthermore, although this test better simulates the confining nature of mortar in concrete, aggregate evaluations may take nearly five months to complete.[11]

3.1.4 Powers Slow Cool (ASTM C 671)

In this test, concrete specimens are maintained in a constant temperature bath at 1.7°C (35°F).[12] Once every two weeks, the specimens are immersed in a water-saturated kerosene bath and the temperature is lowered from 1.7°C (35°F) to -9.4°C (15°F) at the rate of 2.8°C (5°F) per hour. Length changes are measured during cooling. After they are cooled, the specimens are returned to the original water bath. The test is terminated once the specimens exceed critical dilation or until the specimens have completed a desired number of cycles. Critical dilation is the dilation that occurs during the last cycle before the dilation begins to increase by a factor of 2 or more. The number of cycles during which the difference between successive dilations remains constant is termed the *period of frost immunity*. Some highly frost-resistant aggregates may never produce critical dilations.

As with the rapid freezing and thawing test, this test is time-intensive and requires costly equipment.

3.1.5 Single-Cycle Slow Freeze[13] (Virginia Polytechnic Institute and State University)

This test uses concrete specimens made and cured in accordance with ASTM C 192. Stainless steel strain plugs are placed, 25 cm (10 in.) apart, into the prisms. Initial measurements of transverse frequency, weight, and length are recorded. Specimens are placed in a freezing apparatus with an air temperature of -17.8°C (0°F). Length change measurements are made at 5- to 15-minute intervals over a 4-hour cooling period.

From the results, two correlations are made. The first is temperature versus length change. The minimum 2.8°C (5°F) temperature slope is the minimum slope that can be found within a 2.8°C (5°F) or more range on the length change-temperature curve obtained during the first freeze of a specimen. The second correlation is time versus length change. The cumulative length change is plotted versus time, and the time slope is determined as the minimum slope that can be found within a 1/3-hour or greater time range.

This test requires approximately three days to perform once curing is completed. It has been found to produces fairly accurate results for distinguishing between very durable and nondurable aggregates. However, for aggregates of questionable durability, it is recommended that the Rapid Freezing and Thawing test should be performed.

3.2 Aggregate Index Property Tests

The tests developed to correlate aggregate properties to field performance are generally relatively quick compared to the environmental simulation tests described above, and with one exception require relatively inexpensive equipment. These tests include the following:

1. Mercury Intrusion Porosimeter
2. Iowa Pore Index
3. Absorption-Adsorption
4. Petrographic Analysis

3.2.1 Mercury Intrusion Porosimeter

One of the major ways of determining the pore size distribution of a porous solid is by mercury porosimetry, which is based on a relation presented by Washburn.[14] The mercury intrusion porosimeter apparatus has been used in many studies of the pore characteristics of aggregates.[11, 15, 16, 17, 18, 19] The non-wetting liquid is almost always mercury because of its low vapor pressure and relative inertness to chemical reaction with the aggregate, and because it is non-wetting for most surfaces.[15] However, the problems with this test include the following:

- Washburn's equation is for pores that are cylindrical and interconnected. This is not normally the case with aggregate. The pore size distribution is weighted toward smaller pore sizes because the void volumes of pores with entrances narrower than the body, termed "ink-bottle pores," will be recorded according to the entrance size.
- Values must be assumed for the contact angle and surface tension of the non-wetting liquid.
- The sample size is very small, usually 2-5 g. Therefore, the test may not yield a representative result, especially when testing heterogeneous sources.
- The equipment is expensive and requires special handling.

3.2.2 Iowa Pore Index Test

The Iowa pore index test (IPIT) was developed on the basis of earlier evidence that D-cracking is related to freezing and thawing and, more specifically, to the pore sizes of coarse aggregate.[11] The objective in developing the test was to readily identify a correlation between an aggregate's susceptibility to critical saturation and its potential to cause D-cracking.[1]

The test procedure consists of placing a 9000-g oven-dried aggregate sample in a modified air pressure meter container, filling the container with water, and then applying 241 kPa (35 psi) of air pressure.[11] The test procedure defines the "primary load" as the amount of water

injected during the first minute. This reading is assumed to correspond to the filling of the aggregate's macropores. A large primary load is considered to be an indication of a beneficial limestone property.

The amount of water injected between 1 and 15 minutes is defined as the "secondary load" and is believed to represent the quantity of water injected into the aggregate's micropore system. The secondary load is used as the IPIT test result.

Aggregates with histories of producing D-cracking concrete have had IPIT readings of 27 mL or more.[1, 11] Comparing the IPIT and the mercury intrusion porosimeter to aggregate field performance, Shakoor and Scholer concluded that the IPIT test is a reliable, less expensive, and quicker test than mercury intrusion porosimetry.[18] They also state that the IPIT results are more representative of the parent rock because of the large sample volume used.

Other studies have found problems with the IPIT.[20, 21] These problems include variable and erroneous results for aggregates with reasonably rapid rates of early absorption and no discernible trends in the results from gravels. Furthermore, IPIT cannot indicate to what extent a reduction in maximum aggregate size will improve performance, and the test does not discriminate between absorption by a few highly porous particles or absorption by many moderately porous particles.

3.2.3 Absorption-Adsorption

An extensive study of D-cracking by Klieger et al. attempted to develop a test that would distinguish between durable and nondurable aggregates and that would require a minimum amount of sample preparation, time, and test equipment.[22] They developed an absorption-adsorption test and compared the test results to pavement service records.

After conducting this test with a large variety of aggregate sources, they concluded that the absorption-adsorption test tended to be overly conservative in identifying durable and potentially nondurable aggregates. The test predicted poor resistance to freezing and thawing for a large percentage of material from several sources with good service records.

3.2.4 Petrographic Analysis (ASTM C 295)

Many studies of aggregate resistance to freezing and thawing have incorporated petrographic analysis either to identify aggregate properties that affect concrete durability or to predict aggregate performance in freezing and thawing tests.[8, 13, 23, 24, 25, 26] Petrographic examination is a visual analysis of an aggregate's lithology and individual particle properties.[27, 28] It requires the skills of a well trained and experienced petrographer. The examination uses small sample sizes, which require a large amount of work to provide accurate results.[28] Also, the analysis is not able to provide definite specification limits because information so obtained is the result of subjective appraisal by the petrographer and can be reduced to a numerical quantity only through personal interpretation.[27]

4.0 Washington Hydraulic Fracture Test

4.1 Objectives

The importance of identifying D-cracking susceptible aggregates has led to a considerable number of aggregate identification test procedures. Unfortunately, the more reliable of the procedures may require eight weeks or longer, expensive equipment, and highly skilled operators. In response to this problem, the goal of this research has been to develop a rapid, reliable test method for identifying D-cracking susceptible aggregates. The ideal procedure should also be relatively inexpensive so as not to be prohibitive for routine testing. The following sections will describe the procedure, called the Washington Hydraulic Fracture Test, that has been developed.

4.2 Test Description

The test is conducted as follows.

1. Place a washed, oven-dried, and surface-treated (to be hydrophobic) specimen of known mass, number of particles, and size range (smallest size is retained on 12.5 mm sieve) into the pressure chamber.

2. Bolt the chamber shut and fill it with water.

3. Apply an internal pressure of 7930 kPa (1150 psi) to the chamber.

4. Rapidly release the chamber pressure.

5. After ten repetitions of steps 3 and 4 remove the specimen from the chamber oven and count the particles.

Two days are required for specimen preparation (washing, oven drying, surface treating, and grading) and an additional day for each ten pressurization cycles (actual operator time is less than one hour per specimen per day). After the last pressurization day, the results are analyzed. A total of eight days are required for test results. Results are given in terms of the increase in number of pieces larger than the 4.75 mm (#4) sieve as a percentage of the total number of initial pieces for each ten cycles of pressurization. This is termed the *percent fracture*. From these values an index is determined that indicates the number of pressurization cycles necessary to produce 10 percent fracturing. Lower values of this index indicate an aggregate more susceptible to D-cracking than aggregates with higher values.

4.3 Test Mechanism

This test method is based on the assumption that the hydraulic pressures expected in concrete

aggregates during freezing and thawing can be simulated by subjecting sample aggregates, submerged in water, to high pressures. As the external chamber pressure increases, the water penetrates into smaller and smaller pores. If this external pressure is rapidly released, air compressed within any pores will push the water back out, thereby simulating the hydraulic pressures generated during freezing. Fracturing of the aggregate should result if the pressure in the pores cannot be dissipated quickly and the aggregate is unable to elastically accommodate the high internal pressure.

Kaneuji et al. observed qualitative correlations between concrete durability and pore size distributions of aggregates.[17] At a constant total pore volume, aggregates with smaller pore sizes result in a lower durability. For aggregates with similar predominating pore sizes, a greater pore volume results in a less durable aggregate. By correlating aggregate service records with mercury porosimeter studies, Marks and Dubberke found that, with one exception, the nondurable aggregates analyzed exhibited a predominance of pore diameter sizes in the 0.04 to 0.2 μm range, while aggregates with good to excellent service records had a majority of pores that were larger than the 0.04 to 0.2 μm diameter pore sizes.[11]

Using Washburn's equation

$$P = 4T \cos \Theta / d \qquad (1)$$

where:

T	=	surface tension (72 dynes/cm for water)
Θ	=	contact angle (0° for water)
d	=	pore diameter

absolute pressures of between 1450 kPa (210 psi) and 7240 kPa (1050 psi) can be used to force water into pore diameters within the range of 0.2 to 0.04 μm.

The advantages of this proposed test are:

- theoretically, the test should be able to simulate the hydraulic pressures that many believe cause D-cracking in nondurable aggregates;
- the cost for special equipment is relatively low;
- compared to existing tests, this test should be relatively fast, and therefore, economical; and
- the uniform pressure applied to individual aggregate particles within the chamber, along with the rate of pressure application, final pressure, and holding time, which can be easily standardized and controlled, make this test easily reproducible.

The testing procedure depends upon hyperbaric pressure forcing water into the aggregate pores. The release of the pressure causes a critical gradient of pressure from inside to

outside the aggregate of sufficient magnitude to cause fracturing. Winslow[21] pointed out that some aggregates absorb water extremely quickly. If an aggregate is at a relatively high degree of saturation prior to pressurization in the Washington Hydraulic Fracture Test, the pressure gradient necessary for fracture after the pressure was released may not develop. This was found to be true for a limestone used early in the test development. Winslow's absorption rates[21] are shown in Figure 2-1 for four aggregates. Both gravels and one of the limestones (the non-D-cracking limestone) have similar absorption rates while the other limestone (which is D-cracking susceptible) has a much higher absorption rate. While absorption rate itself is not an indicator of D-cracking susceptibility[21], this higher absorption rate could prevent the above fracture mechanism from working with rapidly absorbing aggregates.

A way to avoid problems with aggregates that have high absorption rates is to make the pores hydrophobic rather than hydrophilic. One method of accomplishing this is to treat the aggregate with a silane-based sealer. The literature[29] suggests that the primary effect of the silane is to change the water/solid contact angle in the aggregate pores. This would not affect the pore size, but would effect the absorption of water into the pore by surface tension effects.

Figure 2-2 is a plot of the absorption rates for the untreated and treated ILA limestone. As can be seen, the absorption rate is indeed decreased. The slower-absorbing limestone (ILB) was also treated for comparison purposes. Previous work[30, 31] has shown that the treatment does not affect the fracture results of slow-absorbing aggregates.

4.4 Equipment

The main part of the testing apparatus is the pressure chamber, which is developed from a commercially available 100 bar (10,000 kPa, 1500 psi) pressure membrane extractor (similar to the equipment described in ASTM D 3152). A second top plate replaces the normal bottom plate and drain line provided with the extractor. The three holes already threaded into the pressure chamber cylinder are used for pressure application/relief, water supply, and water drainage. The water drain hole has a piece of copper tubing inserted to act as a siphon so that the chamber may be drained while in a horizontal position.

The pressure application/relief mounting consists of two valves. One valve isolates the pressure chamber from the pressure source (compressed nitrogen). The other valve serves as an overflow valve during filling and a pressure relief valve at the end of testing.

A rock tumbler is used after removing the aggregate sample from the test apparatus to ensure that the effect of sample handling is relatively uniform, therefore making any mass loss associated with handling also uniform. In addition, the tumbler is used to facilitate fracturing initiated by the pressurization process.

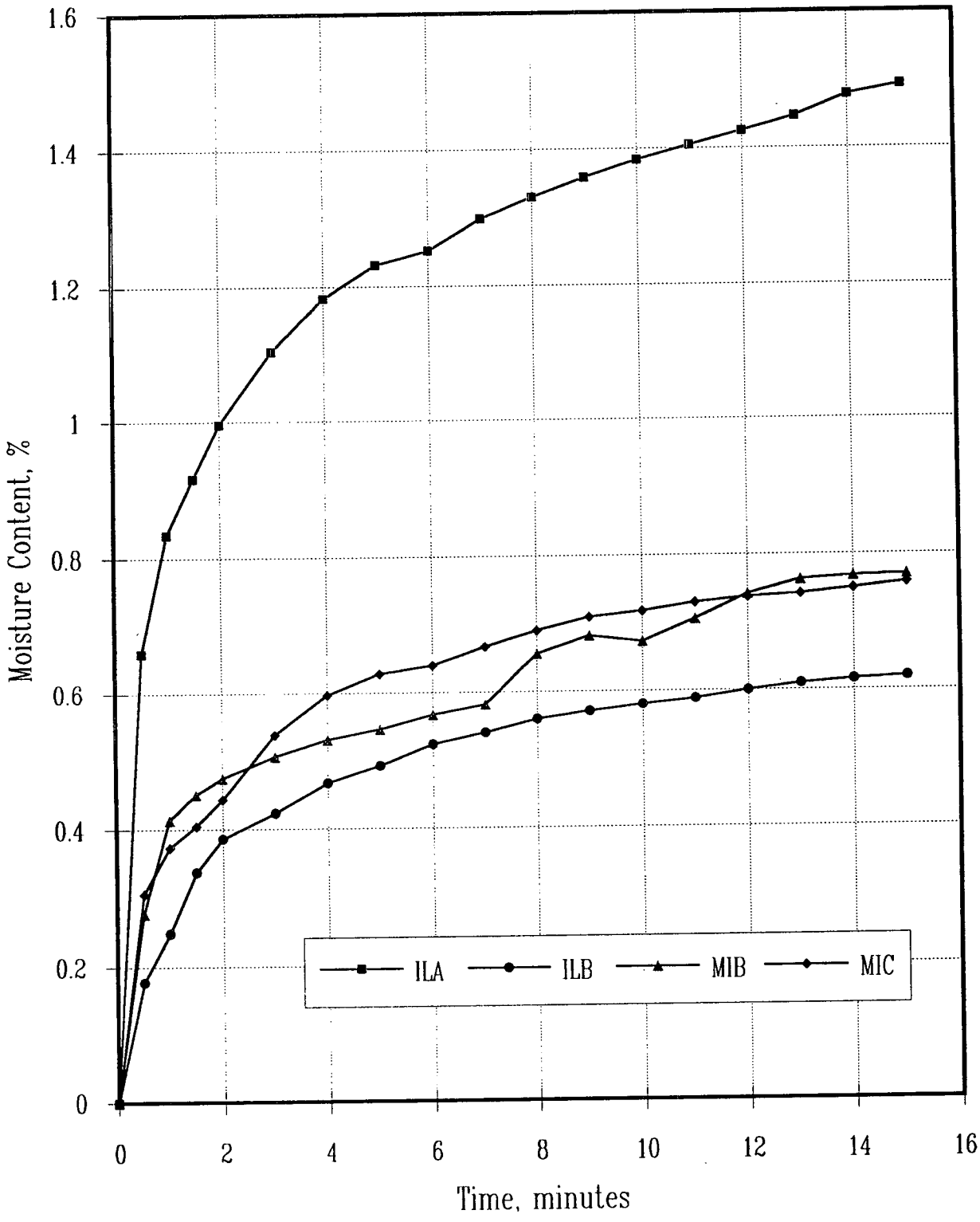

Figure 2-1 Winslow Absorption Rates for Four Aggregates.[21]

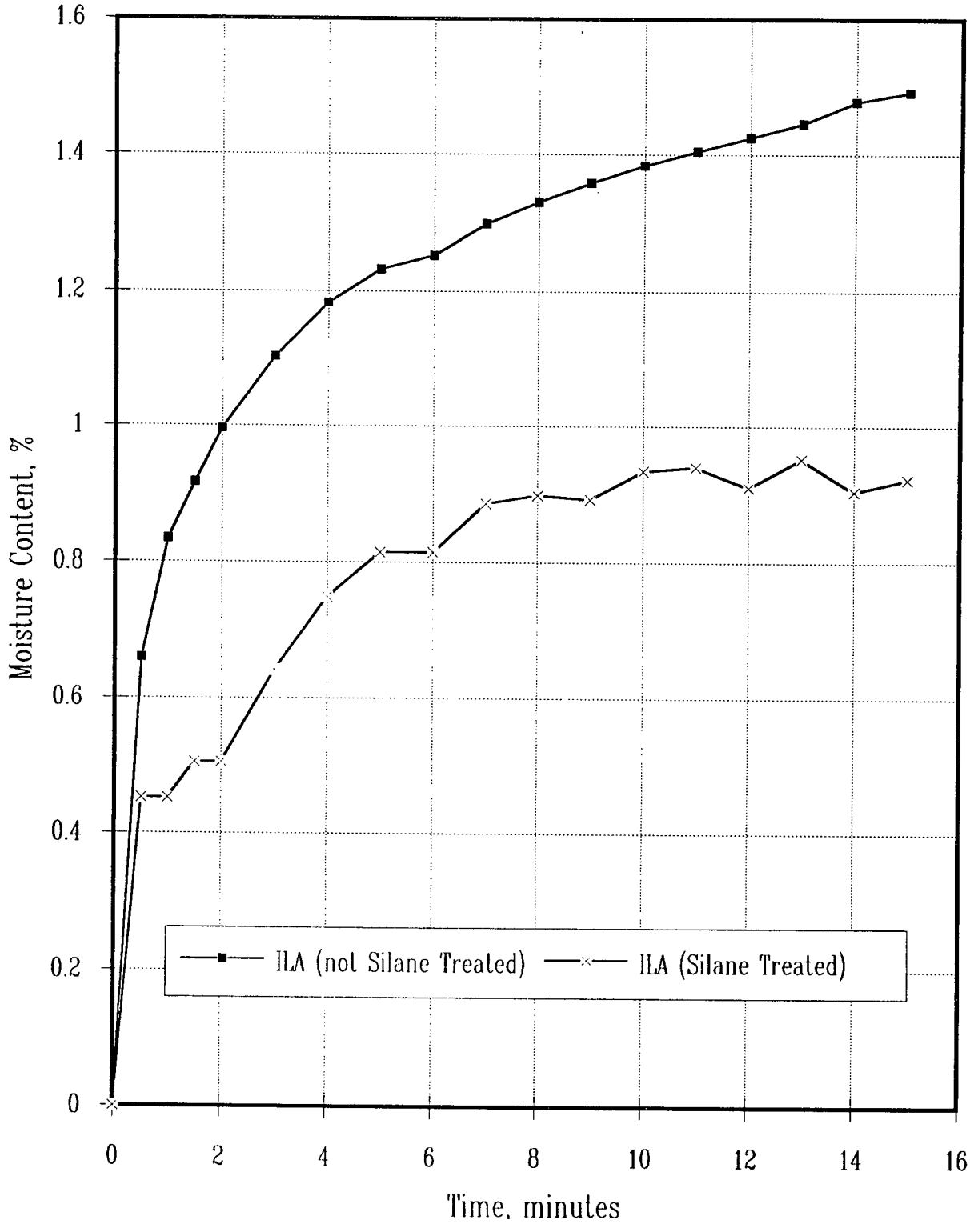

Figure 2-2 Winslow Absorption Rates for Silane-Treated and Untreated ILA Crushed Limestone.[21]

4.5 Test Procedure

Before testing, each aggregate sample is separated by sieving into appropriate size ranges: 12.5 to 19.0 mm (1/2 to (3/4 in.) and 19.0 to 31.5 mm (3/4 to 1-1/4 in.). The size range used is relatively narrow in order to determine the effect of particle size on D-cracking potential. The aggregate is then washed and oven dried at 121°C (250°F) for at least 12 hours. Each specimen was then immersed for 30 seconds in a water-soluble solution of silane sealer, drained, and again oven dried at 121°C (250°F) for at least 12 hours.

The pressure chamber holds a sample size of approximately 3200 g (7.0 lb), depending upon the range analyzed. This is equivalent to approximately 450 pieces in the 12.5 to 19 mm (1/2 to 3/4 in.) range and 150-225 pieces in the 19.0 to 31.5 mm (3/4 to 1-1/4 in.) range. Each sample is initially placed in the rock tumbler for one minute and then all pieces passing the 9.5 mm (3/8 in.) are removed. This ensures that there are no pre-existing fractures in the aggregates prior to testing. The sample initial weight and number of particles are then determined and recorded. Next, the sample is placed in the chamber and the chamber bolted shut. The chamber is then turned on edge, so that the pressure application/relief mount is vertical, and is filled with water up to the overflow/relief valve. Once the water supply and overflow/relief valves are secured, the pressure is applied by opening the valve from compressed nitrogen to the chamber. The pressure at the selected level is maintained for 5 minutes. The compressed nitrogen valve is then closed and the overflow/relief valve is rapidly opened. This quickly releases the pressure within the chamber. The small amount of water that sprays out when the relief valve is opened is replaced by briefly refilling the chamber with water. After 30 seconds the chamber is re-pressurized. The pressure is then released after 2 minutes. An additional eight cycles of 2 minutes of pressure, followed by pressure release and no pressure for 30 seconds, are applied. At the end of the 10 total cycles the pressure chamber is drained and opened. The specimen is oven dried at 121°C (250°F) overnight. The following day, the sample is tumbled for one minute in a rock tumbler and then separated using 9.5 mm (3/8 in.) and No. 4 sieves. All particles of the sample retained on both sieves are weighed and counted. The material retained on the 9.5 mm (3/8 in.) sieve is subjected to an additional ten pressurization cycles. The pressurization is repeated for a total of 50 cycles (five days) for each aggregate sample. A description of the procedure in the format of an AASHTO test procedure is presented in appendix 2A. A guide for using the current equipment is given in appendix 2B.

4.6 Analysis of Results

The example results discussed below are for one D-cracking susceptible and one non-D-cracking susceptible gravel. Results for additional materials are presented under "Reliability and Repeatability."

4.6.1 Calculations

A primary value determined from testing is the percentage of fractures. Percentage of fractures is calculated by dividing the number of additional pieces by the original number of aggregate pieces prior to any pressurization. Materials retained on the 9.5 mm (3/8 in.) sieve are counted as whole pieces (that is, they count as "one"), while particles passing the 9.5 mm (3/8 in.) sieve but retained on the 4.75 mm (No. 4) sieve are counted as partial pieces (the number of pieces is divided by 2 in the calculation). This is shown in Equation 2:

$$FP_i = 100\,(n4_i/2 + n_i - n_0)/n_0 \qquad (2)$$

where FP_i = percent fractures after i pressurization cycles,
$n4_i$ = number of pieces passing the 9.5 mm (3/8 in.) sieve but retained on the 4.74 mm (No. 4) sieve after i pressurization cycles,
n_i = number of pieces retained on the 9.5 mm (3/8 in.) sieve after i pressurization cycles
n_0 = initial number of pieces tested.

The percentage of fractures is used to calculate a value called the hydraulic fracture index (HFI), which can be thought of as the number of cycles necessary to produce 10 percent fracturing. It is determined by one of the following methods, depending upon what percentage of fracturing exists after 50 cycles of pressurization.

If 10 percent fracturing is achieved in 50 or fewer cycles, calculate the HFI as a linear interpolation of the number of cycles that produced 10 percent fractures.

$$HFI = A + 10 \cdot [(10\text{-}FP_A)/(FP_B - FP_A)] \qquad (3a)$$

where A = number of cycles just prior to achieving 10 percent fracturing
FP_A = percentage of fracturing just prior to achieving 10 percent fracturing
FP_B = percentage of fracturing just after achieving 10 percent fracturing

If 10 percent fracturing is not achieved in 50 pressurization cycles, calculate the HFI as an extrapolation from no fracturing at 0 cycles through the amount of fracturing at 50 cycles.

$$HFI = 50 \cdot (10/FP_{50}) \qquad (3b)$$

where FP_{50} = percentage of fracturing after 50 pressurization cycles.

The mass of material as a percentage of the original specimen that is no longer retained on the 9.5 mm (3/8 in.) sieve is called the percentage of mass loss (ML), and is determined as follows on the next page:

$$ML_i = (100/m_0) \cdot [m_0 - (m4_i + m_i)] \quad (4)$$

where ML_i = percentage of mass loss after i cycles of pressurization
$m4_i$ = cumulative mass of the material passing the 9.5 mm (3/8 in.) sieve but retained on the 4.75 mm (No. 4) sieve after i pressurization cycles,
m_i = mass of the pieces retained on the 9.5 mm (3/8 in.) sieve after "i" pressurization cycles
m_0 = initial mass of the specimen tested

While no interpretation has yet been determined for the ML values, this value is calculated and recorded for possible future use.

4.6.2 Pressure Effect

According to the test mechanism proposed above, the magnitude of the pressure used should affect the amount of fracturing produced. Original development of the procedure started with a pressure of 7240 kPa (1050 psi). When this pressure did not produce much fracturing, the pressure was increased to 7930 kPa (1150 psi). Figures 2-3 and 2-4 display changes in the percentage of fracturing due to this increase in pressure. As would be expected, an increase in pressure increases the percentage of fractures. This suggests that higher pressures might produce better results. Above some pressure, however, many non-susceptible aggregates would be expected to show considerable fracturing. This would make differentiating between durable and non-durable materials difficult.

4.6.3 Aggregate Size Effect

A comparison was made with regard to change in particle size. Figures 2-5 and 2-6 present comparisons of plus 19.0 mm (3/4 in.) and minus 19.0 mm (3/4 in.) samples of the susceptible and non-susceptible gravels, respectively. It is shown that there is a decrease in the percentage of fractures as the size of the material tested is reduced. This would be expected since the flow path in the minus 19.0 mm (3/4 in.) material should be much shorter than the plus 19.0 mm (3/4 in.) material, therefore providing a shorter path for the release of hydraulic pressure. This size effect agrees with Stark and Klieger[2], Traylor[20] and others who reported that D-cracking severity was reduced by reducing the maximum aggregate size.

4.7 Reliability and Repeatability

Table 2-1 shows the HFI values for 13 aggregate sources for materials in the 19.0 to 31.5 mm (3/4 to 1-1/4 in.) size range. Seven of these aggregates were reported as susceptible to D-cracking by the agencies that provided them while six of the aggregates were reported as not susceptible to D-cracking. All of the D-cracking susceptible aggregates, with the exception of one of the limestones from Iowa, had HFI values below 60. The Iowa limestone with the high HFI value had durability factors, as determined in accordance with AASHTO T 161, of 65, 83, and 87 in a properly air-entrained mix[32].

All of the aggregates, except one, that were reported as durable had HFI values above 100. The one durable aggregate that gave a low HFI value was described by the Iowa Department of Transportation as a coarse-grained crinoidal limestone with a low specific gravity (2.57) and a high absorption (2.5 percent).[32] No explanation has been developed to explain the high degree of fracturing of this aggregate in the Washington Hydraulic Fracture Test.

Table 2-2 shows the coefficients of variation for the HFI values as determined from a range of sample sizes. This table suggests that the minimum sample size should be in the range of 600-800 pieces in order to provide a reliable HFI value. Unfortunately this was not known when many of the samples were solicited, and adequate sample sizes were not available for many of the aggregates tested. Qualitative observation of the testing suggests that this sample size limitation is more critical for bedrock sources than for gravel sources. With gravels, the fractures appear to occur frequently in the same rock type for a given source. This suggests that for gravels, the majority of the particles are either clearly durable or clearly non-durable. The durability of a source would then depend upon the number of nondurable particles included in the material. It would appear that bedrock sources, however, are more uniform within a given range of a given ledge. It would also appear that bedrock sources could be more likely to contain particles that had borderline durabilities. Therefore, a larger specimen size would be necessary to provide reliable results.

Between laboratory variabilities are shown in table 2-3. The agreement between tests run at University of Washington and tests run at Michigan State University are in most cases quite good, despite the lower than ideal sample sizes (shown as # part in the table). The testing at University of Illinois provided consistently higher HFI values. Recalibration of the pressure gauge on the equipment used at University of Illinois determined that it was off by about 350 kPa (50 psi). The effect of pressure on HFI values has been previously discussed. Greater care will need to be taken in the future to ensure that the pressure gauges are properly calibrated upon installation.

4.8 Chamber Modification

The sample size effects discussed above suggest that a larger chamber capable of testing a larger sample size would be appropriate. Previous discussions have also suggested that pressure magnitude and the rate of pressure release could play critical roles in producing the desired fracturing in nondurable aggregates. Figure 2-7 shows the average pressure release history for the original chamber pressurized to 7,930 kPa (1150 psi). A linear fit to the central portion of the curve gave a pressure release rate of 209,000 kPa/sec (30,350 psi/sec) over a range of over 3,600 kPa (520 psi). Ideally, an alternate chamber (either larger or of a different design) should produce a similar pressure release rate over a similar pressure range.

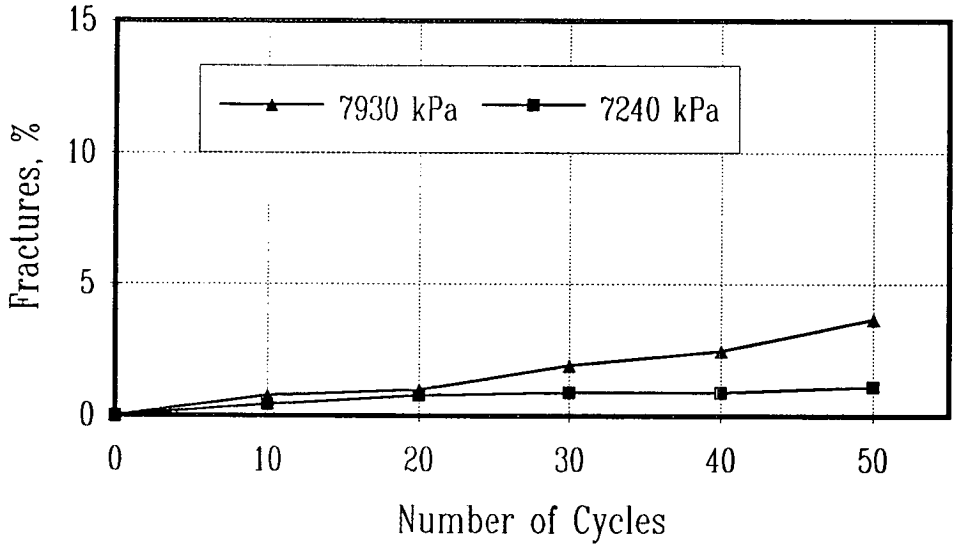

Figure 2-3 Comparison of Percent Fractures for plus 19.0 mm (3/4 in.) Durable Gravel, at both 7240 kPa (1050 psig) and 7930 kPa (1150 psig) Testing Pressures

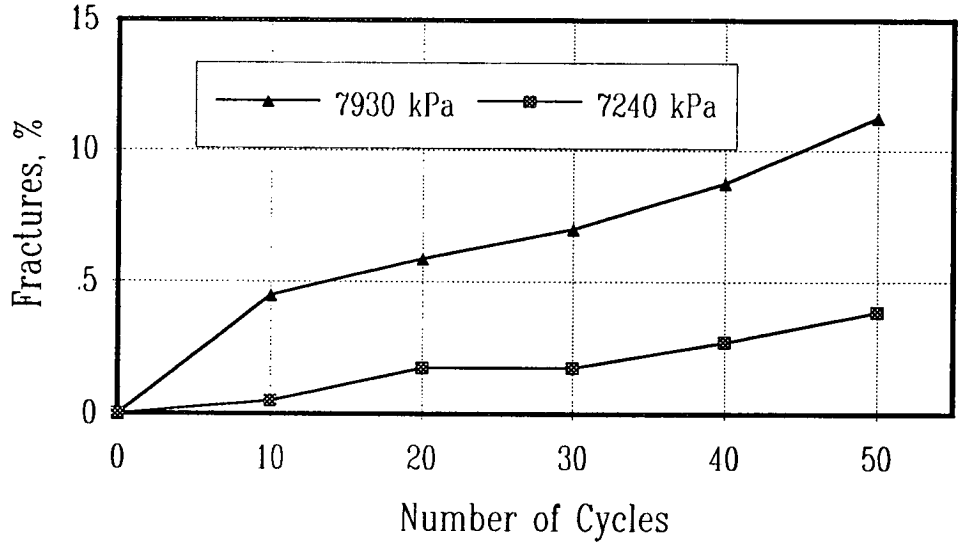

Figure 2-4 Comparison of Percent Fractures for plus 19.0 mm (3/4 in.) Nondurable Gravel, at both 7240 kPa (1050 psig) and 7930 kPa (1150 psig) Testing Pressures

Table 2-1 WHFT Results, > 19 mm (3/4 in.) size.

Sample ID	Source State	Field Performance	Hydraulic Fracture Index
IAB	Iowa	D-Cracking	49
IAD	Iowa	D-Cracking	*160
IAF	Iowa	D-Cracking	43
ILA	Illinois	D-Cracking	52
MIA	Michigan	D-Cracking	43
OHC	Ohio	D-Cracking	11
OHD	Ohio	D-Cracking	32
IAA	Iowa	Non D-Cracking	106
IAC	Iowa	Non D-Cracking	45
IAE	Iowa	Non D-Cracking	109
ILB	Illinois	Non D-Cracking	286
MIB	Michigan	Non D-Cracking	241
WAA	Washington	Non D-Cracking	129

* Aggregate has produced durability factor (DF) values of 65, 83, and 87 in AASHTO T161 when tested by Iowa Department of Transportation. This aggregate is reported as being D-Cracking susceptible in the field.

Table 2-2 Effect of Sample Size on Variability

Sample ID	Coefficient of Variation (%) (Average number of particles)			
IAA	114 (185)	35 (370)	25 (555)	9 (740)
IAB	41 (177)	15 (354)	—	—
IAC	27 (145)	10 (290)	—	—
IAD	72 (181)	29 (362)	12 (543)	—
IAE	52 (156)	23 (312)	—	—
IAF	37 (183)	20 (366)	—	—

— no data available

Table 2-3 Between Laboratory Results

Sample ID	UW[a] HFI (# part)	MSU[b] HFI (# part)	UI[c] HFI (# part)
IAA	106 (924)	91 (200)	148 (178)
IAB	50 (530)	54 (190)	162 (178)
IAC	45 (435)	38 (180)	91 (110)
IAD	168 (725)	40 (200)	230 (138)
IAE	109 (468)	95 (190)	165 (314)
IAF	44 (550)	26 (180)	51 (195)

[a]University of Washington
[b]Michigan State University
[c]University of Illinois

A taller cylinder was obtained for the existing equipment, which increased the chamber volume by a factor of five. Because a larger volume of water would escape when the pressure was released (due to expansion of the larger chamber under pressure and also compression of a larger volume of water in the chamber) modifications of the valves and piping were required. Figure 2-8 shows the pressure release history for the larger chamber with modifications to the valves and fittings made in order to duplicate the original pressure release rate. The pressure release histories of the original and the larger chamber are very close, with a rate of 206,000 kPa/sec. (29,930 psi/sec) for the large chamber compared to a rate of 209,000 kPa/sec (30,350 psi/sec) for the original. The new larger chamber for the Washington Hydraulic Fracture Test is shown in Figure 2-9. While the pressure release histories look quite alike, testing of actual aggregate specimens will be necessary to determine if similar amounts of aggregate fracturing are produced in the large chamber.

Experience with the Washington Hydraulic Fracture Test suggests that the test procedure distinguishes between durable and nondurable aggregate pieces by fracturing the non-durable pieces while leaving the durable pieces unbroken. Experience also suggests that gravel sources often contain both clearly durable and clearly nondurable particles. That is, tests repeated on duplicate specimens of gravel sources usually produce substantial fracturing in the same individual rock types for that gravel source. Experience also suggests that bedrock sources, such as those that produce crushed limestone aggregate, can contain particles that are less clearly durable or nondurable. That may explain the large sample size (about 600-800 pieces) necessary to bring the coefficient of variability down to 10 percent. What this means is that in order to evaluate the modification to the Washington Hydraulic Fracture test equipment, a bedrock aggregate of marginal durability may be a better choice of test material than a gravel that contains a range of rock types. A wider range of pressure release rates would probably fracture the same clearly nondurable pieces in a gravel, while a marginal bedrock source would require more exact duplication of the pressure release history in order to produce the same fracturing.

5.0 Mitigation of Existing D-Cracking

Section 2.2 described how and why a D-cracking susceptible aggregate, freezing, and moisture are necessary for D-cracking to occur. Mitigation of D-cracking would require eliminating one of these conditions. In-place treatment of a D-cracking susceptible aggregate in existing concrete would probably not be possible. Materials may not be environmentally acceptable in the quantities required, so eliminating the D-cracking susceptible aggregate in existing concrete may not be a feasible option. The remaining methods of mitigating D-cracking in existing concrete are to eliminate either the freezing or the moisture condition.

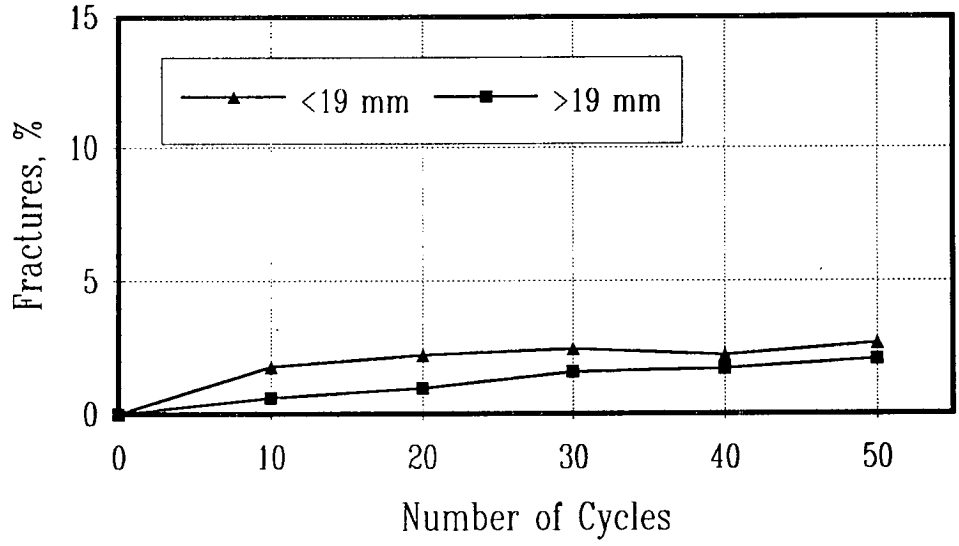

Figure 2-5 Comparison of Percent Fractures for plus 19.0 mm (3/4 in.) and minus 19.0 mm Durable Gravels

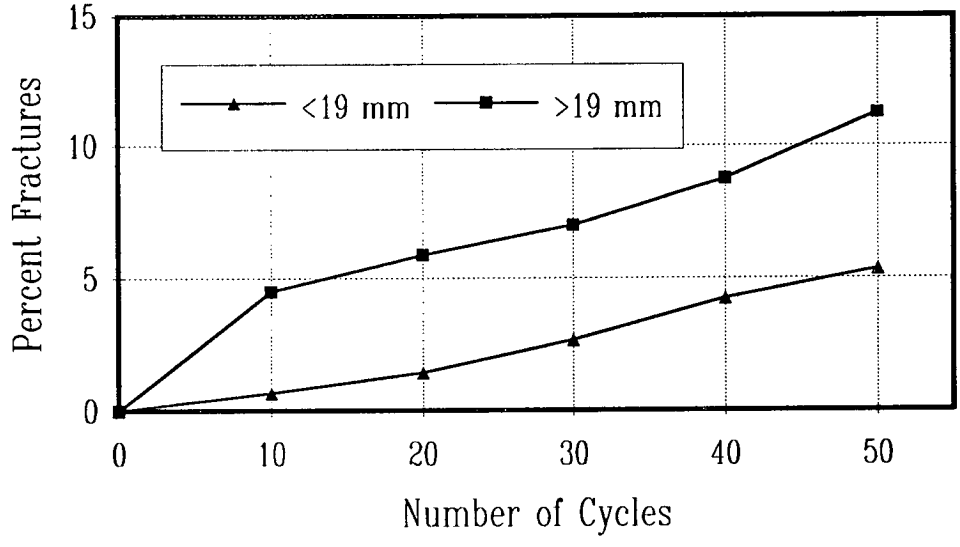

Figure 2-6 Comparison of Percent Fractures for plus 19.0 mm (3/4 in.) and minus 19.0 mm Nondurable Gravels

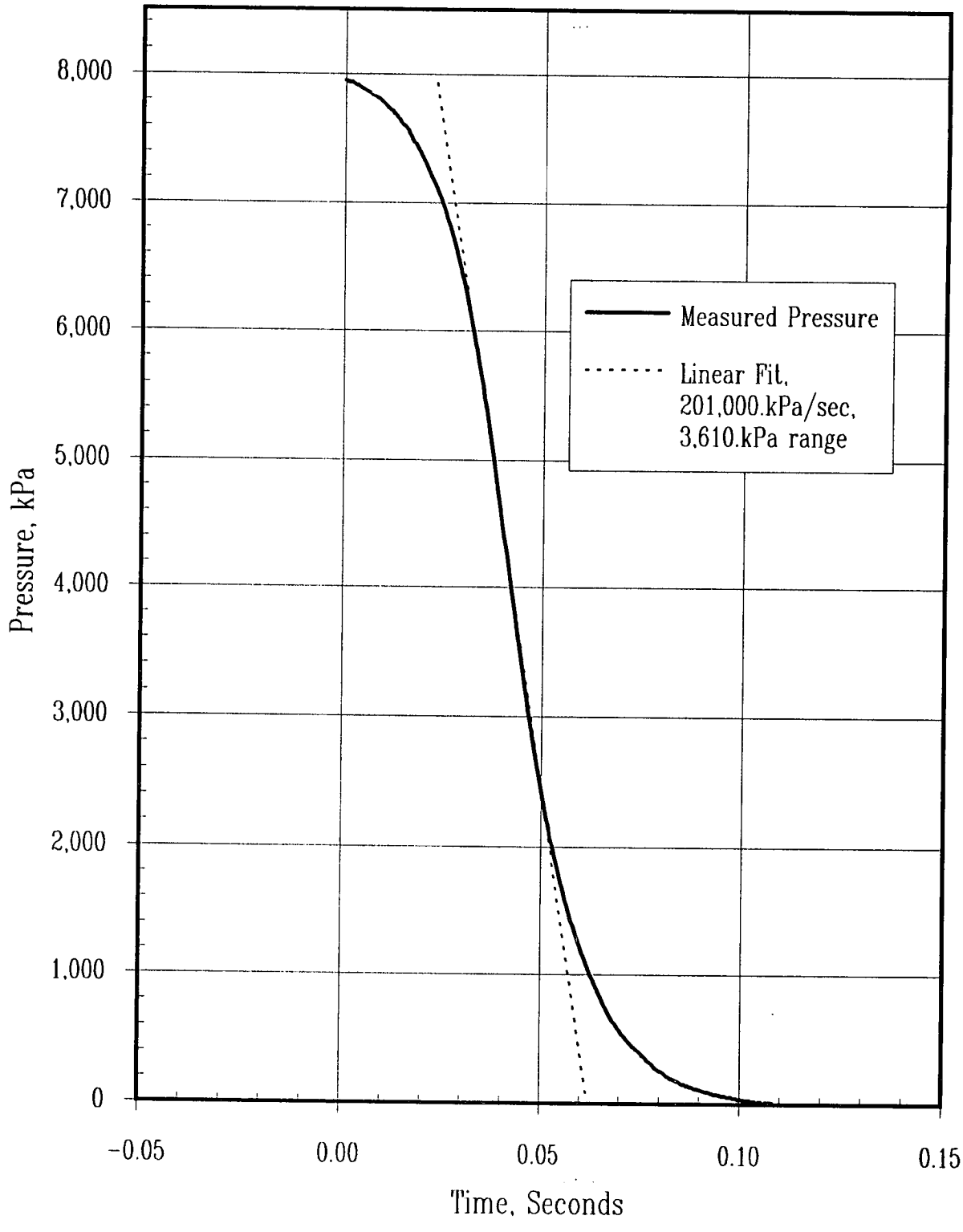

Figure 2-7 Pressure Release History for Original Chamber

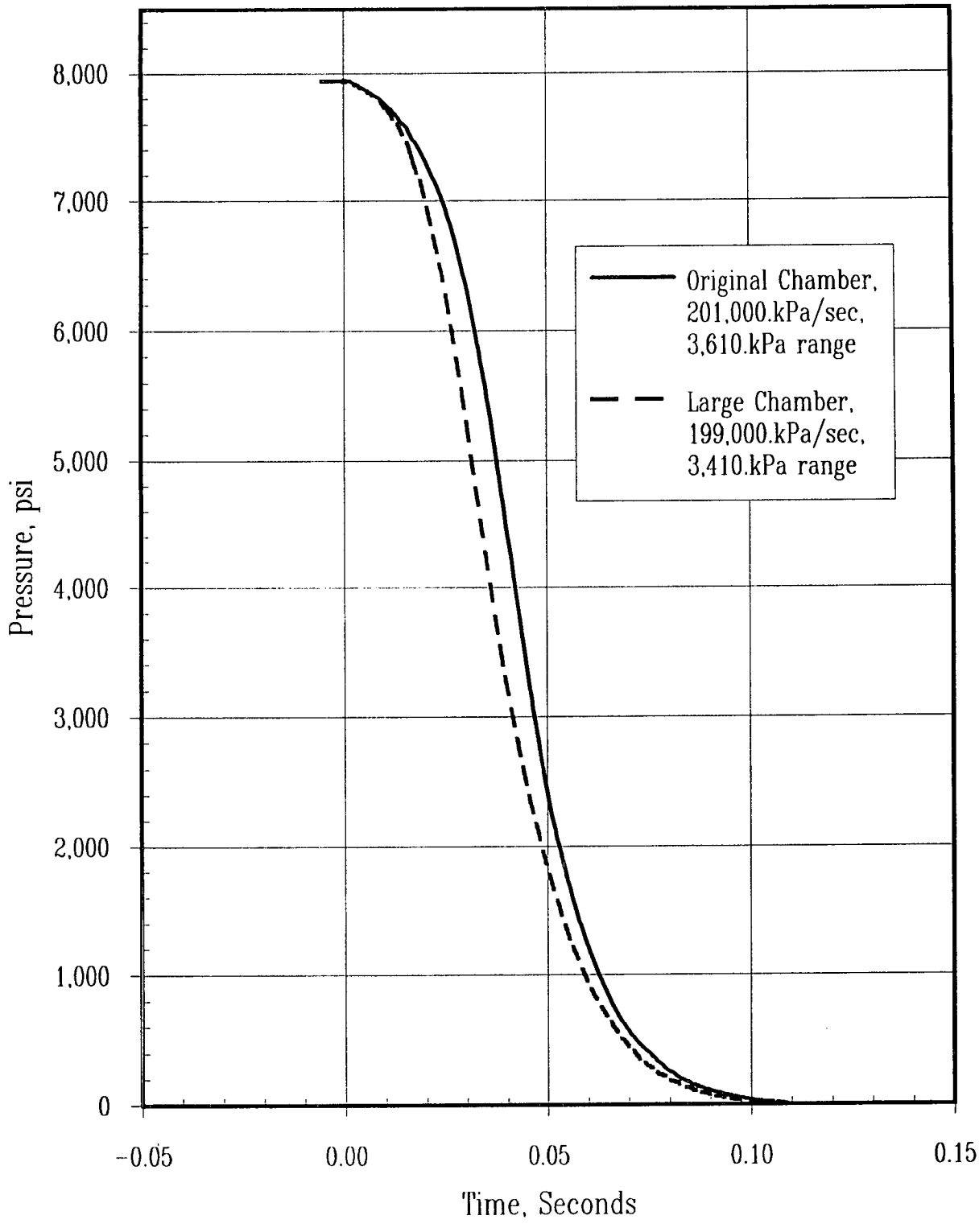

Figure 2-8 Pressure Release Histories for Original and Large Chambers

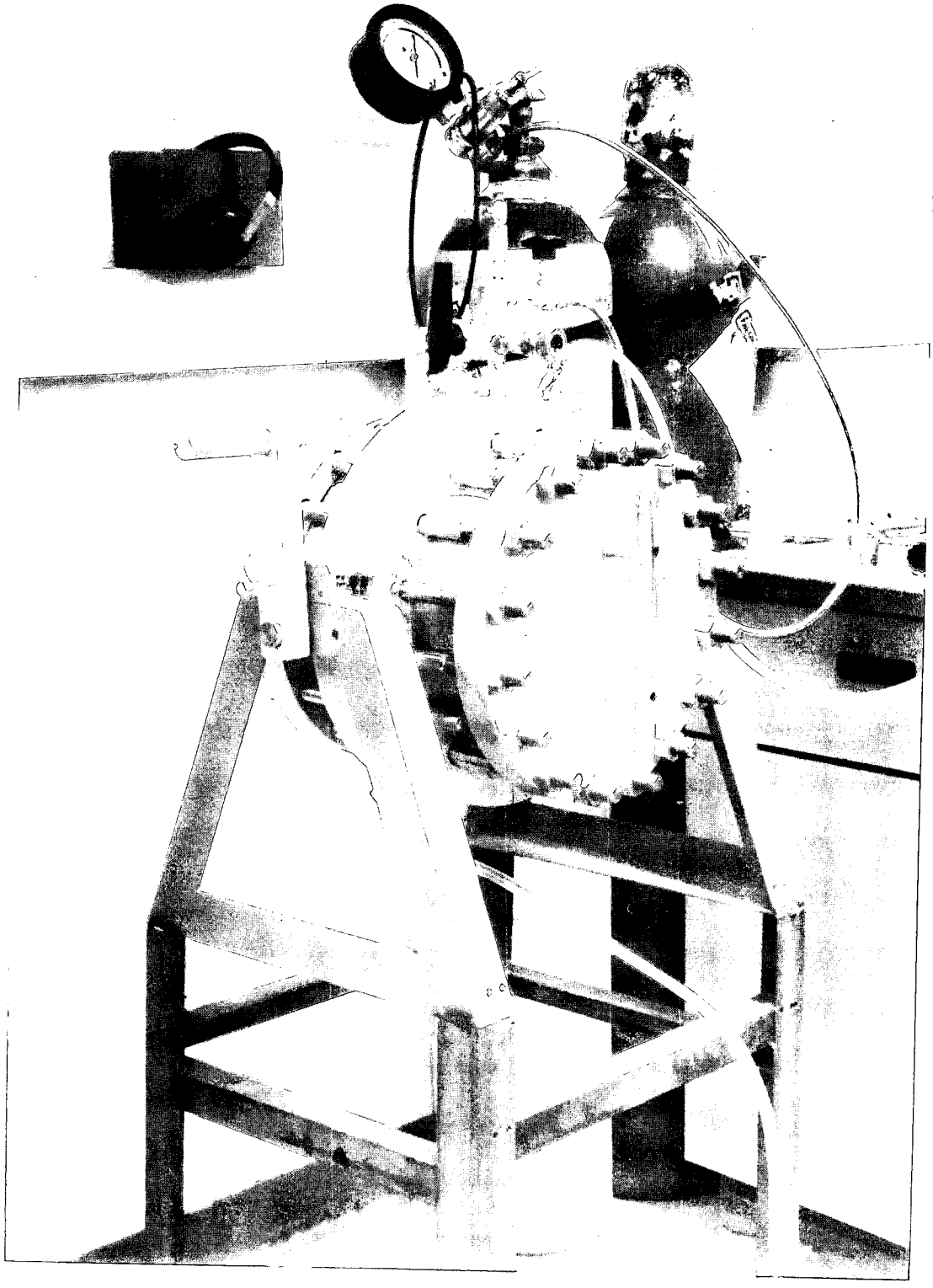

Figure 2-9 The Large Washington Hydraulic Fracture Test Apparatus

5.1 Preventing Freezing

Portland cement concrete pavements often receive asphalt concrete overlays as rehabilitation treatments to improve the condition of the pavement and extend the life of the pavement. In climates that do not often get below freezing in winter, freezing in a concrete pavement that contains D-cracking susceptible aggregates could possibly be prevented by covering the portland cement concrete with a sufficient thickness of asphalt concrete. Previous work[4,5] suggests that the freezing must almost be completely prevented in the concrete in order to stop the progression of D-cracking; merely decreasing the number of cycles of freezing and thawing with an overlay could actually accelerate the rate of D-cracking. This is possibly due to the decrease in evaporation of moisture in the overlaid concrete resulting in the concrete having a higher degree of saturation.

Temperature simulations[33] of overlaid and non-overlaid concrete pavement sections were conducted using historic weather data for at least nine years for five locations in the central latitudes of the United States. The locations studied were Tulsa, Oklahoma; Topeka, Kansas; Lexington, Kentucky; Evansville, Indiana; and Dodge City, Kansas. The average number of annual cycles of freezing and thawing at the surface of the concrete and depths of 50 and 100 mm (2 and 4 in.) into the concrete are shown for conditions of no overlay, 50 mm (2 in.) overlay, 100 mm (4 in.) overlay, and 150 mm (6 in.) overlay in table 2-4. This table shows that even 150 mm (6 in.) of asphalt concrete overlay is not sufficient to prevent freezing from occurring at the surface of the concrete pavement for these locations. As an overlay that thick is seldom used due to the grade corrections that would be necessary to meet highway safety guidelines, using an asphalt concrete overlay to prevent freezing in concrete made with D-cracking susceptible aggregates is probably not an effective D-cracking mitigation method.

5.2 Reducing Moisture

Sections 2.1 and 2.2 stated that D-cracking usually occurs first at joints or cracks and especially at the intersections of joints or cracks. At these locations, moisture is available vertically from the surface, vertically from the subbase, and laterally from the joint or crack. The same concrete, away from the joint or crack often shows no signs of D-cracking. Jointed reinforced concrete pavements with joint spacings of 12 m (40 ft) often contain 10 m (34 ft) or more of concrete with little or no D-cracking. Replacing 1m (3 ft) on each end of concrete slab gives the appearance of a completely restored concrete pavement. Unfortunately, the patching process produces two new joints. D-cracking appears on the old concrete side of the joints within about five years. If lateral moisture movement at these new joints could be prevented, the rate of D-cracking progression at the new joints could possibly be slowed.

Table 2-4 Effect of Asphalt Overlay Thickness on Reducing Freezing in Concrete Pavement

Location	Overlay Thickness (in.)	Number of Freeze Thaw Cycles at various depths in Portland Cement Concrete (PCC)		
		PCC Depth		
		0"	2"	4"
Tulsa, OK	0	31.1	9.7	3.5
	50	11.2	2.5	1.2
	100	4.7	1.0	0.3
	150	1.7	0.5	0.4
Topeka, KS	0	52.6	17.5	7.1
	50	28.8	7.0	5.0
	100	11.5	5.5	4.0
	150	6.0	4.6	2.6
Lexington, KY	0	42.6	15.9	6.5
	50	23.6	6.5	3.7
	100	11.5	4.1	2.6
	150	4.8	3.1	2.5
Evansville, IN	0	40.7	--	--
	50	24.2	5.2	3.9
	100	10.9	2.8	2.0
	150	2.9	2.2	1.3
Dodge City, KS	0	54.2	16.9	5.9
	50	25.7	5.2	3.4
	100	10.7	3.7	2.9

-- Data not available
1 in. = 25.4 mm

To test this hypothesis, 100 mm (4-in.) cores were taken from intact portions of a portland cement concrete pavement made with D-cracking susceptible aggregates (see section 3 of Part III of this report for a full description of the D-cracking susceptible pavement core locations). The cores were cut lengthwise, and air-dried for at least 30 days. The sides of half of each core were then coated with one of four types of concrete sealers. (The intent was not to determine the best sealer for this application, but rather to determine if any sealer would work.) The uncoated and coated halves were then placed together and subjected to repeated cycles of freezing and thawing in accordance with AASHTO T 161. Durability factor (DF) results of this testing is shown in table 2-5.

Table 2-5 Durability Factors of Sealer-Tested Cores from D-cracking to Pavement Susceptibility

Treatment	Treated	Untreated	Difference
Water-Based Silane	106	88	18
	78	75	3
	102	88	14
Solvent-Based Silane	98	84	13
	108	95	13
	97	90	7
Penetrating Oil	40	84	-44
	92	70	22
	85	87	-2
Two-Part Resin	91	95	-4
	84	88	-4
	100	73	27

For the untreated specimens, the overall average DF is 85, the standard deviation is 7.9, and the range between highest and lowest values is 25. AASHTO T 161 (Procedure A) suggests that the expected standard deviation should not exceed 5.7 for that DF range, and that the acceptable range between high and low specimens should not exceed 16. This greater-than-acceptable variability is probably due to a combination of factors including small specimen size, the fact that the specimens were dried prior to testing, and the fact that the specimens were cut to rather than cast in their final shape.

The average DF of 85 is higher than would be expected for concrete containing D-cracking-susceptible aggregate. This high DF is probably due to drying of the cores prior to freezing and thawing.

Considering the silane-treated (both water-based and solvent-based) specimens as a separate group gives a standard deviation of 6.7 and a maximum range of 20. While still greater than the AASHTO T 161 values, these are closer to the acceptable variability.

The difference between DF values for the treated and untreated core halves are also shown in table 2-5. All of the silane treated group show the treated halves having higher DF values (less deterioration) than the untreated halves. This indicates that the sealer appeared to slow down the rate of deterioration of D-cracking susceptible concrete exposed to repeated cycles of freezing and thawing in the laboratory. A full description of the field test of this D-cracking mitigation method along with detailed statistical analysis of the laboratory data is presented in section 3 of Part III of this report.

References

1. Schwartz, D. R., "D-Cracking of Concrete Pavements," *NCHRP Synthesis of Highway Practice No. 134*, 1987.

2. Stark, D. and P. Klieger, "Effects of Maximum Size of Coarse Aggregate on D-Cracking in Concrete Pavements," *Highway Research Record 441,* 1973, pp. 33-43.

3. Bjegovic, D. Mikulic, and V. Ukraincik, "Theoretical Aspect and Methods of Testing Concrete Resistance to Freezing and Deicing Chemicals," *Concrete Durability SP 100,* 1987, Vol. 1, pp. 947-971.

4. Janssen, D. J., "The Effect of Asphalt Concrete Overlays on the Progression of Durability Cracking in Portland Cement Concrete," Ph.D. dissertation, University of Illinois, Department of Civil Engineering, Urbana, Ill., 1985.

5. Janssen, D. J., J. D. DuBose, A. J. Patel, and B. J. Dempsey, "Predicting the Progression of D-Cracking," Civil Engineering Studies, *Transportation Engineering Series No. 44*, University of Illinois, 1986.

6. Larson, T., P. D. Cady, M. Franzen, and J. Reed, "A Critical Review of Literature Treating Methods of Identifying Aggregates Subject to Destructive Volume Change When Frozen in Concrete and a Proposed Program of Research," 1964, *NCHRP Sp Rpt 80.*

7. Thompson, S. R., M.P.J. Olsen, and B. J. Dempsey, "D-Cracking in Portland Cement Concrete Pavements," FHWA/IL/UI-187, Ill. Dept. of Transportation, Bureau of Materials and Physical Research, Springfield, Ill., 1980.

8. Larson, T. D. and P. D. Cady, "Identification of Frost-Susceptible Particles in Concrete Aggregates," 1969, *NCHRP Rpt 66.*

9. *AASHTO Materials, Part II, Tests,* 15th Edition, The American Association of State Highway and Transportation Officials, 1990.

10. Sturrup, V., R. Hooton, P. Mukherjee, and T. Carmichael, "Evaluation and Prediction of Concrete Durability—Ontario Hydro's Experience," *Durability of Concrete SP 100,* 1987, Vol. 2, pp. 1121-1154.

11. Marks, V. J., and W. Dubberke, "Durability of Concrete and the Iowa Pore Index Test," *Transportation Research Record 853*, 1982, pp. 25-30.

12. *Annual Book of ASTM Standards, Vol. 04.02, Concretes and Aggregates,* American Society for Testing and Materials, 1992.

13. Walker, R. D., Identification of Aggregates Causing Poor Concrete Performance When Frozen, 1965, *NCHRP Rpt 12.*

14. Dolch, W. L., "Porosity," *ASTM STP-169B,* 1978, pp. 646-656.

15. Winslow, D. N., and S. Diamond, "A Mercury Porosimetry Study of the Evolution of Porosity in Portland Cement," *Journal of Materials*, Vol. 5, No. 3, 1970, pp. 564-585.

16. Hiltrop, C. L. and J. Lemish, "Relationship of Pore-Size Distribution and Other Rock Properties to Serviceability of Some Carbonate Aggregates," *Highway Research Board Bull. 239*, 1960, pp. 1-23.

17. Kaneuji, M., D. N. Winslow, and W. L. Dolch, "The Relationship Between An Aggregate's Pore Size Distribution and Its Freeze Thaw Durability in Concrete," *Cement and Concrete Research,* Vol. 10, No. 3, 1980, pp. 433-441.

18. Shakoor, A. and C. F. Scholer, "Comparison of Aggregate Pore Characteristics as Measured by Mercury Intrusion Porosimeter and Iowa Pore Index Tests," *Journal of the American Concrete Institute*, 1985, pp. 453-458.

19. Walker, R. D. and T. Hsieh, "Relationship Between Aggregate Pore Characteristics and Durability of Concrete Exposed to Freezing and Thawing," *Highway Research Record 226,* 1968, pp. 41-49.

20. Traylor, M. L., "Efforts to Eliminate D-Cracking in Illinois," *Transportation Research Record 853*, 1982, pp. 9-14.

21. Winslow, D. N., "The Rate of Absoption of Aggregates," *Cement, Concrete, and Aggregates*, Vol. 9, No. 2, 1987, pp. 154-158.

22. Klieger, P., G. Monfore, D. Stark, and W. Teske, "D-Cracking of Concrete Pavements in Ohio," Final Report, 1974, Ohio-DOT-11-74.

23. Harman, J. W., P. D. Cady, and N. B. Bolling, "Slow-Cooling Tests for Frost Susceptibility of Pennsylvania Aggregates," *Highway Research Record 328,* 1970, pp. 26-37.

24. Larson, T. D., A. Boettcher, P. Cady, M. Franzen, and J. Reed, "Identification of Concrete Aggregates Exhibiting Frost Susceptibility," 1965, *NCHRP Rpt. 15.*

25. Mysyk, W. K., "Petrological Studies on Carbonate Aggregate Responsible for Pavement D-Cracking in Southern Manitoba, Canada," *Transportation Research Record 1110*, 1987, pp. 10-15.

26. Walker, R. D., H. J. Pence, W. H. Hazlett, and W. J. Ong, "One-Cycle Slow-Freeze Test For Evaluating Aggregate Performance In Frozen Concrete," 1969, *NCHRP Report 65*.

27. Rhoades, R. and R. C. Mielenz, "Petrography of Concrete Aggregate," *Journal of American Concrete Institute*, Vol. 17, No. 6, 1946, pp. 581-600.

28. ACI Committee 621, "Selection and Use of Aggregates for Concrete," *Journal of American Concrete Institute*, Vol. 58, No. 5, 1961, pp. 513-541.

29. Perenchio, W. F., "Durability of Concrete Treated with Silanes", *Concrete International*, Vol. 10, No. 11, 1988, pp. 34-40.

30. Almond, D. K., "A Test for Identifying Aggregates Susceptible to Freeze-Thaw Damage," Masters' Thesis, Department of Civil Engineering, University of Washington, 1990.

31. Janssen, D. J. and D. K. Almond, "A Comparison of Four Aggregates Using the Washington Hydraulic Fracture Test," *Transportation Research Record No. 1301*, 1991, pp. 57-67.

32. "Recently Active Aggregate Sources," *Instruction Memorandum,* Iowa Department of Transportation, 1990.

33. Dempsey, B. J., "A Heat-Transfer Model for Evaluating Frost Action and Temperature Effects in Multilayered Pavement Systems," Ph.D. Dissertation, University of Illinois, Department of Civil Engineering, Urbana, Ill., 1969.

Appendix 2A
Washington Hydraulic Fracture Test Procedure
AASHTO Test Procedure Format

Proposed Method of Test
for
Hydraulic Fracture of Coarse Aggregate

1. Scope

1.1 This test method assesses the resistance of aggregates to fracture by using a sudden increase of internal gas pressure to expel water from aggregate pores. The procedure assists in the identification of aggregates that may cause deterioration in concrete when exposed to repeated cycles of freezing and thawing (D-cracking).

1.2 This procedure may involve hazardous materials, operations, and equipment. This procedure does not purport to address all of the safety problems associated with its use. It is the responsibility of whosoever uses this procedure to consult and establish appropriate safety and health practices and determine the applicability of regulatory limitations prior to use.

2. Referenced Documents

2.1 *AASHTO Standards*

T 2	Sampling Aggregates
T 161	Resistance of Concrete to Rapid Freezing and Thawing
M 92	Wire Cloth Sieves for Testing Purposes
M 231	Weights and Balances Used in The Testing of Highway Materials

2.2 *ASTM Standards*

C 702	Method for Reducing Field Samples of Aggregate to Testing Size
D 3152	Standard Test Method for Capillary Moisture Relationships for Fine-Textured Soils by Pressure-Membrane Apparatus
D 3665	Practice for Random Sampling of Construction Materials

3. Significance and Use

3.1 As noted in the scope, the procedure described in this method is intended to aid in the identification of D-cracking susceptible aggregates. Aggregates that exhibit a high percentage of fracturing under repeated pressurization cycles are considered to be more likely to cause D-cracking in field applications.

3.2 The relative short time (approximately eight working days) required for completion of this procedure makes it appropriate for use as a screening test to identify questionable aggregates that require additional testing (such as AASHTO T 161) prior to approval.

3.3 This method is sensitive to the size of the aggregate pieces, and may be appropriate for identifying maximum aggregate size reductions necessary to avoid D-cracking.

3.4 This method is also sensitive to the number of nondurable particles in a sample, and may be appropriate for determining the percentage of durable aggregate that must be blended with nondurable aggregate in order to produce a blend that provides acceptable performance.

4. Apparatus

4.1 *Tumbling Apparatus:*

4.1.1 The tumbling apparatus (hereafter referred to as the tumbler) shall consist of a rubber drum for holding the sample and a motorized drive unit.

NOTE 1 - A suitable tumbler is available commercially for polishing rocks. Various sizes are available.

4.1.2 The rubber drum shall have inside dimensions of approximately 6-3/4 in. in diameter by 8 in. deep (170 by 200 mm). The inside shall be faceted to assist in the tumbling of the aggregate pieces. The drum shall have a removable cover to facilitate placing the sample in the drum, and the cover should not interfere with the rotation of the drum when in the motorized drive unit.

4.1.3 The motorized drive unit shall be capable of rotating the drum on its side at a rate of 30 ($\pm$5) revolutions per minute.

4.2 *Pressurization Apparatus:*

4.2.1 The pressurization apparatus shall consist of a pressure chamber able to safely withstand operating pressures of 1500 psi (10,000 kPa), a compressed nitrogen source, an adjustable pressure regulator with gauge having an output capacity of up to 1500 psi (10,000 kPa), appropriate valves and fittings to permit filling with water and draining along with pressurization/rapid pressure release, and a stand to permit a 90° rotation of the pressurization apparatus.

4.2.2 The inside dimensions of the pressure chamber shall be 10 in. in diameter by 10 in. high (254 by 254 mm). The chamber shall consist of three pieces: a cylinder with three through holes tapped from the outside, 1 in. (25.4 mm) from the end, for 3/8 in (9.5 mm). National Pipe Thread (NPT), a top plate with a handle for lifting, and a bottom plate. All pieces shall be at least 1 in. thick (25.4 mm). The three tapped holes shall be spaced around the cylinder with the second 22.5° from the first and the third 180° from the first. Grooves in each end of the cylinder should accept an O-ring for sealing. The top and bottom plates should be drilled to clear the high-strength bolts used to hold the chamber shut. A photograph of the equipment is included in appendix A.

NOTE 2 - A similar pressure chamber is available as a 100 Bar Pressure Membrane Extractor for testing soils in accordance with ASTM D 3152 at pressures up to 1500 psi (10,000 kPa). For use with the Hydraulic Fracture procedure, the 100 Bar Pressure Membrane Extractor should be purchased with a second top plate substituted for the standard bottom plate, and a 10-in. (254 mm) tall cylinder substituted for the standard 2-in. (50.8 mm) tall cylinder.

NOTE 3 - Shop-built pressure chambers are not recommended due to the difficulty with obtaining pressure-tight seals at the high pressures involved, as well as the hazards associated with high pressures. If a shop-built pressure chamber is used, it should be pressure-certified to provide a safety factor of at least 5 to 1.

4.2.3 The cylindrical part of the pressure chamber shall be fitted with necessary valves and fittings to permit the application of pressure (pressure valve), release of pressure (pressure release valve), filling with water (fill valve), and draining (drain valve). Additional valves and fittings may be provided where appropriate by the equipment manufacturer in order to achieve the necessary pressure-release rate.

4.2.4 A pressure regulator and gauge that attaches directly to a compressed nitrogen cylinder shall be provided. The regulator shall have a capacity of 1500 psi (10,000 kPa). The gauge shall have a precision of 0.25 percent of full scale.

NOTE 4 - An appropriate regulator with gauge is available from the manufacturer of the pressure chamber referred to in NOTE 2.

4.2.5 A stand shall be provided to permit rotation of the assembled pressure chamber from horizontal position for filling and assembly to vertical for testing.

4.3 *Drying Oven:*

The drying oven should allow free circulation of air through the oven and should be capable of maintaining a temperature of 121°C ±5°C (250°F ±9°F).

4.4 *Balance:*

The balance should conform to the requirements of AASHTO M 231 for the class of general purpose balance required for the principal sample weight of the sample to be tested.

5. Special Solutions Required

5.1 A solution of alkylalkoxysilane in water (referred to as silane solution) is used in Step 7.3 as part of the sample preparation.

5.2 Appropriate precautions in handling the silane solution should be observed.

NOTE 5 - An appropriate silane solution is available commercially as Enviroseal 40 from Hydrozo, Inc.

NOTE 6 - Some aggregates absorb water at a very rapid rate, which prevents them from fracturing in the following test procedure. The silane treatment described in Step 7.3 reduces the absorption rate by effectively making the aggregates more hydrophobic. This treatment has been demonstrated to have no effect on the hydraulic fracture performance of aggregates with slower absorption rates.

6. Samples

6.1 Representative samples of aggregate sources should be obtained by appropriate means and in accordance with accepted procedures such as AASHTO T 2 and ASTM C 702 and D 3665.

6.2 Samples will be divided into individual size ranges (Step 7.1 below). Appropriate size ranges may include passing the 1-1/4 in. (31.5 mm) but retained on the 3/4 in. (19.0 mm) sieves and passing the 3/4 in. (19.0 mm) but retained on the 1/2 in. (12.5 mm) sieves.

6.3 Duplicate specimens may be run to obtain acceptable variability, and sufficient material should be collected in the initial sample to provide the necessary number of particles in each desired size range. Preliminary work has indicated that 600-800 particles in a given size range provides a coefficient of variation of less than 10 percent in the final results.

7. Preparation of Test Sample

7.1 Separate the sample into appropriate size ranges by sieving to refusal using approved wire screens (AASHTO M 92). Individual specimens should contain sufficient aggregate to fill the pressure chamber.

NOTE 7 - Approximately 15 kg (34 lb) are needed for a test specimen in the passing 1-1/4 in. (31.5 mm) but retained on the 3/4 in. (19.0 mm) sieve size range. This is approximately 800 particles. The actual amount depends upon the size and shape of the individual particles.

7.2 The aggregate specimens should be thoroughly washed and dried to a constant mass in an oven at a temperature of 120°C ±5°C (250°F ±9°F), and allowed to cool to room temperature.

NOTE 8 - Adequate ventilation should be supplied for the following three steps. The use of a fume hood may be appropriate.

7.3 Place the aggregate specimen in the silane solution, making sure that all aggregate pieces are covered. Allow the specimen to remain in the silane solution for 30 (±5) seconds.

7.4 Remove the specimen from the silane solution and allow the excess solution to drain for 5 minutes.

NOTE 9 - Strainers suitable for immersing the aggregate in the silane solution and draining are readily obtainable from restaurant supply sources.

NOTE 10 - The silane solution may be reused if it is placed in a sealed container between uses. The solution should be discarded if it begins to thicken.

7.5 Dry the specimen to a constant mass at a temperature of 120°C ±5°C (250°F ±9°F), and allow to cool to room temperature.

8. Procedure

8.1 Place enough of the specimen into the tumbler to fill it approximately halfway and tumble for 1 minute. Separate out any pieces passing the 3/8 in. (9.5 mm) sieve. Repeat for the remainder of the specimen. Determine the mass to the nearest gram and count the number of pieces retained on the +3/8 in. (9.5 mm) sieve. Record these numbers as the initial mass and number of particles, m_0 and n_0, respectively.

8.2 Place the specimen into the pressure chamber, and close the chamber as directed in the manufacturer's instructions. Rotate the apparatus from the filling (horizontal) to the testing (vertical) position.

8.3 Close the pressure valve and open the main valve on the nitrogen tank. The pressure regulator should be set to 1150 psi. (7930 kPa).

8.4 Fill the pressure chamber with water in accordance with the manufacturers' instructions. After the water has run from the drain line for approximately 30 seconds, turn off the water supply and close the fill, pressure release, and drain valves.

8.5 Pressurize the chamber for 5 minutes (±5 seconds) by opening the pressure valve. Adjust the pressure regulator as necessary to maintain 1150 psi (7930 kPa). At about 4-1/2 minutes, close the pressure valve and disconnect the drain line from the pressure release valve.

8.6 After 5 minutes (±5 seconds) of pressurization, *while wearing ear protection*, release the pressure by rapidly opening the pressure release valve.

8.7 Refill the pressure chamber by re-attaching the drain line to the pressure release valve, opening the fill valve, and turning on the water supply. Allow water to fill for approximately 30 seconds, rotating the chamber slightly to remove any air bubbles in the chamber. Turn off the water supply and close the fill and pressure release valves.

8.8 Re-pressurize the chamber after a total elapsed time of 1 minute (±5 seconds), without pressure. Adjust the regulator as necessary to maintain a pressure of 1150 psi (7930 kPa). This pressurization time is 2 minutes (±5 seconds). At about 1-1/2 minutes, close the pressure valve and disconnect the drain line from the pressure release valve.

8.9 Release the pressure after 2 minutes (±5 seconds), *while wearing ear protection*, by rapidly opening the pressure release valve (as in 8.6 above).

8.10 Repeat Steps 8.7 through 8.9 eight additional times for a total of ten pressurization cycles. Rotate the pressure chamber back to horizontal for draining.

8.11 Turn off the valve on the nitrogen bottle and open the drain valve. Drain the water from the pressure chamber by slowly opening the pressure valve and allowing the compressed gas in the line to force the water out of the chamber.

8.12 Unbolt the chamber and remove the specimen. Dry the specimen to a constant mass at a temperature of 120°C ±5°C (250°F ±9°F), and allow it to cool to room temperature.

8.13 Place enough of the specimen into the tumbler to fill it approximately halfway, and tumble for 1 minute (±5 seconds). Repeat with the remaining portion of the specimen. Separate out any pieces passing the 3/8 in. (9.5 mm) sieve but retained on the No. 4 sieve. Determine the masses of both the +3/8 in. (9.5 mm) and cumulative -3/8 in. (9.5 mm), + No. 4 sieve particles to the nearest gram. Record these values as m_i and $m4_i$ respectively for the i number of pressurization cycles completed. Count the number of pieces retained on the 3/8 in. (9.5 mm) sieve and record this number as n_i. Count the cumulative number of pieces passing the 3/8 in. (9.5 mm) sieve but retained on the No. 4 sieve and record this number as $n4_i$.

8.14 Repeat Steps 8.2 through 8.13 for a total of 50 pressurization cycles.

9. Calculations

9.1 *Percentage Fracture* - Calculate the percentage of fracturing after each ten pressurization cycles as follows:

$$FP_i = 100 \cdot (n4_i/2 + n_i - n_0)/n_0 \qquad (1)$$

where FP_i = percent fractures after i pressurization cycles
$n4_i$ = cumulative number of pieces passing the 9.5 mm (3/8 in.) sieve but retained on the No.4 sieve after i pressurization cycles,
n_i = number of pieces retained on the 9.5 mm (3/8 in.) sieve after "i" pressurization cycles, and
n_0 = initial number of pieces tested

Report FP values to the nearest integer.

9.2 *Hydraulic Fracture Index* - Calculate the hydraulic fracture index (HFI) as the number of cycles necessary to produce 10 percent fracturing as follows:

If 10 percent fracturing is achieved in 50 or fewer cycles, calculate the HFI as a linear interpolation of the number of cycles that produced 10 percent fractures:

$$HFI = A + 10 \cdot [(10\text{-}FP_A)/(FP_B - FP_A)]$$

where A = cycles just prior to achieving 10 percent fracturing
FP_A = percentage of fracturing just prior to achieving 10 percent fracturing, and
FP_B = percentage of fracturing just after achieving 10 percent fracturing

If 10 percent fracturing is not achieved in 50 pressurization cycles, calculate the HFI as an extrapolation from zero fracturing at 0 cycles through the amount of fracturing at 50 cycles.

$$HFI = 50 \cdot (10/FP_{50})$$

where FP_{50} = percentage of fracturing after 50 pressurization cycles.

Report HFI values to the nearest integer.

9.3 *Percent Mass Loss* - Determine the percent mass loss as follows:

$$ML_i = (100/m_0) \cdot [m_0 - (m4_i + m_i)] \quad (2)$$

where ML_i = percentage of mass loss after i cycles of pressurization,
$m4_i$ = cumulative mass of the material passing the 9.5 mm (3/8 in.) sieve but retained on the No. 4 sieve after i pressurization cycles,
m_i = mass of the pieces retained on the 9.5 mm (3/8 in.) sieve after i pressurization cycles, and
m_0 = initial mass of the specimen tested

Report ML values to the nearest integer.

NOTE 11 - When data from more than one specimen are combined for determining final results, the raw data, m_0, n_0, $m4_i$, $n4_i$, m_i, and n_i, should be combined prior to calculation of ML_i, FP_i and HFI.

10. Report

10.1 The report shall include the following information and data:

10.2 *Sample Identification:*

10.2.1 Report the person or agency submitting the sample for testing.

10.2.2 List the source or identifying code for the aggregate.

10.3 *Initial Specimen Size:*

10.3.1 Report the particle size range(s) tested as determined in Section 7 of this procedure.

10.3.2 Report the initial mass and initial number of particles as determined in Step 8.1 above.

10.4 *Percentage Fracture*

Report the percentage fracture after each series of ten pressurization cycles.

10.5 *Percentage Mass Loss*

Report the percentage mass loss after each series of ten pressurization cycles.

10.6 *Hydraulic Fracture Index*

Report the hydraulic fracture index for the specimen

10.7 When multiple specimens are tested from the same source and particle size range, list individual and combined specimen values.

NOTE 12 - A graph of fracture percentage versus number of cycles is often useful in presenting the data.

NOTE 13 - An example report form is shown in appendix B.

11. Precision

11.1 *Within-Laboratory Precision* - The precision of results from a single aggregate source appears to depend upon the number of pieces tested. Data is currently being collected in order to determine the within-laboratory precision. Preliminary data is given in appendix C.

11.2 *Between Laboratory Precision* - Data is currently being collected to determine the between-laboratory precision.

Appendix A
Hydraulic Fracture Apparatus

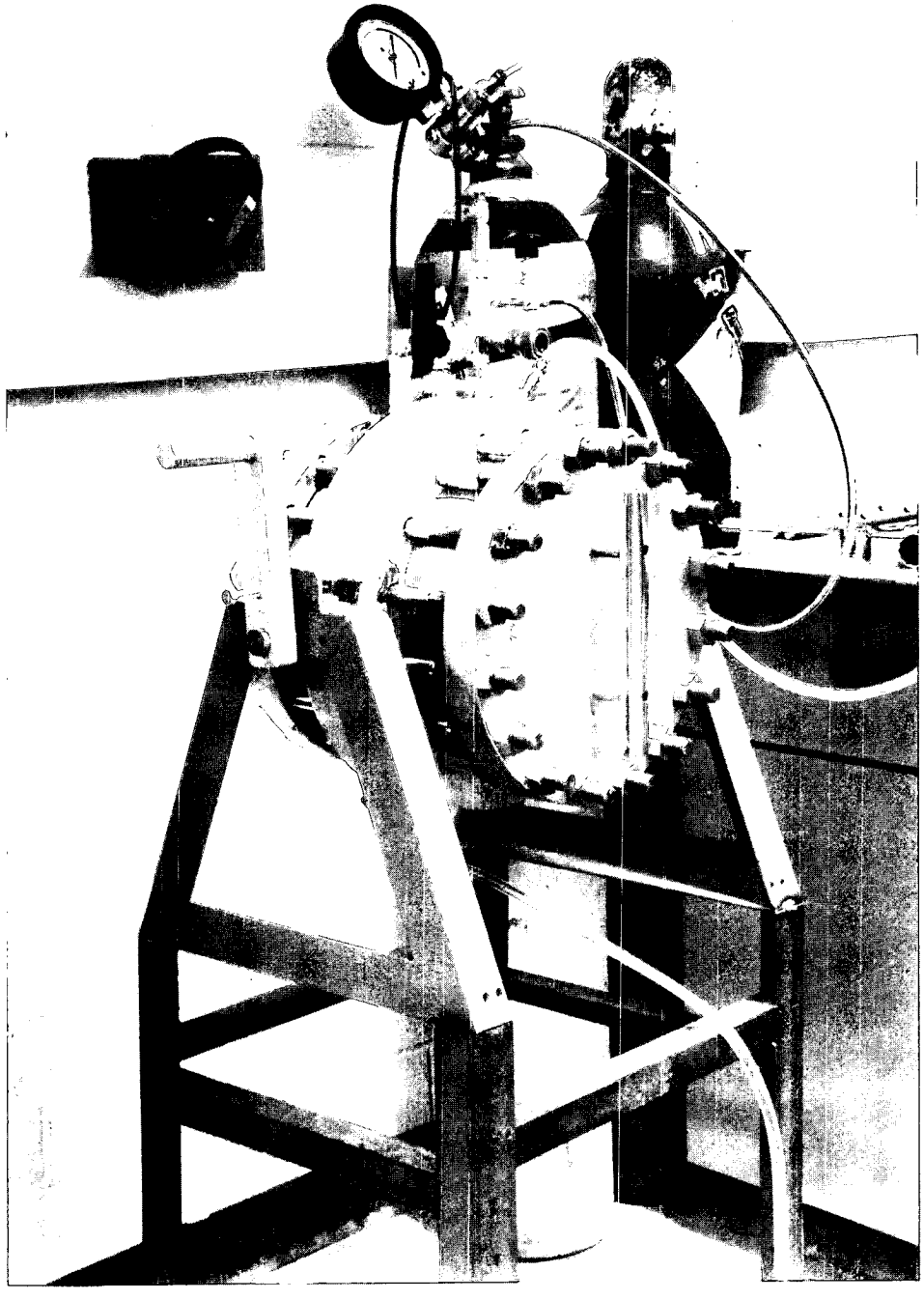

Hydraulic Fracture of Coarse Aggregate

Appendix B
Sample Data Sheet

WHFT Data Sheet

Source		Submitted by		Received by		Date	
	Size Range		Initial Mass		Initial	# Particles	
Testing	Cumulative	Mass	Mass	Count	Count	% Mass	Percent
Date	# of Cycles	(+9.5mm)	(9.5 to 4.76mm)	(+9.5mm)	(9.5 to 4.76mm)	Loss	Fractures
	10						
	20						
	30						
	40						
	50						
						HFI =	

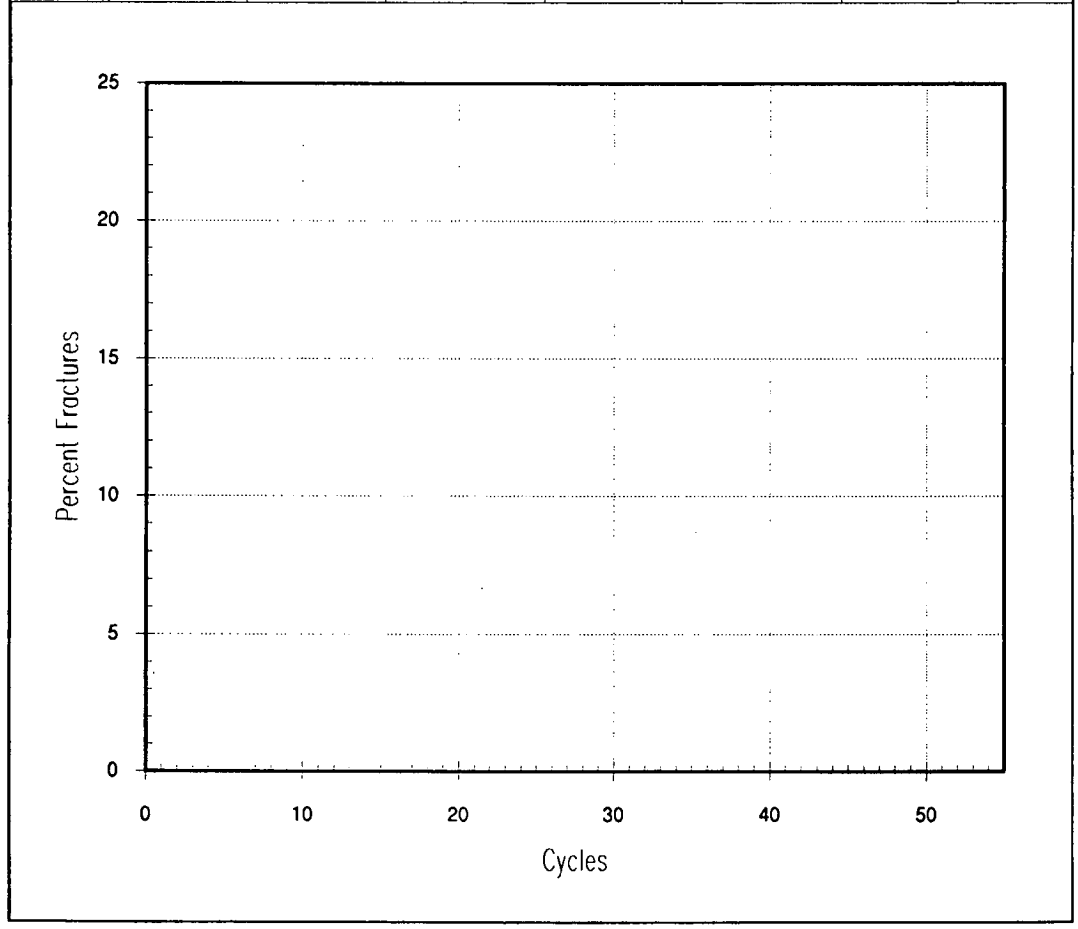

Appendix C
Preliminary Variability Data

Sample ID	Coefficient of Variation (%) (Average Number of Particles)			
IA**A	114 (185)	35 (370)	25 (555)	9 (740)
IA**B	41 (177)	15 (354)	-	-
IA**C	27 (145)	10 (290)	-	-
IA**D	72 (181)	29 (362)	12 (543)	-
IA**E	52 (156)	23 (312)	-	-
IA**F	37 (183)	20 (366)	-	-

Appendix 2B
Assembling and Operating the Washington Hydraulic Fracture Test Apparatus: Large Chamber

Parts Description

The large chamber apparatus for the Washington Hydraulic Fracture Test consists of a number of individual pieces.

Cylinder Assembly -The cylinder assembly includes the cylinder portion of the pressure chamber containing the valves and fittings, along with the attached pivot collar and stand. The cylinder portion has a machined channel for the O-ring seal (called an O-ring channel) on each end. The "bottom" of the cylinder is the end closest to the three sets of valves and fittings.

A handle is attached to the pivot shaft on one side of the stand. A locking bolt on the handle can be turned in to engage one of three positioning holes in the stand if necessary to prevent the cylinder assembly from moving.

O-Rings - Two O-rings are used to seal the pressure chamber when it is assembled and pressurized. The O-rings should be regularly inspected for cuts and imbedded rock particles. Replace the O-rings as necessary.

End Plates - Two interchangeable end plates with handles complete the pressure chamber portion of the apparatus.

High-Strength Bolts - Sixteen high-strength bolts are used to hold the end plates to the cylinder. These bolts are tightened to approximately 60 to 80 inch-pounds (6.8 to 9.0 newton-meters).

Assembly Rods - Two 3/4-in. (19 mm) diameter threaded rods, 14 in. (356 mm) long, are used to assemble the pressure chamber. Each rod has a hole approximately 5 in. from each end through which 1/4 in. (6 mm) diameter rods (assembly pins) are inserted during the assembly process.

Pressure Regulator - A pressure regulator (0-1500 psi outlet pressure) with inlet and outlet pressure gages attaches directly to a high-pressure compressed nitrogen cylinder (user supplied) and connects via a flexible pressure line to the pressure chamber.

Water Line - A flexible plastic water line connects the pressure chamber to a water source. (A user-supplied connection to an anti-siphon laboratory water source is suggested.)

The connection to a water source should comply with local plumbing codes and regulations.

Drain Line - A flexible plastic water line connects to the pressure chamber (through a quick-disconnect fitting) and leads to a water drain. Attaching the hose so that the free end drains into a sink is adequate.

Second Drain Line (optional) - A second drain line can be used with the apparatus, or the single drain line can be interchanged between the drain and pressure release connections.

The specific valve and fitting assemblies are described below:

Fill Assembly - This assembly consists of the fill valve and the connection to the water line.

Fill Valve - This is a plug valve with a green lever handle. On-off is accomplished by a 90-degree turn. Occasional maintenance includes replacing worn or damaged O-rings on the valve plug, and applying a thin film of silicone grease when the valve is reassembled.

Water Line Connection - This is a compression-type connection to the plastic water line, and should not need to be changed after the original assembly.

Drain Assembly - This assembly consists of a drain valve, a connection to the drain line, and a copper drain pipe.

Drain Valve - This valve is identical to the fill valve described previously.

Drain Line Connection - This connector consists either of a female half of a quick disconnect if a single drain line is used, or it can be replaced with a compression-type connector for use with a second drain line.

Copper Drain Pipe - A short section of flexible copper pipe is inserted into a hole on the inside of the pressure cylinder. This pipe serves to help siphon water from the pressure chamber at the conclusion of testing. When the chamber is being assembled, the open end of this pipe should contact the bottom plate for complete drainage. If the copper drain pipe becomes loose with usage, either a few wraps of Teflon tape or flexible caulking can be used to re-attach the pipe.

Pressure Assembly - This assembly includes four valves and connections for both a drain line and the pressure line.

Pressure Valve - This is a screw-type valve with a large round handle. The valve connects directly to the pressure line by threaded-pipe connection.

Standpipe Valve - This is also a screw-type valve and has a small round handle. Nothing is connected to the outlet side of this valve.

Pressure Isolation Valve - This is a ballvalve with a small black lever handle. Maintenance for this valve consist of periodically tightening the packing around the ball whenever a slow leak develops. This is accomplished by removing the lever handle (attached with a set-screw) and using a wrench to tighten the two-sided nut exposed under the handle. The nut should be tightened in 1/16th turns until leaking stops.

Pressure Release Valve - This is a ball-valve with a large black lever handle. Maintenance is the same as for the pressure isolation valve described above.

Pressure Release Connector - This is the female half of a quick-disconnect. The drain line is connected here while the pressure chamber is being filled with water, and removed for pressure release.

Chamber Assembly

The pressure chamber is assembled by the following steps:

1. With the pressure cylinder in the inverted position (bottom of cylinder up), wipe any dirt or rock chips out of the O-ring channel. Place an O-ring in the channel.

2. Place one of the end plates on the end of the cylinder and visually align the holes in the end plate with the holes in the pivot collar surrounding the cylinder.

3. With a nut turned onto one end of an assembly rod, insert the assembly rod into one of the holes in the end plate. Insert an assembly pin into the hole in the assembly rod on the far side of the pivot collar.

   Repeat this procedure with the second assembly rod, using the hole in the end plate on the opposite side as the assembly rod already inserted. Finger-tighten the nuts on each of the assembly rods.

4. Turn the pressure cylinder right-side up, and make sure that the copper drain tube is touching the bottom end plate.

5. Place the aggregate specimen into the pressure cylinder. (The cylinder holds a specimen of approximately 15 kg. [33 lbs.]).

6. Clean the O-ring channel and insert the O-ring.

7. Place the remaining base plate over the protruding ends of the assembly rods and onto the pressure cylinder.

8. Place a nut on each of the protruding assembly rods, and finger-tighten.

9. Pivot the pressure chamber sideways.

10. Insert the bolts into the holes in one of the base plates, through the pivot collar, and through the other base plate. Place nuts on all of the bolts.

11. Finger-tighten the two nuts on either side of each of the assembly rods.

12. Remove the assembly rods, place the remaining two bolts in the holes vacated by the assembly rods, and place the remaining nuts on the remaining bolts.

13. Tighten the nuts to 60-80 in-lbs. (6.8-9.0 N.m.) in the following pattern:

    a) Tighten two nuts on opposite sides of the pressure cylinder (nuts 1 and 9 if the nuts are numbered consecutively going around the cylinder).
    b) Tighten the nut on each side, midway between the nuts already tightened (nuts 5 and 13).
    c) Tighten nuts 3, 7, 11, and 15.
    d) Tighten the remaining nuts.
    e) Check the nuts to make sure none have loosened as the O-rings were compressed. Tighten any loose nuts, and recheck all nuts for tightness.

14. Attach the drain line to the pressure release connector.

15. Open the fill and pressure release valves and fill the chamber with water by turning on the water source.

16. After the chamber is full (excess water is coming out of the drain line that is connected to the pressure release valve), fill the standpipe by opening the pressure isolation valve and briefly opening the standpipe valve until a small amount of water comes out (a beaker can be used to catch this overflow water). Also fill the copper drain pipe by briefly opening the drain valve until a small amount of water comes out.

17. Remove any air bubbles in the pressure chamber by pivoting the chamber back and forth, leaving the bottom end (the end closest to the valves and fittings) slightly higher than the top end.

18. Shut off the water source, close the fill valve, close the pressure release valve, and disconnect the drain line.

Chamber Operation

Pressurization

At this point, the chamber is ready for pressurization. All valves on the chamber should be shut except for the pressure isolation valve (the ball valve with the small black lever handle). Open the valve on the top of the compressed nitrogen cylinder and adjust the regulator to the desired testing pressure. Pressurize the chamber by opening the chamber pressure valve (large round knob) approximately one-half to one turn.

Pressure Release

To release the pressure, close the pressure isolation valve (small black lever handle), and quickly open the pressure release valve. This should be done while wearing ear protection.

Repressurization

To repressurize the chamber, use the following procedure:

1. Purge any accumulated gas bubbles in the chamber by opening the fill valve and turning on the water source.

2. Close the pressure valve and release pressure in the standpipe by opening the standpipe valve. (If the valve is opened rapidly, the pressure release can be noisy. The hearing protection should be worn for this step.)

3. Open the standpipe valve to refill the standpipe. Close the standpipe valve when water starts to come out.

4. Remove any air bubbles in the pressure chamber by pivoting the chamber back and forth, leaving the bottom end (the end closest to the valves and fittings) slightly higher than the top end.

5. Turn off the water source and close the fill and pressure release valves.

6. Open the pressure valve.

Chamber Opening

After the pressure has been released, the water can be drained by the following procedure:

1. Attach the drain tube to the quick-release connector at the drain valve.

2. Close the pressure release valve and open the drain valve.

3. Pivot the pressure chamber so that the chamber is right side up (the bottom plate should be parallel to the floor).

4. Close the valve on the nitrogen cylinder. Slowly open the pressure isolation valve, allowing the gas pressure to force the water out of the pressure chamber.

5. If necessary, close the pressure isolation valve, open the valve on the nitrogen cylinder to repressurize the pressure line, and then close the valve on the nitrogen cylinder. Slowly open the pressure isolation valve.

6. When all the water has been removed from the pressure chamber, close the pressure valve and pivot the chamber to the sideways position.

7. Remove two bolts on opposite sides of the pressure chamber.

8. Replace the two bolts with the assembly rods. Insert the assembly pins into the holes in the assembly rods on the top side of the pivot flange.

9. Finger tighten nuts on both ends of the assembly rods.

10. Loosen the nuts on the remaining bolts and remove the bolts.

11. Remove the nuts on the top ends of the assembly rods and remove the top base plate.

12. Remove the aggregate specimen from the pressure chamber.

13. Take the O-ring out of the top O-ring channel and clean both the O-ring and the O-ring channel.

14. Invert the pressure cylinder, loosen the remaining nuts on the assembly rods, remove the assembly pins, and remove the assembly rods.

15. Remove the bottom base plate and clean the inside faces of both base plates.

16. Remove the O-ring from the O-ring channel, and clean the O-ring and the O-ring channel.

Part III - Field Testing Program

1.0 Introduction

This part describes field testing of the findings described in Part I and Part II. A field trial of a D-cracking mitigation method and cooperative testing of SHRP high-performance concrete program field mixes are also described in this part. Goals and objectives, the test program design, construction details, laboratory test results, and preliminary findings of this task are presented.

Since long-term performance monitoring efforts must extend well beyond the end of this SHRP contract, performance monitoring programs are also proposed and described herein.

2.0 Paste Test Program

2.1 Objectives

The goal of the paste test program was to perform field validation of the conclusion of Parts I and II. Specific objectives included:

1. To use the findings and models to develop durable concrete mixtures that may use current chemical and mineral admixtures.

2. To validate the findings and models concerning the air void/water pore system parameters required for the production of frost-resistant concrete, especially for concretes that use chemical and mineral admixtures.

To meet these objectives, a series of concrete mixes representative of current mixture proportions and covering a range of expected durabilities were tested in the field in locations that experience freezing and thawing.

The test program design considerations, construction summaries, and preliminary findings of this work are described below.

2.2 Test Program Design

2.2.1 Site Selection

The site selection process began in early 1991. Selected SHRP regional coordinators and

state highway agencies were contacted in order to find planned concrete construction projects that could be easily modified to include selected concrete mixtures that feature air void-water pore systems that will provide field documentation of the performance hypotheses described in Parts I and II. Each test site needed to accommodate six or more different mixtures so that the performance hypotheses could be tested over a broad range of variables and expected durability performance.

Candidate test sites were identified in Michigan, Ohio, Washington, Minnesota, Iowa, and Illinois, with some states offering multiple site options. These sites included both pavements and bridge decks and offered the potential to include conventional mixtures as well as high-performance concretes. The sites included a variety of climates and deicing salt application rates.

Factors that were considered in the final site selection process included local climate, ability to accommodate the placement of several trial mixtures (including some that might be expected to be nondurable), deicing salt application rates, traffic mix and volume, availability of useful construction and monitoring data, and level of cooperation offered by the highway agency. The two test sites that were eventually selected are located in Ohio and Minnesota.

2.2.2 Mixture Selection

The control mixture at each site was based upon applicable state concrete specifications and was selected with the cooperation of the responsible state agency. The remaining mixtures were based upon the control mixtures with minor adjustments of the batch quantities of air-entraining admixture as necessary to achieve the desired range of air contents. Since one goal of the field studies was to validate the results of the laboratory tests, the range of air void contents was selected (based upon the laboratory results) to produce a range of performances, including mixtures that were expected to fail prematurely. Durable local aggregates were used in each mixture.

2.2.3 Ohio Test Site Experimental Design Details

The Ohio test site is the site of the original Ohio D-cracking study that was conducted by David Stark of Construction Technology Laboratories (CTL) on Route 2 in Erie and Lorain Counties, between mileposts 29.14 and 0.00. The reinforced concrete pavement is generally 23 cm (9 in.) thick and features various slab lengths and base types. The project is 7.89 km (4.90 miles) in length and carries an average of 14,330 vehicles per day, including about 15 percent truck traffic.

Several of the panel joints and cracks were showing signs of D-cracking by 1990. Full-depth repairs of selected joints and cracks were planned for 1992. Ninety of these full-depth repair locations (outer lane only) were selected for cooperative work with the SHRP high-performance concrete program. Construction began in September, 1992. Each repair was approximately 1.9 m (6 ft) in length, 3.8 m (12 ft) wide, and 23 cm (9 in.) thick,

placed upon existing base materials, and constructed with two dowelled joints.

Seventy of the repairs were placed in cooperation with the SHRP high-performance concrete program and featured seven different mixtures designed for early opening to traffic (curing times ranging from 2 to 24 hours). These mixtures were variants of the VES (Very Early Strength) and HES (High Early Strength) mixtures developed under the SHRP high-performance concrete program, and several proprietary mixtures (C-205 project). The actual as-placed batch quantities for these mixtures are presented in table 3-1.

Ten additional repairs were constructed using Ohio Department of Transportation (ODOT) Class FS concrete, another HES material. The basic Class FS mixture is an ODOT standard. The mixture proportions used for this project were modified somewhat by CTL in response to the results of their laboratory testing of the standard mixture using the contractor's aggregate sources and the desire for extremely rapid strength gain. The resulting mixture used Type III cement and rather large quantities of air entraining admixture. The actual batch quantities used for the mixtures are also presented in table 3-1.

The ODOT class FS mixture was used as the basis for the five additional mixtures placed at the request of the SHRP concrete frost resistance program project team because the class FS mixture represents a typical state standard concrete mixture and uses typical materials (i.e., does not *require* Type III cement or other proprietary cements and aggregates). The mixture proportions are also fairly typical, other than the large amount of cement required for early strength and the large amount of air-entraining admixture recommended by the SHRP high-performance concrete program project team.

Ten repairs were allocated for the placement of the SHRP concrete frost resistance program mixes. Mixture proportions were selected to be identical to the ODOT Class FS repairs with the exception of varying air-entraining admixture dosage and minor adjustments to aggregate quantities to maintain workability. Mixing water was adjusted to account for variations in aggregate absorption, but cement content and w/c were held constant. The air-entraining admixture dosage was to be varied (0.05, 0.20, 0.40, 0.60, and 0.80 of the Class FS dosage) to produce five mixtures. This resulted in a range of air contents varying from a small amount (0.05 of the Class FS dosage) to slightly less than the Ohio Class FS mixture. Each of these mixtures was placed in two repairs, which resulted in the placement of a total of 6 different mixtures in 20 repairs (including the 10 standard Class FS repairs being placed by the ODOT). These mixtures and repairs were in addition to the 7 mixtures and 70 repairs placed in conjunction with the SHRP high-performance concrete program.

The use of the six variations of the ODOT Class FS mixtures allowed the placement of a complete spectrum of mixtures ranging from those with reasonable air-void systems expected to show no failure from field freezing and thawing, to those expected to show substantial deterioration. This will provide valuable information concerning what air-void system is necessary to provide protection from a specific field exposure to freezing and thawing.

Table 3-1. Summary of Field Mixtures used on Ohio D-Cracking Test Road Site (cast 9/1/92 to 9/11/92)

Batch quantities per cubic meter

Mixture	Description	Sand (kg, SSD)	CA (kg, SSD)	Water (kg)	Cement (kg)	w/c	A/E (ml)	WR/HRW (ml)	Accel. or Retarder (ml or kg)	Fresh Air Content (%)	Slump (mm)
A-HES	High Early Strength	443	941	200	497	0.40	2595	7784	151	9.8	146
B-FTI	Fast Track	806	711	213	445	0.48	2029	1739	0	5.5	19
C-PC1	Pyrament #1	851	816	143	536	0.27	0	0	0	2.8	32
D-RSC1	Rapid Set #1	814	755	176	439	0.40	859	0	6.6	7.0	98
E-VES	Very Early Strength	683	631	235	530	0.44	2763	3454	228	8.3	102
F-PC2	Pyrament #2	820	792	139	481	0.29	0	0	0	7.3	216
G-RSC2	Rapid Set #2	854	793	198	397	0.50	0	0	5.9	3.3	38
H1	ODOT Class FS (morning)	606	861	218	546	0.40	3559	0	Note 12	3.8	13
H2	ODOT Class FS (afternoon)	589	837	212	530	0.40	3459	0	Note 12	6.5	41
I1	H1 w/0.8*A/E dosage	598	821	214	520	0.41	2714	0	Note 12	7.0	44
I2	H1 w/0.6*A/E dosage	622	826	216	523	0.41	2048	0	Note 12	5.6	70
I3	H1 w/0.4*A/E dosage	619	821	215	521	0.41	1357	0	Note 12	6.2	89
I4	H1 w/0.2*A/E dosage	622	825	216	523	0.41	682	0	Note 12	5.8	76
I5	H1 w/0.05*A/E dosage	640	849	223	538	0.41	176	0	Note 12	3.1	64

Note 1: All masses are for SSD aggregate conditions.
Note 2: Air contents and slumps shown are for batch used to cast lab specimens; other batches varied
Note 3: Cement is St. Mary's Type III unless noted otherwise
Note 4: Cement in mixtures C and F is Pyrament by Lone Star Industries
Note 5: Cement in mixtures D and G is RapidSet Cement by CTS Manufacturing Co.
Note 6: High-Range Water Reducer in mixture A is Catexol 1000SPMN by Axim Tech. Co.
Note 7: High-Range Water Reducer in mixture E is Melment, by Cormix Construction Materials
Note 8: Water reducer in mixture B is Catexol 1000N by Axim Tech. Co.
Note 9: DCI corrosion inhibitor by W. R. Grace used as set accelerator in mixtures A and E.
Note 10: Set retarder used in mixtures D and G is 1.5% citric acid by Midland Co.
Note 11: Water from DCI already included in water quantities shown.
Note 12: 2% (10.7 kg) $CaCl_2$ set accelerator used. Catexol 1000R set retarder used at 522 ml/m^3.

Table 3-2 Raw Material Properties for Ohio Field Tests

Coarse Aggregate:

Source: Sandusky Crushed Stone, Sandusky, Ohio
Grading: Typical

Sieve No.	% Passing
1/2"	100
3/8"	88
4	16
8	3
16	1

Specific Gravity: 2.59 (Avg. of 3 tests)
Absorption: 2.18 % (Avg. of 3 tests, Moisture content at mixer varied daily)
Durability: Unacceptable (4% avg. mass loss in soundness test, freeze-thaw expansion area = 4.81 avg. @ 350 cycles)

Fine Aggregate:

Source: Norwalk Sand and Gravel, Norwalk, Ohio
Grading: Typical

Sieve No.	% Passing
3/8"	100
4	100
8	86
16	59
30	30
50	13
100	6
200	2.2

Specific Gravity: 2.58 (Avg. of 3 tests)
Absorption: 1.51 % (Avg. of 3 tests, Moisture content at mixer varied daily)
Fineness Modulus: 3.07

Cement: Type: III (High Early Strength)
Source: St. Mary's Peerless

Air-Entraining Admixture: Catexol AE260 by AXIM Tech. Co.
High-Range Water Reducers: Catexol 1000SPMN by AXIM Tech. Co.
Melment by Cormix Construction Materials
Water Reducer: Catexol 1000N by AXIM Tech. Co.
Set Accelerator: DCI Corrosion Inhibitor by W. R. Grace Co.

Table 3-3 Layout of SHRP Concrete Frost Resistance Program Repairs and Concrete Sealers in Ohio

Repair Type	Station	AASHTO Aggregate Grading	Sealer Type Approach	Leave
FS	152+94	4/6	N	SS
FS	152+53	4/6	WS	LS
I3	152+14	4/6	2P	N
FS	151+11	4/6	N	WS
I4	150+76	4/6	SS	2P
I5	150+28	4/6	LS	N
I1	149+97	6	SS	WS
FS	149+48	6	LS	2P
I5	149+14	6	N	LS
FS	148+66	6	2P	N
I2	147+82	6	WS	SS
FS	147+57	8	N	LS
I3	147+43	8	LS	WS
I4	147+17	8	N	N
FS	147+03	8	WS	SS
FS	146+68	8	SS	2P
I2	145+97	8	2P	N
FS	145+04	4/6	WS	2P
I1	144+64	4/6	2P	N
FS	144+25	4/6	N	WS

Notes:

Centerline joint sealer matches leave joint sealer

Concrete Sealer Legend:
N = None
2P = 2-Part Epoxy Resin
LS = Penetrating Oil Sealer
WS = Water-Based Silane
SS = Solvent-Based Silane

Concrete Mixture Legend:
FS = ODOT Class FS Standard Mixture
I1 = FS with 0.8 AE dose
I2 = FS with 0.6 AE dose
I3 = FS with 0.4 AE dose
I4 = FS with 0.2 AE dose
I5 = FS with 0.05 AE dose

Modern information of this type was not identified by searches conducted in the first two years of this project.

The final batch quantities that were used for all of the Ohio mixtures, including both the SHRP high-performance concrete and concrete frost resistance program mixtures, are presented in table 3-1. Table 3-2 summarizes details concerning the materials that were used at the Ohio test site, including material sources, gradings, and other physical characteristics.

It was originally desired that each mixture be replicated in four repairs in the outer lane and that different mixtures be distributed randomly along the project to reduce the possibility of bias due to moisture, support, or other variations along the project. The placement of repairs in the inner lane was also desired to provide some documentation of the combined effects of climate and traffic load variance on the material performance. Unfortunately, only two replicates were placed for each mixture and only the outer lane of the westbound lanes was used (due to site design and construction limitations). However, the repairs were constructed in a random sequence along the project length, as shown in table 3-3, which provides a list of repair materials used and repair locations (by station). Furthermore, mixture performance comparisons that account for traffic effects can still be obtained by observing deterioration in the wheel tracks and between the wheel tracks.

The Ohio project site was also used to test several concrete sealers in an effort to determine their potential effectiveness in mitigating D-cracking. Details concerning these tests are presented in section 3.0 of this report.

2.2.4 Minnesota Test Site Experimental Design Details

The Minnesota Department of Transportation agreed to allow the placement of a series of concrete mixtures in support of the SHRP concrete frost resistance program in 6.1 by 4.6 m (20 by 15 ft) test pads at the Minnesota Road Research Project (Mn/ROAD) which is currently under construction along I-94 about 65 km (40 miles) northwest of Minneapolis. These test pads were constructed in October of 1992 and will not be subjected to traffic.

The basic concrete mixture used for concrete surface paving at the Mn/ROAD test site includes 15 percent class C fly ash and sufficient air-entraining admixture to produce 5.5 percent total air content. This mixture was also placed in the first test pad. The actual mixture design batch quantities used are presented as mixture MN1 in table 3-4.

Six of the remaining seven mixtures that were placed in test pads at the Mn/ROAD project site are based upon MN1. These mixtures include ranges of fly ash contents (from 0 to 30 percent by mass replacement of cement) and air contents (from less than 2 to more than 6 percent). Specifically, the following mixtures were constructed as outlined on the next page:

Mixture	Description
MN2	Same as MN1 except air-entraining admixture dosage reduced by 50 percent or as needed to obtain an air content of approximately 2.5 percent.
MN3	Same as MN1 except further reduction in air-entraining admixture to produce a very low air content.
MN4	Similar to mixture MN2 (air-entraining admixture dosage reduced to obtain an air content of approximately 2.5 percent) except use 341 kg (530 lbs) cement, no fly ash.
MN5	Similar to mixture MN3 (adjust air-entraining admixture dosage to produce a very low air content) except use 241 kg (530 lbs) cement, no fly ash.
MN6	Similar to mixture MN2 (air-entraining admixture dosage reduced to obtain an air content of approximately 2.5 percent) except use 169 kg (372 lbs) cement and 71.8 kg (158 lbs) Class C fly ash.
MN7	Similar to mixture MN3 (adjust air entraining admixture dosage to produce a very low air content) except use 169 kg (372 lbs) cement and 71.8 kg (158 lbs) Class C fly ash.

In summary, a matrix of these seven test mixtures could be presented as:

Fly Ash Content (%)	Air Void/Water Pore System		
	Nondurable (1.5 %)	Marginal (2.5 %)	Durable (5.5 %)
0	MN 5	MN 4	
15	MN 3	MN 2	MN 1
30	MN 7	MN 6	

Actual batch quantities for the test mixtures are given in table 3-4.

Table 3-4 Summary of Field Mixtures Used at the Minnesota Road Research Site (Cast 10/15/92)

Batch quantities per cubic meter

Mixture	Goal	Sand (kg, SSD)	CA (>19 mm) (kg, SSD)	CA (<19 mm) (kg, SSD)	Water (kg)	Cement (kg)	Fly Ash (kg)	w/c	w/(c+p)	% Flyash (%C+P)	A/E (ml)	Fresh AIr Content (%)	Slump (mm)
MN1	MnDOT Standard	720	548	540	163	304	51	0.54	0.46	14.4	250	3.9	85.7
MN2	MN1 w/marginal air	727	557	542	169	306	53	0.55	0.47	14.8	133	2.7	76.2
MN3	MN1 w/low air	731	562	553	167	315	48	0.53	0.46	13.3	45	2.0	50.8
MN4	MN1 w/marg. air, no FA	733	558	550	166	367	0	0.45	0.45	0.0	135	2.5	82.6
MN5	MN1 w/low air, no FA	737	556	548	178	362	0	0.49	0.49	0.0	45	1.5	114.3
MN6	MN1 w/marg. air, 30% FA	716	548	534	167	247	105	0.68	0.47	29.7	131	3.8	120.7
MN7	MN1 w/low air, 30% FA	725	559	557	172	253	108	0.68	0.48	29.9	20	1.4	127.0
MN8	MnDOT Experimental Mix	656	0	1116	169	327	0	0.52	0.52	0.0	0	5.6	88.9

Note 1: All masses are for SSD aggregate conditions.
Note 2: Water is 75% hot (85 deg. F), 25% cold (40 deg. F).
Note 3: Cement is Type I.
Note 4: Fly ash is Class C.
Note 5: Test pads were placed with mixture MN1 at west end of pad area, MN8 at east end, with MN2 through MN7 ordered sequentially in between.
Note 6: MN8 mixed with "High Carbon Concrete Admixture" at a dosage of 5 parts water to 1 part HCC admixture. 1148 kg of admixture was used, which included 191.3 kg HCC.
Note 7: A/E is Contech Pro-Crete.

Table 3-5 Raw Material Properties for Minnesota Field Tests

Coarse Aggregate:

Source: Barton Sand and Gravel, Barton, Minnesota (Pit No. 171004)

Grading (50%-50% blend of 3/4"+ and 3/4"- materials)
(average results of 10 sieve analysis tests):

Sieve No.	3/4"+ % Passing	3/4"- % Passing	Blend % Passing
2"	100	100	100
1-1/2"	100	100	100
1-1/4"	79	100	90
1"	33	100	67
3/4"	4	96	50
5/8"	1	86	44
1/2"	0	62	
3/8"		32	
#4		2	

Specific Gravity: 2.72 (3/4"+), 2.69 (3/4"-), 2.705 (blend)
Absorption: 0.72% (3/4"+), 1.21% (3/4"-), 0.965% (blend)
Moisture Content: 0.8% (3/4"+), 1.8% (3/4"-), 1.3% (blend)
Durability: No Durability Testing Performed: 0.00% Chert, 4.25% Limestone, 0.6% Soft Rock.

Fine Aggregate:

Source: Barton Sand and Gravel, Barton, Minnesota

Grading (average results of 10 sieve analysis tests):

Sieve No.	% Passing
4	100
8	95
16	70
30	34
50	9
100	2
200	0.6

Specific Gravity: 2.64
Absorption: 0.73 %
Moisture Content at Mixer: 4.35 %

Cement:
Type: I (Normal)
Source: Lehigh Portland Cement Company, Mason City, Iowa
Specific Gravity: 3.15
Air-Entraining Admixture: ProCrete by Contech

The eighth mixture included a proprietary admixture to produce a mixture called "High Carbon Concrete." This material was incorporated in the SHRP concrete frost resistance test program at the request of the Minnesota DOT. This mixture was called MN8.

The final batch quantities that were used for all of the Minnesota mixtures are presented in table 3-4. Table 3-5 summarizes details concerning the materials that were used at the Minnesota test site, including material sources, gradings, and other physical characteristics.

2.3 Construction Summaries

Construction of the Ohio test section was completed between September 1 and September 11, 1992, with the SHRP high-performance concrete program mixtures being placed between September 1 and September 10. The Ohio Class FS and SHRP concrete frost resistance test program mixtures were placed on September 11. Air content and slump information for all of the mixes is included in table 3-1.

It should be noted that the air-entraining admixture dosage recommended by CTL for the Ohio Class FS mixture was apparently well in excess of that required to produce suitably large fresh air contents. This is apparent because initial reductions in air-entraining admixture dosage (decrements of 20 percent of original dosage) produced no real reductions in air content. In fact, the air content of some mixtures actually increased with reduced air-entraining admixture dosage. This may have been because the coarse aggregate quantities were decreased slightly and the fine aggregate quantities were increased slightly to compensate for the loss of workability that was expected to accompany the decrease in air-entraining admixture and air content. However, these batch quantity adjustments may have overcompensated for the expected loss of air, resulting in a more workable mixture, more vigorous mixing and more efficient air entrainment in spite of the reduced air-entraining admixture dosage. The effect of this apparent air-entraining admixture overdose in the control mixture was that only one mixture was placed with a relatively low air content (Mixture I5, air content = 3.1 percent).

Construction of the Minnesota test pads was completed on October 15, 1992. This construction operation went very smoothly and the desired ranges of air content and mix designs were easily achieved. Air content and slump measurements for the eight experimental mixtures placed near Mn/ROAD are given in table 3-4.

Each test pad was 19 cm (7.5 in.) thick on a dense-graded granular base material. Each test pad was constructed independently and away from other test pads. Each pad measured 6.1 by 4.6 m (20 by 15 ft), and contraction joints were sawed to a depth of 7.5 cm [3 in] to produce four slabs measuring 3.1 by 2.3 m (10 by 7.5 ft). The joints were left unsealed to maximize the potential for saturation of the concrete in the joint areas. This lack of joint sealant should not produce significant spalling because the pads are not exposed to traffic. In addition, the joints are all undowelled.

2.4 Monitoring Programs

2.4.1 Construction Monitoring

Construction monitoring at both project sites was accomplished by the Michigan State University (MSU) project team at both the concrete batch plant and on the job site. A member of the MSU project team was present for the placement of all SHRP concrete frost-resistance test program mixtures and worked in coordination with appropriate DOT and contractor personnel to ensure the proper mixture proportions and placement of the test concrete. In addition, experienced research assistants from MSU were present (three in Minnesota, up to five in Ohio) to perform all air content and slump tests, cast test beams and cylinders, and generally assist in the construction of the test sections.

Air content was measured using a pressure meter. Companion cylinders and beams were cast for each mixture for laboratory testing as follows:

- Twelve cylinders were cast for compressive strength measurements at 24 hours, 72 hours, 7 days, and 28 days. These cylinders were generally 15.2 by 30.5 cm (6 by 12 in.) at the Ohio test site and 10.2 by 20.3 cm (4 by 8 in.)] at the Minnesota test site.

- Two 15.2 by 30.5 cm (6 by 12 in.) cylinders were cast for permeability and freezable water testing.

- Four to six beams 7.6 by 10.2 by 40.6 cm (3 by 4 by 16 in.) were cast for durability testing according to proposed AASHTO T 161 (ASTM C 666) Procedure C. One beam specimen was selected from each mixture to be sliced and polished for microscopic analysis of the air void system (linear traverse), leaving three to five for testing for resistance to freezing and thawing. These beams were cured at 23°C (73.4°F) in a lime water bath for 27 days (for a total curing period of 28 days) before testing.

The SHRP concrete frost resistance program project team also assisted in the construction and monitoring of several of the SHRP high-performance concrete program mixtures at the Ohio test site, including the local adaptation of the SHRP HES (High-Early Strength) mixture, the SHRP VES (Very Early Strength) mixture, and the two mixtures that used Pyrament cement. Companion specimens were cast and tested for these mixtures (as described above) independently of the tests performed by the SHRP high-performance concrete program contractor.

The SHRP concrete frost resistance program project team also performed the application of concrete sealers to the vertical faces of the repair joints prior to placement of the concrete at the Ohio test site. This operation is described in more detail in section 3.3.

The tests performed on the companion specimens (and the results of this testing) are described in section 2.5.

2.4.2 Performance Monitoring

No performance monitoring was accomplished after construction of the field test sections under the SHRP concrete frost resistance program contract because the test sections were constructed only a few months before the end of the contract. The following recommendations are made for future performance monitoring.

Performance monitoring should consist of at least two types of data collection efforts. The first should consist of an annual 100 percent condition survey of the test sections and surrounding concrete pavement. This condition survey should be conducted in accordance with LTPP standard condition data collection procedures and will focus upon indicators of frost resistance problems in either the surrounding mainline pavement or the repairs themselves. Critical distresses will include D-cracking, scaling, joint sealant damage, spalling, and popouts. Repair failures should be documented in terms of these distresses. Nondestructive (impact hammer) tests should also be considered for monitoring changes in the mechanical properties of the concrete that can be expected to occur with frost damage.

An alternative to NDT testing of dynamic modulus is to obtain cores from the field installations and perform resonant frequency analyses to estimate the dynamic modulus of the concrete. This type of test offers the advantage of being able to measure variance in deterioration within and between wheel paths at the Ohio test site, and to measure variance in deterioration between the joints and mid-slab at either the Minnesota or Ohio locations. In addition, the cores could then be subjected to laboratory testing for resistance to freezing and thawing to estimate the remaining durable life of the field installations. However, this type of test could be performed only a limited number of times because of its destructive nature and the limited number of sites at each installation that would be suitable for coring. If this alternate test method is selected, tests should be performed approximately every three to four years (or at shorter intervals, if needed) with an initial measurement obtained immediately.

The second proposed data collection effort involves the collection of data that will be useful in defining the exposure of the test sections to traffic and environmental effects. This task will be relatively simple for the Minnesota test site since the test pads will not be subjected to traffic and a first-order weather station is present at the road test site. Weather data are being collected on a continuous basis at this site, and additional information concerning roadbed soil moisture, slab temperature gradients, etc. will be available for the concrete pavements that are installed in the nearby test road.

This task is not as simple in Ohio. Weigh-in-motion instruments are currently operational in the westbound lanes approximately two miles east of the project site. The nearest first order weather stations are more than 30 miles away in Cleveland and in Urbana. Obtaining project site weather data will require some interpolation of weather data from these distant sites.

The Ohio test site is part of a major travel corridor. Although this site has long been used by the ODOT for field tests of various pavement materials and designs, any test programs that are present may be terminated when the performance of the in-service pavement becomes unacceptable. Thus, coordination must be maintained with the ODOT to ensure that any agency interested in monitoring the performance of this test site is notified prior to removal or rehabilitation of any portion of the roadway.

Similarly, the Minnesota DOT is responsible for the maintenance and continuance of the SHRP concrete frost resistance program mixtures placed at Mn/ROAD. Coordination must be maintained to ensure proper treatment of these test pads and advance notification of any modification or removal of the test pads.

2.5 Laboratory Tests

All of the SHRP concrete frost resistance program field mixtures and selected SHRP high-performance concrete program field mixtures were subjected to numerous laboratory tests. These tests and their results are described below.

Compressive strength tests were performed on cylinders after 24 hours, 72 hours, 7 days, and 28 days. All cylinders were cured in the molds for 24 hours and moist cured according to applicable AASHTO and ASTM specifications until they were broken. Capping and testing was also performed in strict accordance with applicable AASHTO and ASTM specifications. Detailed compression test data is presented in table 3-6 for the Ohio mixtures and table 3-7 for the Minnesota mixtures. Summaries of the compression test data for each mixture are presented with the results of air void measurements in table 3-8 (for the Ohio mixtures) and table 3-9 (for the Minnesota mixtures).

Tests for resistance to freezing and thawing were conducted in accordance with AASHTO T161 (ASTM C 666) Procedure B, except that each beam was wrapped in a snug-fitting terrycloth wrap (see notes regarding proposed Procedure C in Part I). This procedure was consistent with the laboratory testing conducted throughout this project. In addition, all field test specimens tested at Michigan State University were obtained by the MSU project team and were cured for 28 days prior to freezing. Several specimens were also provided by the SHRP high-performance concrete program contractor to the University of Washington for testing after only 14 days of curing. A summary of the results of all of the freezing and thawing testing is presented in table 3-10 for the Ohio mixtures and table 3-11 for the Minnesota mixtures. In addition, appendices A and B of this report provide graphs of the test histories for each mixture placed at the Ohio and Minnesota sites, respectively, including plots of dilation, mass loss, relative dynamic modulus and relative damping factor versus number of cycles of freezing and thawing.

Linear traverse testing was performed on samples from each test mixture in accordance with applicable AASHTO and ASTM specifications to measure air void parameters. The results of these measurements are provided in table 3-8 for the Ohio mixtures and table 3-9 for the

Minnesota mixtures. The measurements tabulated for the SHRP high-performance concrete program mixtures placed in Ohio were provided by CTL. All other measurements were performed at MSU.

Specimens were collected for measuring concrete permeability and freezable moisture. These tests are being conducted at the University of Washington. However, these tests require several months to complete. Thus, permeability and freezable moisture data are not yet available for the field mixtures.

Table 3-6 Summary of Laboratory Compression Test Results on Materials from the Ohio D-Cracking Test Road Site (Cast 9/1/92 - 9/11/92)

Mixture	Description	24-hour (MPa)	3-day (MPa)	7-day (MPa)	28-day (MPa)
A-HES	High Early Strength	25.2	27.8	29.8	43.3
B-FTI	Fast Track				
C-PC1	Pyrament #1	16.3	35.9	56.5	58.9
D-RSC1	Rapid Set #1				
E-VES	Very Early Strength	24.7	31.8	34.6	37.3
F-PC2	Pyrament #2	14.6	44.0	47.7	50.0
G-RSC2	Rapid Set #2				
H	ODOT Class FS	41.4	43.6	49.8	50.6
I1	H1 w/0.8*A/E dosage	33.6	36.8	39.9	44.6
I2	H1 w/0.6*A/E dosage	39.6	45.1	46.3	50.7
I3	H1 w/0.4*A/E dosage	39.6	41.6	43.6	48.3
I4	H1 w/0.2*A/E dosage	37.0	43.0	43.9	50.2
I5	H1 w/0.05*A/E dosage	44.2	46.1	50.4	57.7

Table 3-7 Summary of Laboratory Compression Test Results on Materials from the Minnesota Road Research Site (Cast 10/15/92)

Mixture	Description	24-hour (MPa)	3-day (MPa)	7-day (MPa)	28-day (MPa) (Estimated)	6-month (MPa)
MN1	MnDOT Standard	9.4	17.2	22.9	30.5	44.4
MN2	MN1 w/marginal air	12.6	14.2	24.7	26.5	40.7
MN3	MN1 w/low air	11.3	23.9	29.5	38.5	44.5
MN4	MN1 w/marginal air, no FA	11.0	24.7	26.6	36.5	42.9
MN5	MN1 w/low air, no FA	10.7	24.7	36.3	40.5	44.1
MN6	MN1 w/marginal air, 30% FA	8.5	15.1	25.8	29.0	39.3
MN7	MN1 w/low air, 30% FA	9.2	16.5	23.1	26.5	29.0
MN8	MnDOT Experimental Mixture	9.2	13.3	16.5	23.0	39.6

Table 3-8
Summary of Laboratory Durability Test Results
Ohio D-Cracking Test Road Site (Cast 9/1/92 - 9/11/92)

Air Void/Water Pore System Characteristics

Mixture	Description	Fresh Air (%)	Hardened Air (%)	Hardened Air (ent, %)	Spacing Factor (mm)	Spacing Factor (ent, mm)	Specific Surface (mm-1)	Specific Surface (ent, mm-1)	Voids/mm	Voids/mm (ent)	Avg. Ch. Length (mm)	Paste-to-Air Ratio	28-day f'c (MPa)
A-HES	High Early Strength (14-day)	9.8	6.6	5.8	0.099	0.093	49.1	55.1	0.810	0.800	0.081	5.6	Note 4
A-HES	High Early Strength	9.8	2.3	2.1	0.305	0.293	27.9	30.2	0.163	0.161	0.143	19.7	43.3
B-FTI	Fast Track (14-day)	5.5	4.3	3.0	0.174	0.144	33.7	48.0	0.360	0.360	0.119	8.4	Note 4
C-PC1	Pyrament #1 (14-day)	2.8	2.8	1.4	0.468	0.350	14.5	25.8	0.100	0.090	0.176	11.6	Note 4
C-PC1	Pyrament #1	2.8	n/a	n/a	n/a	n/a	n/a	n/a	n/a	n/a	n/a	n/a	53.1
D-RSC1	Rapid Set #1 (14-day)	7.0	3.1	2.2	0.293	0.251	22.1	30.0	0.170	0.170	0.181	10.5	Note 4
E-VES	Very Early Strength (14-day)	8.3	6.5	5.6	0.097	0.090	53.1	61.6	0.860	0.860	0.075	6.4	Note 4
E-VES	Very Early Strength	8.3	7.6	7.2	0.108	0.106	47.8	50.3	0.914	0.911	0.084	6.4	37.3
F-PC2	Pyrament #2 (14-day)	7.3	4.5	3.4	0.296	0.262	17.9	23.0	0.200	0.190	0.223	6.7	Note 4
F-PC2	Pyrament #2	7.3	4.9	3.5	0.337	0.290	16.6	22.3	0.203	0.196	0.241	7.5	50.0
G-RSC2	Rapid Set #2 (14-day)	3.3	7.5	n/a	0.127	n/a	25.1	n/a	0.473	n/a	n/a	n/a	n/a
H1	ODOT Class FS (morning)	3.8	4.9	2.6	0.246	0.179	24.2	44.2	0.298	0.286	0.165	8.7	50.6
H1	ODOT Class FS (morning, 14-day)	4.5	3.4	2.4	0.222	0.187	30.8	42.4	0.260	0.250	0.130	11.8	Note 4
H2	ODOT Class FS (afternoon)	6.5	4.7	2.6	0.350	0.360	25.2	43.5	0.296	0.287	0.159	9.0	n/a
I1	H1 w/0.8*A/E dosage	7.0	4.1	2.8	0.157	0.128	42.1	61.0	0.431	0.425	0.095	11.0	44.6
I2	H1 w/0.6*A/E dosage	5.6	4.4	3.0	0.176	0.147	36.1	50.6	0.393	0.386	0.111	10.1	50.7
I3	H1 w/0.4*A/E dosage	6.2	4.1	2.6	0.470	0.387	14.0	20.7	0.143	0.135	0.286	10.8	48.3
I4	H1 w/0.2*A/E dosage	5.8	5.2	4.5	0.213	0.200	27.7	31.3	0.359	0.355	0.144	8.5	50.2
I5	H1 w/0.05*A/E dosage	3.1	2.7	1.8	0.382	0.318	20.2	28.8	0.138	0.132	0.198	15.5	57.7

Note 1: All specimens cured 28 days (including 27 days in lime water) unless noted otherwise.
Note 2: All air void measurements for 14-day cures performed at University of Washington.
Note 3: All air void measurements for 28-day cures performed at Michigan State University.
Note 4: Compression tests not performed at 14-day.
Note 5: RSC2 data obtained from CTL report; seperate traverse not conducted for this project.
Note 6: 28-day Pyrament #1 linear traverse data not available.

Table 3-9
Summary of Laboratory Durability Test Results from the Minnesota Road Research Site (Cast 10/15/92)

Air Void/Water Pore System Characteristics

Mixture	Description	Fresh Air (%)	Hardened Air (%)	Hardened Air (ent, %)	Spacing Factor (mm)	Spacing Factor (ent, mm)	Specific Surface (mm-1)	Specific Surface (ent, mm-1)	Voids/mm	Voids/mm (ent)	Avg. Ch. Length (mm)	Avg. Ch. Length (ent, mm)	Paste-to-Air Ratio	28-day f'c (MPa)
MN1	Mn/DOT Standard	3.9	3.5	2.9	0.249	0.228	24.5	29.0	0.216	0.213	0.163	0.138	9.2	30.5
MN2	MN1 w/marginal air	2.7	1.2	0.9	0.353	0.306	28.0	36.2	0.080	0.079	0.143	0.111	27.7	26.5
MN3	MN1 w/low air	2.0	1.0	0.7	0.907	0.780	11.3	15.3	0.029	0.027	0.353	0.262	30.6	38.5
MN4	MN1 w/marg. air, no FA	2.5	1.7	1.4	0.377	0.344	21.8	26.1	0.094	0.092	0.183	0.153	18.2	36.5
MN5	MN1 w/low air, no FA	1.5	2.2	1.7	0.378	0.336	19.4	24.7	0.109	0.105	0.206	0.162	13.9	40.5
MN6	MN1 w/marg. air, 30% FA	3.8	1.6	1.4	0.277	0.261	31.2	35.0	0.128	0.126	0.128	0.114	20.2	29.0
MN7	MN1 w/low air, 30% FA	1.4	2.7	1.5	0.390	0.304	17.6	28.9	0.116	0.108	0.228	0.138	11.9	26.5
MN8	Mn/DOT Experimental Mixture	5.6	7.3	4.4	0.215	0.166	20.7	33.9	0.379	0.370	0.190	0.118	4.6	23.0

Note 1: All specimens cured 28 days (including 27 days in lime water).
Note 2: All air void measurements performed at Michigan State University.

Table 3-10
Summary of Laboratory Durability Test Results from the Ohio D-Cracking Test Road Site (Cast 9/1/92 - 9/11/92)

Mix	Description	Durability Test Results									
		Durability Facto		Cycles to 60% RDM		Cycles to 0.1% Dilation		% Mass Loss @ 60% RDM or 300 Cycles		% Dilation @ 60% RDM or 300 Cycles	
		Mean	Std. Dev.	Mean	Std. Dev.	Mean	Std. Dev.	Mean	Std. Dev.	Mean	Std. Dev.
A-HES	High Early Strength (14-day)	80.4	3.5	380	19.1	327	40.8	0.65	0.22	0.073	0.031
A-HES	High Early Strength	75.8	2.3	394	17.4	307	32.3	0.67	0.14	0.098	0.014
B-FTI	Fast Track (14-day)	24.7	1.7	124	8.3	124	15.1	-0.46	0.22	0.093	0.059
C-PC1	Pyrament #1 (14-day)	14.9	0.8	75	14.0	46	2.1	-0.84	0.07	0.193	0.025
C-PC1	Pyrament #1	13.2	0.4	66	3.1	48	3.0	-0.64	0.02	0.164	0.020
D-RSC1	Rapid Set #1 (14-day)	63.6	7.5	303	11.5	227	20.4	3.27	2.66	0.260	0.040
E-VES	Very Early Strength (14-day)	15.1	1.8	76	8.8	67	5.9	1.78	0.45	0.133	0.015
E-VES	Very Early Strength	56.4	7.0	275	20.3	251	26.2	5.61	2.41	0.128	0.018
F-PC2	Pyrament #2 (14-day)	13.5	1.7	68	8.5	69	2.0	1.77	1.26	0.147	0.015
F-PC2	Pyrament #2	13.8	2.1	70	11.4	46	4.5	-0.58	0.03	0.164	0.018
G-RSC2	Rapid Set #2 (14-day)	101	0.4	***	***	***	***	0.10	0.10	-0.020	0.010
H1	ODOT Class FS (morning)	17.2	1.7	87	6.2	72	2.1	-0.72	0.01	0.179	0.006
H1	ODOT Class FS (morning, 14-day)	13	0.6	65	2.9	62	8.1	-0.86	0.11	0.127	0.025
H2	ODOT Class FS (afternoon)	18.5	0.5	92	2.5	73	3.0	-0.51	0.01	0.180	0.037
I1	H1 w/0.8*A/E dosage	18.8	1.0	95	5.3	82	8.2	-0.32	0.07	0.151	0.029
I2	H1 w/0.6*A/E dosage	14	0.8	71	3.3	66	4.1	-0.83	0.05	0.144	0.016
I3	H1 w/0.4*A/E dosage	17.6	2.4	89	10.4	75	6.1	-0.87	0.05	0.170	0.017
I4	H1 w/0.2*A/E dosage	12.8	0.4	64	0.7	56	1.0	-0.90	0.04	0.150	0.010
I5	H1 w/0.05*A/E dosage	7.75	0.4	41	2.3	33	0.9	-0.69	0.03	0.156	0.007

Note 1: All specimens cured 28 days unless noted otherwise.
Note 2: All frost resistance testing was accomplished in accordance with AASHTO T161 (ASTM C 666) Procedure B, except for use of cloth wraps and cure periods noted.
Note 3: All frost resistance testing for 14-day cures performed at University of Washington.
Note 4: All frost resistance testing for 28-day cures performed at Michigan State University.
Note 5: *** indicates data not available.

Table 3-11
Summary of Laboratory Durability Test Results from the Minnesota Road Research Site (Cast 10/15/92)

Mixture	Description	Durability Facto		Cycles to 60% RDM		Cycles to 0.1% Dilation		% Mass Loss @ 60% RDM or 300 Cycle		% Dilation @ 60% RDM or 300 Cycle	
		Mean	Std. Dev.	Mean	Std. Dev.	Mean	Std. Dev.	Mean	Std. Dev.	Mean	Std. Dev.
MN1	Mn/DOT Standard	98.9	0.4	300+	-	300+	-	0.1001	0.0066	-0.0090	0.0216
MN2	MN1 w/marginal air	98.4	0.6	300+	-	300+	-	0.1028	0.0206	0.0019	0.0019
MN3	MN1 w/low air	97.6	1.1	300+	-	300+	-	0.1185	0.0083	0.0088	0.0019
MN4	MN1 w/marg. air, no FA	97.9	0.3	300+	-	300+	-	0.0989	0.0205	0.0084	0.0024
MN5	MN1 w/low air, no FA	92.5	3.2	300+	-	300+	-	0.0460	0.0084	0.0267	0.0142
MN6	MN1 w/marg. air, 30% FA	99.2	0.5	300+	-	300+	-	0.1054	0.0123	0.0030	0.0050
MN7	MN1 w/low air, 30% FA	91.4	6.5	300+	-	300+	-	0.0731	0.0154	0.0209	0.0029
MN8	Mn/DOT Experimental Mixture	98.4	0.3	300+	-	300+	-	0.0467	0.0506	0.0087	0.0053

Note 1: All specimens cured 28 days (27 days in lime water).

Note 2: All frost resistance testing conducted in accordance with AASHTO T161 (ASTM C 666) Procedure B, modified (use of cloth wraps).

2.6 Preliminary Findings

It is obvious that few findings can be drawn as yet from observations of the field performance of the mixtures placed in either Minnesota or Ohio. However, some inferences can be drawn from the results of tests conducted to date on the companion laboratory specimens.

The most obvious trend apparent in the laboratory data obtained from the Ohio companion test specimens is that nearly all of the specimens exhibited very poor resistance to freezing and thawing in spite of the measurement of air contents in excess of 5 percent, very high strengths, and low w/c ratios (see tables 3-1 and 3-10). Only the HES and VES mixtures exhibited durability factors of 50 or more; none of the other mixtures tested endured more than 100 freeze-thaw cycles before failure. Consideration of the data in table 3-8 suggests a strong correlation between durability factor and spacing factor, although good durability does not necessarily accompany spacing factors of less than 0.2 mm (0.008 in.). The good durability of the VES and HES mixtures may be attributed to the measurement of spacing factors of less than 0.05 mm (0.002 in.). Other mixtures were found to have spacing factors of less than 0.2 mm (0.008 in.), but more than 0.05 mm (0.002 in.); these were nondurable in spite of the high strengths and low w/c ratios. The poor durability of the mixtures with normally adequate air void systems may be caused by microcracking of the concrete during exposure to the extremely high temperatures that were generated during the hydration of the cement (some of the repairs were observed to be steaming on a warm day when the insulation boards were removed). This suggests that much more stringent air void system requirements may be necessary for HES concretes that may be subject to high temperatures and microcracking. It is also possible that the short mixing time and rapid setting of the concrete prevented the formation of satisfactory air void systems or that the air void system was substantially changed during the consolidation of the test specimens used in the laboratory test.

It was also observed that there was very little difference in durability between specimens that were cured for 14 days and those that were cured for 28 days. The only exception to this was for the SHRP high-performance program VES mixture, which was found to have a durability factor of only 15 at the University of Washington after 14 days of curing, and a durability of 56 at Michigan State University after 28 days of curing. There is no apparent explanation for the effect of curing time on the VES concrete. However, the lack of effect of curing time on the durability of the other mixtures indicates that most of the factors that influence durability (e.g., air void system, water pore system, strength, etc.) are well established after 14 days.

It is also worth noting that almost all of the Ohio mixtures exhibited large amounts of scaling, particularly the HES and VES mixtures, which endured more cycles of freezing and thawing than the other mixtures.

One final possibility that might explain the poor durability of all of the Ohio mixes is the use of a nondurable coarse aggregate. However, this is not expected to be a factor because of the very fine nominal maximum size gradation (9.5-cm [3/8-in.] top size) that was used.

The laboratory data from the Minnesota mixtures offer only subtle trends for consideration. All of the mixtures exhibit excellent durability thus far (more than 400 cycles of freezing and thawing completed to date). Projections of durability indicate that the most durable mixtures will be those that include 15 percent fly ash, with decreasing air content producing higher spacing factors and slightly lower durabilities within that group. However, all three of these mixes are expected to have durability factors of 95 or more, yet have high spacing factors (0.33 mm [0.013 in.] and 0.77 mm [0.030 in.]) and 7-day compressive strengths that are generally less than 28 MPa (4000 psi). This indicates that the pozzolanic effects of the 15 percent fly ash may have optimally decreased the permeability and freezable water content of the mixtures. The use of 0 percent fly ash or 30 percent fly ash produced marginally less durable concrete than the use of 15 percent fly ash. Within each fly ash replacement group, durability generally decreased slightly with decreasing air content and increasing spacing factor.

3.0 D-Crack Mitigation Test Program

3.1 Objectives

The primary goal of Task 4 of this research project was to develop a reliable and practical test to identify aggregates that produce concrete with low frost resistance. A secondary goal was to identify and develop promising methods of treating pavements with existing aggregate damage due to freezing and thawing. It is this secondary goal which was the focus of some field work in this project.

The research effort associated with identifying aggregate susceptible to D-cracking and mitigation of D-cracking is described fully in section 3 of Part II of this final report.

3.2 Test Program Design

The most promising method for mitigating the effects of D-cracking in concrete was to use concrete surface and penetrating sealers to prevent the saturation of the concrete with water. Four concrete sealers were identified as having good potential for use in delaying the onset of aggregate-related D-cracking: a two-part epoxy-resin; penetrating oil; a water-based silane; and a solvent-based silane.

As described earlier, the Ohio field test site is the site of the original Ohio D-cracking study that used three different aggregate sources with varying gradings in concrete pavement that was placed over various base courses. This site was determined to be ideal for a study of

concrete sealer effectiveness because the durability history of the existing concrete is well documented and some D-cracking has taken place over the last sixteen years (most of which was removed during the placement of the full-depth repairs).

The twenty repairs used for the SHRP concrete frost resistance study were selected for this study. The sealers were applied to the joint faces of the existing concrete pavement when the deteriorated concrete was removed. The coarse aggregate source used for the old concrete pavement was constant throughout this area (National Lime and Stone Company plant at Marion, Ohio), although the nominal maximum size of the original coarse aggregate had been varied from 13 to 38 mm (0.5 to 1.5 in.) to determine the effects of grading in the incidence of D-cracking. The sealer applications were distributed with equal frequency over concrete made using each of these aggregate gradings.

Other design factors that were identified as having possible effects on the concrete sealer performance were joint location (approach versus leave) and joint sealant (sealed versus unsealed joints). All sealers were distributed over both approach and leave joints and all approach joints were sealed while leave joints were left unsealed. This approach was selected because studies conducted by ERES Consultants and the University of Illinois have indicated that many repairs tend to move against the flow of traffic over time, resulting in the closure of the approach joint (possible producing spalling if the joint is unsealed and incompressibles are present) and opening of the leave joint (possibly producing joint sealant failure). The selected field experimental design protects the approach joint while allowing the differentiation of the relative benefits of joints sealing and concrete sealing as related to D-cracking mitigation.

Cores 100 mm in diameter (4 in.) were obtained from the repair area at station 152+14 for use in laboratory testing of the sealant materials. This program is detailed under section 3.5.

3.3 Construction Summaries

Table 3-3 summarizes the application of concrete surface sealers at the Ohio test site. All sealer applications were performed by the MSU project team using materials and application equipment provided by the material manufacturers. The penetrating oil and solvent-based silane treatments were applied using commercially available spray bottles of the type used for misting flowers.

Each joint face was thoroughly cleaned by scraping and wire brushing the sawing slurry from the concrete face. Each joint face was allowed to air dry until it no longer appeared damp before applying the sealer. This was done to ensure that at least a small amount of sealer would penetrate the concrete surface.

It should be noted that the joint face cleaning and drying process was tedious, time-consuming, and generally impractical for a production operation. A quicker way must be used for reliably cleaning and drying the concrete surface.

Visual observations of the sealer application process and results suggested that the solvent-based silane treatment might be the most effective and practical of the four treatments that were used. This is based on the fact that it was easy to apply, and water was observed beading on the concrete surface when the contractor moistened the foundation prior to placement of the concrete mixes. The two-part sealer also did an excellent job of sealing the surface, but was difficult to work with in the field because the application nozzle delivered a stream rather than a spray, requiring the use of a brush to spread the sealer. In addition, the nozzle clogged fast as the two-part material would thicken and begin to set within a minute.

3.4 Monitoring Program

No performance monitoring was accomplished after construction of the field test sections under the SHRP concrete frost resistance program because the test sections were constructed only a few months before the end of the contract. However, the following recommendations are made for performance monitoring.

Performance monitoring should be accomplished according to the same guidelines as described under section 2.3. Of particular importance will be the annual 100 percent condition survey of the test sections and surrounding concrete pavement. Monitoring personnel should be especially careful to examine the old pavement around each repair (particularly in the vicinity of unsealed transverse joints) for evidence of D-cracking. As before, nondestructive (impact hammer) tests and coring of the joints may also provide useful information concerning the effectiveness of the various treatments.

3.5 Laboratory Tests

The cores obtained from the Ohio field test site (as described previously) were trimmed (i.e., the bottom portion of each core was sawed to produce a relatively smooth, flat surface). Each core was then measured, tested for longitudinal resonant frequency, and ranked according to dynamic modulus of elasticity.

Each core was then sawed in half longitudinally to produce two matched half cylinders. One of each pair of half cylinders was then treated on all sides (but not the top or bottom) with one of the four concrete sealers used in the field. The other half was left untreated. Treatments were assigned to each core with consideration of original core location (inner wheel path vs. outer wheel path) and concrete dynamic modulus, as described in ASTM C 215 (three blocks of approximately equal dynamic modulus were established and each treatment was assigned to one core in each block). In this way, each sealer was applied to six different half cylinders, as shown in table 3-12.

Half of the test cylinders were sent to the University of Washington for future testing and half remained at MSU for testing under this research effort. Freeze-thaw tests were conducted on each matched pair of half-cylinders at MSU in accordance with ASTM C666, proposed Procedure C. Measurements of mass loss, relative dynamic modulus and quality

factor (Q) were made periodically. The results of these tests provide an indication of the effectiveness of surface treatments and sealers in mitigating D-cracking. They also predict the performance that can be expected at the Ohio field test site.

3.6 Laboratory Test Results

The results of the laboratory freeze-thaw tests of the treated and untreated core halves from the Ohio test road are summarized in tables 3-13 (water-based silane treatment), 3-15 (solvent-based silane treatment), 3-17 (penetrating oil treatment) and 3-19 (two-part resin sealant treatment). Tables 3-14, 3-16, 3-18 and 3-20 summarize the results of statistical analyses that were conducted to determine whether the differences in performance (i.e., differences in relative dynamic modulus, relative Q and mass loss after 300 cycles of freezing and thawing) between treated and untreated core halves are statistically significant. These tables also contain 90 and 95 percent confidence intervals for the differences in mean performance measures between the treated and untreated core halves. All of the statistical analyses were conducted using the t-distribution as an approximation to the reference distribution for the paired comparison experimental design.

3.6.1 Water-based Silane Treatment

The data presented in tables 3-13 and 3-14 indicate that the water-based silane sealant was effective in reducing the effects of freezing and thawing on concrete that contains aggregate susceptible to D-cracking. The average difference in relative dynamic modulus (RDM) between treated and untreated specimens after 300 cycles of freezing and thawing was 11.4 percent, a difference that is significant at the 0.06 level. In other words, there is approximately a 94 percent probability that the water-based silane treatment produced a significant improvement in this performance measure; the 90 and 95 percent confidence intervals for the actual magnitude of this improvement are also presented in table 3-14.

The benefits of water-based silane treatment are also apparent in the mass loss portions of tables 3-13 and 3-14. The negative mass loss measurements indicate that the specimens actually gained weight due to the absorption of water necessary to saturate the specimens (they were initially air-dry prior to treatment and testing) and continued absorption as the pore structure of the concrete was dilated during freezing and thawing. This increase in mass was eventually offset, in part, by mass losses due to scaling, popouts, etc. For this reason, the treated specimens show a greater residual mass gain than the untreated specimens. The difference is exceptionally significant (significance level = 0.002).

Table 3-12 Ohio Core Measurements and D-Cracking Mitigation Treatments

Core #	Dia-1 (mm)	Dia-2 (mm)	Avg. Diam. (mm)	Length-1 (mm)	Length-2 (mm)	Avg. Length (mm)	Long. Freq.	Wt. (kg)	Treat-ment	Test Location
O-3	99.57	99.70	99.63	224.36	220.24	222.30	1059	4.071	1	UW
I-12	100.46	100.33	100.39	227.58	225.60	226.59	1076	4.141	1	MSU
O-11	100.30	100.97	100.63	225.43	221.54	223.48	1137	4.120	2	UW
I-5	100.58	100.48	100.53	225.48	225.93	225.70	1157	4.165	2	MSU
I-6	100.74	100.58	100.66	227.23	224.74	225.98	1189	4.163	3	UW
O-4	100.46	100.84	100.65	223.34	224.16	223.75	1269	4.063	3	MSU
I-2	100.36	100.38	100.37	225.35	225.25	225.30	1252	4.170	4	UW
O-1	100.74	100.89	100.81	221.11	220.09	220.60	1323	4.026	4	MSU
I-4	100.20	100.58	100.39	223.85	225.96	224.90	1300	4.142	4	MSU
O-12	100.30	100.97	100.63	225.43	221.54	223.48	1334	4.141	4	UW
I-8	100.33	100.33	100.33	226.03	224.92	225.48	1330	4.156	3	MSU
I-3	100.48	100.33	100.41	224.94	224.71	224.83	1362	4.110	3	UW
O-9	100.30	100.97	100.63	225.43	221.54	223.48	1403	4.009	2	MSU
O-2	100.33	100.58	100.46	222.89	223.34	223.11	1401	4.094	2	UW
O-8	100.30	100.97	100.63	225.43	221.54	223.48	1409	4.065	1	MSU
I-9	100.58	100.56	100.57	226.44	227.08	226.76	1434	4.213	1	UW
I-14	100.33	100.08	100.20	228.09	225.68	226.89	1439	4.201	3	MSU
O-10	100.30	100.97	100.63	225.43	221.54	223.48	1522	4.093	2	UW
I-7	99.44	99.19	99.31	226.31	226.47	226.39	1534	4.084	1	MSU
I-16	100.58	100.33	100.46	228.07	226.70	227.38	1568	4.170	4	UW
I-10	100.33	100.46	100.39	227.69	225.55	226.62	1569	4.193	4	MSU
I-11	99.57	99.47	99.52	223.90	227.56	225.73	1588	4.136	1	UW
I-15	100.10	100.33	100.22	226.03	225.96	226.00	1625	4.171	2	MSU
I-13	100.20	100.33	100.27	224.16	226.19	225.17	1631	4.179	3	UW

Notes:

1. All cores obtained from concrete being replaced at westbound station 152+14.
2. Cores with "O" prefix obtained from driving lane outer wheel path.
   Cores with "I" prefix obtained from driving lane inner wheel path.
3. Treatment key: 1 = 2-part sealer; 2 = penetrating oil; 3 = water-based silane;
   4 = solvent-based silane.
4. Each core was sawed in half longitudinally;
   one-half of each core was treated, one half was left untreated.

Table 3-13 Results of freeze-thaw testing of D-cracking-susceptible concrete treated with water-based silane.

Specimen No.	O-4		I-8		I-14	
Treatment	Treated	Untreated	Treated	Untreated	Treated	Untreated
RDM @ 300 cycles, %	105.5	88.0	78.1	74.8	101.5	88.0
Cycles to 60% RDM	600+	600	408	417	600+	600+
RDM @ 300 cycles, % (Treated - Untreated)	17.5		3.3		13.5	
Rel. Q @ 300 cycles, %	35.2	39.6	42.5	40.0	13.5	30.0
Rel. Q @ 300 cycles, % (Treated - Untreated)	-4.4		2.5		-16.5	
Mass Loss @ 300 cycles, %	-1.75	-0.55	-2.00	-0.57	-1.90	-0.65
Mass Loss @ 300 cycles, % (Treated - Untreated)	-1.20		-1.43		-1.25	

Table 3-14 Significance levels and confidence intervals for results of freeze-thaw testing of D-cracking-susceptible concrete treated with water-based silane.

	RDM @ 300 cycles, % (Treated-Untreated)	Rel. Q @ 300 cycles, % (Treated-Untreated)	Mass Loss @ 300 cycles, % (Treated-Untreated)
Mean Difference	11.43	-6.13	-1.29
Significance Level	0.06	0.195	0.002
90% C.I.	-0.9 to 23.8	-22.3 to 10.1	-1.50 to -1.09
95% C.I.	-6.8 to 29.6	-30.0 to 17.8	-1.59 to -0.99

The treated specimens generally showed lower levels of relative Q after 300 cycles of freezing and thawing. However, the results are not highly significant (significance level = 0.195, which suggests that such results could be obtained due to random errors about once every five tests). Furthermore, the 90 and 95 percent confidence intervals for the true difference between treated and untreated specimens include large ranges of both positive and negative values. Thus, the results of this test are inconclusive for the water-based silane treatment.

In summary, the test results generally show that the water-based silane treatment was effective in reducing the rate of deterioration of concrete containing D-cracking susceptible aggregate and subjected to repeated cycles of freezing and thawing, although the results of comparisons of relative Q are inconclusive.

3.6.2 Solvent-based Silane Treatment

The data presented in tables 3-15 and 3-16 indicate that the solvent-based silane sealant was effective in reducing the effects of freezing and thawing on concrete that contains aggregate susceptible to D-cracking. The average difference in relative dynamic modulus (RDM) between treated and untreated specimens after 300 cycles of freezing and thawing was 10.9 percent, a difference that is significant at the 0.02 level. In other words, there is approximately a 98 percent probability that the solvent-based silane treatment produced a significant improvement in this performance measure; the 90 and 95 percent confidence intervals for the actual magnitude of this improvement are presented in table 3-16.

The benefits of solvent-based silane treatment are also apparent in the mass loss portions of tables 3-15 and 3-16. The negative mass loss measurements indicate that the specimens actually gained weight due to the absorption of water necessary to saturate the specimens (they were initially air-dry prior to treatment and testing) and continued absorption as the pore structure of the concrete was dilated during freezing and thawing. This increase in mass was eventually offset, in part, by mass losses due to scaling, popouts, etc. For this reason, the treated specimens show a greater residual mass gain than the untreated specimens. The difference is highly significant (significance level = 0.075).

The treated specimens showed an average decrease in relative Q after 300 cycles. However, the results are inconclusive (significance level = 0.46), and would be reversed if the results of specimen I-10 were ignored. Thus, the results of this test were highly variable and are considered inconclusive for the solvent-based silane treatment.

In summary, the test results generally show that the solvent-based silane treatment was effective in reducing the rate of deterioration of concrete containing D-cracking susceptible aggregate and subjected to repeated cycles of freezing and thawing, although the results of comparisons of relative Q are inconclusive.

Table 3-15 Results of freeze-thaw testing of D-cracking-susceptible concrete treated with solvent-based silane.

Specimen No.	O-1		I-10		I-4	
Treatment	Treated	Untreated	Treated	Untreated	Treated	Untreated
RDM @ 300 cycles, %	97.1	83.9	107.5	94.6	96.7	90.2
Cycles to 60% RDM	600+	469	600+	600+	600+	590
RDM @ 300 cycles, % (Treated - Untreated)	13.2		12.9		6.5	
Rel. Q @ 300 cycles, %	46.9	37.4	19.8	48.4	59.2	48.2
Rel. Q @ 300 cycles, % (Treated - Untreated)	9.5		-28.6		11.0	
Mass Loss @ 300 cycles, %	-1.43	-0.60	-0.84	-0.45	-0.97	-0.83
Mass Loss @ 300 cycles, % (Treated - Untreated)	-0.83		-0.39		-0.14	

Table 3-16 Significance levels and confidence intervals for results of freeze-thaw testing of D-cracking-susceptible concrete treated with solvent-based silane.

	RDM @ 300 cycles, % (Treated-Untreated)	Rel. Q @ 300 cycles, % (Treated-Untreated)	Mass Loss @ 300 cycles, % (Treated-Untreated)
Mean Difference	10.87	-2.70	-0.45
Significance Level	0.02	0.46	0.075
90% C.I.	4.5 to 17.2	-40.5 to 35.1	-1.04 to 0.14
95% C.I.	1.5 to 20.3	-58.5 to 53.1	-1.32 to 0.42

3.6.3 Penetrating Oil Treatment

The data presented in tables 3-17 and 3-18 are generally inconclusive with respect to the effectiveness of the penetrating oil treatment in reducing the effects of freezing and thawing on concrete that contains aggregate susceptible to D-cracking. The average difference in relative dynamic modulus (RDM) between treated and untreated specimens after 300 cycles of freezing and thawing was -6.9 percent, a difference that favored the untreated specimens. However, this difference is significant only at the 0.36 level. The results of the three pairs of comparisons are highly variable with respect to this measure and the test results are considered inconclusive.

The treated specimens showed consistently lower levels of relative Q after 300 cycles (average difference = 9.2 percent). However, the results range widely and are only somewhat significant (significance level = 0.145). Thus, it appears that the penetrating oil treatment may have resulted in a slight decrease in performance when measured using relative Q, but the results are inconclusive.

The benefits of penetrating oil treatment are suggested in the mass loss portions of tables 3-17 and 3-18. The negative mass loss measurements indicate that the specimens actually gained weight due to the absorption of water necessary to saturate the specimens (they were initially air-dry prior to treatment and testing) and continued absorption as the pore structure of the concrete was dilated during freezing and thawing. This increase in mass was eventually offset, in part, by mass losses due to scaling, popouts, etc. For this reason, the treated specimens show a greater residual mass gain than the untreated specimens. The difference is highly significant (significance level = 0.025).

In summary, the test results are mixed for the penetrating oil treatment, with apparent decreases in performance measured with respect to relative dynamic modulus and relative Q and improvements in performance with respect to mass loss. Based on these results, one cannot determine the effectiveness of the penetrating oil treatment in reducing the rate of deterioration of concrete containing D-cracking susceptible aggregate and subjected to repeated cycles of freezing and thawing. Additional testing should be conducted.

3.6.4 Two-part Resin Surface Sealer Treatment

The data presented in tables 3-19 and 3-20 are generally inconclusive concerning the effectiveness of the two-part resin surface sealer treatment in reducing the effects of freezing and thawing on concrete that contains aggregate susceptible to D-cracking. The average difference in relative dynamic modulus (RDM) between treated and untreated specimens after 300 cycles of freezing and thawing was 6.0 percent, a difference that favored the treated specimens, but is significant only at the 0.295 level because of the variability of the test results. In fact, if specimen I-7 is ignored, the remaining specimens showed a slight reduction in RDM with treatment. Thus, the results of the three pairs of comparisons are highly variable with respect to this measure and are considered inconclusive.

Table 3-17 Results of freeze-thaw testing of D-cracking-susceptible concrete treated with penetrating oil sealer.

Specimen No.	O-9		I-5		I-15	
Treatment	Treated	Untreated	Treated	Untreated	Treated	Untreated
RDM @ 300 cycles, %	43.5	84.0	92.4	70.4	85.0	87.0
Cycles to 60% RDM	200	600+	520	373	422	536
RDM @ 300 cycles, % (Treated - Untreated)	-40.5		22.0		-2.0	
Rel. Q @ 300 cycles, %	22.0	27.0	28.0	29.0	22.0	43.5
Rel. Q @ 300 cycles, % (Treated - Untreated)	-5.0		-1.0		-21.5	
Mass Loss @ 300 cycles, %	-1.10	-0.75	-1.45	-0.79	-1.55	-0.70
Mass Loss @ 300 cycles, % (Treated - Untreated)	-0.35		-0.66		-0.85	

Table 3-18 Significance levels and confidence intervals for results of freeze-thaw testing of D-cracking-susceptible concrete treated with penetrating oil sealer.

	RDM @ 300 cycles, % (Treated-Untreated)	Rel. Q @ 300 cycles, % (Treated-Untreated)	Mass Loss @ 300 cycles, % (Treated-Untreated)
Mean Difference	-6.83	-9.17	-0.62
Significance Level	0.36	0.145	0.025
90% C.I.	-60.0 to 46.3	-27.5 to 9.2	-1.05 to -0.19
95% C.I.	-85.2 to 71.5	-36.2 to 17.8	-1.25 to 0.01

Table 3-19 Results of freeze-thaw testing of D-cracking susceptible concrete treated with two-part resin surface sealer.

Specimen No.	O-8		I-12		I-7	
Treatment	Treated	Untreated	Treated	Untreated	Treated	Untreated
RDM @ 300 cycles, %	90.8	94.6	83.5	88.1	99.8	73.3
Cycles to 60% RDM	600+	600+	440	600+	600+	420
RDM @ 300 cycles, % (Treated - Untreated)	-3.8		-4.6		26.4	
Rel. Q @ 300 cycles, %	35.1	35.1	19.8	39.4	38.1	27.9
Rel. Q @ 300 cycles, % (Treated - Untreated)	0.0		-19.6		10.2	
Mass Loss @ 300 cycles, %	-1.30	-0.70	-1.80	-0.90	-1.90	-0.49
Mass Loss @ 300 cycles, % (Treated - Untreated)	-0.60		-0.90		-1.41	

Table 3-20 Significance levels and confidence intervals for results of freeze-thaw testing of D-cracking susceptible concrete treated with two-part resin surface sealer.

	RDM @ 300 cycles, % (Treated-Untreated)	Rel. Q @ 300 cycles, % (Treated-Untreated)	Mass Loss @ 300 cycles, % (Treated-Untreated)
Mean Difference	-3.8	-4.6	26.4
Significance Level	0.295	0.37	0.03
90% C.I.	-23.8 to 35.8	-28.7 to 22.4	-1.66 to -0.28
95% C.I.	-37.9 to 49.9	-40.8 to 34.5	-1.99 to 0.05

The treated specimens showed generally lower levels of relative Q after 300 cycles of freezing and thawing (average difference = 3.1 percent). However, the results range widely and the trend is not considered significant (significance level = 0.37). Thus, the results of the three pairs of comparisons are highly variable with respect to this measure and are considered inconclusive.

It should be noted here that the two-part resin surface sealer treatment hampered efforts at measuring relative dynamic modulus and relative Q. The presence of the relatively soft resin coating over the entire core half seemed to provide partial attenuation of the impulses provided by the modally-tuned hammer that was used in the test. In addition, the sealer sometimes exhibited small bubbles or areas of debonding with the specimen, possibly caused by the expulsion of water or vapor upon freezing. As a result of these two conditions, the test operator often experienced considerable difficulty in obtaining consistent, reasonable test results for these specimens, which probably contributed the variability of the test results.

The two-part resin surface sealer treatment was effective in reducing the mass loss of the test specimens, as shown in tables 3-19 and 3-20. The negative mass loss measurements indicate that the specimens actually gained weight due to the absorption of water necessary to saturate the specimens (they were initially air-dry prior to treatment and testing) and continued absorption as the pore structure of the concrete was dilated during freezing and thawing. This increase in mass was eventually offset, in part, by mass losses due to scaling, popouts, etc. For this reason, the treated specimens show a greater residual mass gain than the untreated specimens. The difference is highly significant (significance level = 0.03). It was also noted that, although large cracks did develop in the resin specimens, the coating effectively held the loose particles and chunks of concrete in place.

In summary, the test results generally show improvements in the performance of specimens treated with the two-part resin surface sealer treatment, but the improvement in relative dynamic modulus is not strong enough to be conclusive, and a negative trend was observed in relative Q values (also not strong enough to be conclusive). Improvements in mass loss were positive and conclusive.

3.6.5 Summary of Laboratory Test Results

The laboratory freeze-thaw tests conducted on surface treatments of matched, paired specimens provided conclusive evidence that the water-based and solvent-based silane treatments were effective in mitigating the deterioration of concrete containing D-cracking susceptible aggregate. Tests of the penetrating oil and two-part resin treatments were generally inconclusive, although all four treatments were effective in reducing the mass loss of the treated specimens, and the two-part resin treatment was effective in holding cracked concrete intact.

4.0 Other Field Mixes

4.1 Background

Additional field correlation work is being conducted with the cooperation of David Whiting of Construction Technology Laboratories (CTL) and the SHRP high-performance concrete program. Both latex and silica fume mixtures from bridge deck overlays in three different states are being tested in repeated freezing and thawing by the proposed Procedure C of AASHTO T 161 (ASTM C 666). The purpose of this testing is twofold: to provide comparison of the proposed testing procedure with the standard Procedure A as performed at CTL; and to provide laboratory test data on field-placed mixtures.

4.2 Testing Summary

A summary of the results obtained to date are shown below:

Mixture ID	Q-failure (best fit)	Cyles Endured	Relative Dynamic Modulus
Series 1, Latex	>1000	>300	102
Series 1, SF	>1000	>300	93
Series 2, Latex	>1000	195	(97)
Series 2, SF	>1000	195	(92)
Series 3, Latex	>1000	117	(100)
Series 3, SF	-	-	-

The Q-Failure values shown in column 2 are determined as previously described under task 2. The data in column 4 is the durability factor for the Series 1 mixes which have been exposed to over 300 cycles of freezing and thawing. For Series 2 and 3, this column contains the relative dynamic modulus after the number of cycles shown in column 3.

5.0 Conclusions and Summary

The field tests and laboratory tests of field test materials will provide a great deal of information that will be useful in validating the models and concepts presented in parts I and II of this report. In addition, the D-cracking mitigation study incorporated in the Ohio test section, the first such field study to be undertaken on highway pavements, will provide a basis for determining the potential benefits of using concrete sealers to mitigate or prevent the development of D-cracking in concrete pavements constructed using nondurable aggregates.

Appendix A
Freezing and Thawing Test Histories for Ohio Test Mixtures

NOTE: Unless noted otherwise, each series of symbols in the following charts represents the results of tests performed on a single specimen prepared from the same batch of concrete as all other specimens in the same chart. For example, squares might represent data from specimen No. 1 of mixture X, triangles might represent data from specimen No. 2 of mixture X, etc.)

Dilation after Freezing and Thawing

Ohio Mixture A (HES)-28-Day Cure

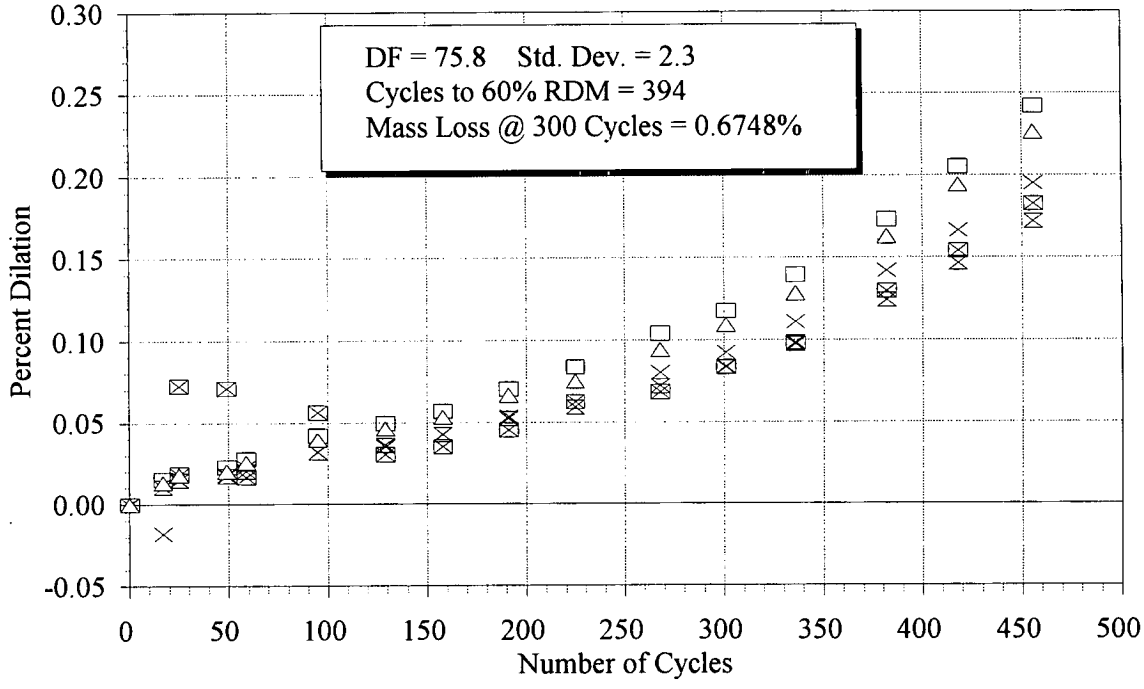

Mass Loss After Freezing and Thawing

Ohio Mixture A (HES)-28-Day Cure

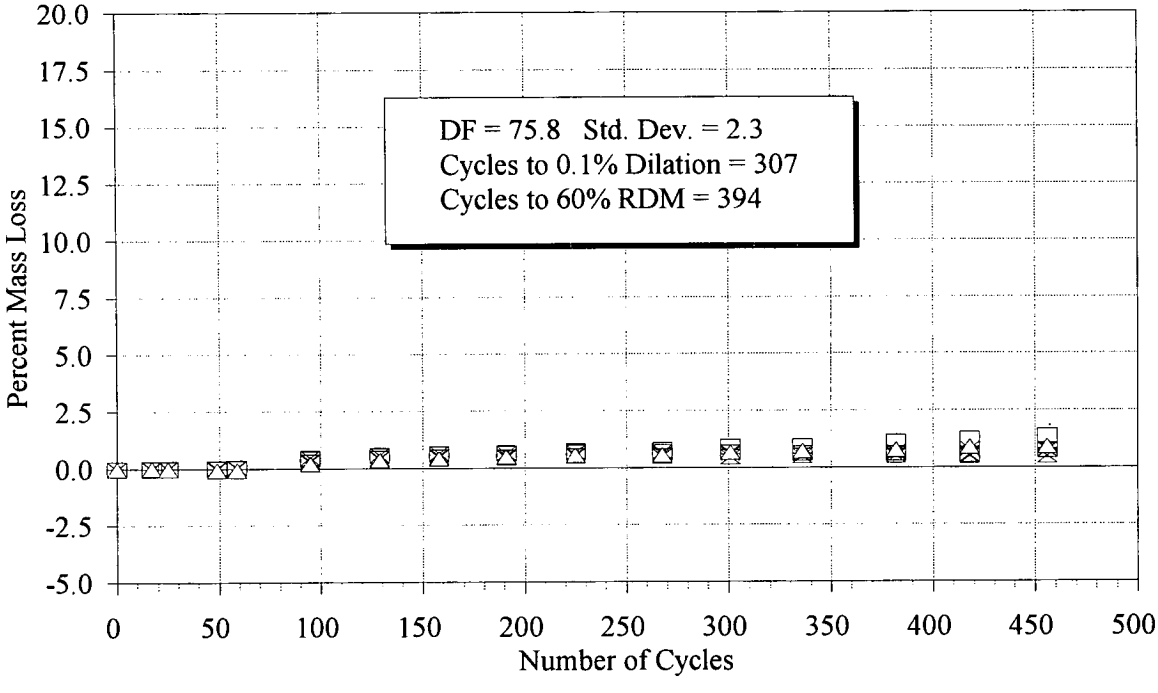

Rel Q Based on Transverse Frequency

Ohio Mixture A (HES)-28-Day Cure

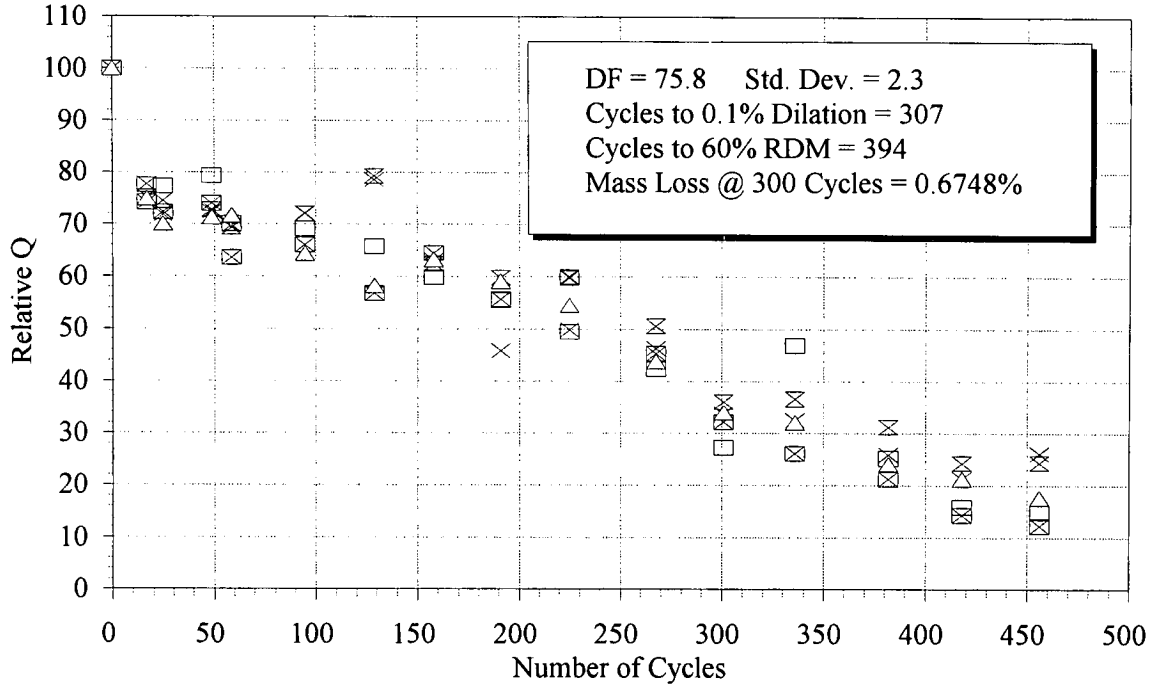

Relative Dynamic Modulus

Ohio Mixture A (HES)-28-Day Cure

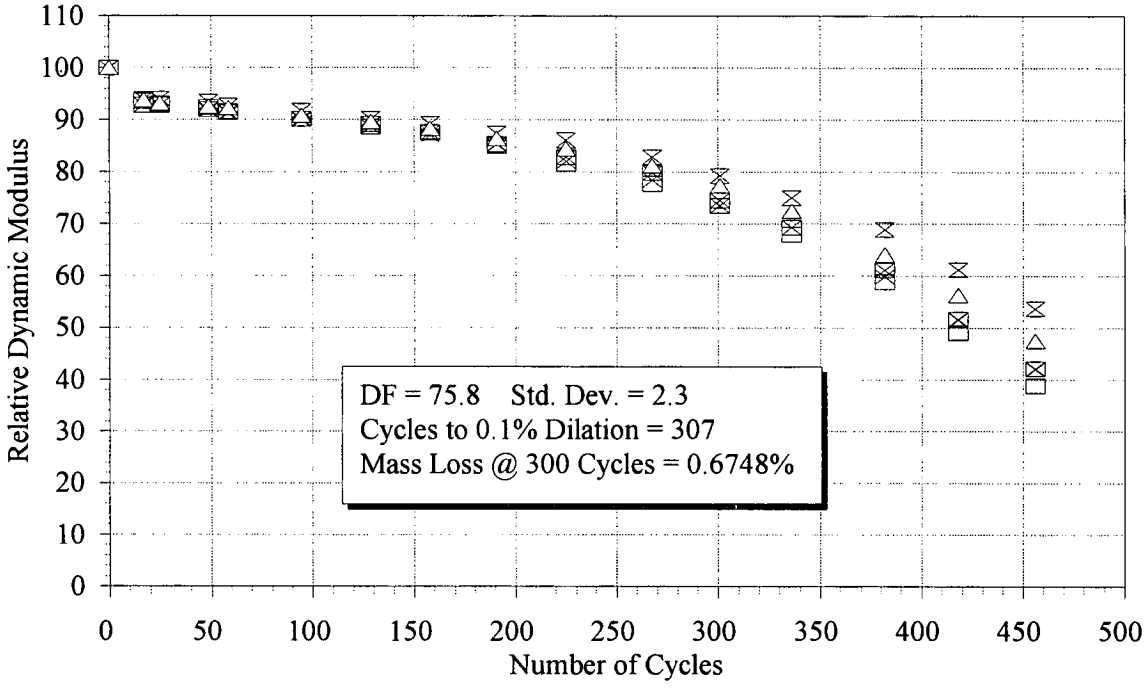

Dilation after Freezing and Thawing

Ohio Mixture C (PC1)-28-Day Cure

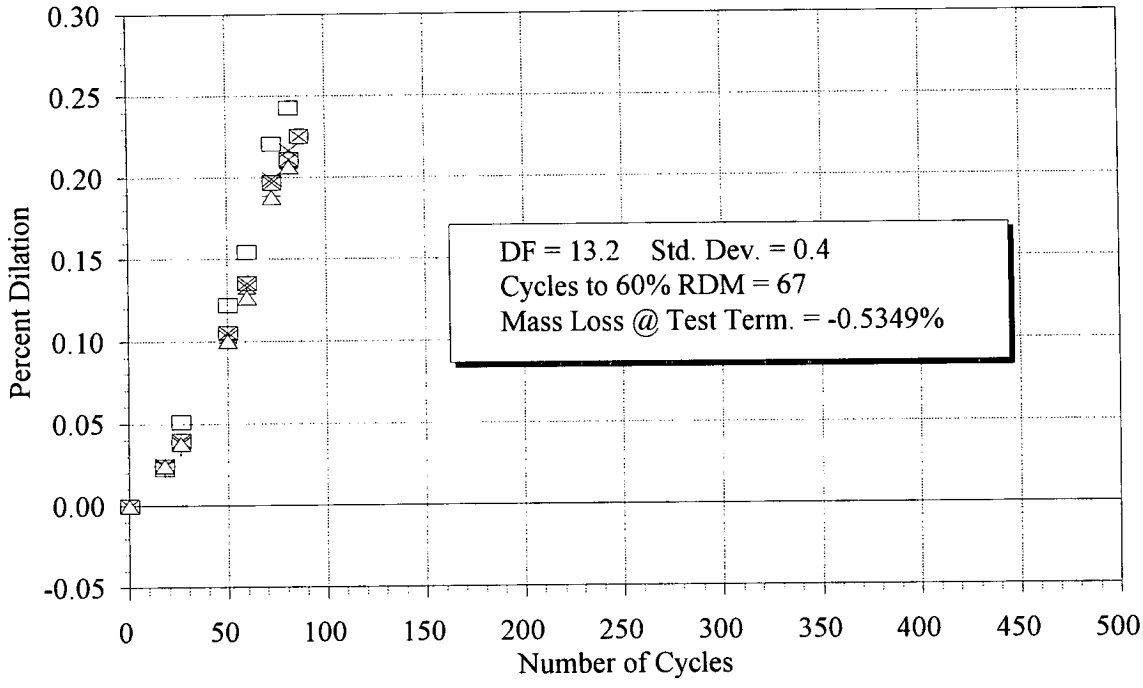

Mass Loss After Freezing and Thawing

Ohio Mixture C (PC1)-28-Day Cure

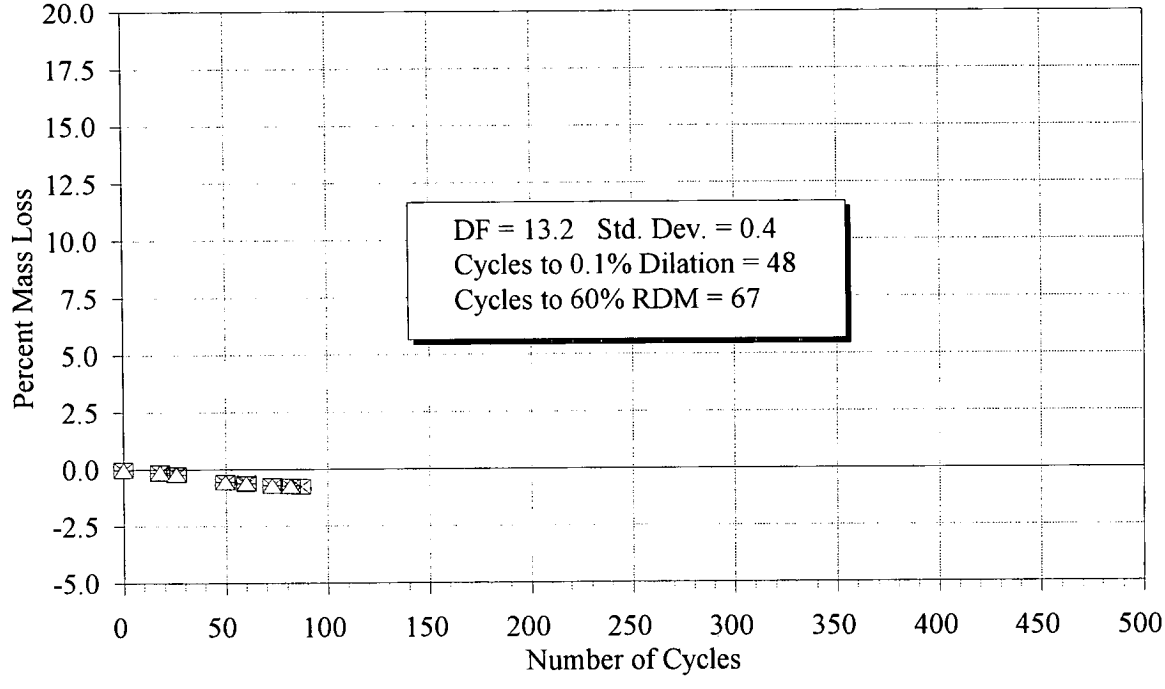

Rel Q Based on Transverse Frequency

Ohio Mixture C (PC1)-28-Day Cure

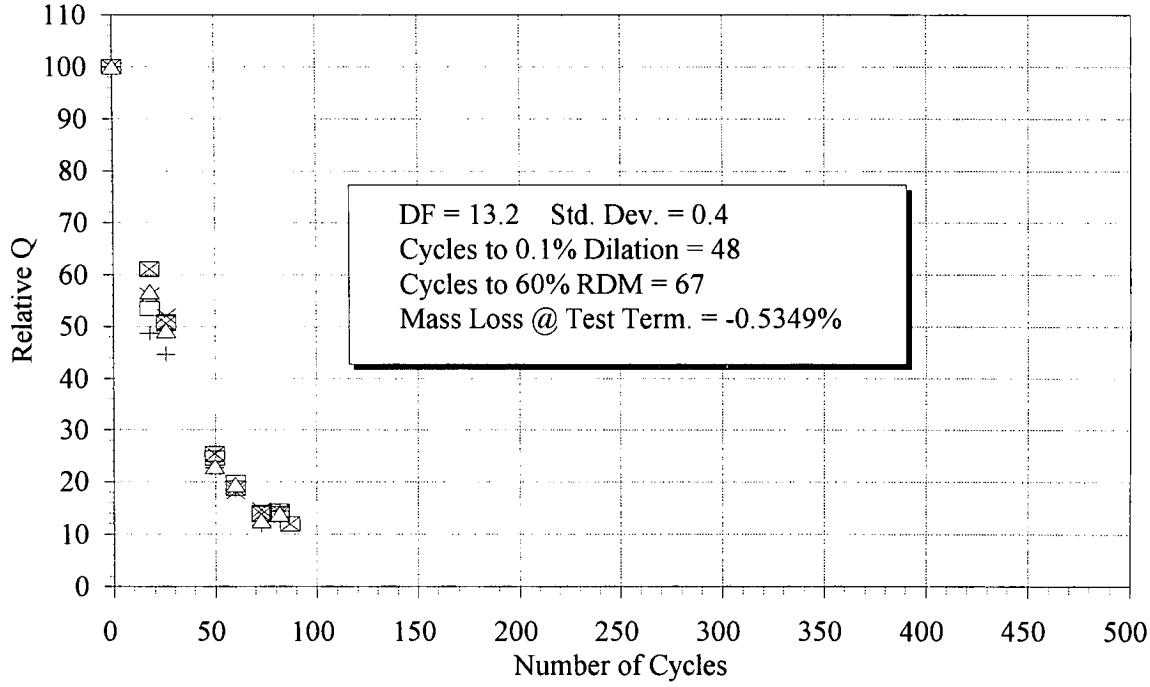

Relative Dynamic Modulus

Ohio Mixture C (PC1)-28-Day Cure

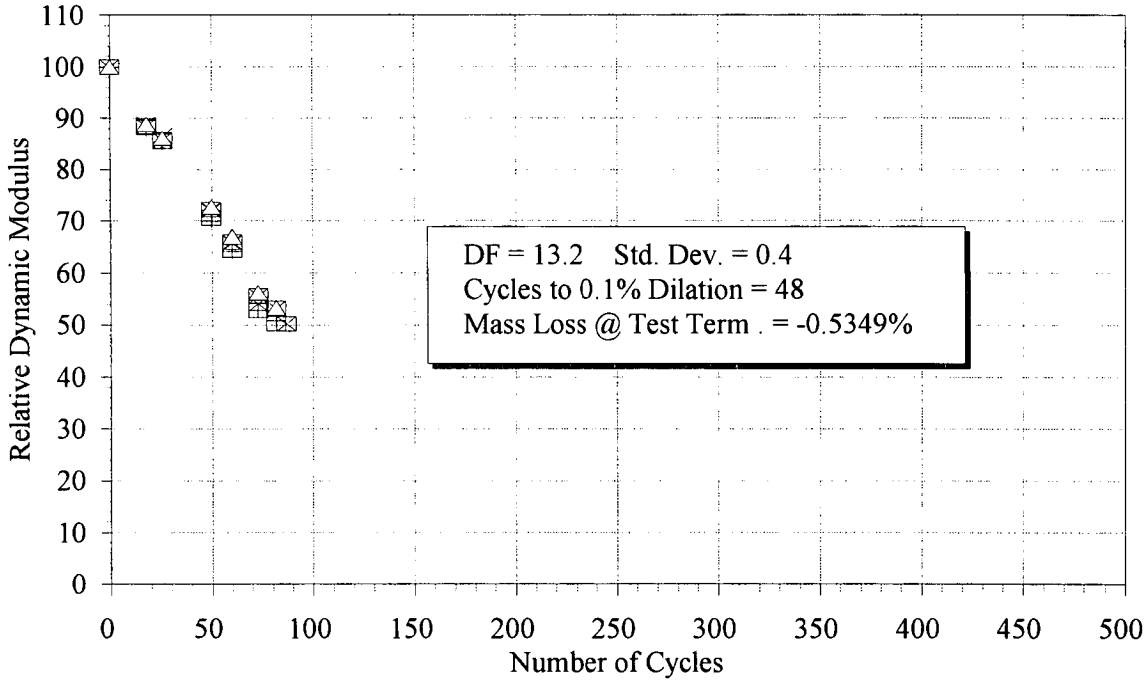

Dilation after Freezing and Thawing

Ohio Mixture E (VES)-28-Day Cure

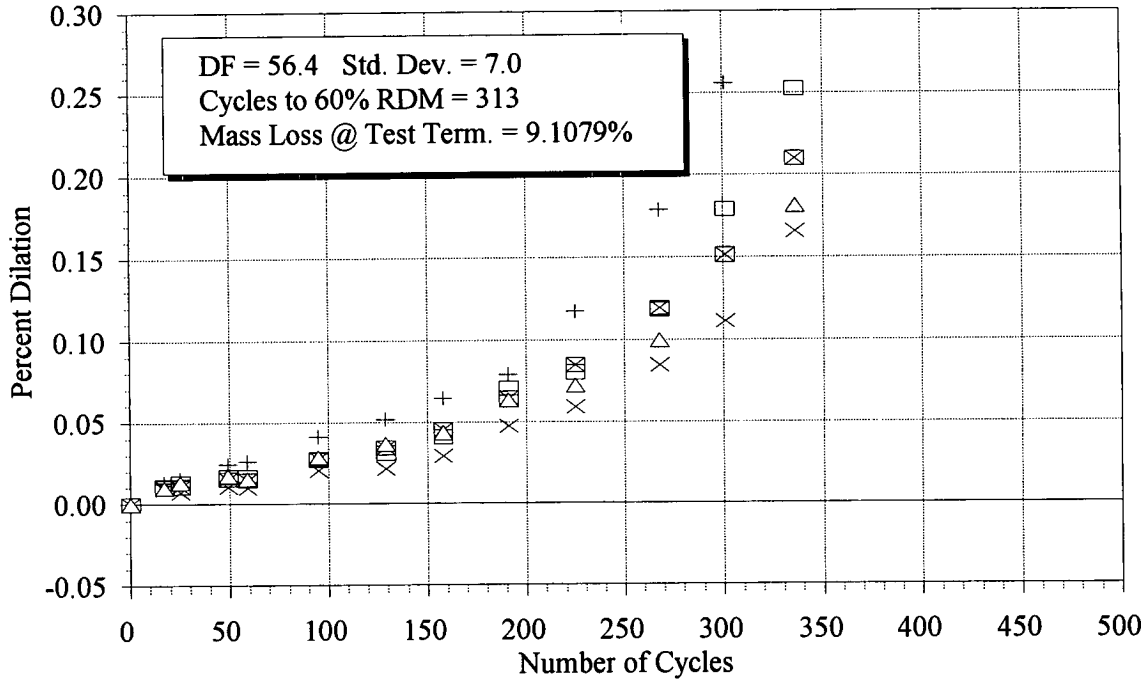

Mass Loss After Freezing and Thawing

Ohio Mixture E (VES)-28-Day Cure

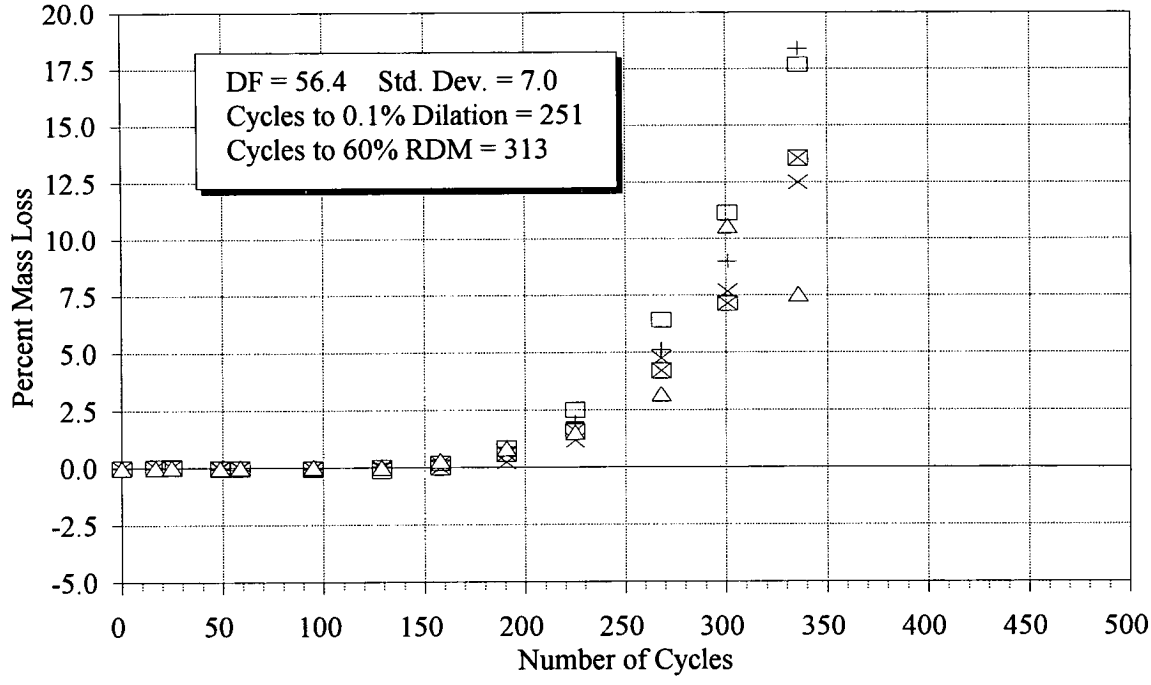

Rel Q Based on Transverse Frequency

Ohio Mixture E (VES)-28-Day Cure

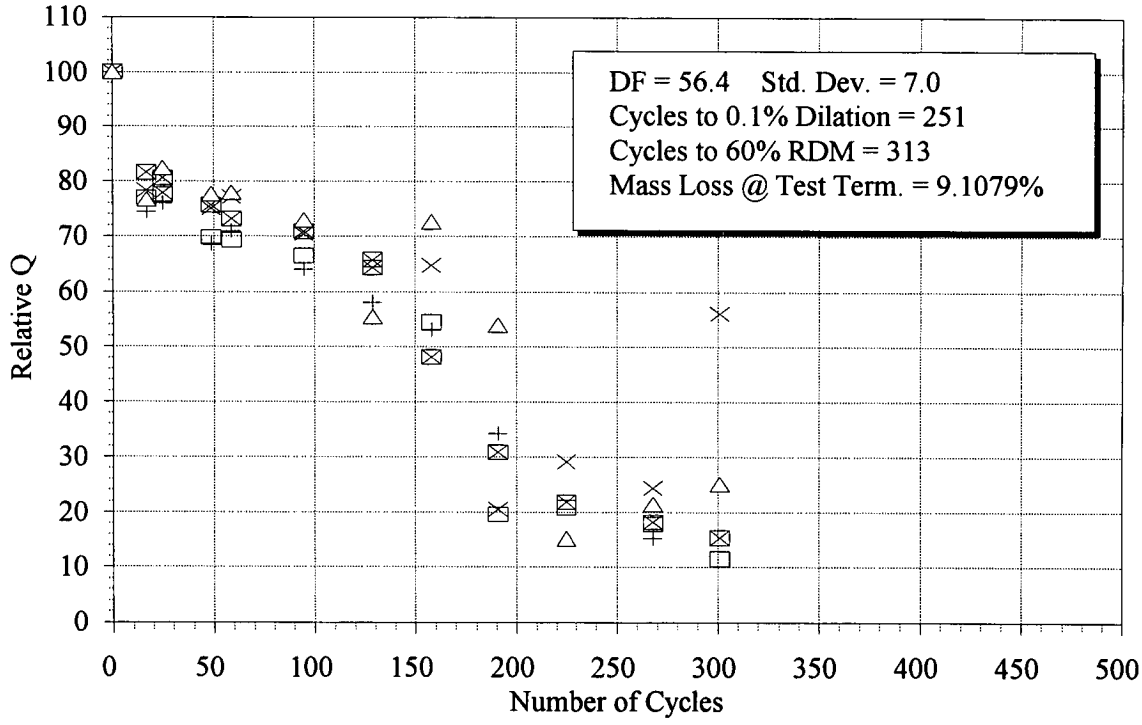

Relative Dynamic Modulus

Ohio Mixture E (VES)-28-Day Cure

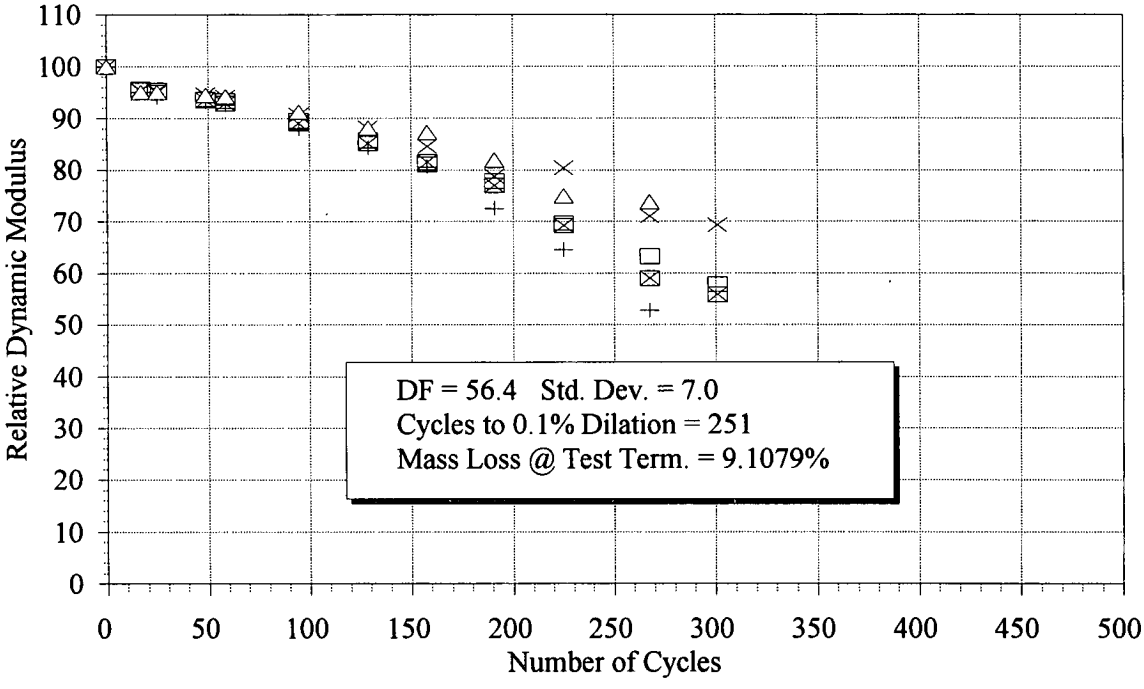

Dilation after Freezing and Thawing

Ohio Mixture F (PC2)-28-Day Cure

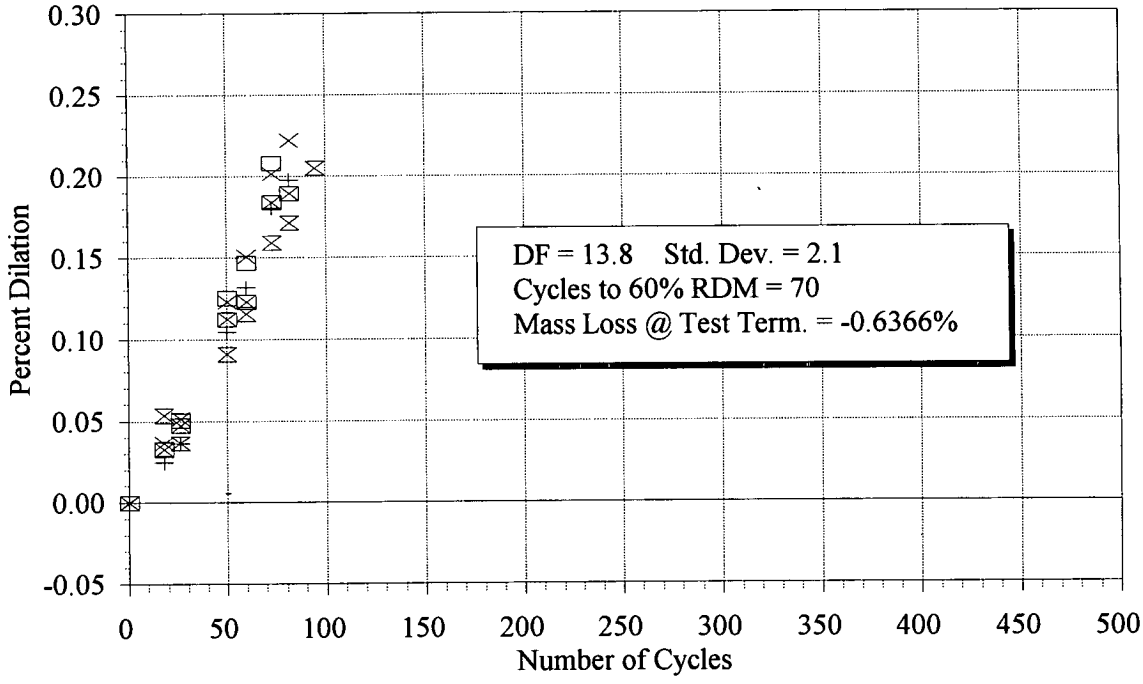

Mass Loss After Freezing and Thawing

Ohio Mixture F (PC2)-28-Day Cure

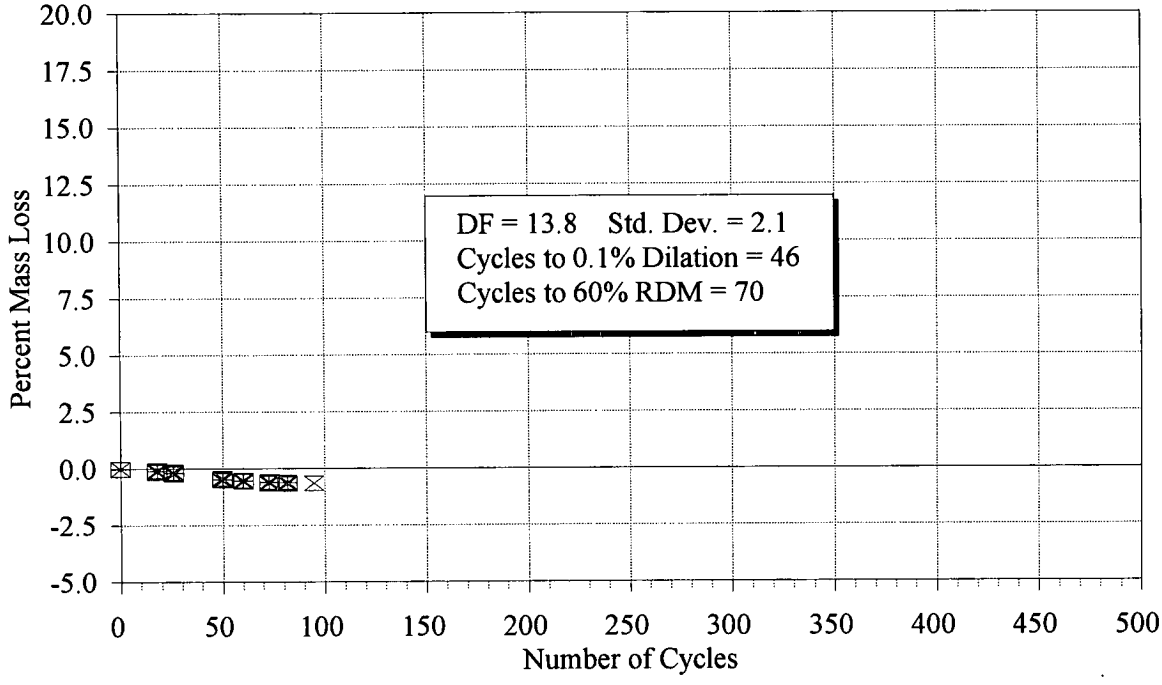

Rel Q Based on Transverse Frequency

Ohio Mixture F (PC2)-28-Day Cure

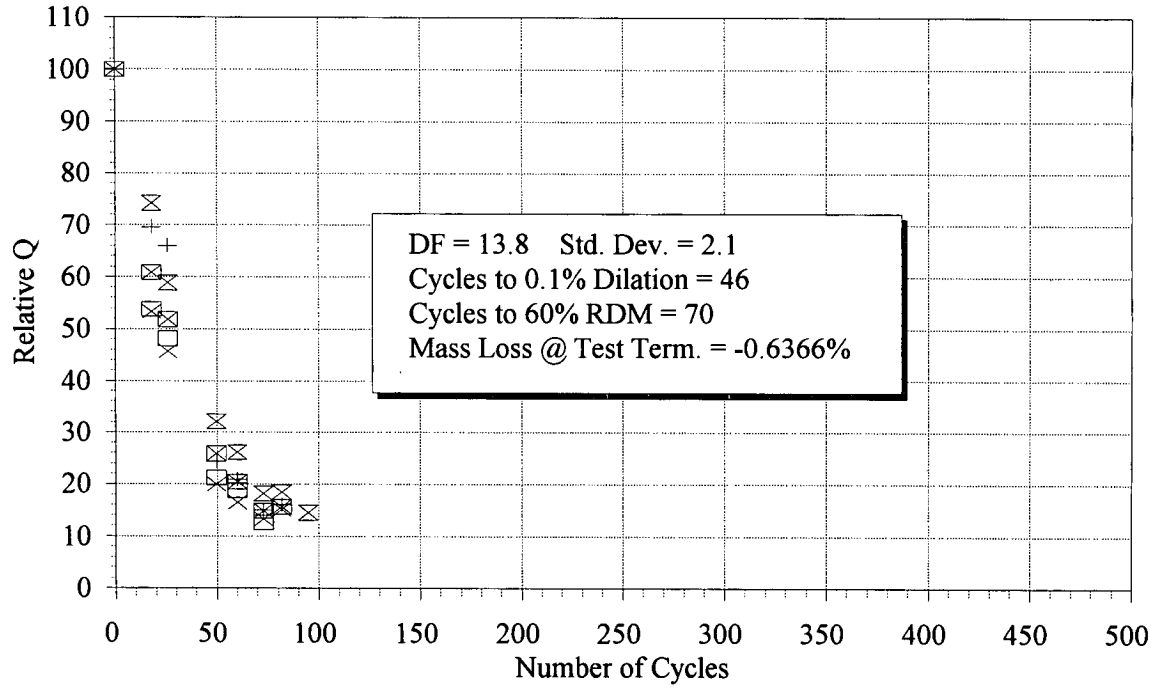

Relative Dynamic Modulus

Ohio Mixture F (PC2)-28-Day Cure

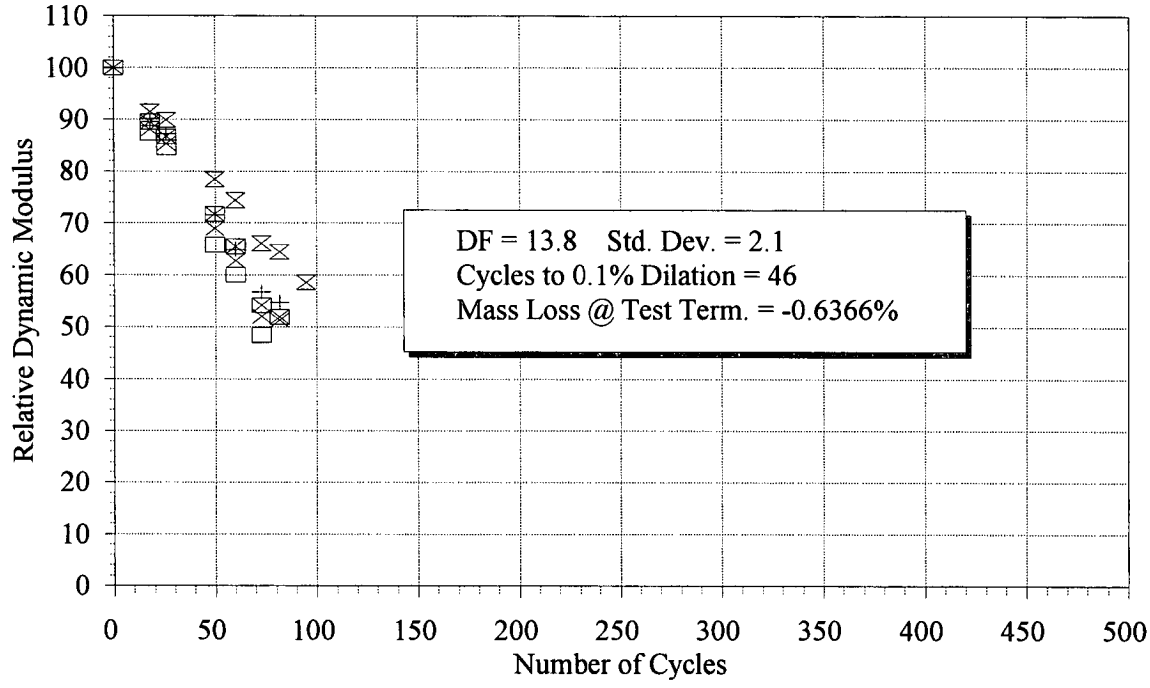

Dilation after Freezing and Thawing

Ohio Mixture H1 (FS)-28-Day Cure

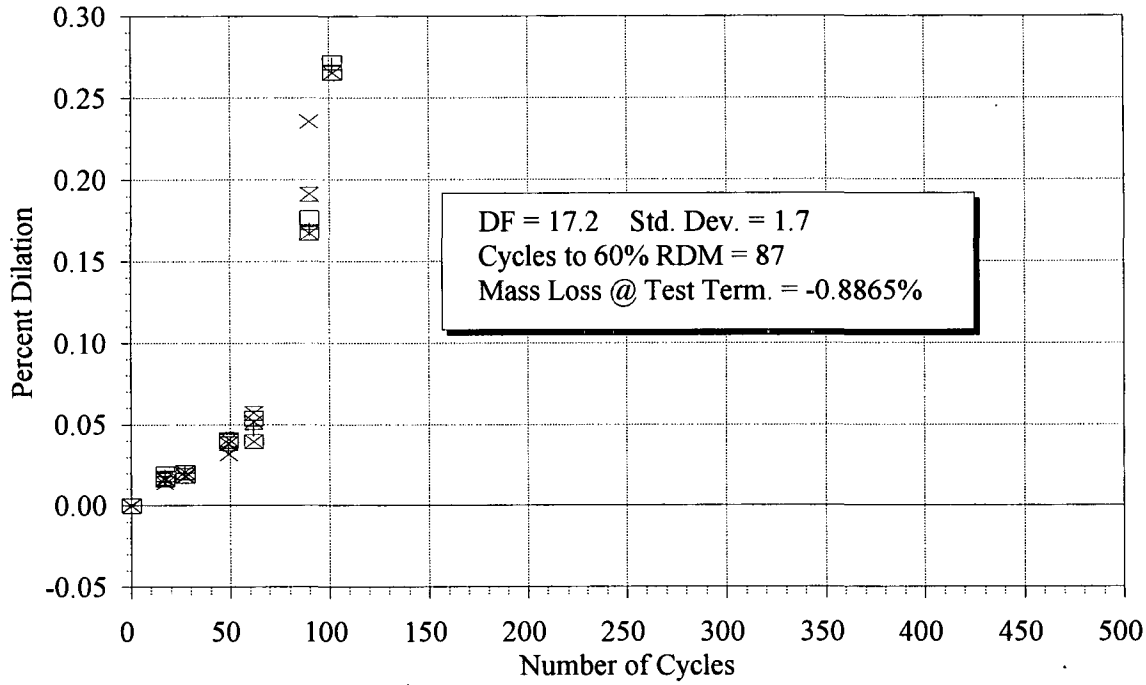

Mass Loss After Freezing and Thawing

Ohio Mixture H1 (FS)-28-Day Cure

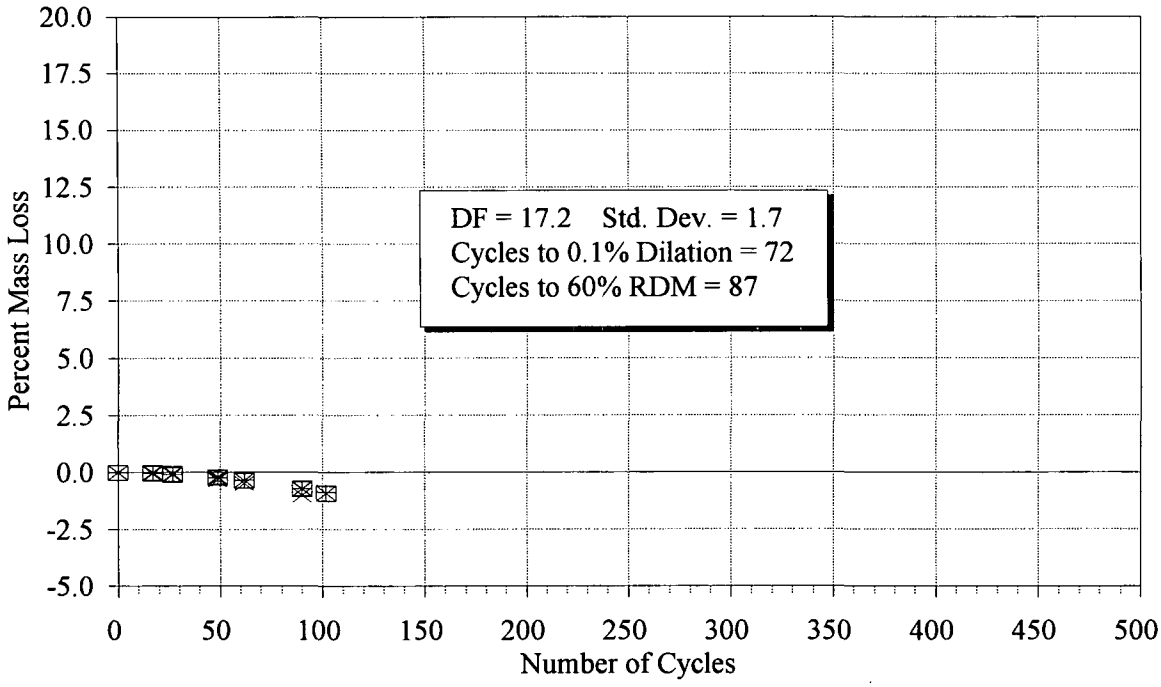

Rel Q Based on Transverse Frequency

Ohio Mixture H1 (FS)-28-Day Cure

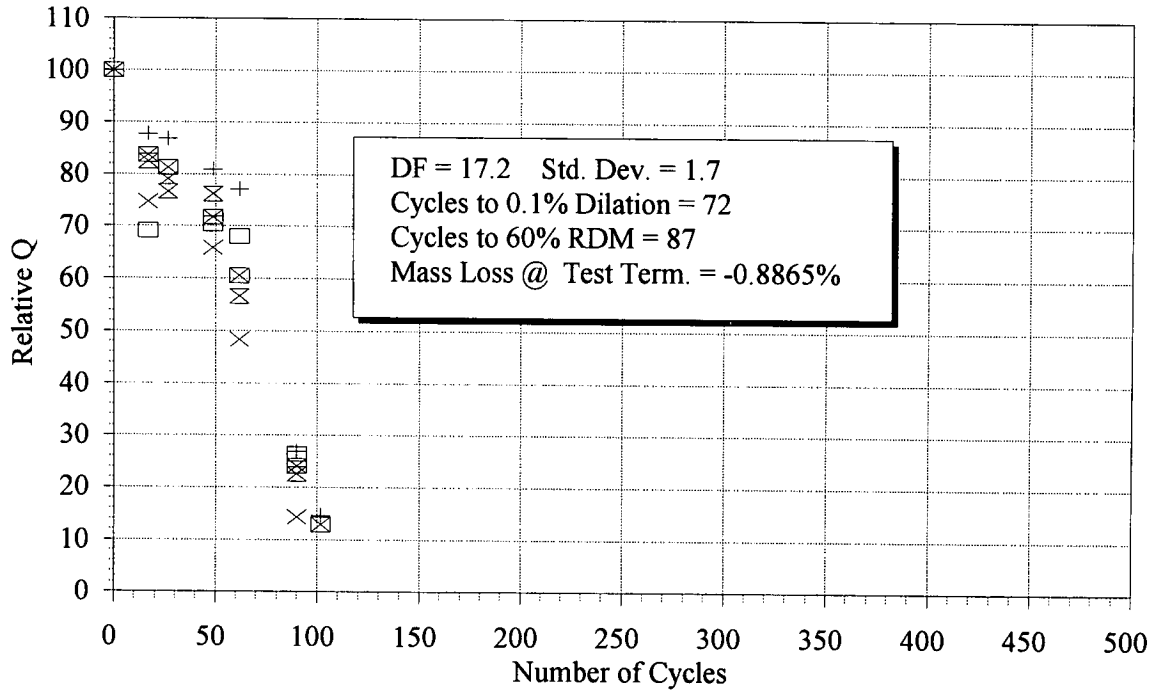

Relative Dynamic Modulus

Ohio Mixture H1 (FS)-28-Day Cure

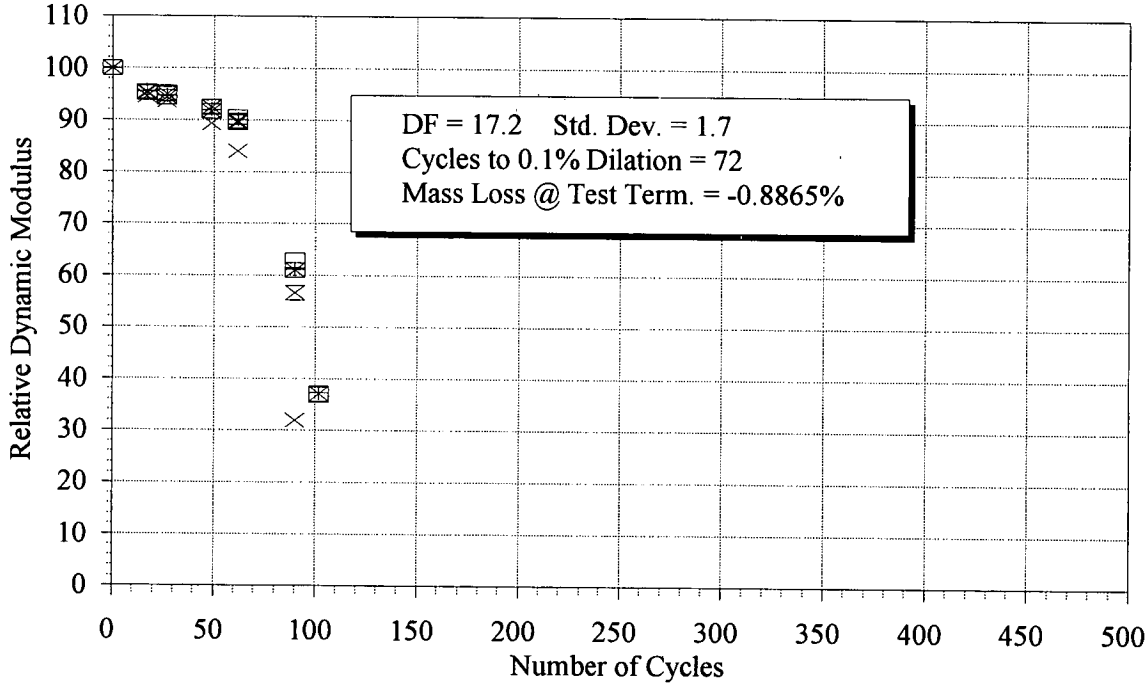

Dilation after Freezing and Thawing

Ohio Mixture H2 (FS)-28-Day Cure

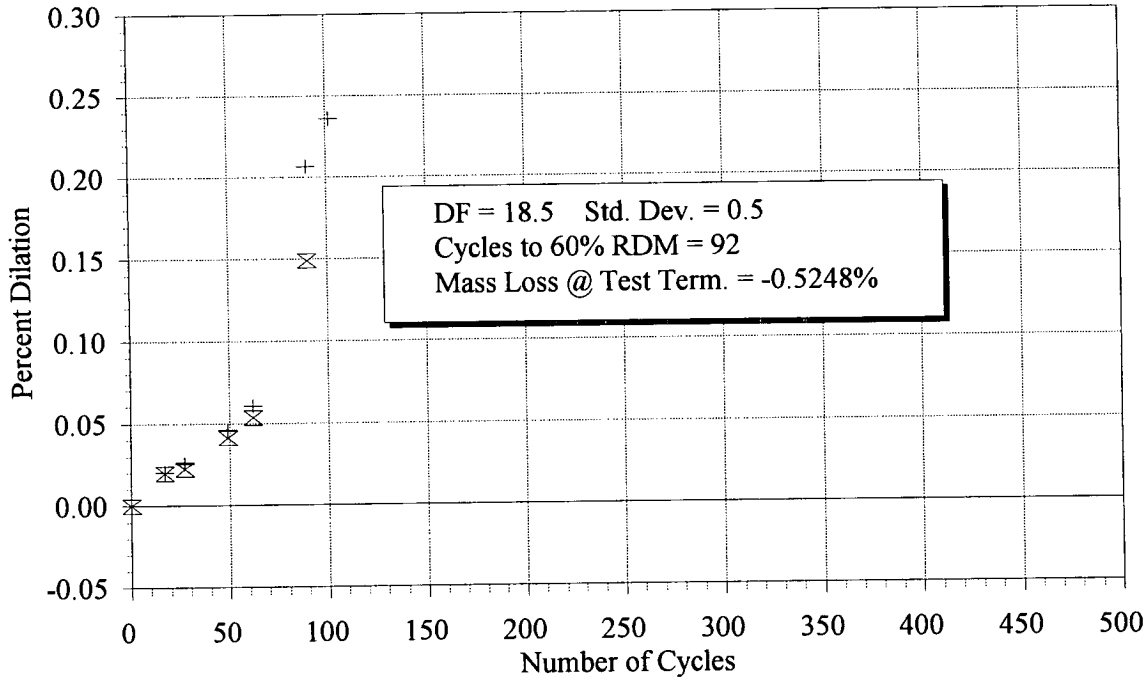

Mass Loss After Freezing and Thawing

Ohio Mixture H2 (FS)-28-Day Cure

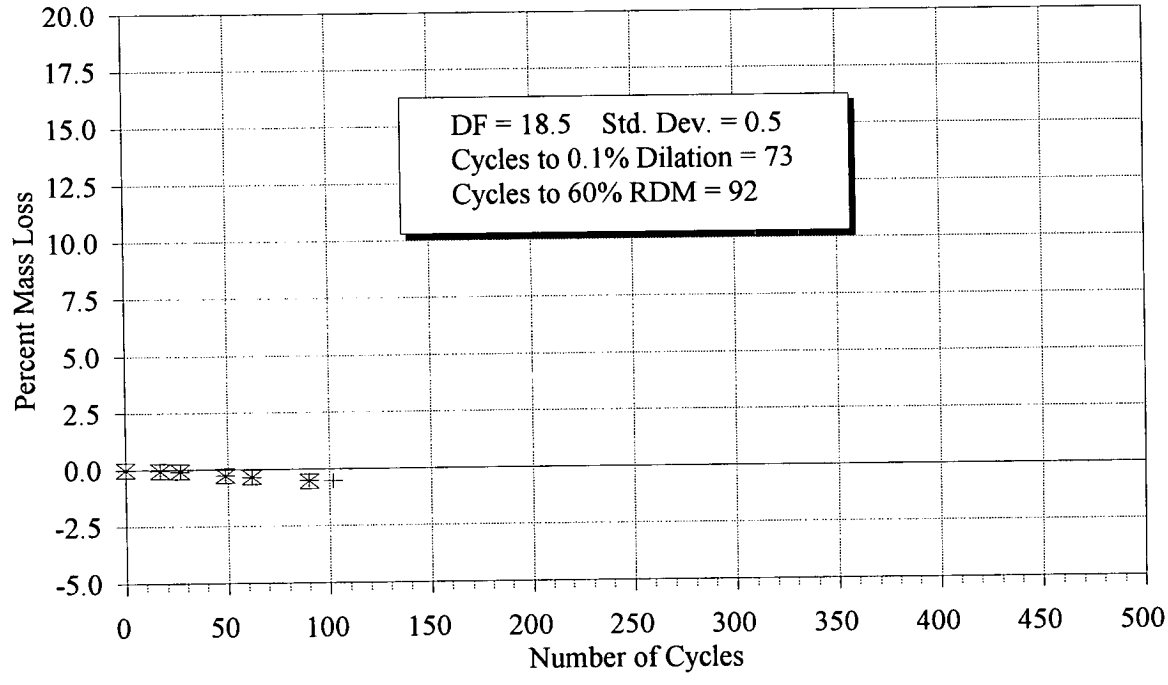

Rel Q Based on Transverse Frequency

Ohio Mixture H2 (FS)-28-Day Cure

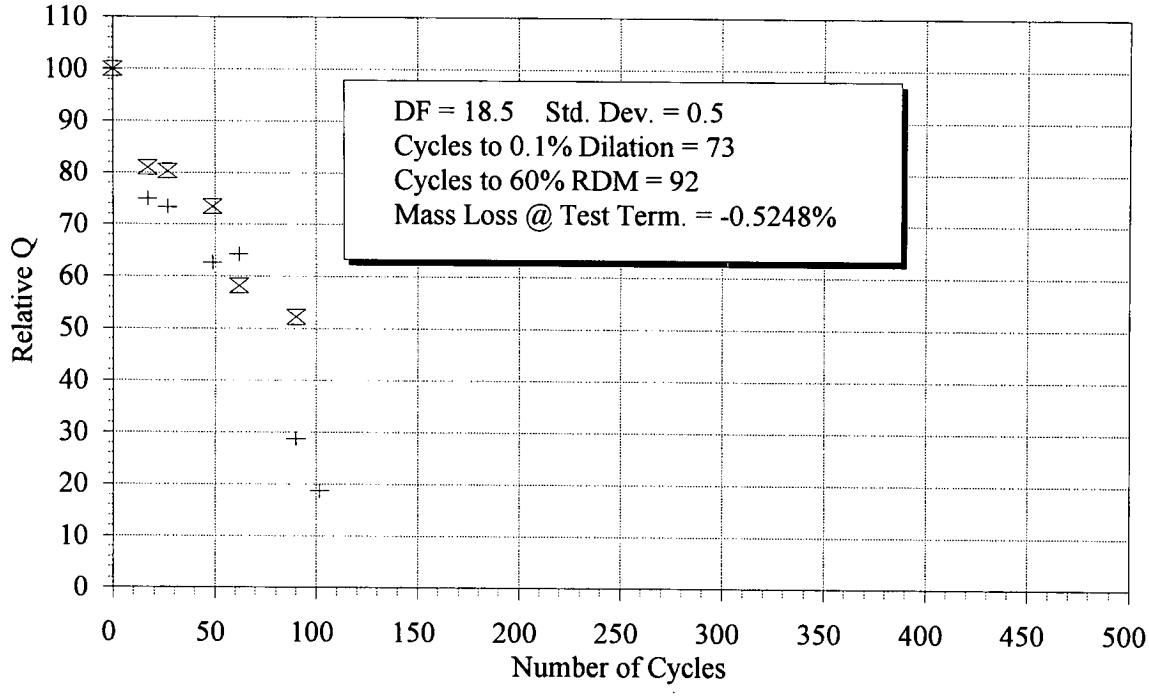

Relative Dynamic Modulus

Ohio Mixture H2 (FS)-28-Day Cure

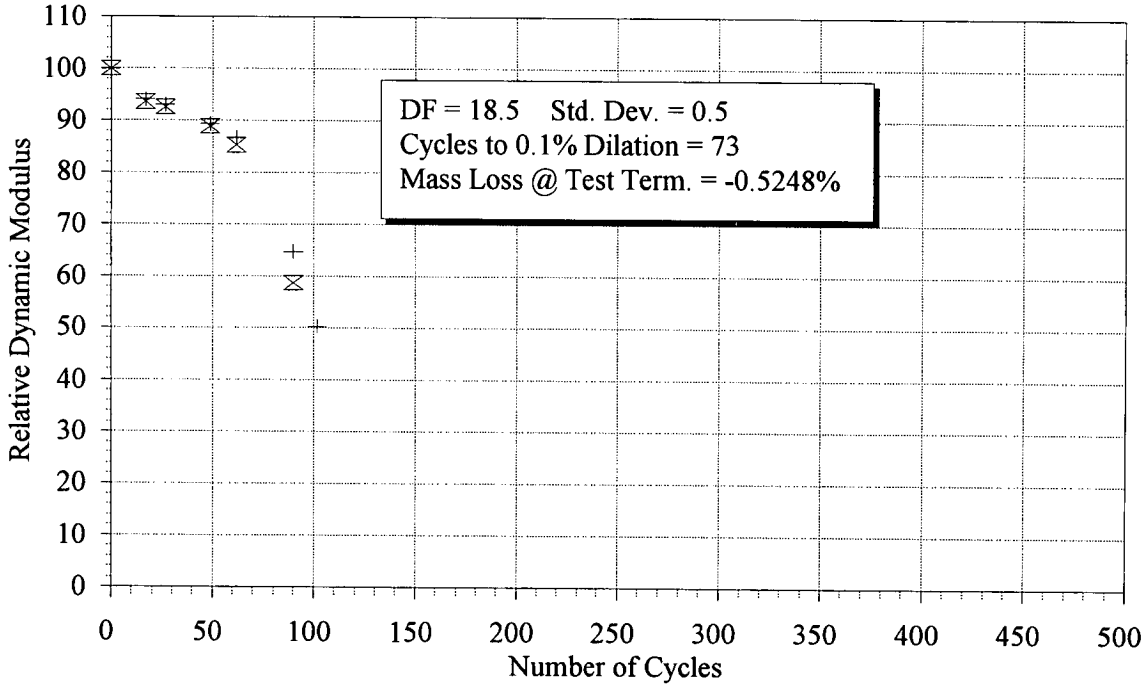

Dilation after Freezing and Thawing

Ohio Mixture I1 (FS mod) - 28-Day Cure

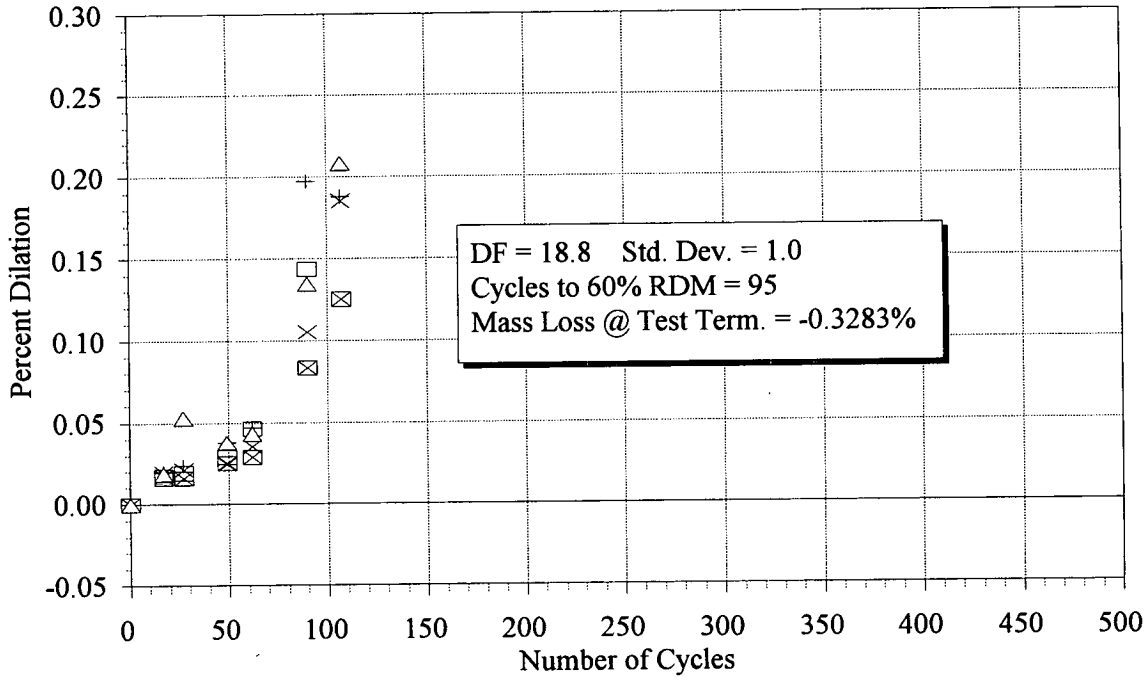

Mass Loss After Freezing and Thawing

Ohio Mixture I1 (FS mod) - 28-Day Cure

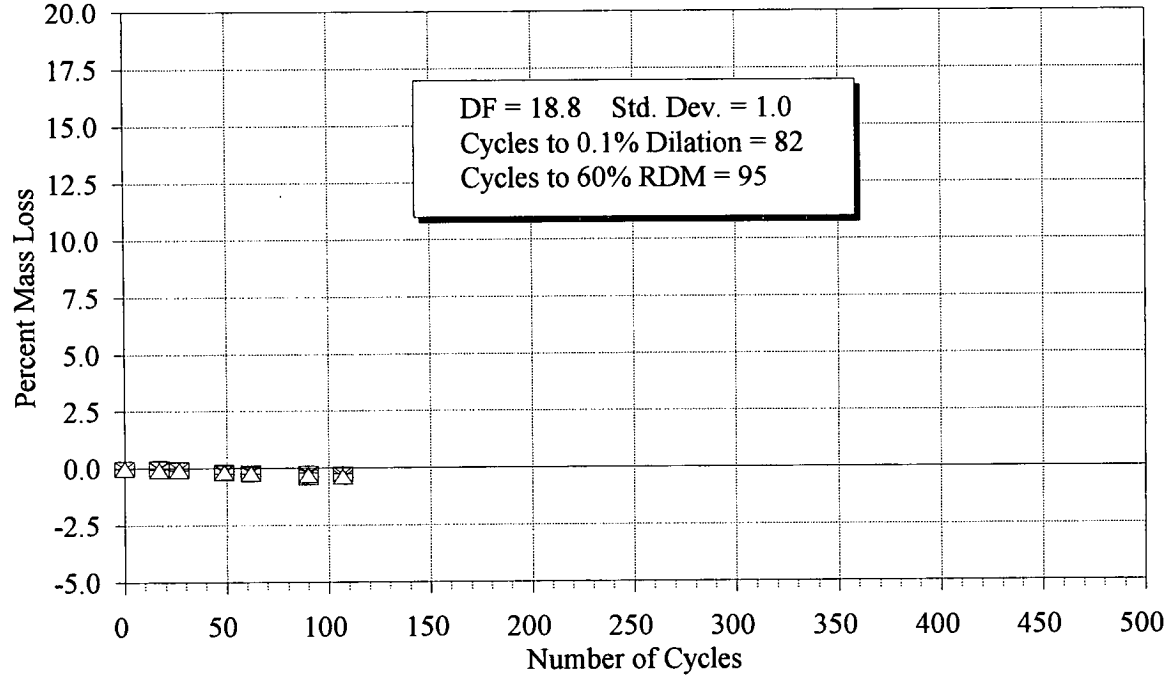

Rel Q Based on Transverse Frequency

Ohio Mixture I1 (FS mod) - 28-Day Cure

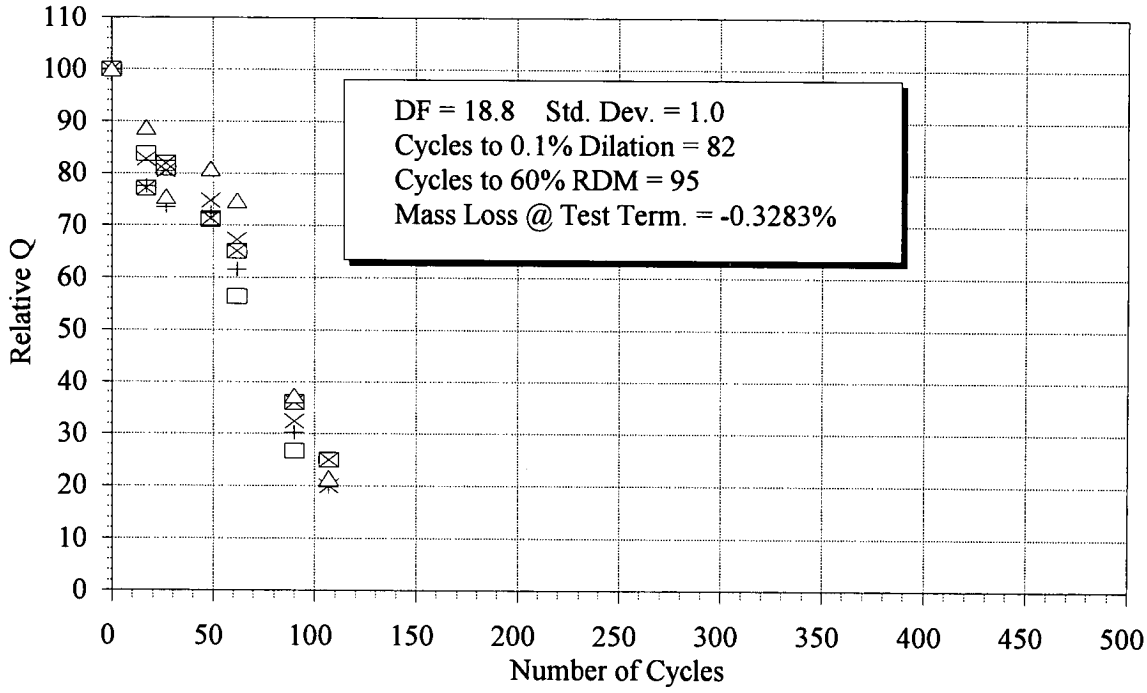

Relative Dynamic Modulus

Ohio Mixture I1 (FS mod) - 28-Day Cure

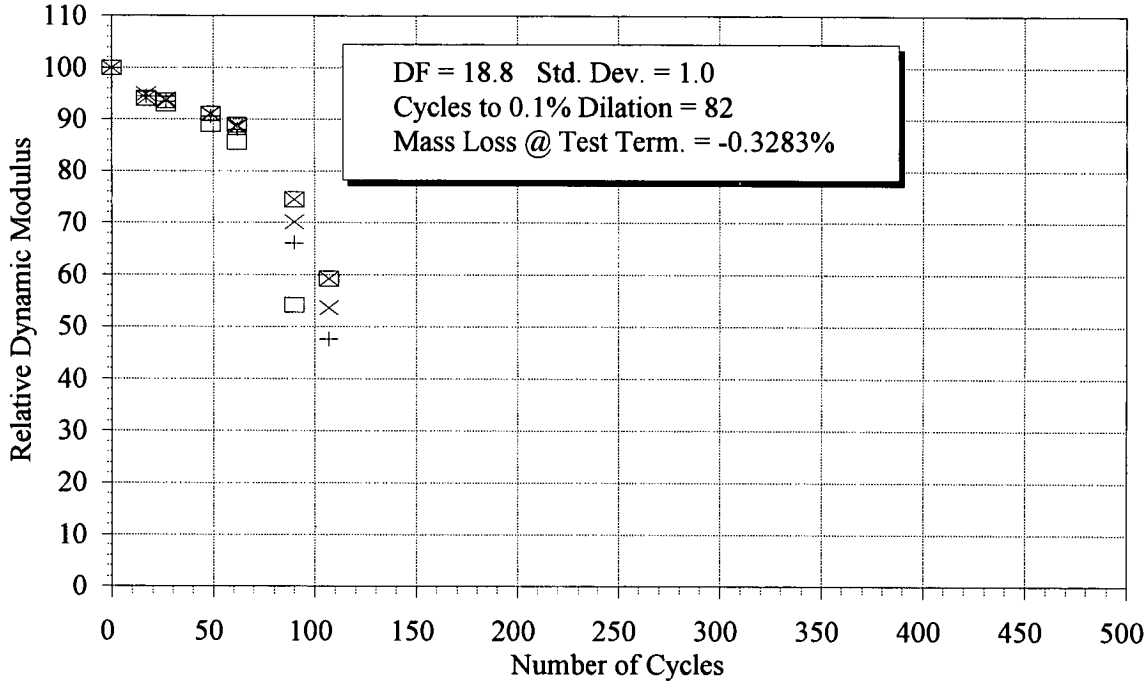

Dilation after Freezing and Thawing

Ohio Mixture I2 (FS mod) - 28-Day Cure

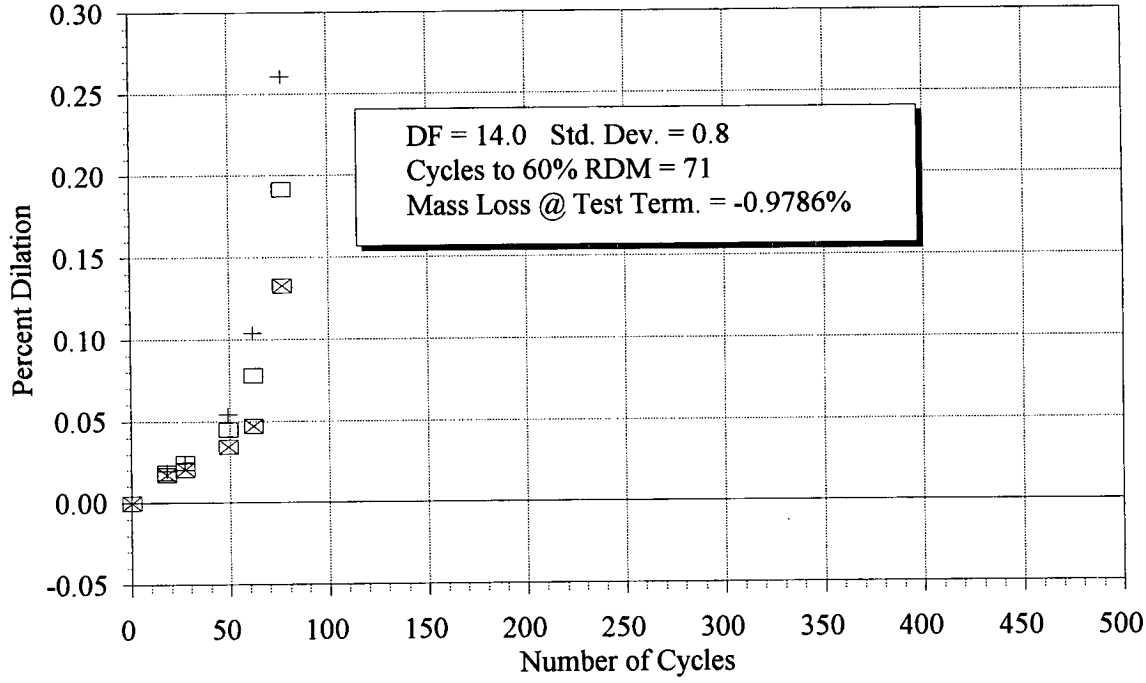

Mass Loss After Freezing and Thawing

Ohio Mixture I2 (FS mod) - 28-Day Cure

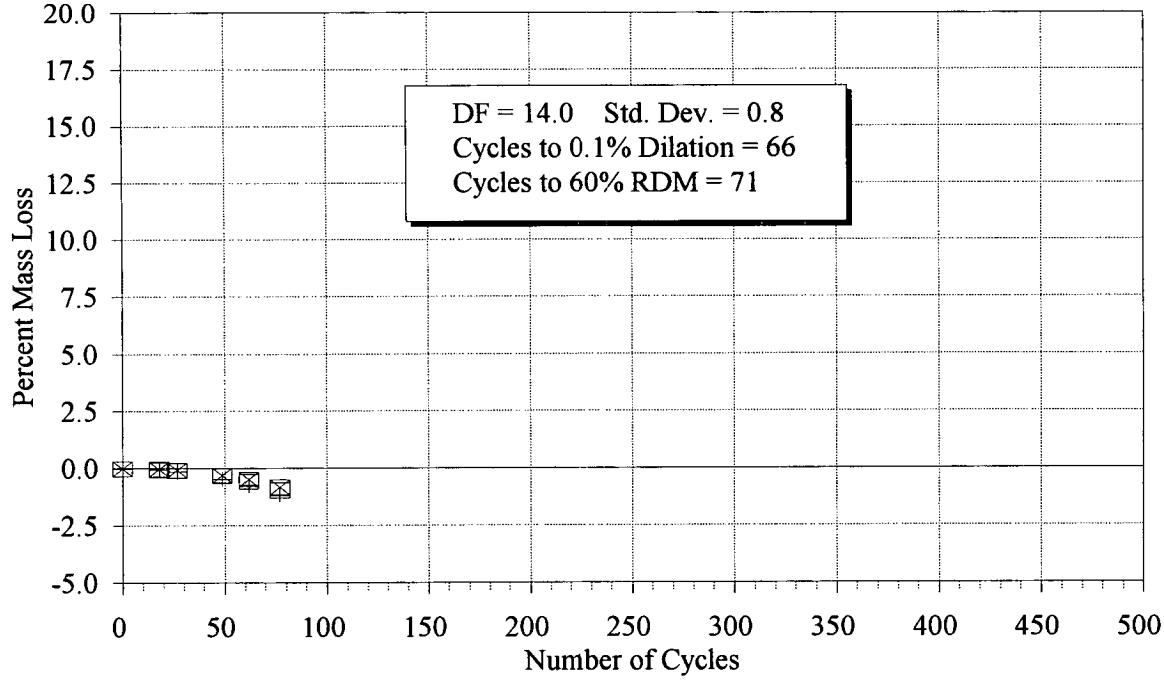

Rel Q Based onTransverse Frequency

Ohio Mixture I2 (FS mod) - 28-Day Cure

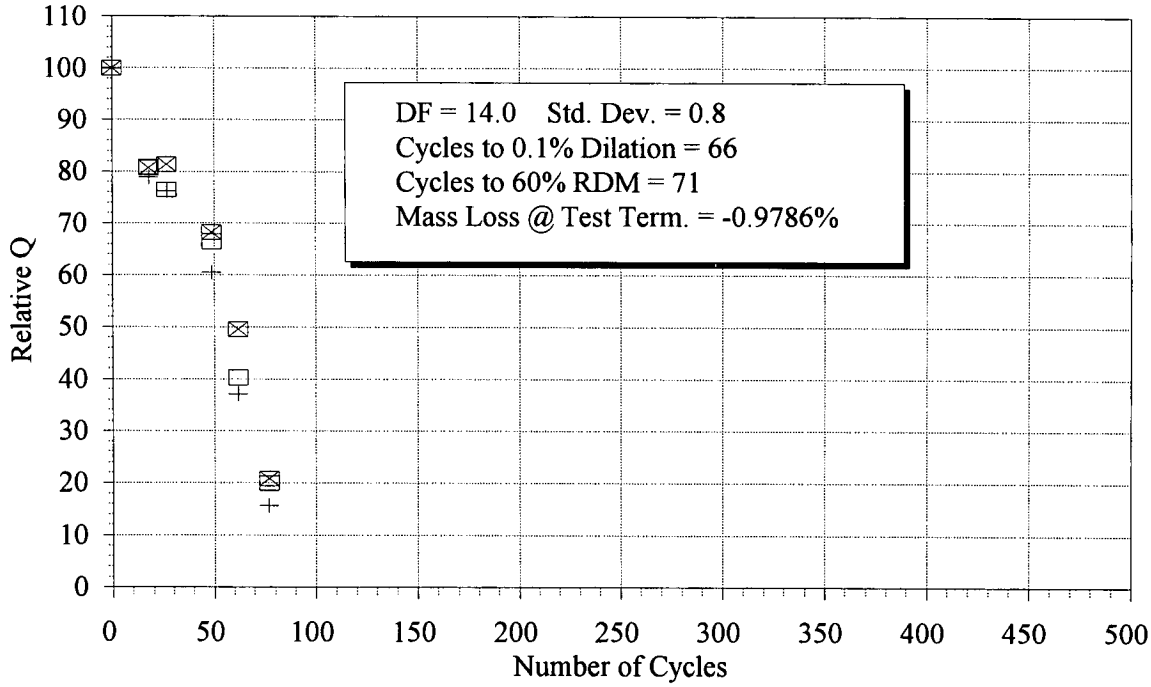

Relative Dynamic Modulus

Ohio Mixture I2 (FS mod) - 28-Day Cure

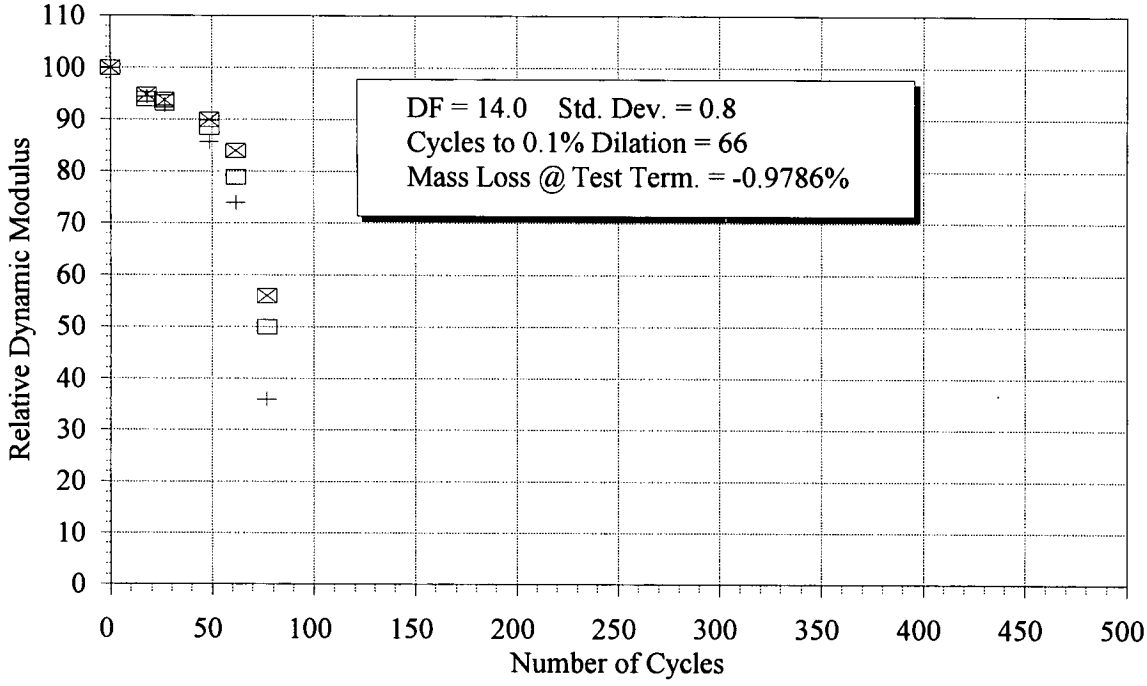

Dilation after Freezing and Thawing

Ohio Mixture I3 (FS mod) - 28-Day Cure

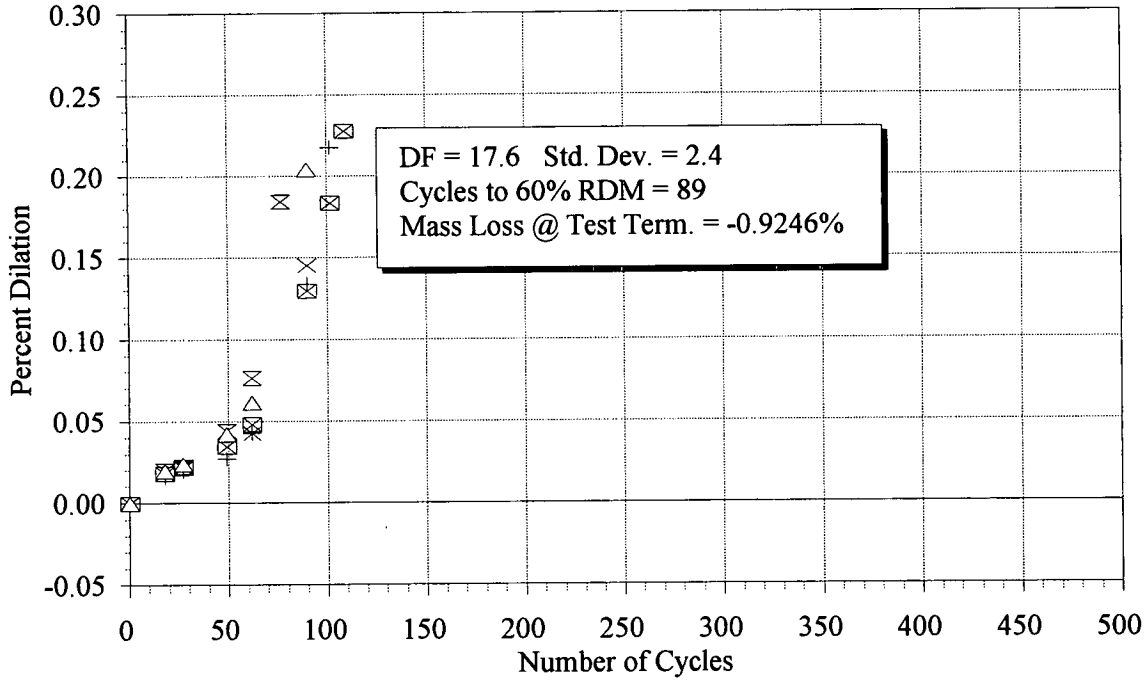

Mass Loss After Freezing and Thawing

Ohio Mixture I3 (FS mod) - 28-Day Cure

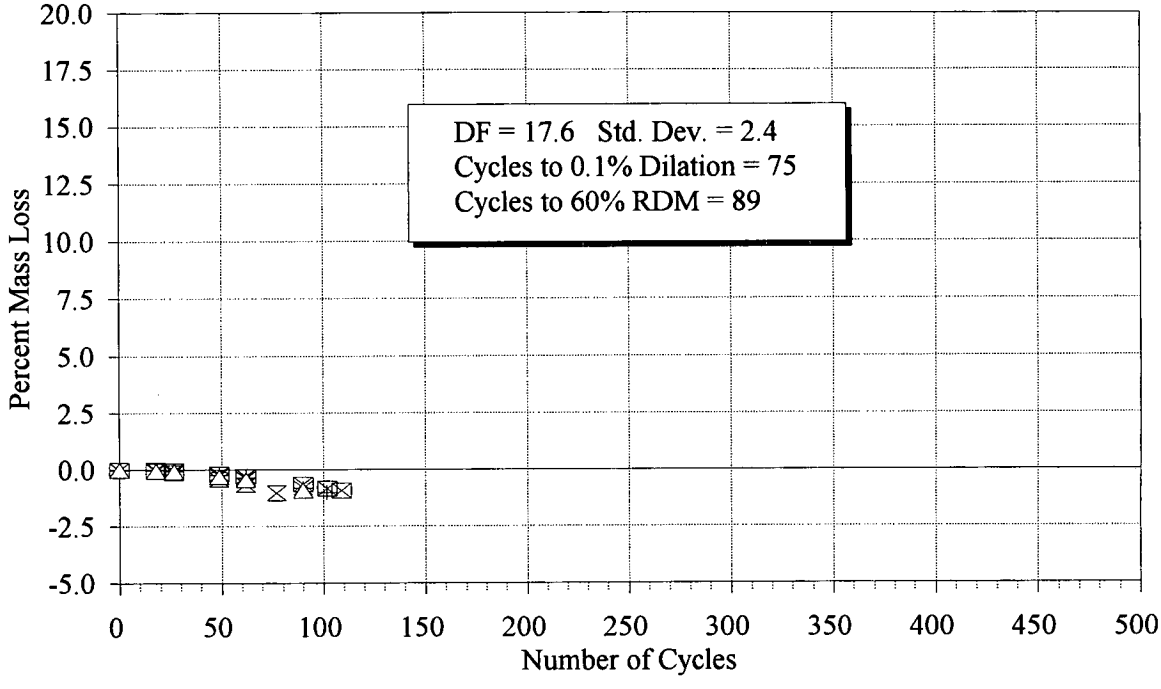

Rel Q Based on Transverse Frequency

Ohio Mixture I3 (FS mod) - 28-Day Cure

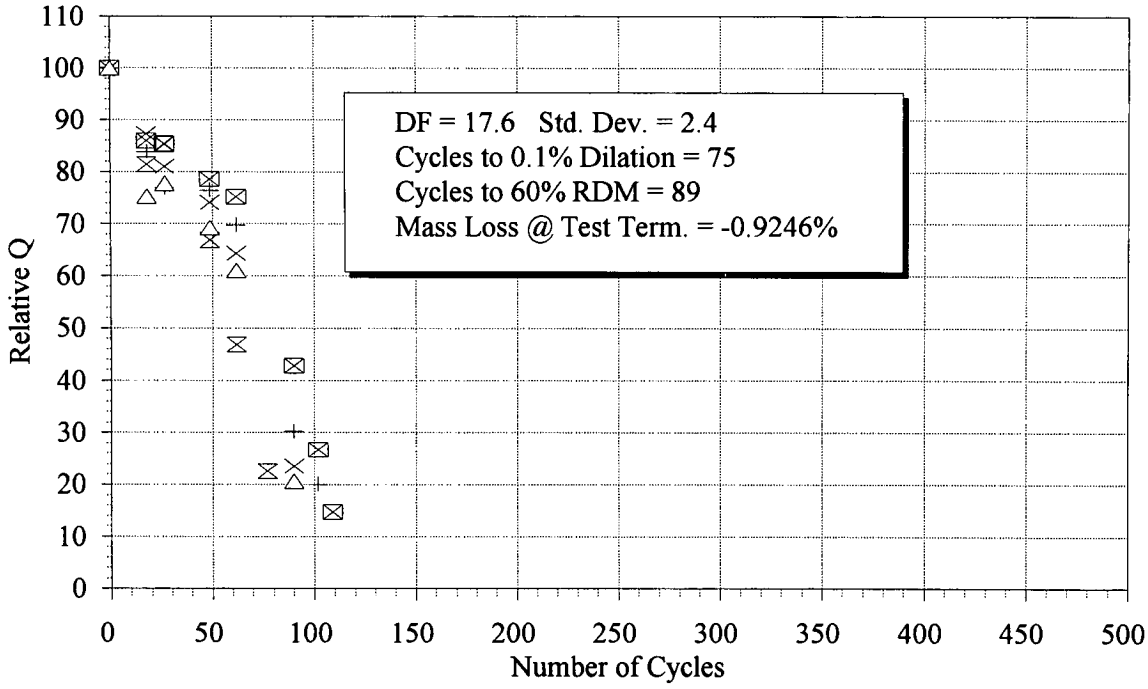

Relative Dynamic Modulus

Ohio Mixture I3 (FS) - 28-Day Cure

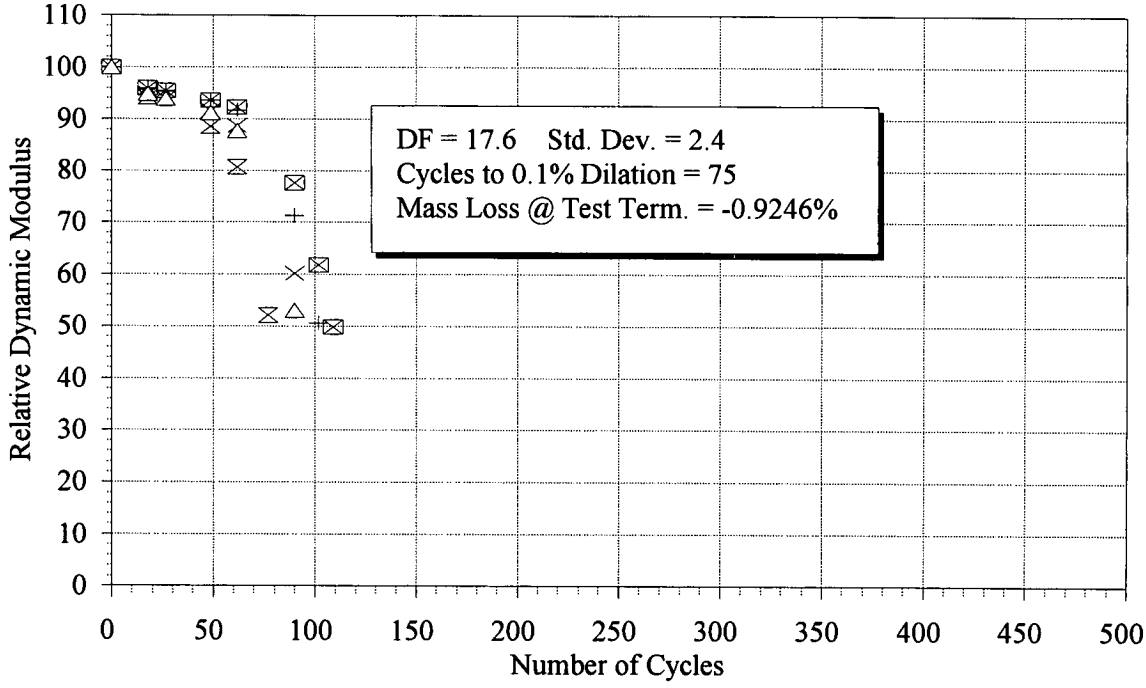

Dilation after Freezing and Thawing

Ohio Mixture I4 (FS mod) - 28-Day Cure

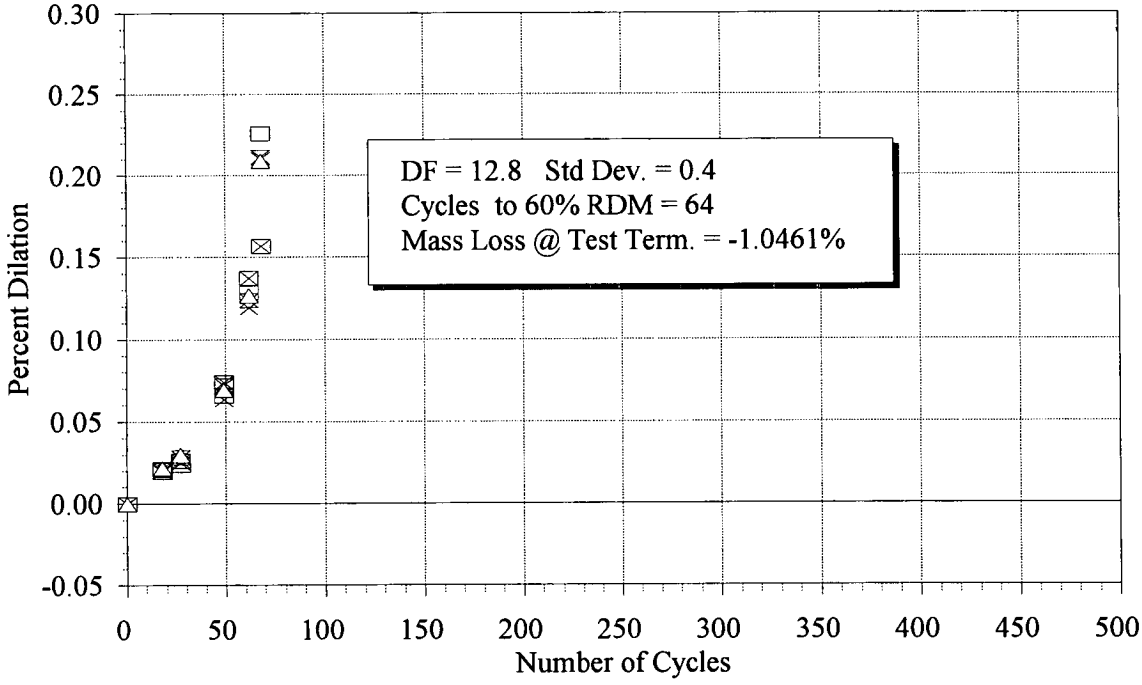

Mass Loss After Freezing and Thawing

Ohio Mixture I4 (FS mod) - 28-Day Cure

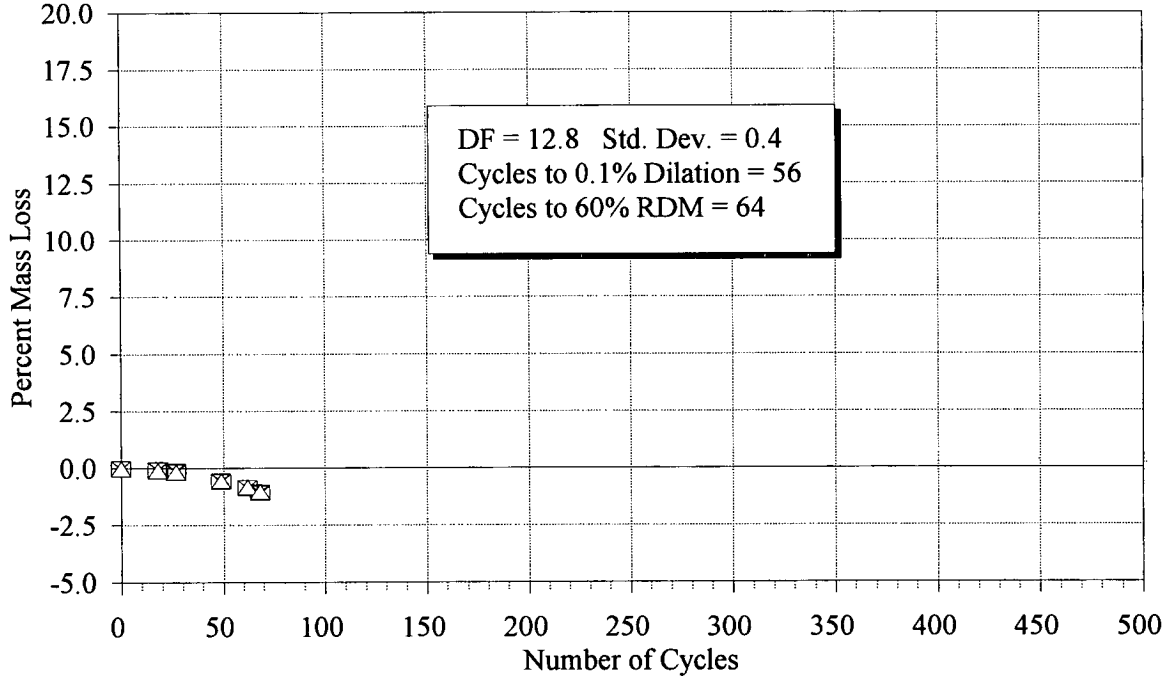

Rel Q Based on Transverse Frequency

Ohio Mixture I4 (FS mod) - 28-Day Cure

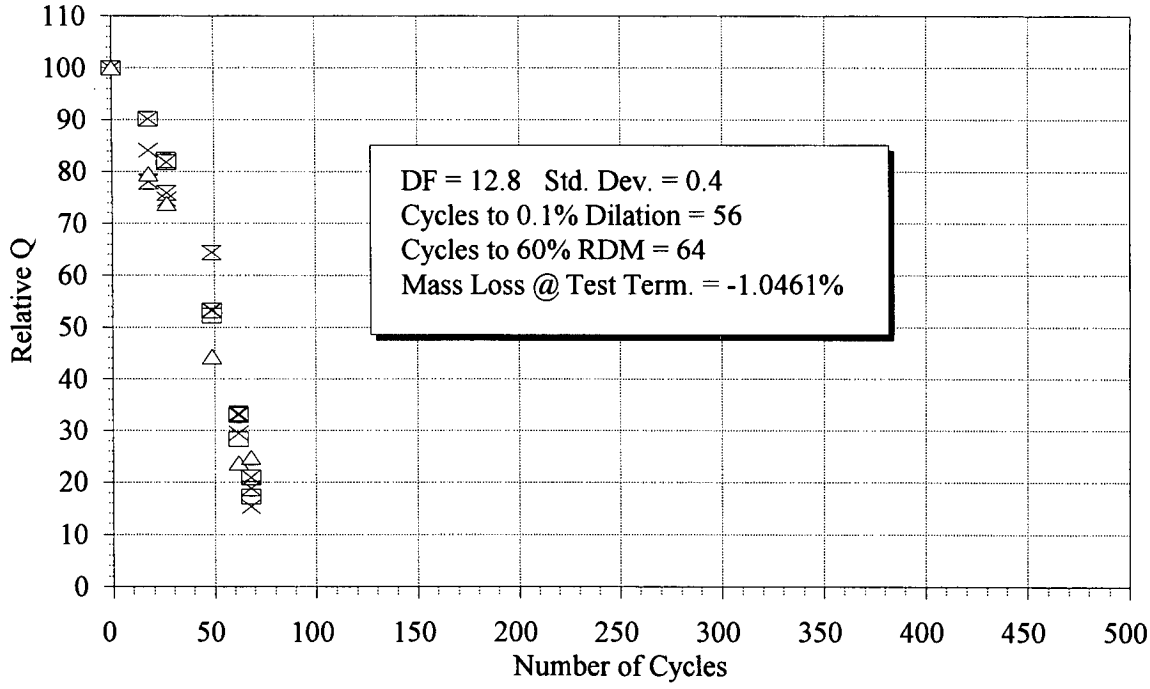

Relative Dynamic Modulus

Ohio Mixture I4 (FS mod) - 28-Day Cure

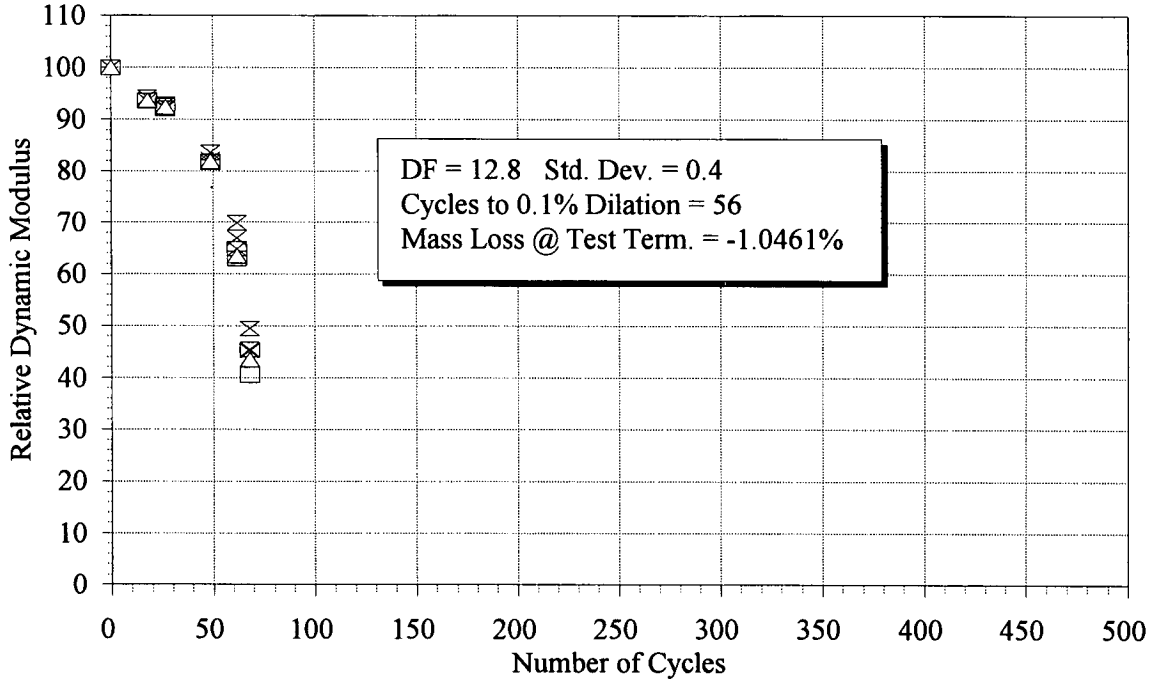

Dilation after Freezing and Thawing

Ohio Mixture I5 (FS mod) - 28-Day Cure

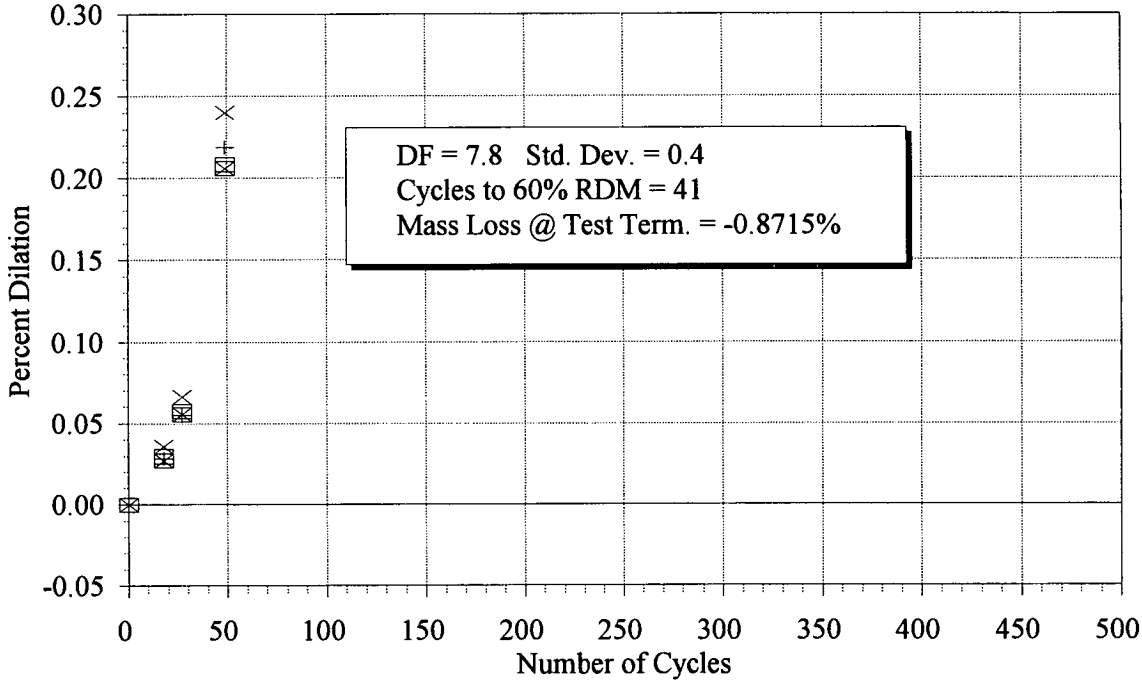

Mass Loss After Freezing and Thawing

Ohio Mixture I5 (FS mod) - 28-Day Cure

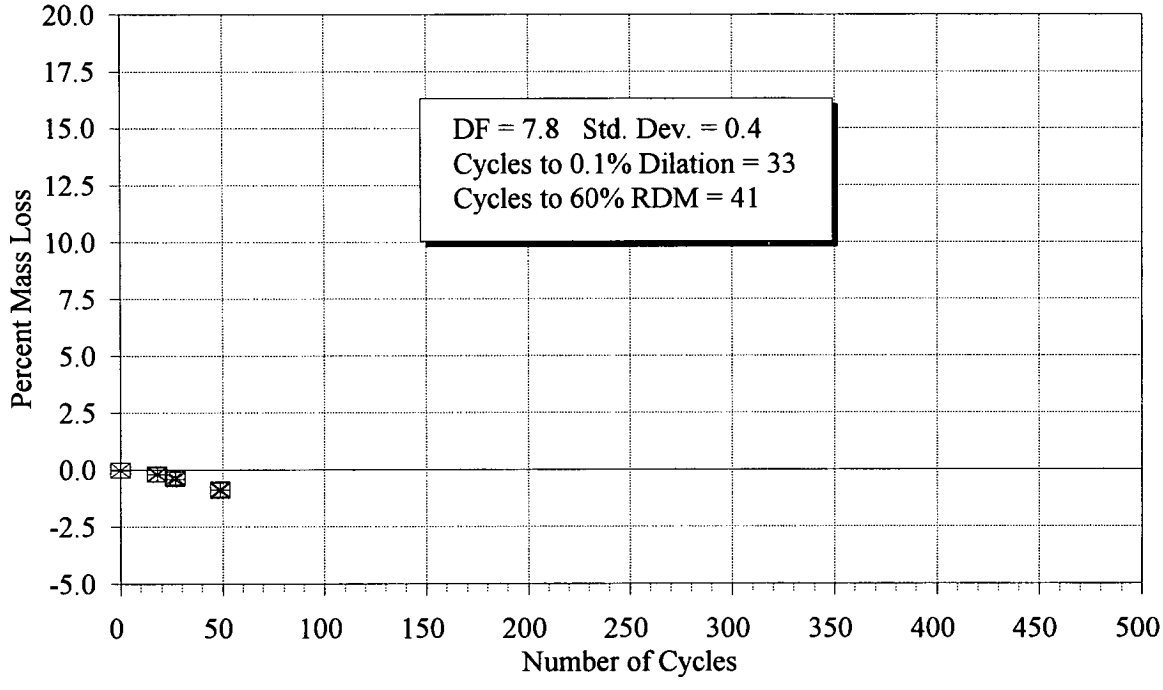

Rel Q Based on Transverse Frequency

Ohio Mixture I5 (FS mod) - 28-Day Cure

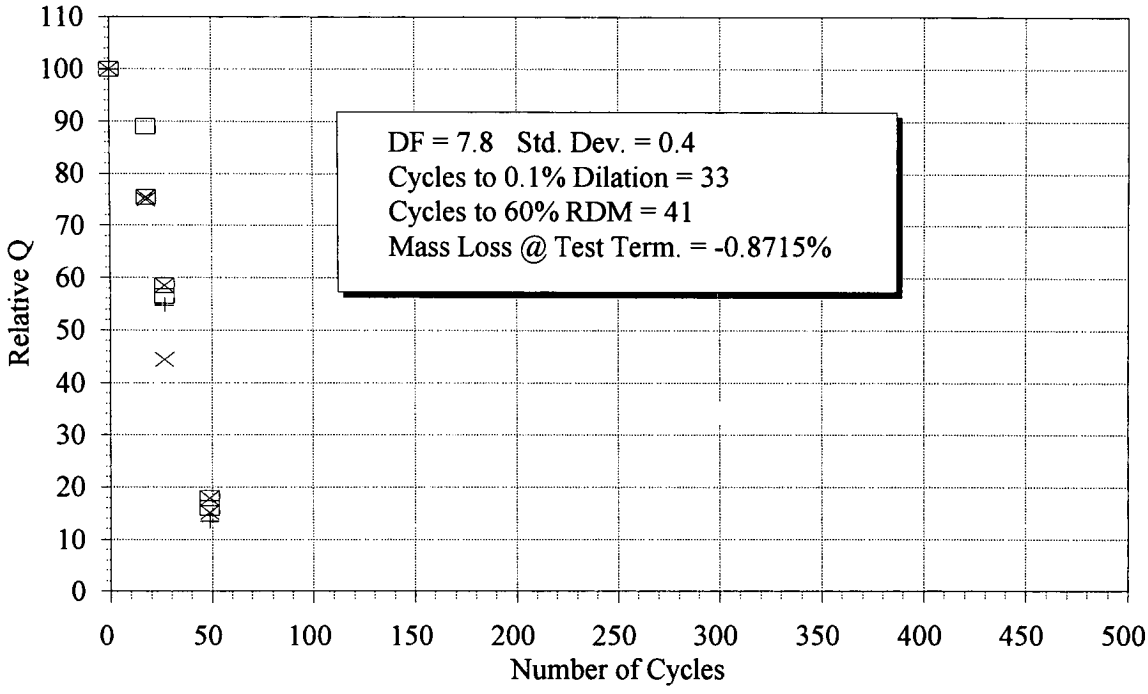

Relative Dynamic Modulus

Ohio Mixture I5 (FS mod) - 28-Day Cure

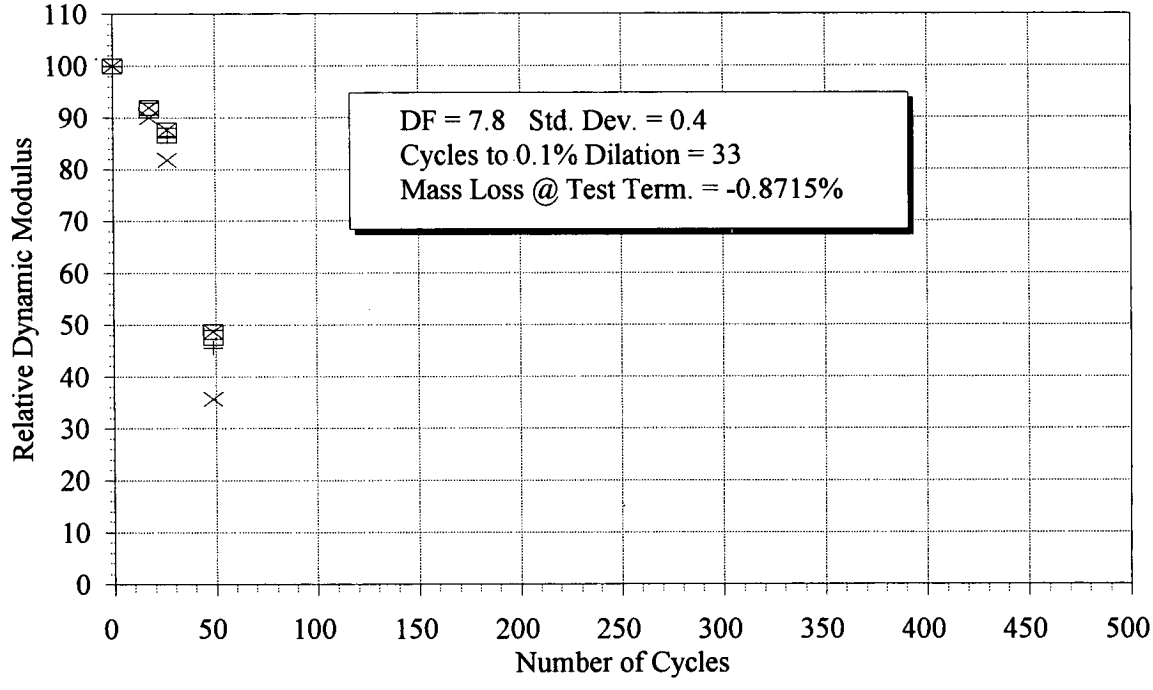

Appendix B
Freezing and Thawing Test Histories for Minnesota Test Mixtures

NOTE: Unless noted otherwise, each series of symbols in the following charts represents the results of tests performed on a single specimen prepared from the same batch of concrete as all other specimens in the same chart. For example, squares might represent data from specimen No. 1 of mixture X, triangles might represent data from specimen No. 2 of mixture X, etc.

Mass Loss After Freezing and Thawing

Mixture MN1 - 28-Day Cure

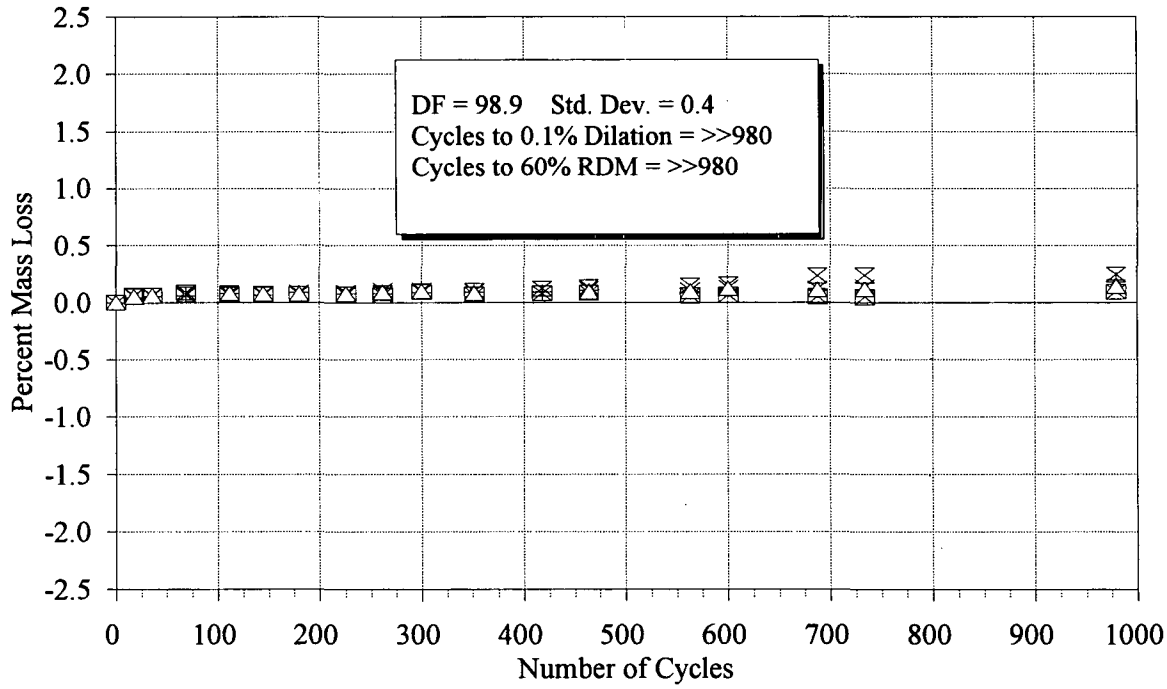

Dilation after Freezing and Thawing

Mixture MN1 - 28-Day Cure

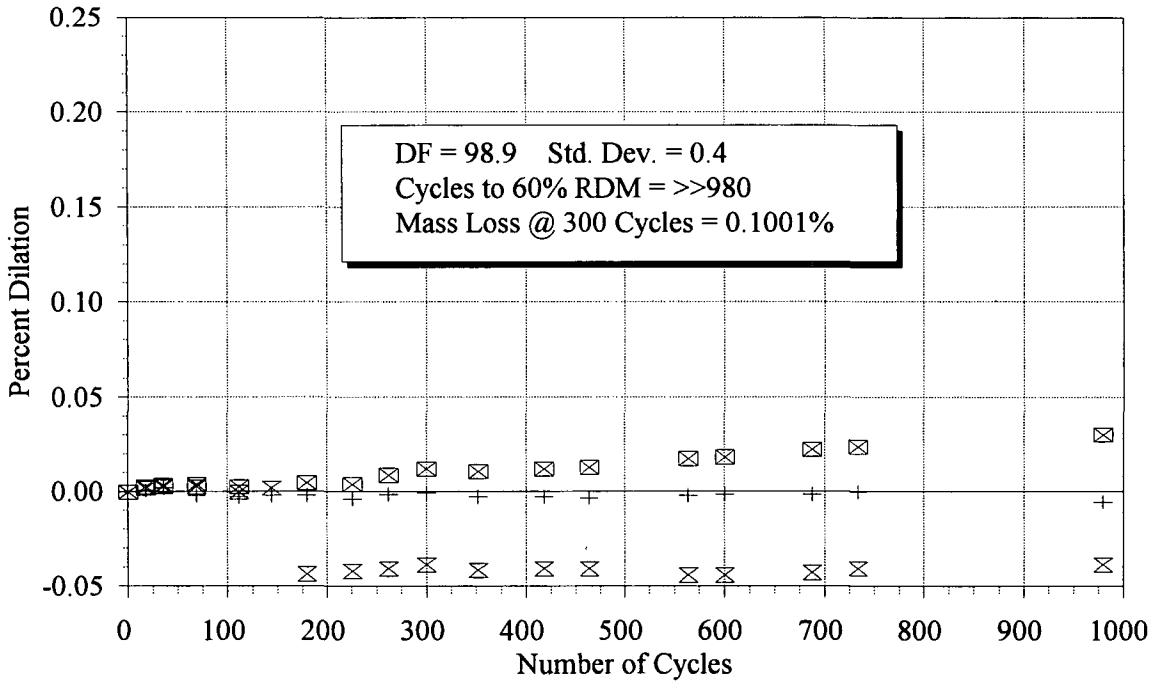

Rel Q Based on Transverse Frequency

Mixture MN1 - 28-Day Cure

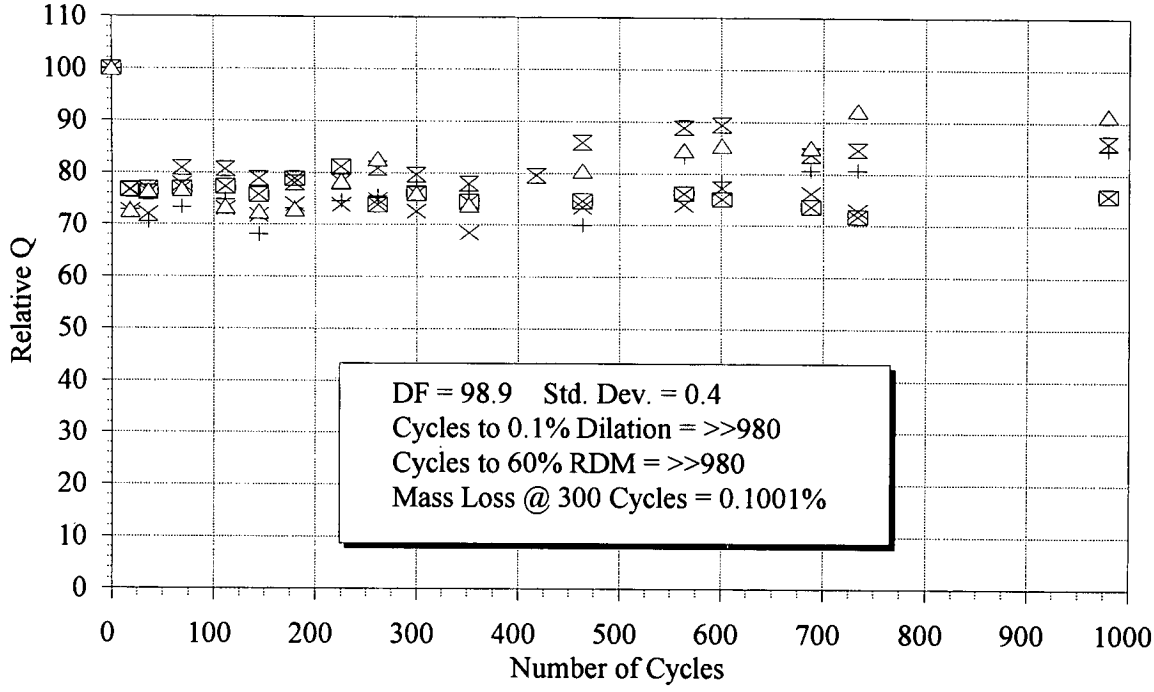

Relative Dynamic Modulus

Mixture MN1 - 28-Day Cure

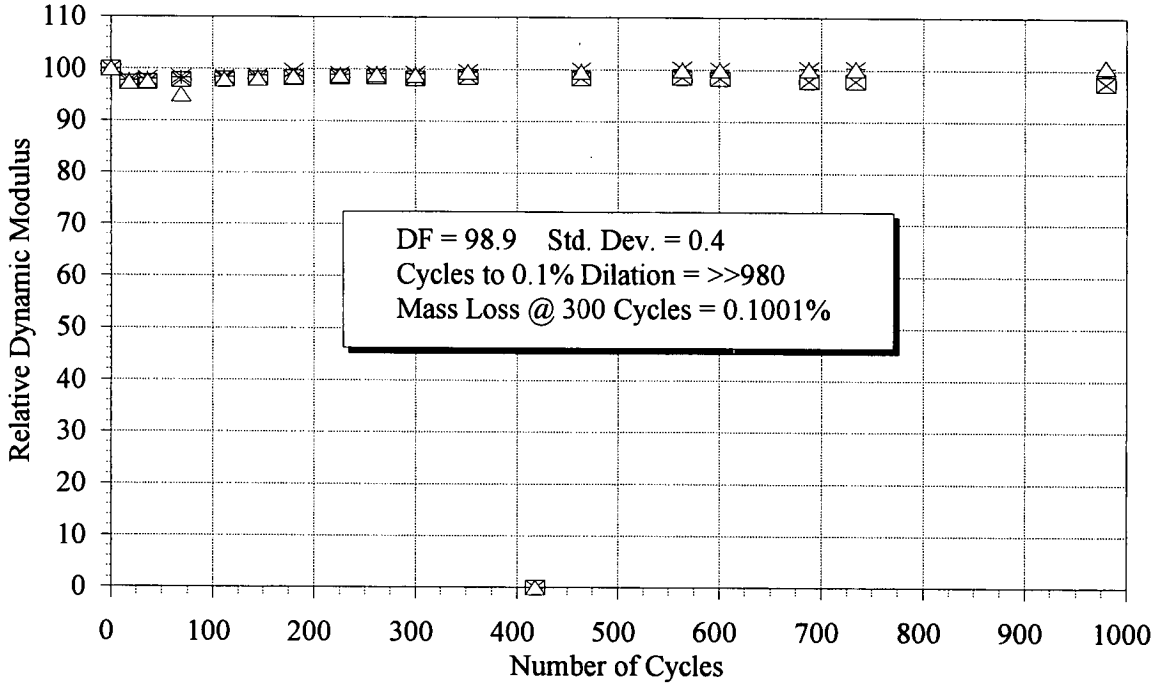

Dilation after Freezing and Thawing

Mixture MN2 - 28-Day Cure

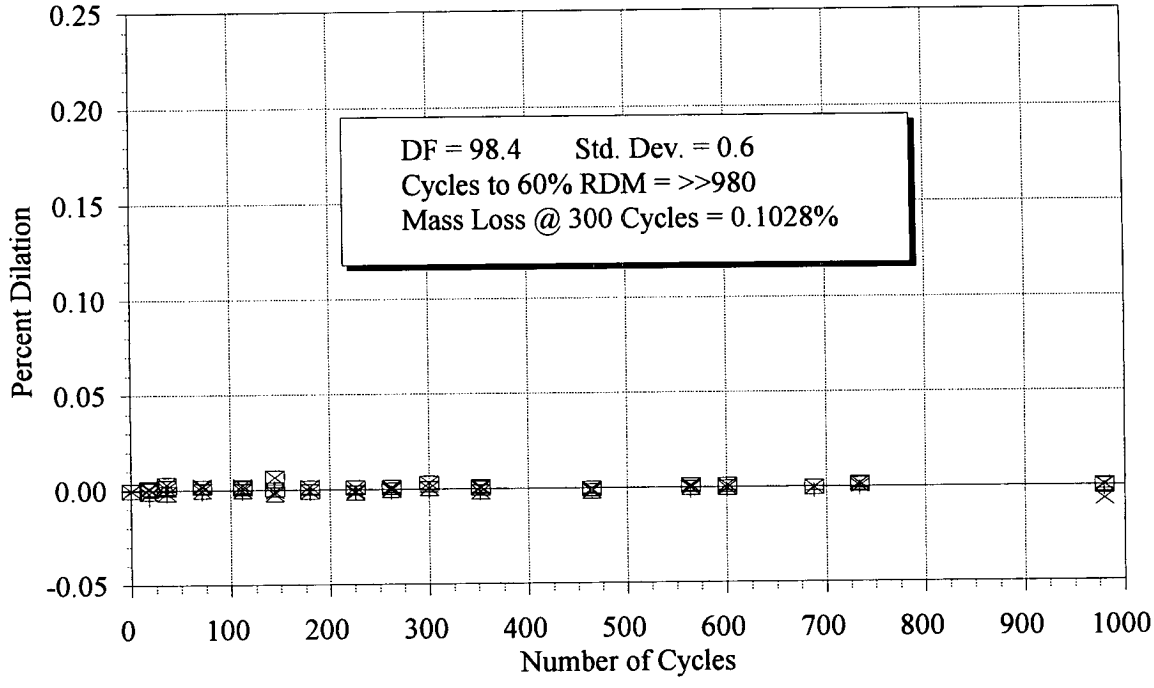

Mass Loss After Freezing and Thawing

Mixture MN2 - 28-Day Cure

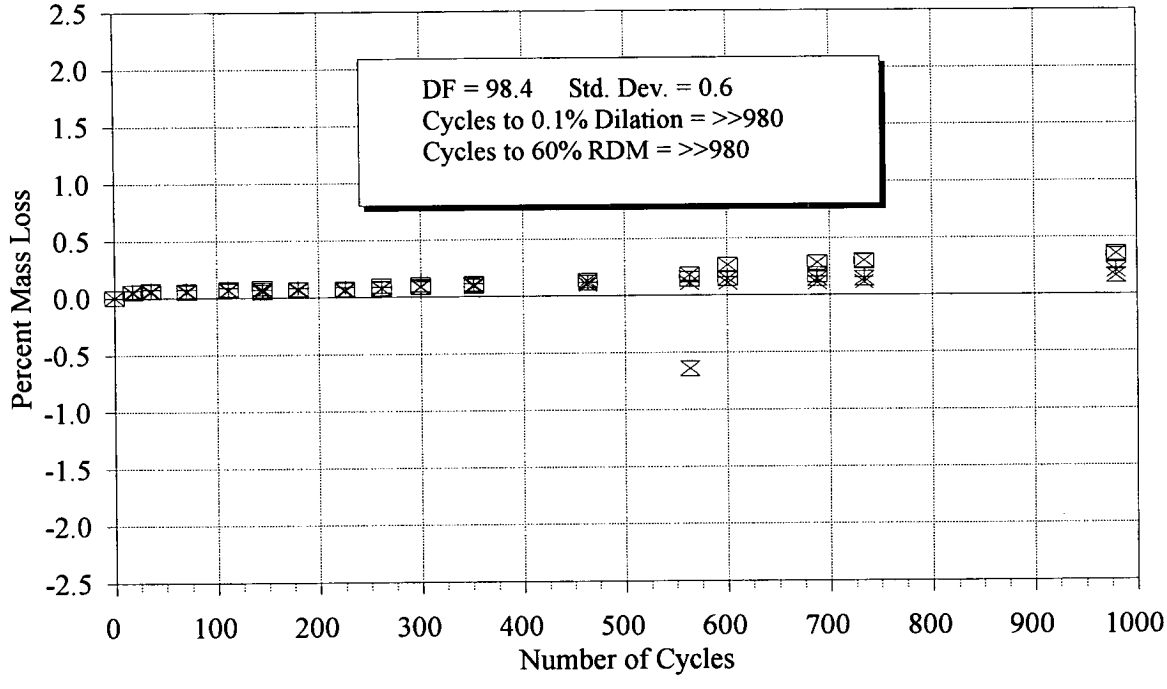

Rel Q Based on Transverse Frequency

Mixture MN2 - 28-Day Cure

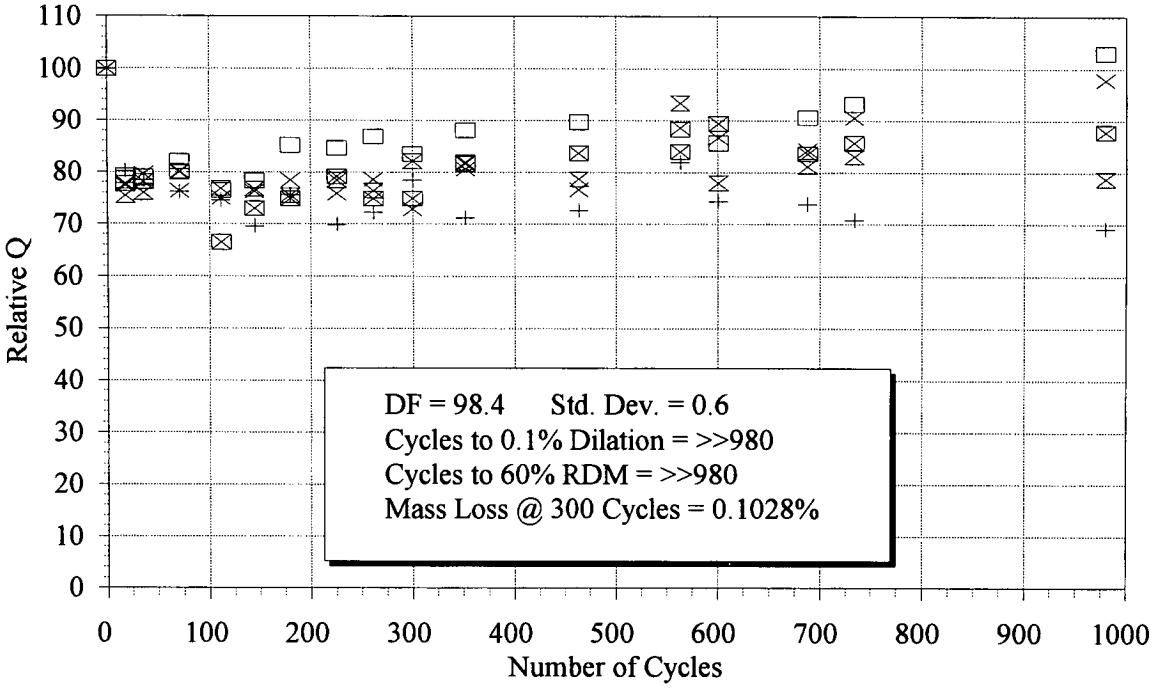

Relative Dynamic Modulus

Mixture MN2 - 28-Day Cure

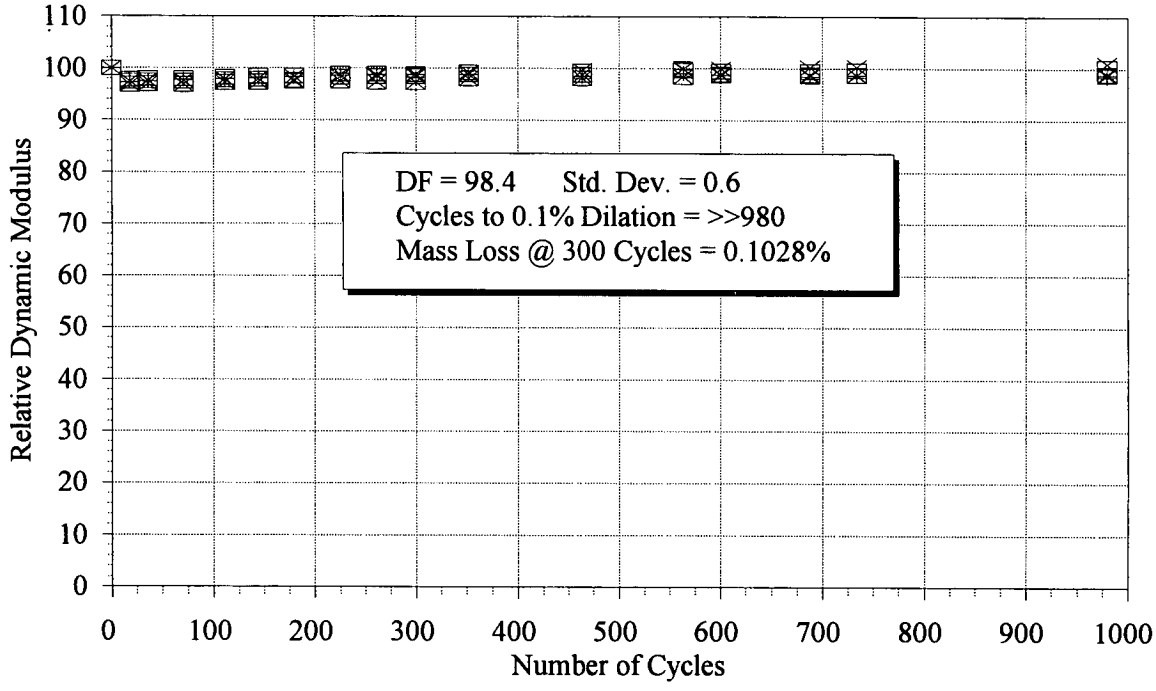

Dilation after Freezing and Thawing

Mixture MN3 - 28-Day Cure

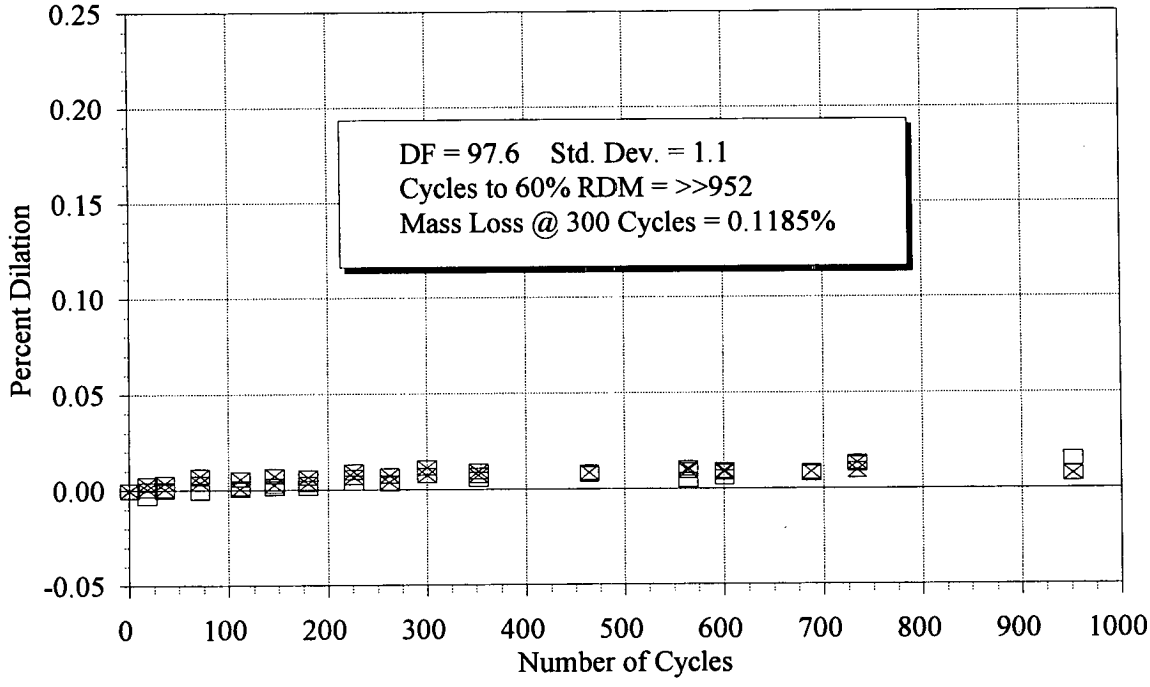

Mass Loss After Freezing and Thawing

Mixture MN3 - 28-Day Cure

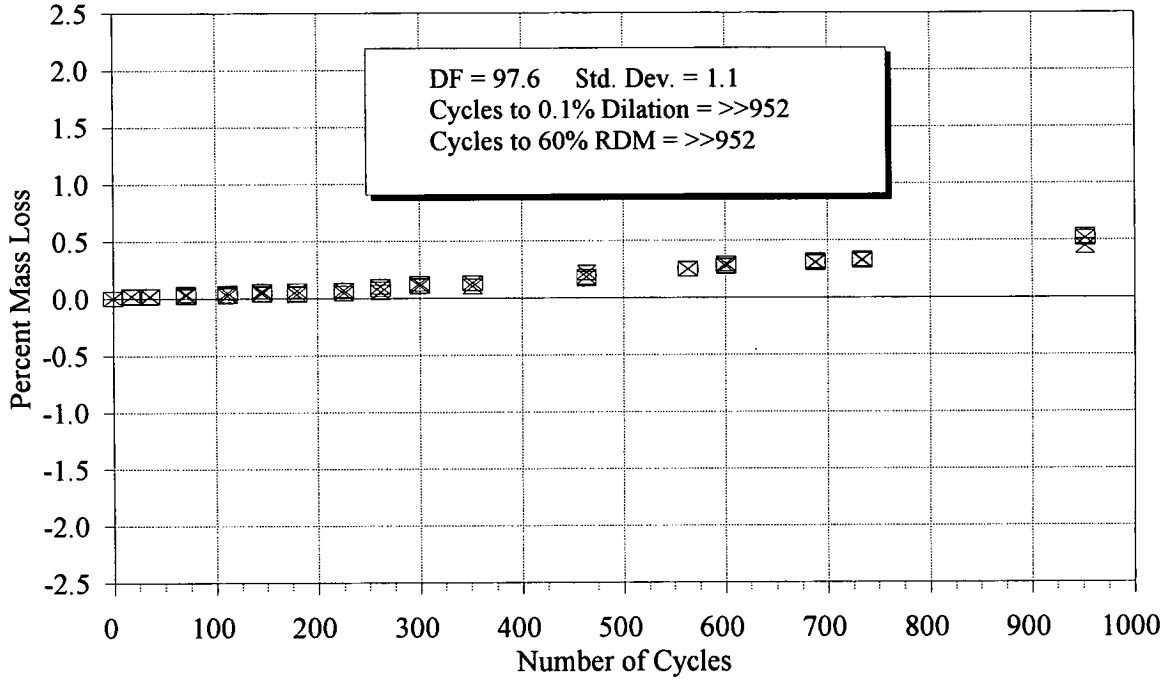

Rel Q Based on Transverse Frequency

Mixture MN3 - 28-Day Cure

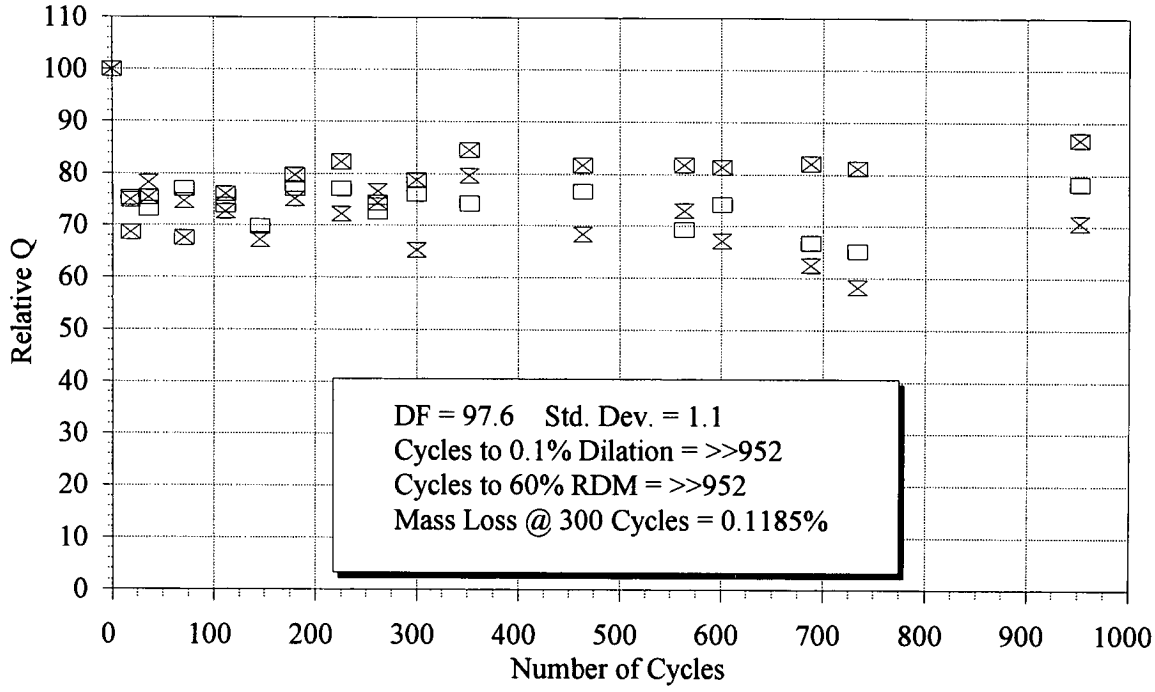

Relative Dynamic Modulus

Mixture MN3 - 28-Day Cure

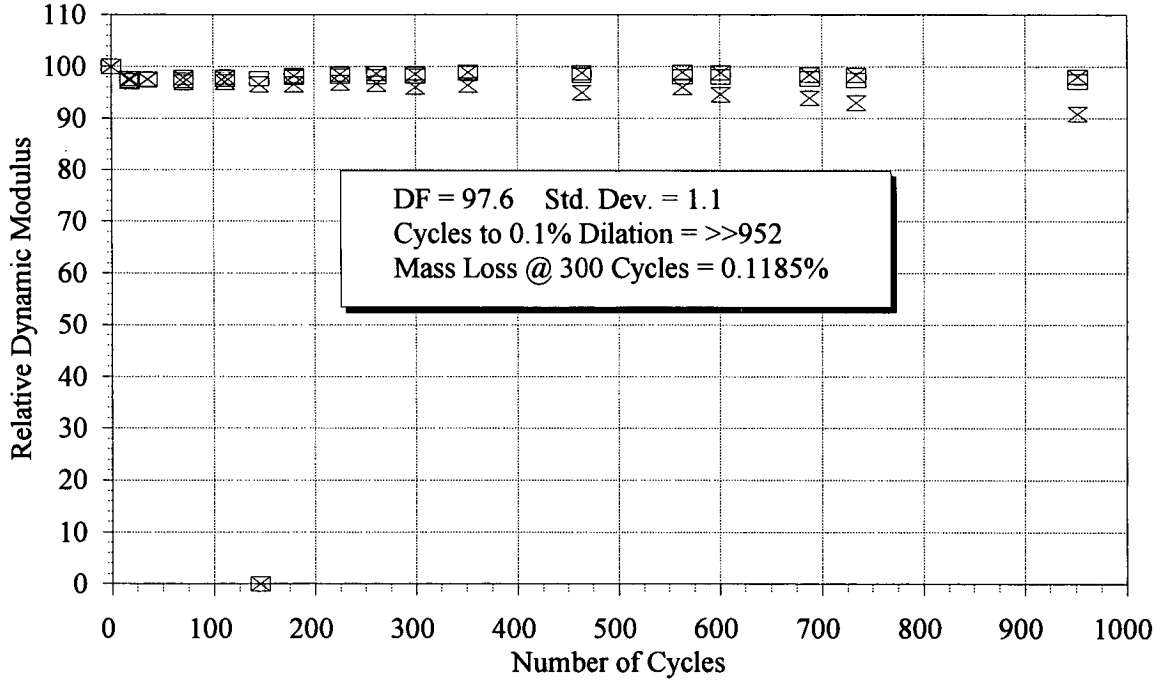

Dilation after Freezing and Thawing

Mixture MN4 - 28-Day Cure

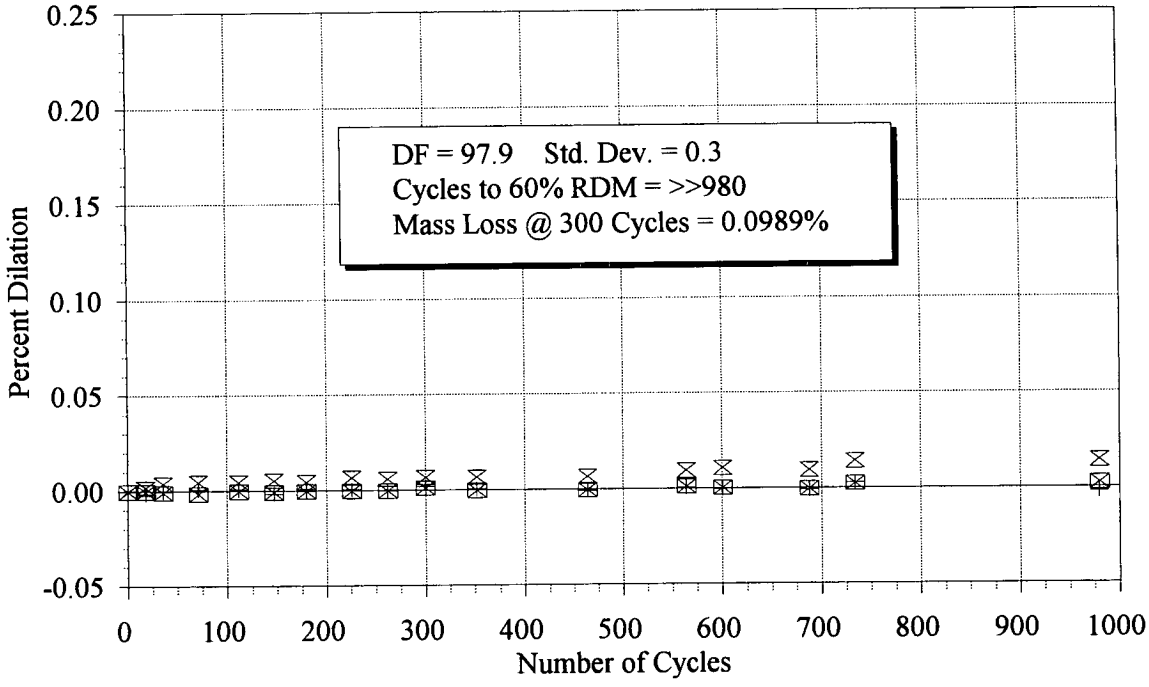

Mass Loss After Freezing and Thawing

Mixture MN4 - 28-Day Cure

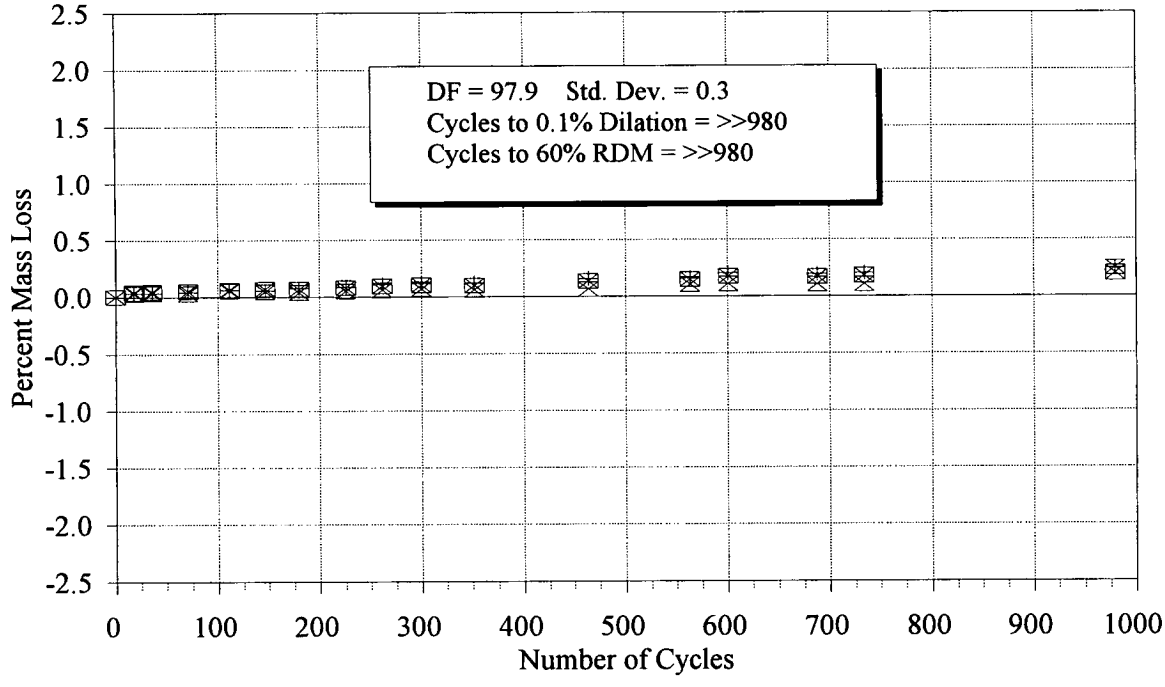

Rel Q Based on Transverse Frequency

Mixture MN4 - 28-Day Cure

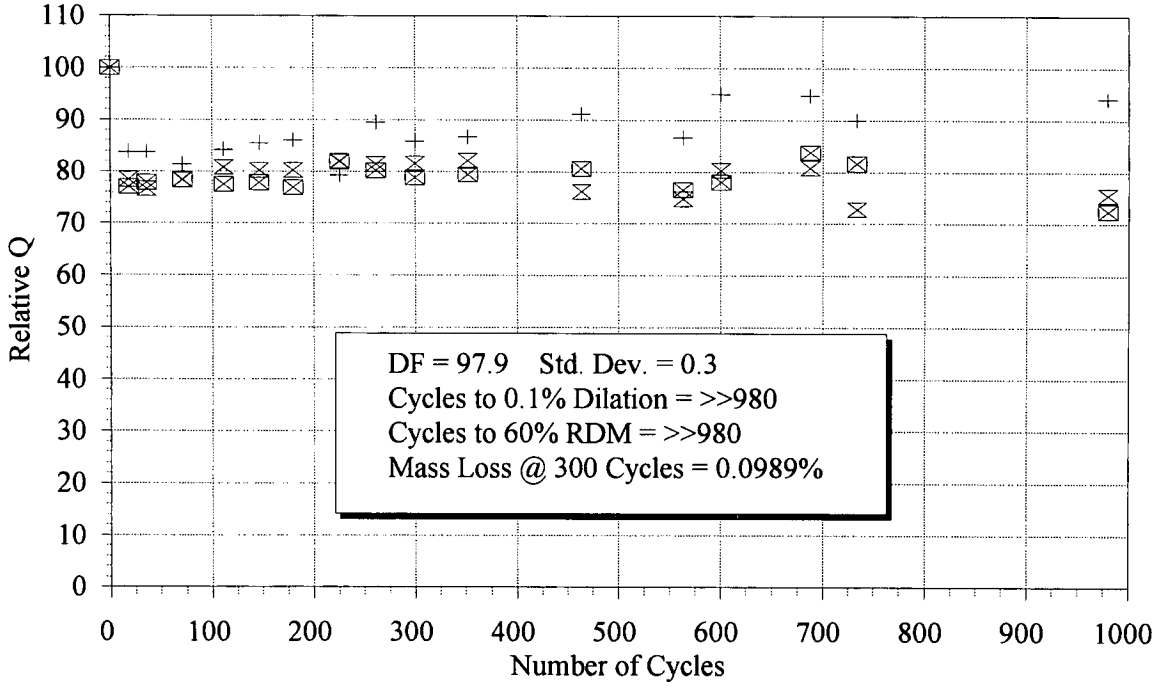

Relative Dynamic Modulus

Mixture MN4 - 28 Day Cure

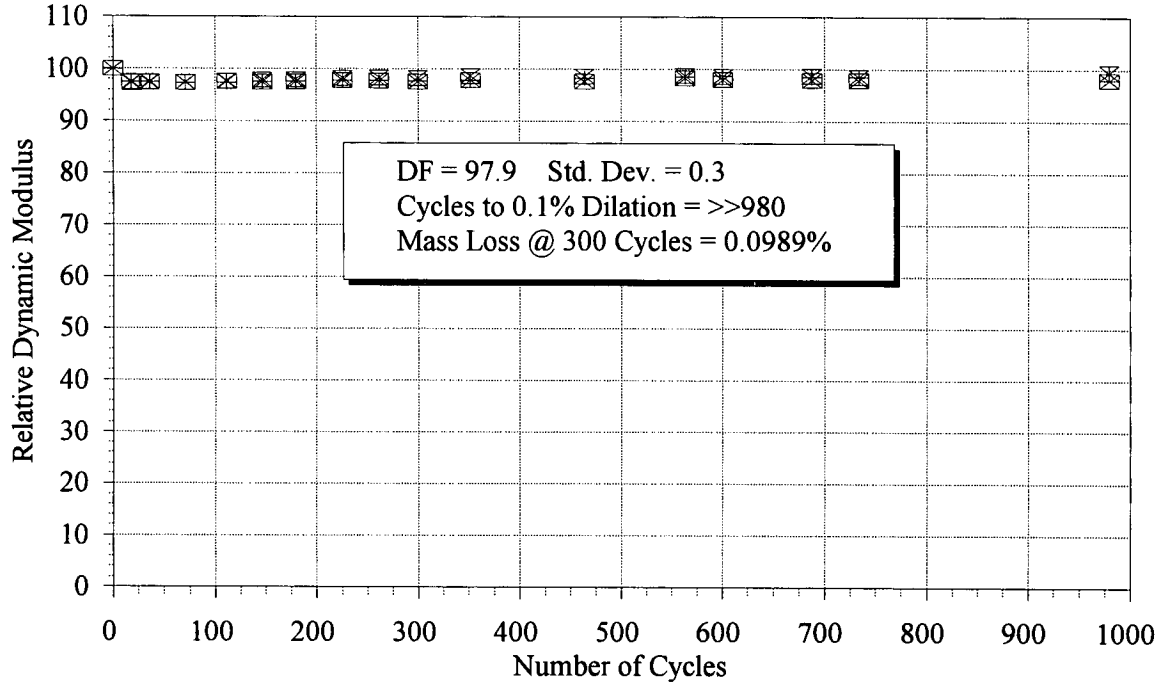

Dilation after Freezing and Thawing

Mixture MN5 - 28-Day Cure

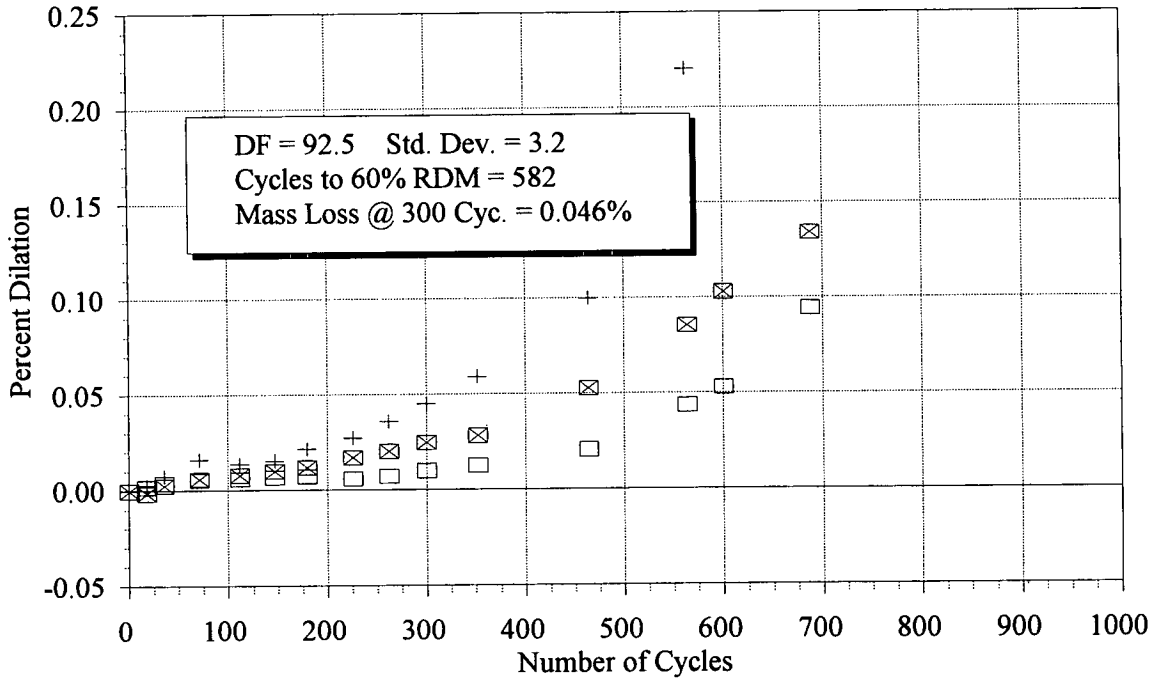

Mass Loss After Freezing and Thawing

Mixture MN5 - 28-Day Cure

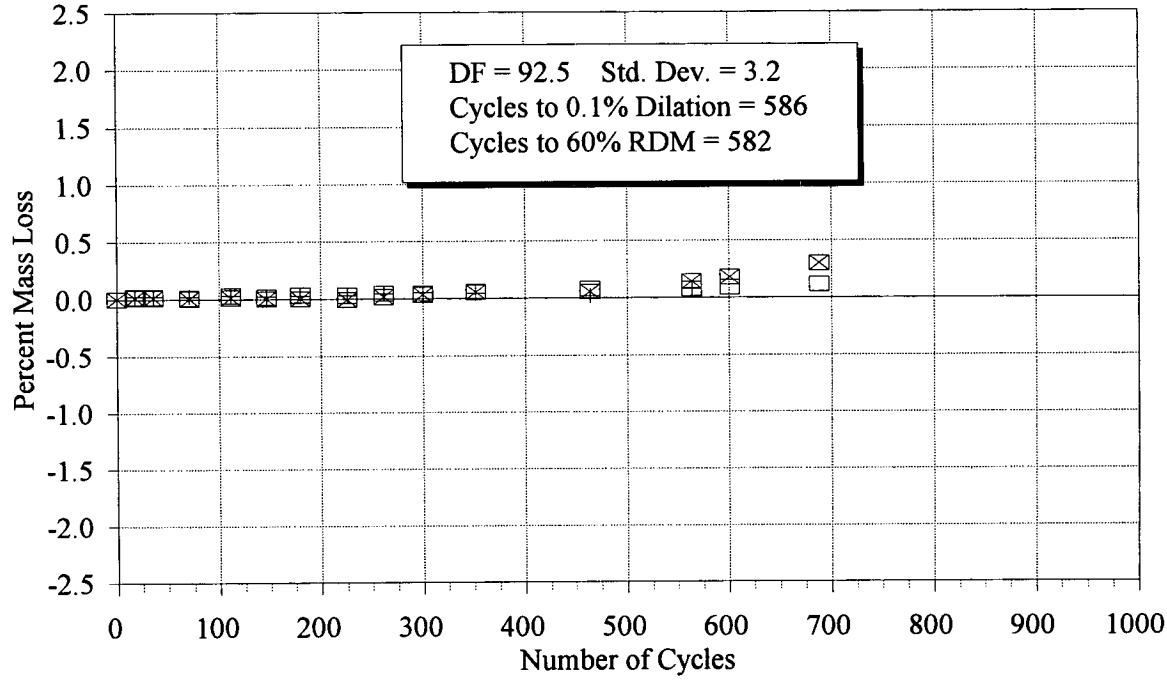

Rel Q Based on Transverse Frequency

Mixture MN5 - 28-Day Cure

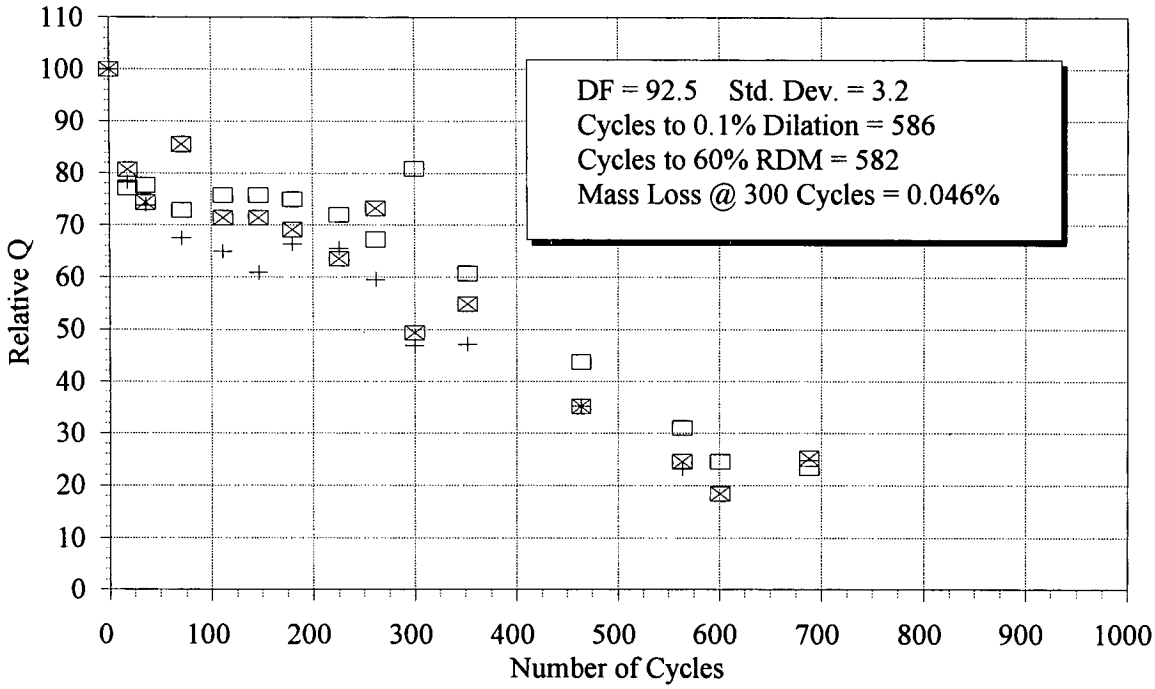

Relative Dynamic Modulus

Mixture MN5 - 28-Day Cure

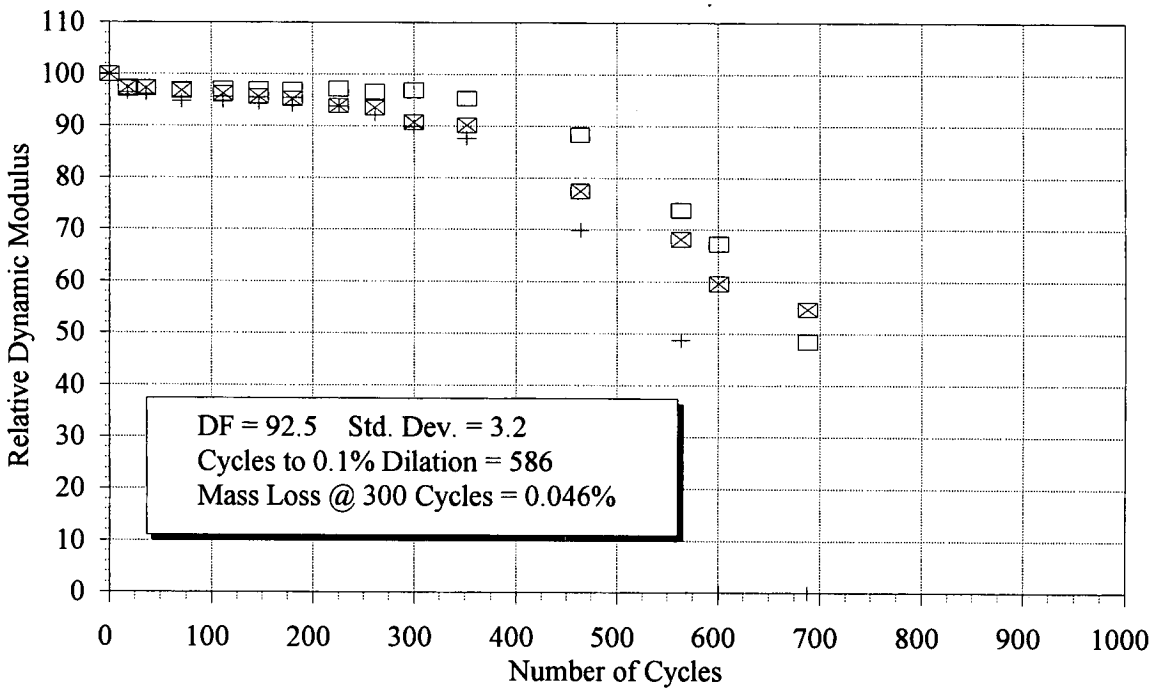

Dilation after Freezing and Thawing

Mixture MN6 - 28-Day Cure

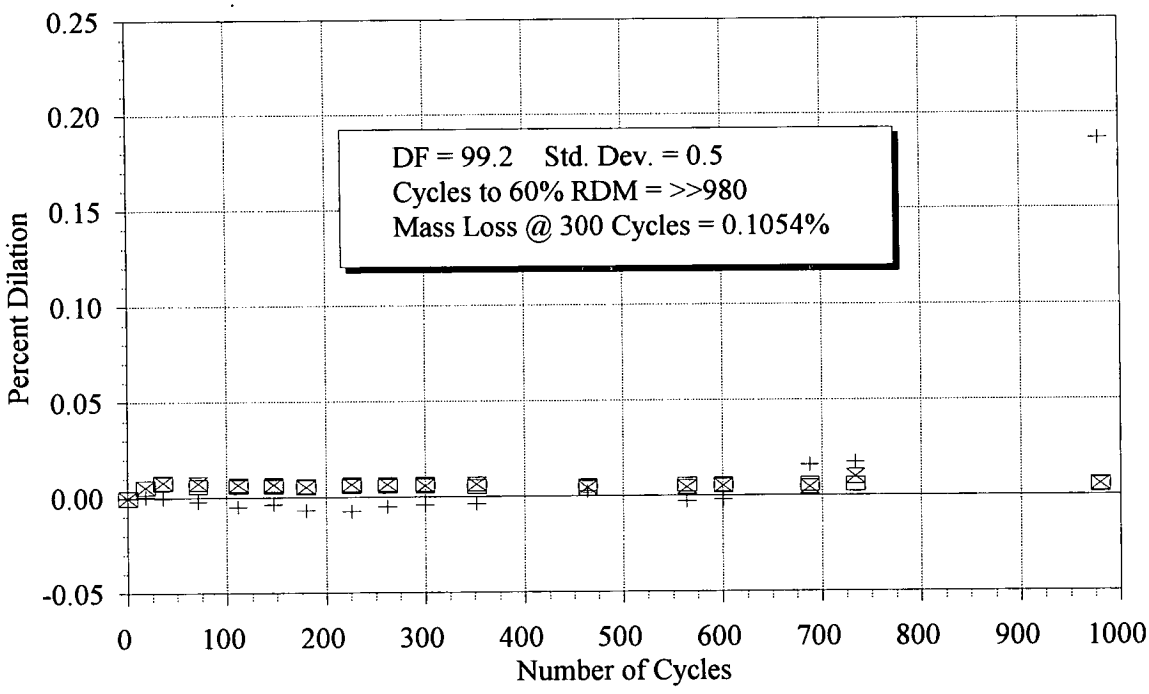

Mass Loss After Freezing and Thawing

Mixture MN6 - 28-Day Cure

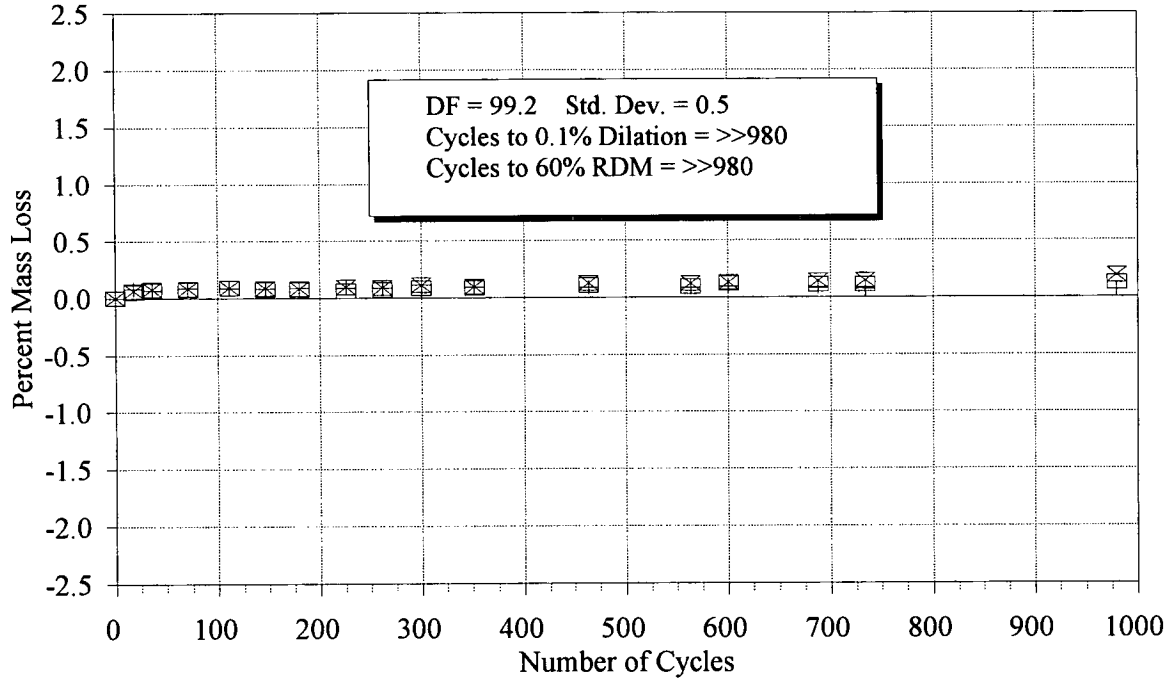

Rel Q Based on Transverse Frequency

Mixture MN6 - 28-Day Cure

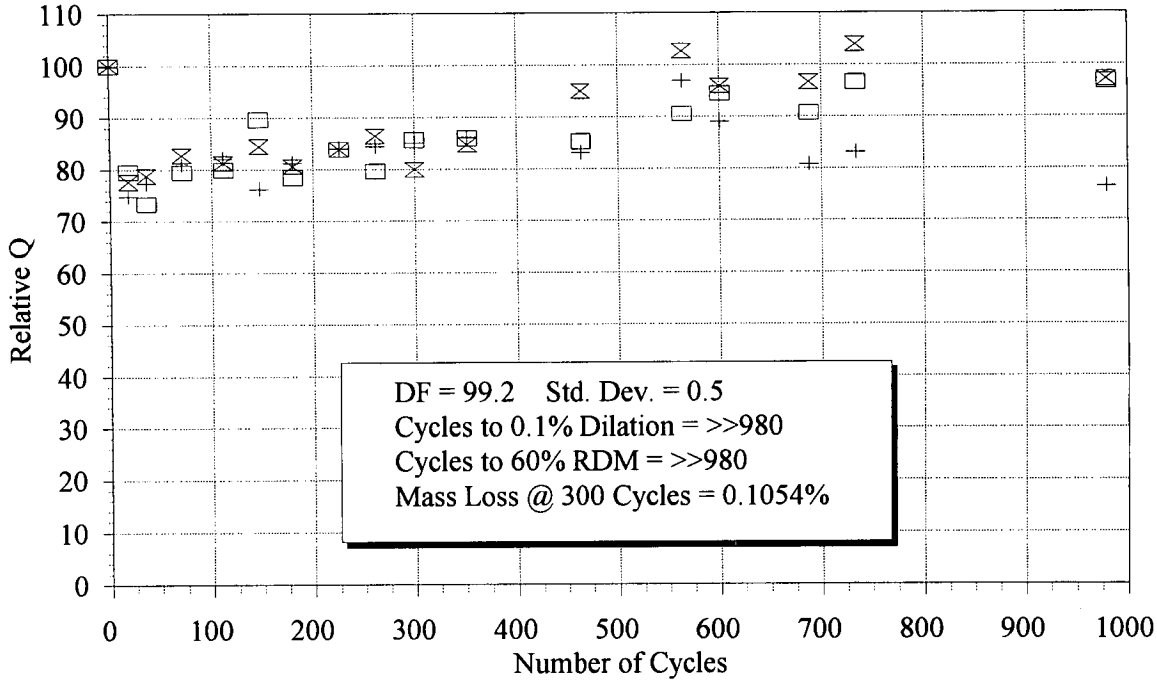

Relative Dynamic Modulus

Mixture MN6 - 28-Day Cure

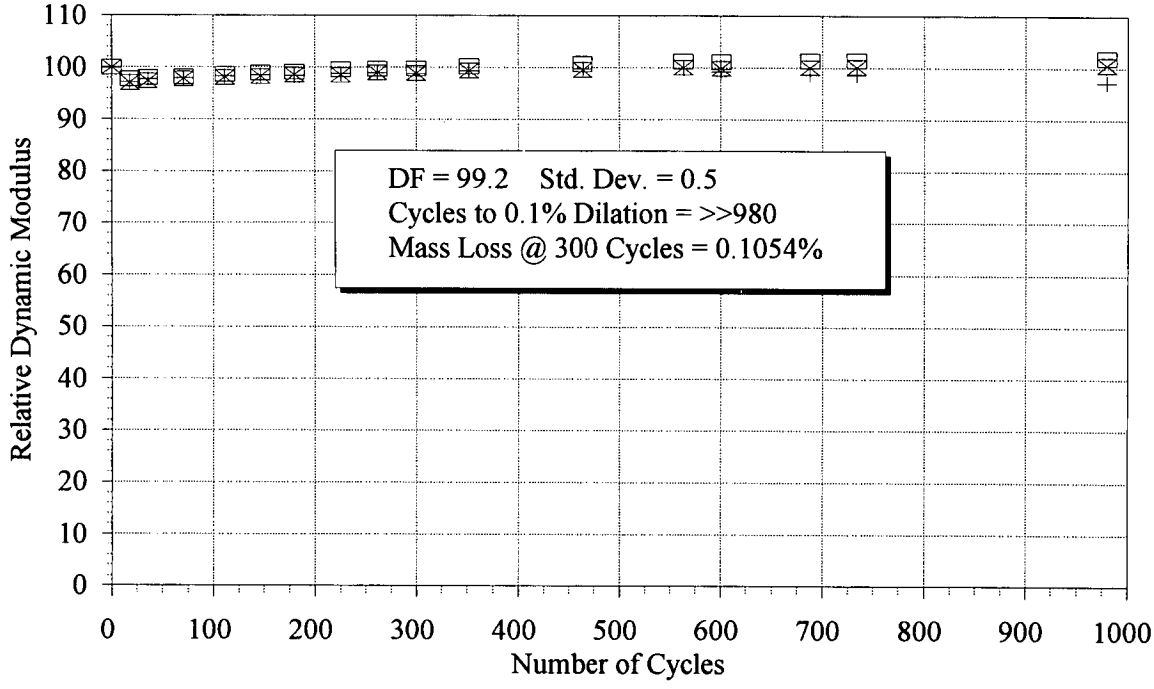

Dilation after Freezing and Thawing

Mixture MN7 - 28-Day Cure

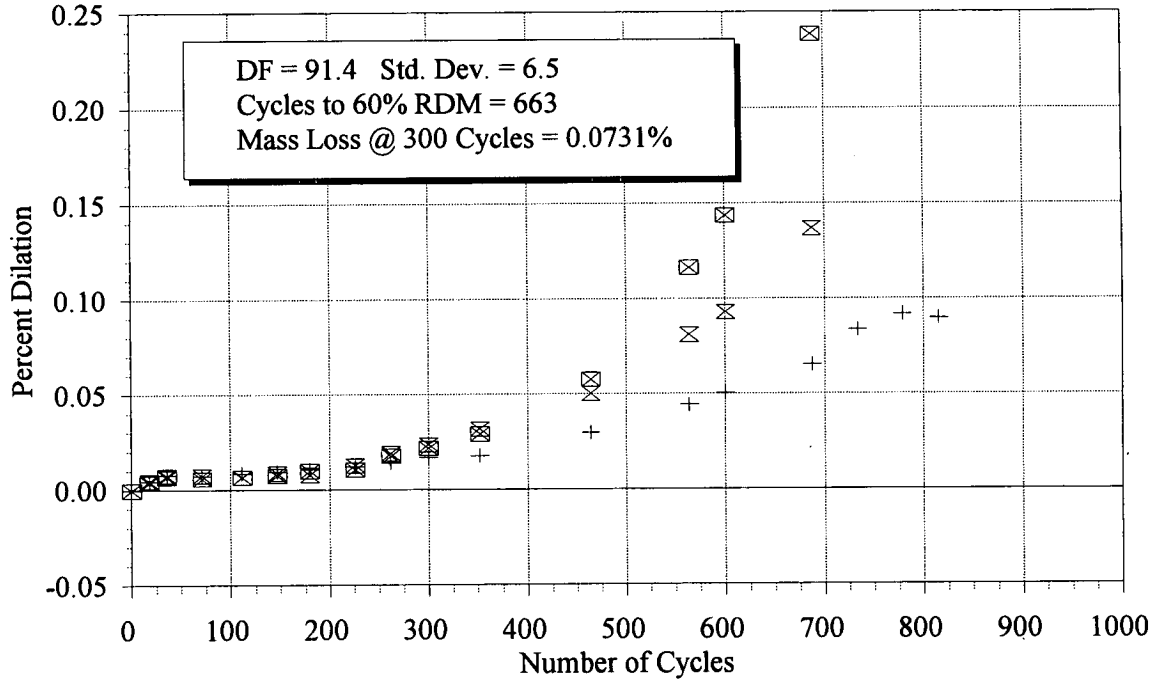

Mass Loss After Freezing and Thawing

Mixture MN7 - 28-Day Cure

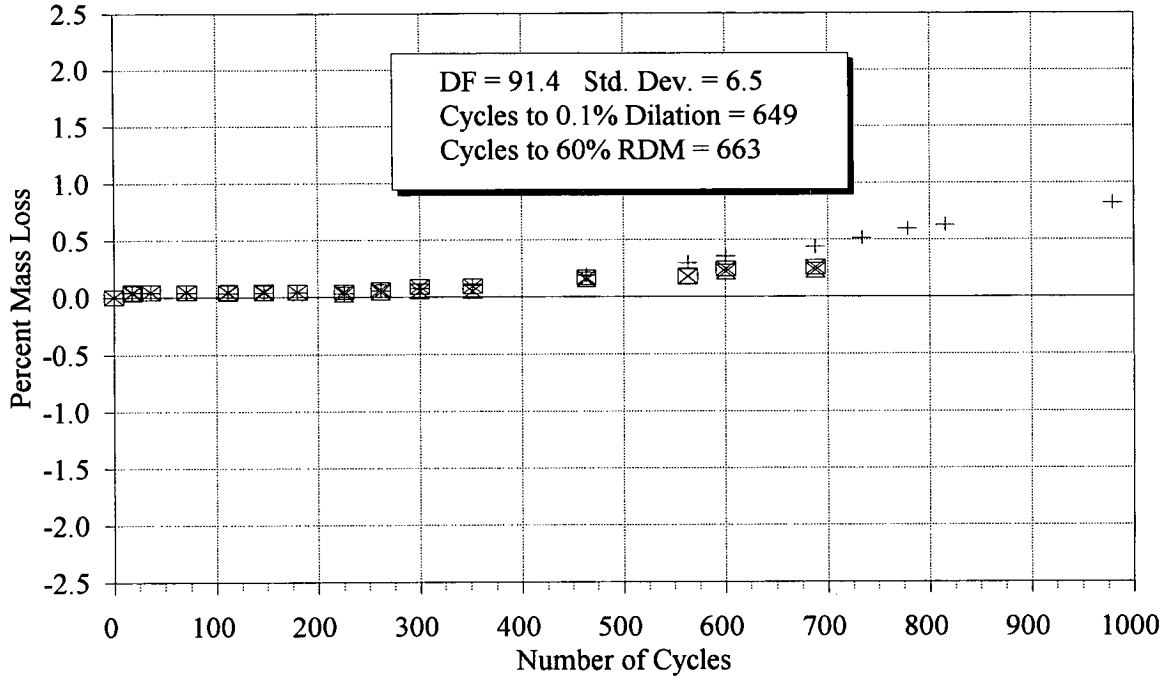

Rel Q Based on Transverse Frequency

Mixture MN7 - 28-Day Cure

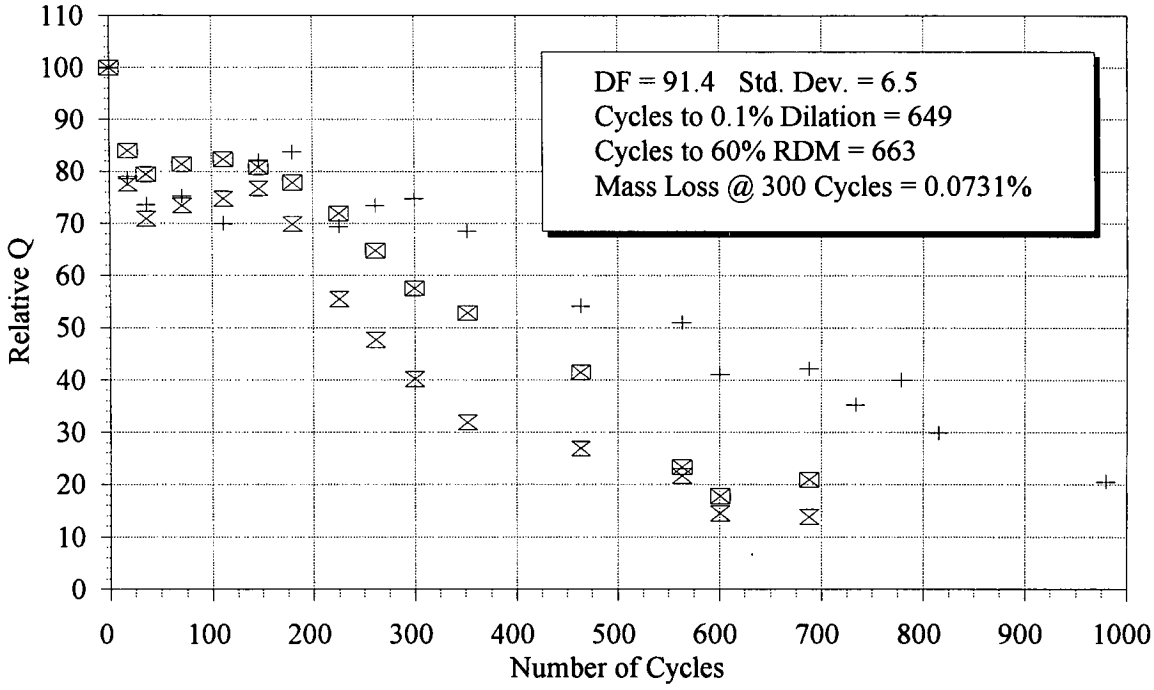

Relative Dynamic Modulus

Mixture MN7 - 28-Day Cure

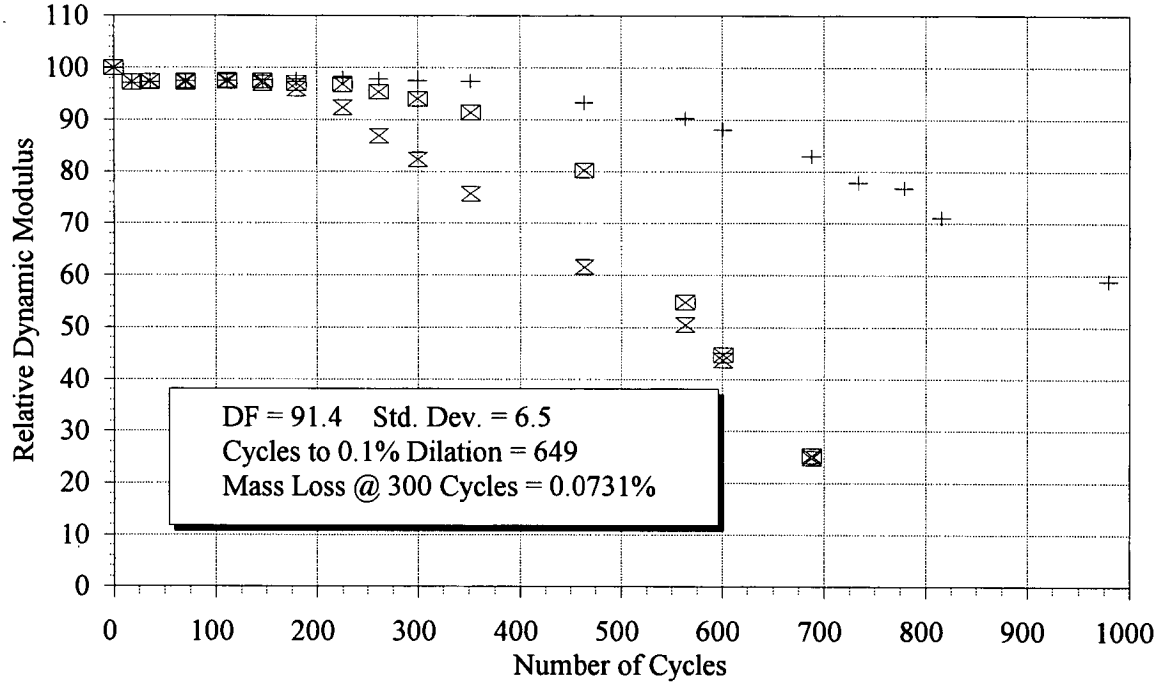

Dilation after Freezing and Thawing

Mixture MN8 - 28-Day Cure

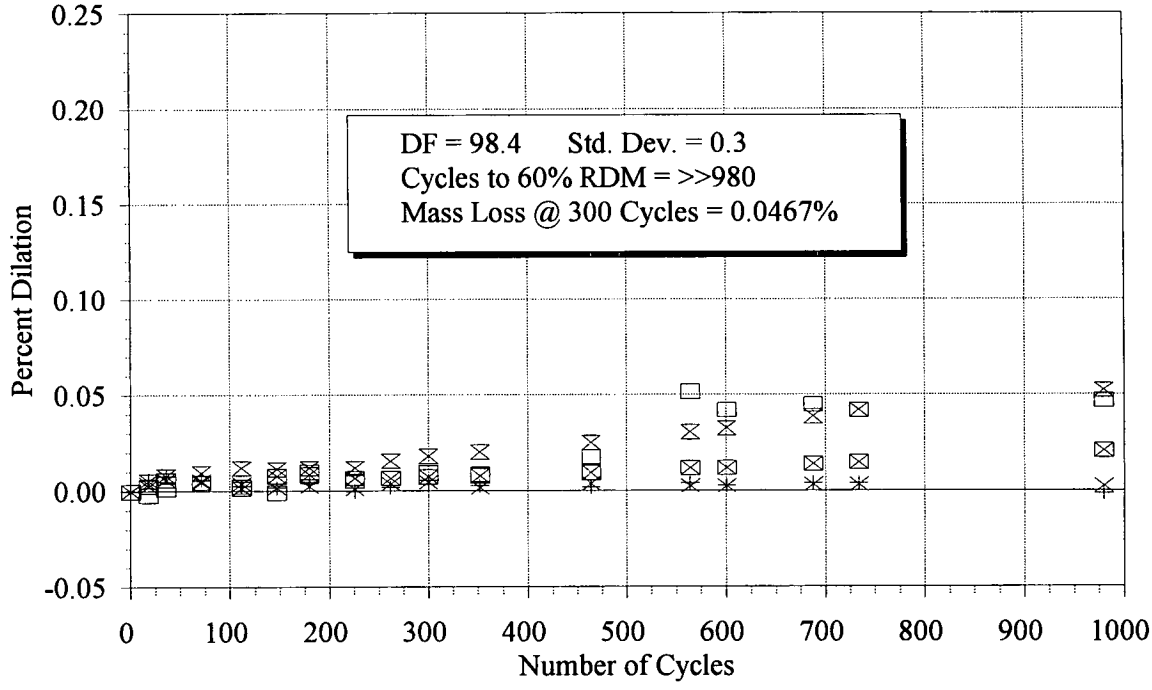

Mass Loss After Freezing and Thawing

Mixture MN8 - 28-Day Cure

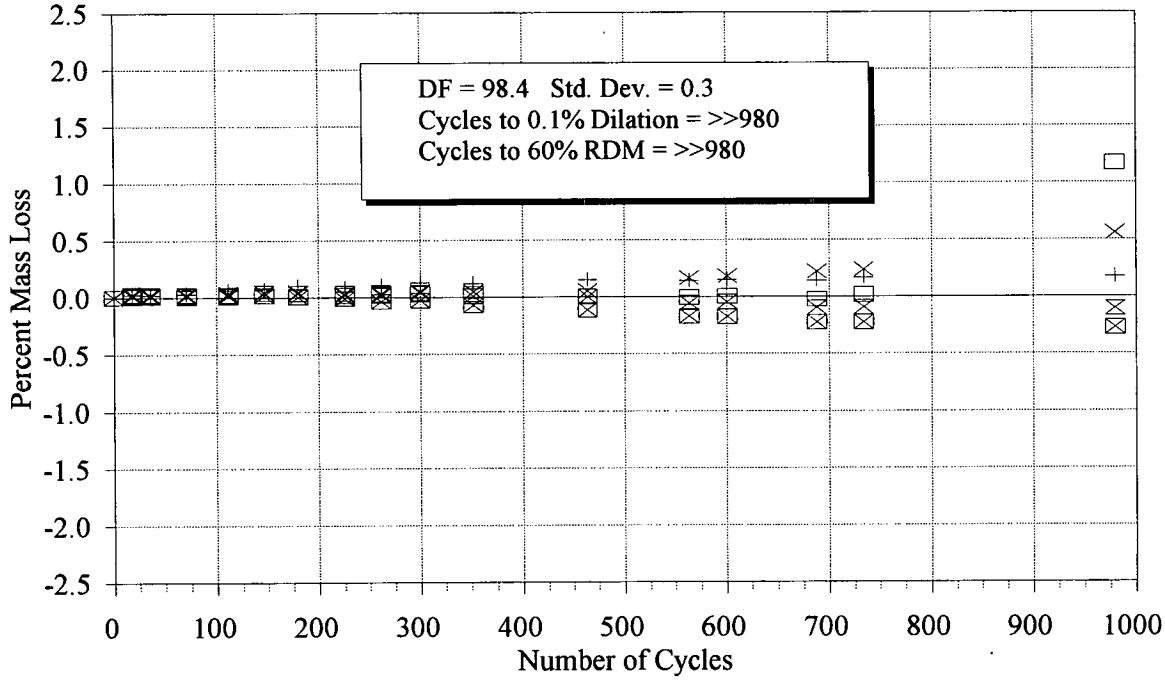

Rel Q Based on Transverse Frequency

Mixture MN8 - 28-Day Cure

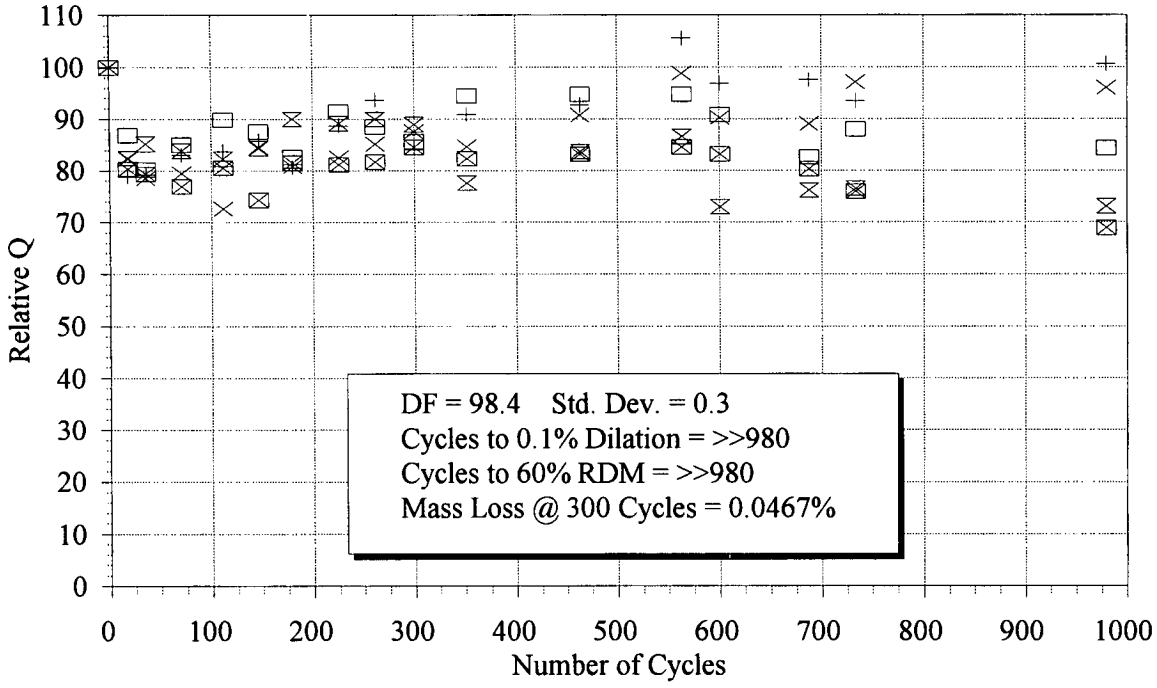

Relative Dynamic Modulus

Mixture MN8 - 28-Day Cure

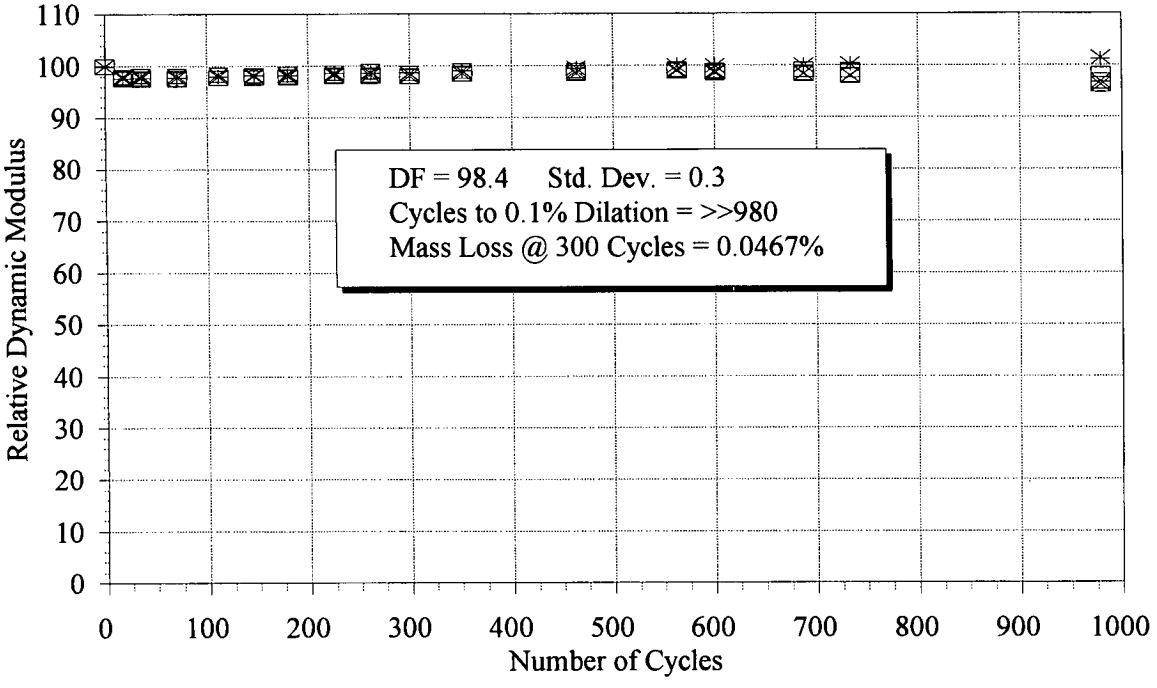

Concrete and Structures Advisory Committee

James J. Murphy, *chairman*
New York Department of Transportation (retired)

Howard H. Newlon, Jr., *vice chairman*
Virginia Transportation Research Council (retired)

Charles J. Arnold
Michigan Department of Transportation

Donald E. Beuerlein
Koss Construction Co.

Bernard C. Brown
Iowa Department of Transportation

Richard D. Gaynor
National Aggregates Association/National Ready Mixed Concrete Association

Robert J. Girard
Missouri Highway and Transportation Department

David L. Gress
University of New Hampshire

Gary Lee Hoffman
Pennsylvania Department of Transportation

Brian B. Hope
Queens University

Carl E. Locke, Jr.
University of Kansas

Clellon L. Loveall
Tennessee Department of Transportation

David G. Manning
Ontario Ministry of Transportation

Robert G. Packard
Portland Cement Association

James E. Roberts
California Department of Transportation

John M. Scanlon, Jr.
Wiss Janney Elstner Associates

Charles F. Scholer
Purdue University

Lawrence L. Smith
Florida Department of Transportation

John R. Strada
Washington Department of Transportation (retired)

Liaisons

Theodore R. Ferragut
Federal Highway Administration

Crawford F. Jencks
Transportation Research Board

Bryant Mather
USAE Waterways Experiment Station

Thomas J. Pasko, Jr.
Federal Highway Administration

John L. Rice
Federal Aviation Administration

Suneel Vanikar
Federal Highway Administration

Expert Task Group

Paul Klieger, *chairman*
Consultant

Stephen Forster
Federal Highway Administration

James G. Gehler
Illinois Department of Transportation

Vernon J. Marks
Iowa Department of Transportation

Bryant Mather
USAE Waterways Experiment Station

Richard Meininger
National Aggregates Association/ National Ready Mix Concrete Association

Larry R. Roberts
W.R. Grace and Company

James H. Stokes
New Mexico State Highway Department

James Woodstrom
Consultant